

2016-2017 Catalog

**CELL-BASED
ASSAYS**

STEM CELL RESEARCH

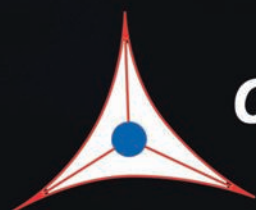
VIRAL EXPRESSION

**OXIDATIVE STRESS /
DAMAGE ASSAYS**

**CELL SIGNALING &
PROTEIN BIOLOGY**

METABOLISM RESEARCH

**PATHOGEN &
TOXIN ASSAYS**



CELL BIOLABS, INC.

Creating Solutions for Life Science Research

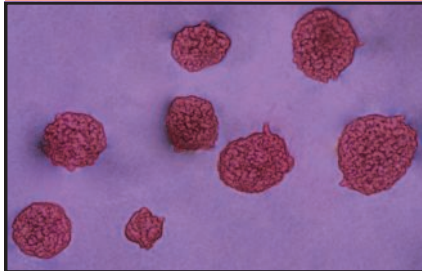
TABLE OF CONTENTS

Ordering Information & Support

4

Ch. 1 Cell-Based Assays

5



TRANSFORMATION
ADHESION
MIGRATION
INVASION
WOUND HEALING

CELL HEALTH
CELL HYPOXIA
PHAGOCYTOSIS
CONTRACTION
ANGIOGENESIS

Ch. 2 Stem Cell Research

31



IPS CELL REPROGRAMMING
RETROVIRAL EXPRESSION SYSTEMS
FEEDER CELLS
COLONY FORMATION ASSAYS
ALKALINE PHOSPHATASE ASSAYS

Ch. 3 Viral Expression

39

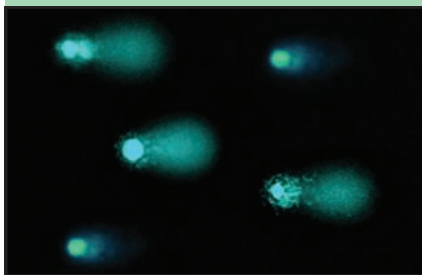


ADENO-ASSOCIATED
VIRUS (AAV)
ADENOVIRUS
LENTIVIRUS
RETROVIRUS

PREMADE VIRUSES
EXPRESSION SYSTEMS
PURIFICATION KITS
TITER KITS
TRANSDUCTION KITS

Ch. 4 Oxidative Stress / Damage

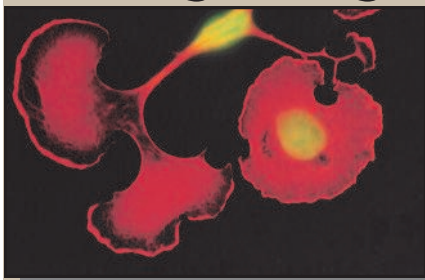
71



PROTEIN OXIDATION/NITRATION
LIPID PEROXIDATION
DNA/RNA DAMAGE AND REPAIR
REACTIVE OXYGEN SPECIES (ROS) ASSAYS
ANTIOXIDANT ASSAYS
OXIDASE/PEROXIDASE ASSAYS

TABLE OF CONTENTS

Ch. 5 Cell Signaling & Protein Biology 103



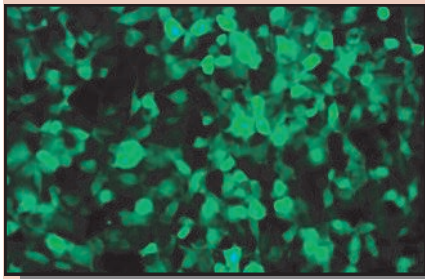
SMALL GTPASE / G-PROTEIN SIGNALING
KINASE ASSAYS
REPORTER ASSAYS AND REAGENTS
EPI TOPE TAGS
PROTEIN ANALYSIS TOOLS

Ch. 6 Metabolism Research 121



LIPOPROTEIN METABOLISM
AMINO ACID ASSAYS
CARBOHYDRATE ASSAYS
RENAL FUNCTION ASSAYS
ALCOHOL ASSAYS

Ch. 7 Pathogen and Toxin Assays 151



VIRAL ANTIGEN ASSAYS
TOXIN ASSAYS

Product Index 156

ORDERING INFORMATION & SUPPORT

Placing an Order within the U.S.

Our Customer Service representatives are available Monday through Friday from 8:00 am to 5:00 pm Pacific Time.

Most orders received by 2:00 pm Pacific Time will be shipped the same day. We will notify you immediately of any backordered item.

We accept VISA®, MasterCard® and American Express® cards. Net 30 day credit terms may be offered upon approval.

Phone 1 858 271 6500
1 888 CBL 0505 (Toll-Free)

Fax 1 858 271 6514

E-mail orders@cellbiolabs.com

Online www.cellbiolabs.com

Mail Attn: Customer Service
7758 Arjons Drive
San Diego, CA 92126

Worldwide Technical Support

Do you have questions about a particular product before you buy? Do you need help with a protocol?

Our Technical Service Scientists have been directly involved in the development and testing of our products, so you get the benefit of their hands-on experience.

Phone 1 858 271 6500
1 888 CBL 0505 (US Toll-Free)

Fax 1 858 271 6514

E-mail tech@cellbiolabs.com

Pricing

Current U.S. prices are available online at www.cellbiolabs.com, or you may request a separate price list by e-mail. Prices are subject to change without notice.

For pricing outside the U.S. please contact your local distributor, which can be found on the inside back cover of this catalog.

Placing an Order outside the U.S.

Please see our list of Worldwide Distributors at www.cellbiolabs.com/international-distributors. We have a network of global distributors serving life science researchers in over 80 countries.

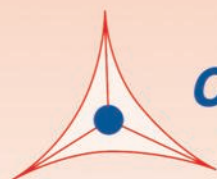
If you don't see your country listed, please contact our U.S. office.

Kit Components

Because our kits are QC tested by lot, individual kit components are generally not available for purchase separately. However, certain components may be available in bulk quantities on a custom basis. For more information please inquire by sending a message to sales@cellbiolabs.com.

Cell-Based Assays

Cell Transformation / Colony Formation	6
Cell Adhesion	10
Cell Migration / Invasion	12
Wound Healing	20
Cell Co-Culture	21
Cell Health	22
Cell Hypoxia	26
Adipogenesis	27
Phagocytosis	28
Cell Contraction	29
Angiogenesis	30
Autophagy	30



CELL BIOLABS, INC.

Creating Solutions for Life Science Research

Tumor Cell / Soft Agar Assays

Transformation of normal cells into neoplastic cells results in a population capable of proliferating independently of internal and external signals that normally restrain growth. The soft agar colony formation assay has traditionally been used to monitor anchorage-independent growth, employing 3-4 weeks of cell growth followed by manual cell counting.

We have advanced the soft agar assay to eliminate tedious manual cell counting, allow high-throughput drug screening, and enable recovery of transformed cells for downstream analysis. These advances have also allowed us to develop a unique kit for the separation of clonogenic cancer cells from normal cells in heterogeneous solid tumors.

CytoSelect™ 96-Well Cell Transformation Assay—Traditional Soft Agar Colony Formation

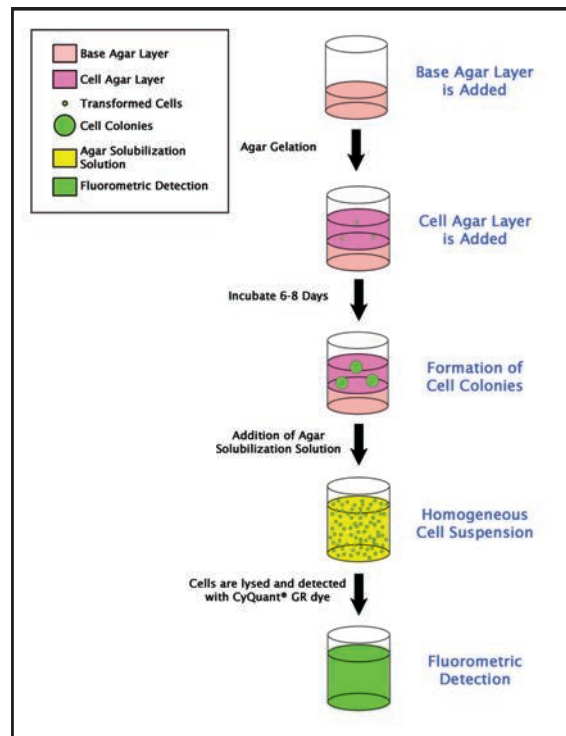
Our CytoSelect™ 96-Well Cell Transformation Assay (Soft Agar Colony Formation) is suitable for measuring malignant transformation where no downstream analysis is required. Transformed cells cannot be recovered; however, no manual cell counting is required.

With this assay, cells are incubated in a semisolid agar medium for 6-8 days, then solubilized, lysed and detected using CyQuant® GR dye in a fluorometric plate reader.

Recent Product Citations

1. Tsukamoto, Y. et al. (2015). Expression of DDX27 contributes to colony forming ability of gastric cancer cells and correlates with poor prognosis in gastric cancer. *Am. J. Cancer Res.* **5**:2998.
2. Ercan, D. et al. (2015). EGFR mutations and resistance to irreversible pyrimidine based EGFR receptors. *Clin. Cancer Res.* **21**:3913-3923.
3. Mayr, C. et al. (2015). 3-Deazaneplanocin A may directly target putative cancer stem cells in biliary tract cancer. *Anticancer Res.* **35**:4697-4705.
4. Hua, G. et al. (2015). YAP induces high-grade serous carcinoma in fallopian tube secretory epithelial cells. *Oncogene* **10.1038/onc.2015.288**.
5. Ukaji, T. et al. (2015). Inhibition of IGF-1 mediated cellular migration and invasion by migracin A in ovarian clear cell carcinoma cells. *PLoS One* **10**:e0137663.
6. Bon, H. et al. (2015). Salt-inducible Kinase 2 regulated mitotic progression and transcription in prostate cancer. *Mol. Cancer Res.* **13**:620-635.
7. Kim, T. et al. (2015). Role of MYC-regulated long noncoding RNAs in cell cycle regulation and tumorigenesis. *J. Nat. Cancer Inst.* **107**:dju505.

- **Fast Results:** 6-8 days vs. 21 days
- **Plate Reader Convenience:** Eliminates manual counting
- **Versatile Format:** Designed for 96-well throughput, but can be adapted for 48, 24, 12 or 6-well



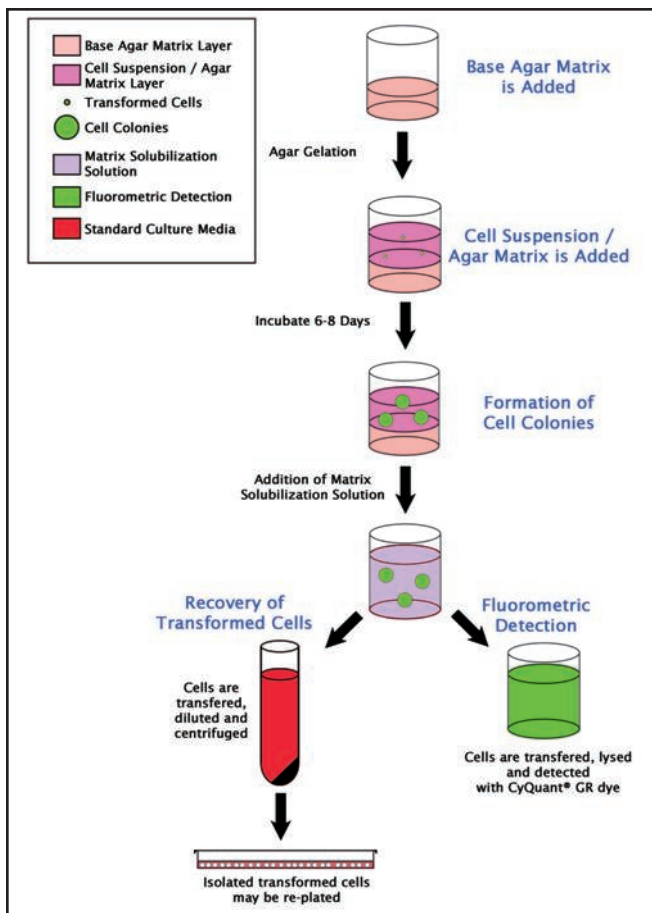
Cell Transformation Assay Principle.

Product Name	Detection	Size	Catalog Number
CytoSelect™ 96-Well Cell Transformation Assay (Soft Agar Colony Formation)	Fluorometric	1 Plate*	CBA-130
		5 Plates*	CBA-130-5

*Each kit provides sufficient reagent quantities to perform 96, 48, 24, 12, or 6 tests in a 96, 48, 24, 12, or 6-well plate, respectively.

CytoSelect™ 96-Well Cell Transformation Assays—Advanced Soft Agar with Post-Incubation Cell Recovery

The CytoSelect™ 96-Well Cell Transformation Assay (Cell Recovery Compatible) provides a robust system for screening oncogenes and cell transformation inhibitors. Transformed cells may be recovered for further downstream analysis following colony formation.



Cell Transformation Assay Principle. Cell colonies form after a 6-8 day incubation with agar matrix. Transformed cells can then be either lysed and detected with a fluorescent dye or recovered and re-plated.

- **Faster Results:** 6-8 days vs. 21 days
- **Cell Recovery:** Transformed cells remain viable for further analysis
- **Plate Reader Convenience:** Eliminates manual counting of cells
- **Versatile Format:** Designed for 96-well throughput, but can be adapted for 48, 24, 12 or 6-well

Recent Product Citations

1. Mardin, B.R. et al. (2015). A cell-based model system links chromothripsis with hyperploidy. *Mol. Syst. Biol.* **11**:828. (CBA-135)
2. Monot, M. et al. (2015). Early steps of Jaagsiekte sheep retrovirus-mediated cell transformation involve the interaction between env and the RALBP1 cellular protein. *J. Virol.* **89**:8462-8473. (CBA-135)
3. Bon, H. et al. (2015). Salt-inducible Kinase 2 regulated mitotic progression and transcription in prostate cancer. *Mol. Cancer Res.* **13**:620-635. (CBA-135)
4. Fatemi, M. et al. (2014). Epigenetic silencing of CHD5, a novel tumor-suppressor gene, occurs in early colorectal cancer stages. *Cancer* **120**:172-180. (CBA-135)
5. Park, H. et al. (2014). Distinct roles of DKK1 and DKK2 in tumor angiogenesis. *Angiogenesis* **17**:221-234. (CBA-135)
6. Wang, X. et al. (2014). Commensal bacteria drive endogenous transformation and tumour stem cell marker expression through a bystander effect. *Gut* **10.1136/gutjnl-2014-307213**. (CBA-135)
7. Bottero, V. et al. (2013). Kaposi's Sarcoma-associated Herpesvirus-positive primary effusion lymphoma tumor formation in NOD/SCID mice is inhibited by neomycin and neamine blocking angiogenin-s nuclear translocation. *J. Virol.* **87**:11806-11820. (CBA-135)
8. Singh, R. et al. (2013). Increasing the complexity of chromatin: functionally distinct roles for replication-dependent histone H2A isoforms in cell proliferation and carcinogenesis. *Nucleic Acids Res.* **10.1093/nar/gkt736**. (CBA-135)
9. Shukla, A. et al. (2013). Extracellular signal-regulated kinase 5: a potential therapeutic target for malignant mesotheliomas. *Clin. Cancer Res.* **19**:2071-2083. (CBA-135)
10. Niccoli, S. et al. (2012). The Asian-American E6 variant protein of human papillomavirus 16 alone is sufficient to promote immortalization, transformation, and migration of primary human foreskin keratinocytes. *J. Virol.* **86**:12384-12396. (CBA-135)
11. Hong, S.W. et al. (2012). Ring finger protein 149 is an E3 ubiquitin ligase active on wild-type v-Raf murine sarcoma viral oncogene homolog B1 (BRAF). *J. Biol. Chem.* **287**:24017-24025. (CBA-135)

Product Name	Detection	Size	Catalog Number
CytoSelect™ 96-Well Cell Transformation Assay (Cell Recovery Compatible)	Colorimetric	1 Plate*	CBA-135
		5 Plates*	CBA-135-5
	Fluorometric	1 Plate*	CBA-140
		5 Plates*	CBA-140-5
CytoSelect™ 384-Well Cell Transformation Assay**	Fluorometric	1 Plate***	CBA-145
		5 Plates***	CBA-145-5

*Each kit provides sufficient reagent quantities to perform 96, 48, 24, 12, or 6 tests in a 96, 48, 24, 12, or 6-well plate, respectively.

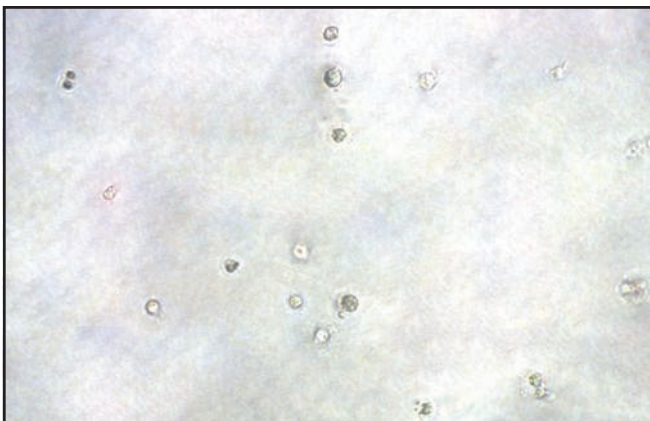
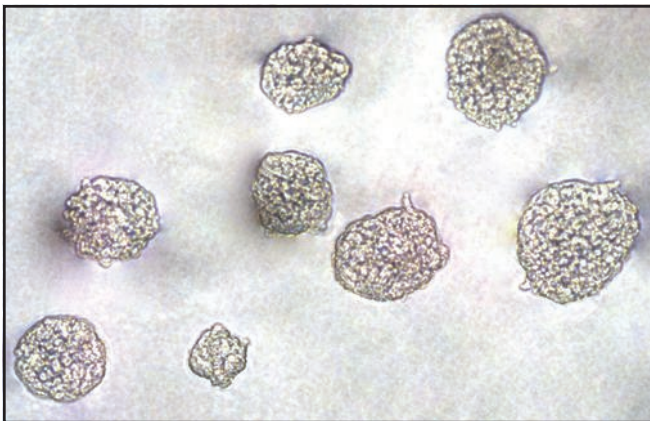
**The 384-well kit does not allow for cell recovery due to small well size.

***Each kit provides sufficient reagents for one or five 384-well plates respectively.

CytoSelect™ 96-Well *In Vitro* Tumor Sensitivity Assay

The CytoSelect™ *In Vitro* Tumor Sensitivity Assay provides a stringent, anchorage-independent model for chemosensitivity testing and possible anticancer drug screening. The assay uses a soft agar matrix to promote the colony formation of neoplastic cells in about a week. Cells are quantified using a standard ELISA plate reader.

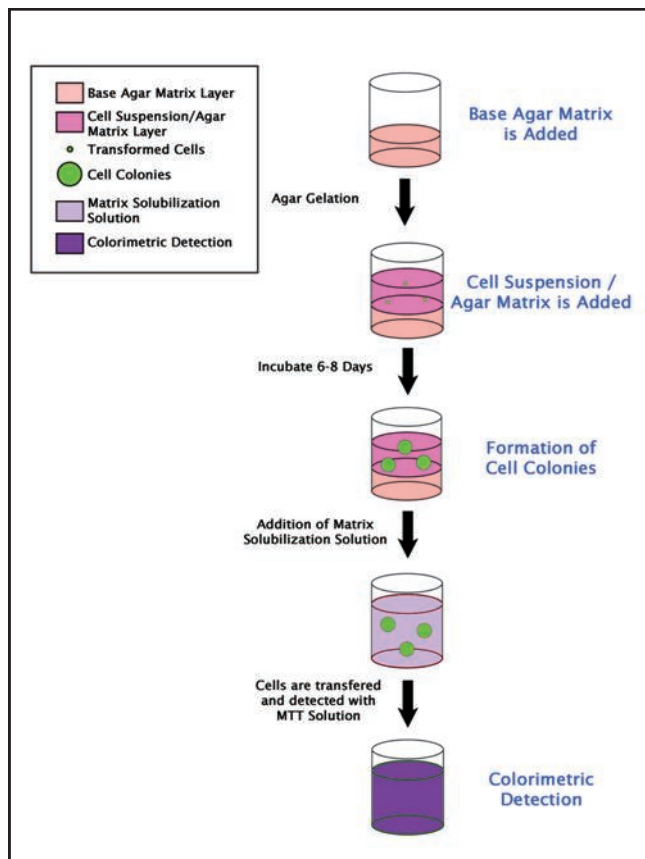
- **Fast Results:** 6-8 days
- ***In Vivo* Simulation:** Resembles a three-dimensional cell environment
- **Plate Reader Convenience:** Eliminates manual counting



Inhibition of HeLa Cell Anchorage-Independent Growth by Taxol. HeLa cells were cultured for 7 days in the absence (top) or presence (bottom) of 1 nM Taxol according to the assay protocol.

Recent Product Citations

1. Meador, C.B. et al. (2015). Optimizing the sequence of anti-EGFR-targeted therapy in EGFR-mutant lung cancer. *Mol. Cancer Ther.* **14**:542-552.
2. Aki, M.R. et al. (2015). Araguspongine C induces autophagic death in breast cancer cells through suppression of c-Met and HER2 receptor tyrosine kinase signaling. *Mar Drugs* **13**:288-311.
3. Peng, Y.T. et al. (2015). Upregulation of cyclin-dependent kinase inhibitors CDKN1B and CDKN1C in hepatocellular carcinoma-derived cells via goniotalamin-mediated protein stabilization and epigenetic modifications. *Toxicol. Rep.* 10.1016/j.toxrep.2015.
4. Suman, S. et al. (2014). The pro-apoptotic role of autophagy in breast cancer. *Bri. J. Cancer* **111**:309-317.
5. Bard-Chapeau, E. et al. (2013). EVI1 oncoprotein interacts with a large and complex network of proteins and integrates signals through protein phosphorylation. *PNAS* **110**:E2885-E2894.
6. Takezawa, K. et al. (2012). HER2 amplification: a potential mechanism of acquired resistance to EGFR inhibition in EGFR-mutant lung cancers that lack the second-site EGFR T790M mutation. *Cancer Discovery* **2**:922-933.



Tumor Sensitivity Assay Principle.

Product Name	Detection	Size	Catalog Number
CytoSelect™ 96-Well <i>In Vitro</i> Tumor Sensitivity Assay	Colorimetric	96 Assays	CBA-150
		5 x 96 Assays	CBA-150-5

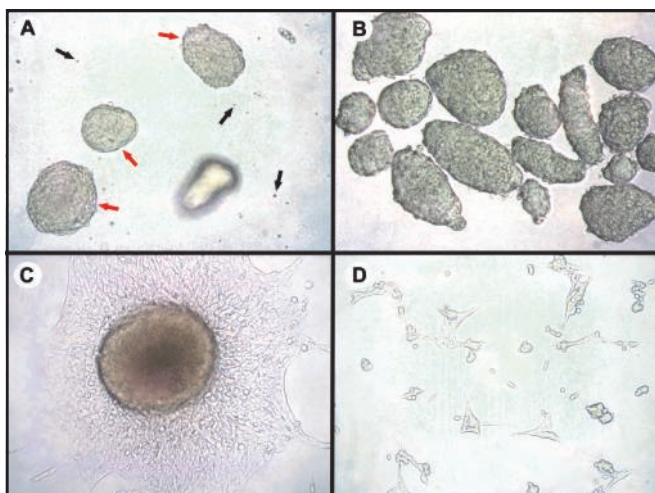
CytoSelect™ Clonogenic Tumor Cell Isolation Kit

Clean separation of clonogenic tumor cells from normal cells is critical for proper analysis of disease state progression. Due to the heterogeneity of many tumors, however, isolation of homogenous tumor cell populations can be difficult.

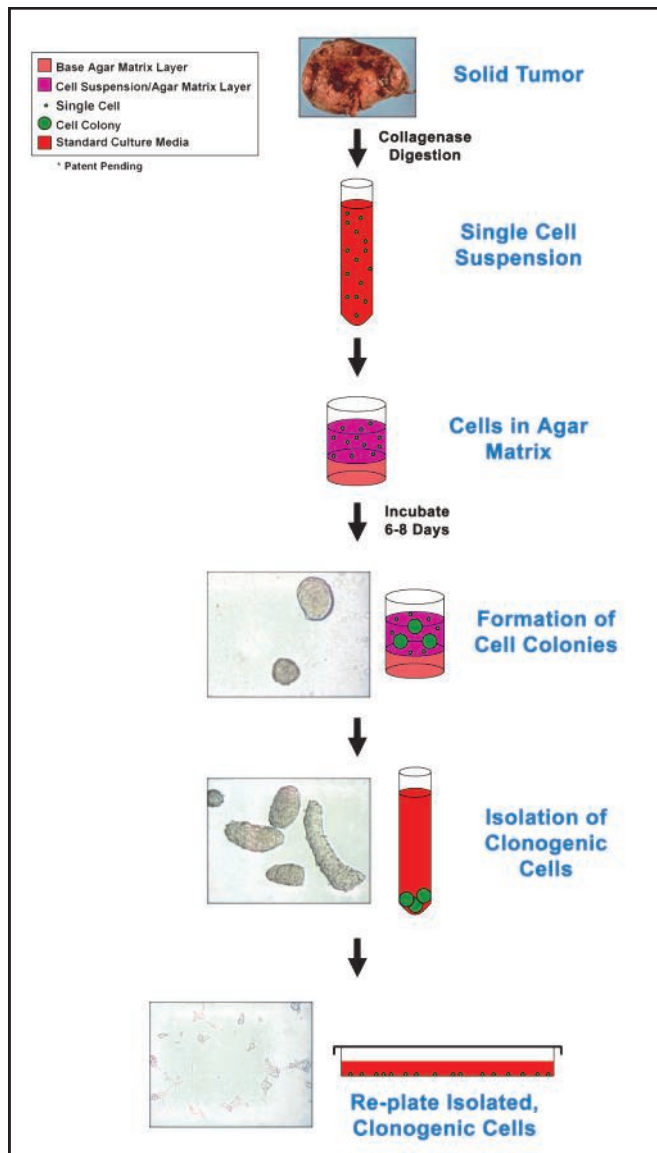
The CytoSelect™ Clonogenic Tumor Cell Isolation Kit uses a proprietary semisolid agar medium to facilitate colony formation by cells from solid tumors.

Colonies are grown in either a 6-well plate or a 35 mm dish. The colonies are then isolated away from single cells by size filtration.

- **Efficient:** Easily eliminates single cells from clonogenic tumor cell population
- **Versatile:** In addition to solid tumors, has potential use in isolating tumor stem cells



Clonogenic Colony Formation, Isolation and Re-plating. **A:** Clonogenic colony formation (red arrows) and single cells (black arrows) after 7 day incubation. **B:** Isolation of clonogenic colonies from single cells. **C:** Re-plated clonogenic colonies after 3 days (no trypsinization). **D:** Re-plated clonogenic colonies 1 day after trypsinization.



Clonogenic Tumor Cell Isolation Procedure.

Product Name	Size	Catalog Number
CytoSelect™ Clonogenic Tumor Cell Isolation Kit	5 Preps	CBA-155
	25 Preps	CBA-155-5

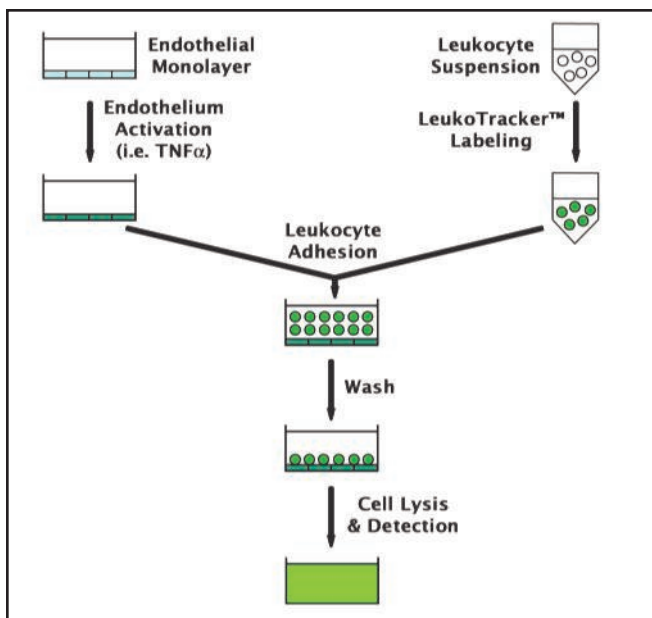
Cell Adhesion Assays

Cell adhesion is a complex mechanism involved in a variety of processes including cell migration/invasion, embryogenesis, wound healing and tissue remodeling. Cells can adhere to the ECM, forming complexes with cytoskeletal components, or to the endothelium.

Our CytoSelect™ Cell Adhesion Assays quantify adhesion of cells using a microplate reader or fluorometer; no manual cell counting is required.

CytoSelect™ Leukocyte Endothelium Adhesion Assays

The CytoSelect™ Leukocyte Endothelium Adhesion Assays provide a robust system for the quantitative determination of interactions between leukocytes and endothelium. Adherent cells can be quantified on a fluorescence plate reader.



CytoSelect™ Leukocyte-endothelium Adhesion Assay Principle.

Recent Product Citations

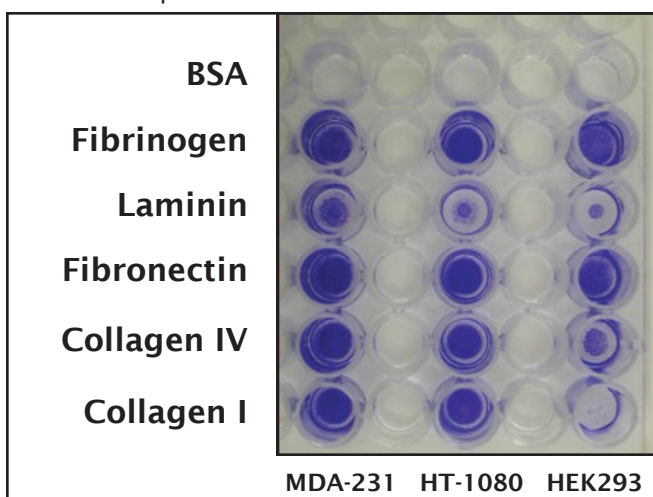
- Huang, M. et al. (2015). Niclosamide inhibits the inflammatory and angiogenic activation of human umbilical vein endothelial cells. *Inflamm. Res.* **64**:1023-1032. (CBA-210)
- Shah, D. et al. (2015). C1q deficiency promotes pulmonary vascular inflammation and enhances the susceptibility of the lung endothelium to injury. *J. Biol. Chem.* **10.1074/jbc.M115.690784**. (CBA-210)
- Campos-Estrada, C. et al. (2015). Simvastatin and benznidazole-mediated prevention of Trypanosoma cruzi-induced endothelial activation: role of 15-epi-lipoxin AA4 in the action of simvastatin. *PLoS Negl Trop. Dis.* **9**:e0003770. (CBA-210)
- Ibrahim, A.S. et al. (2015). A lipidomic screen of hyperglycemia-treated HRECs links 12/15-lipoxygenase to microvascular dysfunction during diabetic retinopathy via NADPH oxidase. *J. Lipid Res.* **56**:599-611. (CBA-210)
- Cao, Q. et al. (2014). Inhibiting DNA methylation by 5-aza-2'-deoxycytidine ameliorates atherosclerosis through suppressing macrophage inflammation. *Endocrinology* **155**:4925-4938. (CBA-210)
- Kapitsinou, P.P. et al. (2014). Endothelial HIF-2 mediates protection and recovery from ischemic kidney injury. *J. Clin. Invest.* **124**:2396. (CBA-210)
- Wu, X.Y. et al. (2014). Regulation of microRNA-515 in endothelial inflammation by targeting nuclear factor (NF)-kappaB p65. *J. Cell Biochem.* **115**:1928-1936. (CBA-210)
- Ghoshal, P. et al. (2014). Glycosylation inhibitors efficiently inhibit P-selectin-mediated cell adhesion to endothelial cells. *PLoS One* **9**:e99363. (CBA-210)
- Jassam, S.A. et al. (2015). TNF-alpha enhancement of CD62E mediates adhesion of non-small cell lung cancer cells to brain endothelium via CD15 in lung-brain metastasis. *Neuro Oncol.* **10.1093/neuonc/nov248**. (CBA-215)
- Finetti, F. et al. (2015). mPGES-1 in prostate cancer controls stemness and amplifies EGFR-driven oncogenicity. *Endocr. Relat. Cancer* **10.1530/ERC-15-0277**. (CBA-215)
- Yang, M. et al. (2014). IgG expression in trophoblasts derived from placenta and gestational trophoblastic disease and its role in regulating invasion. *Immunol. Res.* **60**:91-104. (CBA-215)
- Sasahira, T. et al. (2014). Transport and Golgi organisation protein 1 is a novel tumour porgresssive factor in oral squamous cell carcinoma. *Eur. J. Cancer* **50**:2142-2151. (CBA-215)

Product Name	Detection	Size	Catalog Number
CytoSelect™ Leukocyte-Endothelium Adhesion Assay	Fluorometric	96 Assays	CBA-210
CytoSelect™ Leukocyte-Epithelium Adhesion Assay	Fluorometric	96 Assays	CBA-211
CytoSelect™ Tumor-Endothelium Adhesion Assay	Fluorometric	96 Assays	CBA-215

CytoSelect™ ECM Cell Adhesion Assays

CytoSelect™ ECM Cell Adhesion Assays provide a quantitative method to measure cell adhesion. The 48-well plate is precoated with your choice of substrate. Adherent cells attach, while non-adherent cells are washed away. Adherent cells can be quantified on a colorimetric or fluorometric plate reader.

- **Quantitative:** Measure results in a colorimetric or fluorescence plate reader
- **Flexible:** Uniform substrate layer of your choice of Collagen I, Collagen IV, Fibrinogen, Fibronectin, or Laminin; or choose the ECM array which contains all 5 ECM proteins



CytoSelect™ 48-well Cell Adhesion Assay. Serum starved cells from three different cell lines were allowed to attach to the ECM-coated plate for 1 hr at 100,000 cells/well. Adherent cells were stained according to the assay protocol.

Recent Product Citations

1. Jiang, F. et al. (2015). CYP3A5 functions as a tumor suppressor in hepatocellular carcinoma by regulating mTORC2/Akt signaling. *Cancer Res.* **75**:1470-1481. (CBA-050)
2. Chen, L. et al. (2015). Both mTORC1 and mTORC2 are involved in the regulation of cell adhesion. *Oncotarget.* **6**:7136-7150. (CBA-050 and CBA-056)
3. Aghajani, H. et al. (2014). Semaphorin 3d and semaphorin 3e direct endothelial motility through distinct molecular signaling pathways. *J. Biol. Chem.* **289**:17971-17979. (CBA-052)
4. Lee, J. et al. (2013). Selective inhibition of prostaglandin E2 receptors EP2 and EP4 inhibits adhesion of human endometrial epithelial and stromal cells through suppression of integrin-mediated mechanisms. *Biol. Reprod.* **88**:77. (CBA-057)
5. Montealegre, M.C. et al. (2015). The *Enterococcus faecalis* EbpA pilus protein: attenuation of expression, biofilm formation, and adherence to fibrinogen start with the rare initiation codon ATT. *MBio.* **6**:e00467-15. (CBA-058)
6. Miao, H. et al. (2008). Gene expression and functional studies of the optic nerve head astrocyte transcriptome from normal African Americans and Caucasian Americans donors. *PLoS One* **3**(8):E2847. (CBA-060)
7. Nowakowska, M. et al. (2014). Diverse effect of WWOX overexpression in HT29 and SW480 colon cancer cell lines. *Tumor Biol.* **35**:9291-9301. (CBA-070)
8. Singla, A.K. et al. (2015). Characterization of a murine model of metastatic human non-small cell lung cancer and effect of CXCR4 inhibition on the growth of metastases. *Oncoscience* **2**:263-271. (CBA-070)
9. Jain, M. et al. (2014). ZHF367 inhibits cancer progression and is targeted by miR-195. *PLoS One* **9**:e101423. (CBA-070)
10. Tanoury, Z. et al. (2014). Genes involved in cell adhesion and signaling: a new repertoire of retinoic acid receptor target genes in mouse embryonic fibroblasts. *J. Cell Sci.* **127**:521-533. (CBA-070)
11. Aohra, F.T. et al. (2015). Functional behavior and gene expression of magnetic nanoparticle-loaded primary endothelial cells for targeting vascular stents. *Nanomedicine (Lond.)* **10**:1391-1406. (CBA-071)

Product Name	Detection	Size	Catalog Number
CytoSelect™ 48-Well Cell Adhesion Assay, ECM Array (Contains one row each of Collagen I, Collagen IV, Fibrinogen, Fibronectin, and Laminin)	Colorimetric	48 Assays	CBA-070
		5 x 48 Assays	CBA-070-5
	Fluorometric	48 Assays	CBA-071
		5 x 48 Assays	CBA-071-5
CytoSelect™ 48-Well Cell Adhesion Assay, Collagen I	Colorimetric	48 Assays	CBA-052
	Fluorometric	48 Assays	CBA-053
CytoSelect™ 48-Well Cell Adhesion Assay, Collagen IV	Colorimetric	48 Assays	CBA-060
	Fluorometric	48 Assays	CBA-061
CytoSelect™ 48-Well Cell Adhesion Assay, Fibrinogen	Colorimetric	48 Assays	CBA-058
	Fluorometric	48 Assays	CBA-059
CytoSelect™ 48-Well Cell Adhesion Assay, Fibronectin	Colorimetric	48 Assays	CBA-050
	Fluorometric	48 Assays	CBA-051
CytoSelect™ 48-Well Cell Adhesion Assay, Laminin	Colorimetric	48 Assays	CBA-056
	Fluorometric	48 Assays	CBA-057

Cell Migration & Invasion Assays

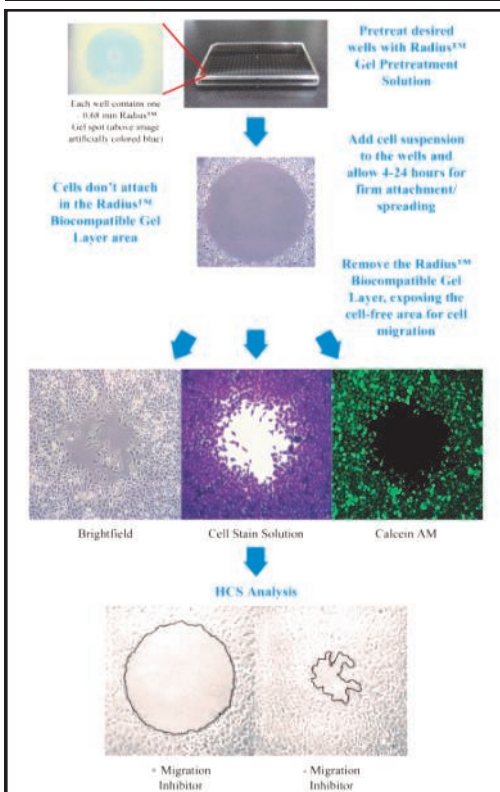
Cell migration and invasion are highly integrated, multi-step processes and play important roles in the progression of various diseases including cancer, atherosclerosis and arthritis.

Our cell migration assays are provided in two formats: 2-Dimensional Gap Closure and Boyden Chamber. Each format has its own advantages and applications. Use the information below to help choose the best format for your cell migration experimental goals.

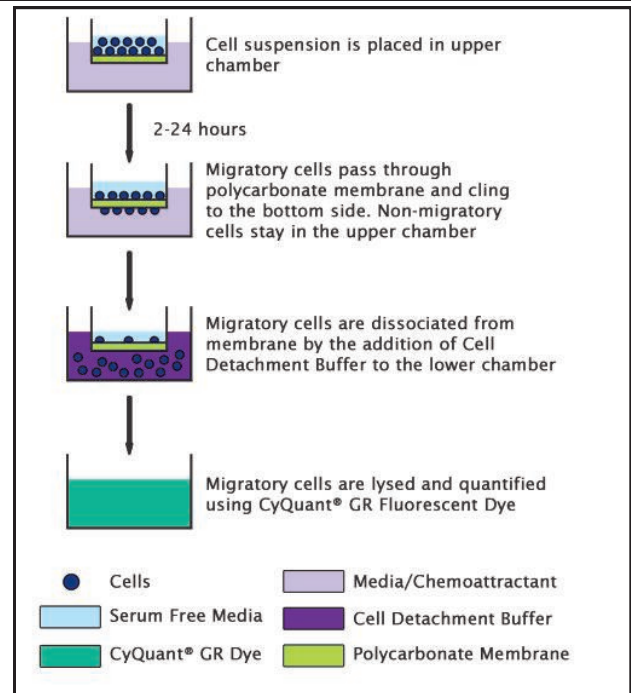
Cell invasion assays are provided in the Boyden Chamber format.

Cell Migration Format Selection Guide

	2D Gap Closure Assays (p. 13)	Boyden Chamber Assays (p. 14-19)
Type of Analysis	Qualitative or Quantitative	Quantitative
Detection Time	Endpoint or Real Time	Endpoint
Detection Method	Microscopy	Plate Reader
Chemoattractant Gradient	No	Yes
Relative Sensitivity	Good	Fair
Adaptability to Automation	Good	Poor
Cell Compatibility	Universal	Choose pore size based on cell size



Assay Principle for the Radius™ 2D Gap Closure Assays.



Example of Boyden Chamber Assay Principle.

Radius™ Cell Migration Assays (2D Gap Closure)

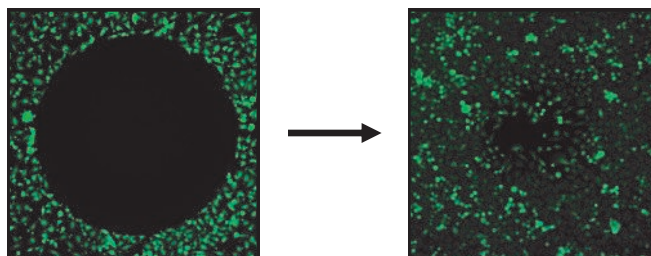
Radius™ Cell Migration Assays provide a unique alternative to the traditional Boyden Chamber migration assay. Radius assays allow you to measure cell migration at endpoint or in real time, and are ideal for time course migration studies.

Radius™ Cell Migration Assays use a cell culture plate containing a proprietary, carefully-defined bio-compatible hydrogel (Radius™ gel) spot centralized at the bottom of each well. Cells seeded in the well will attach everywhere except on the Radius gel spot, creating a cell-free zone. Once cells attach, the Radius gel is removed and migration of cells across the cell-free zone begins. The gel removal step allows synchronization of a zero time point to facilitate well-to-well comparisons.

With Radius™ Cell Migration Assays, there are no cell culture inserts; so you don't need to worry about which pore size to choose for your cell type. Any adherent cell may be used in the assay.

Radius assays are supplied in 24-well, 96-well and 384-well formats. In addition, the 24-well assays are provided with your choice of coatings for proper cell attachment:

- Uncoated
- Collagen I-coated
- Fibronectin-coated
- Laminin-coated
- ECM Array with 6 wells of each of the above (uncoated, Collagen I, Fibronectin, Laminin); ideal if you are unsure which ECM protein may provide the best cell attachment



Example Results using 2D Gap Closure Assay.

Recent Product Citations

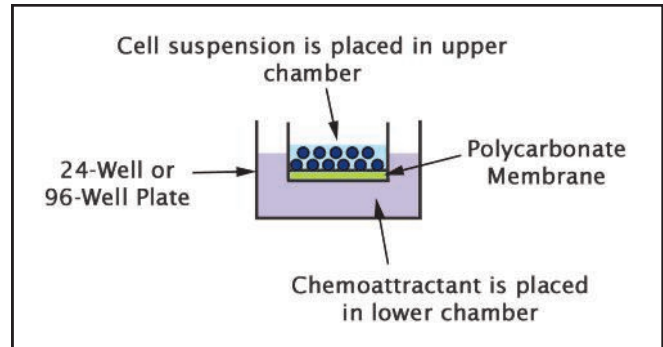
1. Sanna, V. et al. (2015). Nanoencapsulation of natural triterpenoid celastrol for prostate cancer treatment. *Int. J. Nanomedicine* **10**:6835-6846. (CBA-125)
2. Nishikawa, M. et al. (2015). Enhanced sensitivity to sunitinib by inhibition of Akt1 expression in human castration-resistant prostate cancer PC3 cells both in vitro and in vivo. *Urology* **85**:1215-e1. (CBA-125)
3. Pu, J. et al. (2015). BORC, a multisubunit complex that regulates lysosome positioning. *Dev. Cell* **33**:176-188. (CBA-125)
4. Ge, C. et al. (2015). Role of Runx2 phosphorylation in prostate cancer and association with metastatic disease. *Oncogene* **10.1038/onc.2015.91**. (CBA-125)
5. Kim, E.K. et al. (2015). First evidence that ecklonia cava-derived dieckol attenuates MCF-7 human breast carcinoma cell migration. *Mar Drugs* **13**:1785-1797. (CBA-125)
6. Camacho, M. et al. (2015). Prostacyclin-synthase expression in head and neck carcinoma patients and its prognostic value in the response to radiotherapy. *J. Pathol.* **235**:125-135. (CBA-126)
7. Woodard, G.E. et al. (2015). Characterization of discrete subpopulations of progenitor cells in traumatic human extremity wounds. *PLoS One* **9**:e114318. (CBA-126)
8. Felthaus, O. et al. (2014). Migration of human dental follicle cells in vitro. *J. Periodontal Res.* **49**:205-212. (CBA-126)
9. Wong, B. et al. (2013). Adrenomedullin enhances invasion of human extravillous cytotrophoblast-derived cell lines by regulation of urokinase plasminogen activator expression and S-nitrosylation. *Biol. Reprod.* **88**:34. (CBA-126)
10. Ichikawa, A. et al. (2013). CXCL10-CXCR3 enhances the development of neutrophil-mediated fulminant lung injury of viral and nonviral origin. *Am. J. Respir. Crit. Care Med.* **187**:65-77. (CBA-126)

Product Name	Detection	Size	Catalog Number
Radius™ 24-Well Cell Migration Assay	Microscopy	24 Assays	CBA-125
		5 x 24 Assays	CBA-125-5
Radius™ 24-Well Cell Migration Assay (Collagen I Coated)	Microscopy	24 Assays	CBA-125-COL
Radius™ 24-Well Cell Migration Assay (Fibronectin Coated)	Microscopy	24 Assays	CBA-125-FN
Radius™ 24-Well Cell Migration Assay (Laminin Coated)	Microscopy	24 Assays	CBA-125-LN
Radius™ 24-Well Cell Migration Assay (ECM Array Coated)	Microscopy	24 Assays	CBA-125-ECM
Radius™ 96-Well Cell Migration Assay	Microscopy	96 Assays	CBA-126
		5 x 96 Assays	CBA-126-5
Radius™ 384-Well Cell Migration Assay	Microscopy	384 Assays	CBA-127
		5 x 384 Assays	CBA-127-5

CytoSelect™ Cell Migration and Invasion Assays (Boyden Chamber)

The Boyden Chamber has been extensively used and widely published as a tool for measuring cell migration and cell invasion in vitro. Our CytoSelect™ Cell Migration and Invasion Assays use this well-cited method to quantify cell migration and invasion with no manual cell counting required. Migratory or invasive cells are quantified using a colorimetric or fluorometric plate reader.

Cell migration may take on various forms and behaviors depending on the type and location of cells. Such subclasses of cell migration include chemotaxis, haptotaxis, and transmigration. Use the chart below to compare the various subclasses of cell migration as well as cell invasion, which will help you choose the assay best suited to your experimental goals.



Typical Well Setup for Boyden Chamber Assay.

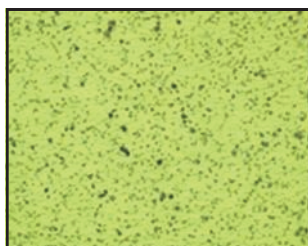
Boyden Chamber Assay Selection Guide

Assay	Definition	Cell Types	Pore Size	Insert Coating	Assay Formats
Chemotaxis (p. 15)	Migration of cells toward a chemoattractant (chemical signal) in the cell's surrounding environment	Neutrophils Leukocytes	3 μm	None	24-Well 96-Well
		Lymphocytes Monocytes Macrophages	5 μm	None	24-Well 96-Well
		Fibroblasts Endothelial Cells Epithelial Cells Tumor Cells	8 μm	None	24-Well 96-Well
		Astrocytes Slow-moving Cells	12 μm	None	24-Well
Haptotaxis (p. 16)	Migration of cells along a gradient of cellular adhesion sites or extracellular matrix-bound chemoattractants	Fibroblasts Endothelial Cells Epithelial Cells	8 μm	Collagen I (bottom)	24-Well
				Fibronectin (bottom)	24-Well
Transmigration (p. 17)	Migration of cells through the vascular endothelium toward a chemoattractant	Leukocytes	3 μm	None	24-Well
		Tumor Cells	8 μm	None	24-Well
Invasion (p. 18-19)	Movement of cells through the 3D extracellular matrix into neighboring tissues; includes ECM degradation and proteolysis	Fibroblasts Endothelial Cells Epithelial Cells Tumor Cells	8 μm	ECM Matrix (top)	24-Well 96-Well
				Collagen I (top)	24-Well 96-Well
				Laminin I (top)	24-Well 96-Well

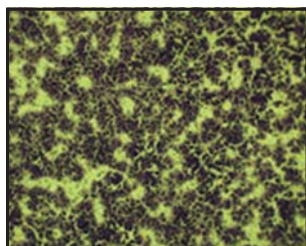
CytoSelect™ Cell Migration Assays—Chemotaxis

CytoSelect™ Cell Migration Assays are ideal for measuring chemotaxis. The kits utilize polycarbonate membrane inserts in 24-well or 96-well plates. Inserts are available with 4 different pore sizes to accommodate a variety of cell types.

- **Fast Results:** Visualize chemotaxis in less than 6 hours with most cell types
- **Flexible:** Bottoms of membrane inserts are uncoated to allow use with any chemoattractant
- **Higher Throughput:** 96-well format available for fluorescence plate readers



0% FBS



10% FBS

Migration of Human Fibrosarcoma HT-1080 Cells. Cells were seeded at 30,000 cells per well of a 24-well plate and allowed to migrate toward 10% FBS for 4 hours. Migratory cells were stained (above) and quantified in a fluorescence plate reader (data not shown).

Recent Product Citations

1. Ran, X. et al. (2015). A quantitative proteomics study on olfactomedin 4 in the development of gastric cancer. *In. J. Oncol.* **47**:1932-1944. (CBA-100)
2. Koenig, J. et al. (2015). Placental mesenchymal stromal cells derived from blood vessels or avascular tissues: what is the better choice to support endothelial cell function? *Stem Cells Dev.* **24**:115-131. (CBA-100)
3. Banerjee, D. et al. (2015). Notch suppresses angiogenesis and progression on hepatic metastases. *Cancer Res.* **75**:1592-1602. (CBA-101)
4. Deng, B. and Feng, Y. (2015). TIPE2 mediates the suppressive effects of Shikonin on MMP13 in osteosarcoma cells. *Cell Physiol. Biochem.* **37**:2434-2443. (CBA-102)
5. Sloniecka, M. et al. (2015). Substance P enhances keratocyte migration and neutrophil recruitment through interleukin-8. *Mol. Pharmacol.* **10.1124/mol.115.101014.** (CBA-103)
6. Kitano, K. et al. (2014). Rho-kinase activation in leukocytes plays a pivotal role in myocardial ischemia/reperfusion injury. *PLoS One* **9**:e92242. (CBA-104)
7. Hargarten, J.C. et al. (2015). *Candida albicans* quorum sensing molecules stimulate mouse macrophage migration. *Infect. Immun.* **83**:3857-3864. (CBA-105)
8. Kondo, Y. et al. (2015). Differential expression of CX3CL1 in hepatitis B virus-replicating hepatoma cells can affect the migration activity of CX3CR1+ immune cells. *J. Virol.* **89**:7016-7027. (CBA-105)
9. Adam, M.G.. et al. (2015). SIAH ubiquitin ligases regulate breast cancer cell migration and invasion independent of the oxygen status. *Cell Cycle* **14**:3734-3747. (CBA-106)
10. Hammer, K. et al. (2015). Engineered adenoviruses combine enhanced oncolysis with improved virus production by mesenchymal stromal carrier cells. *Int. J. Cancer* **10.1002/ijc.29442.** (CBA-107)

Product Name	Pore Size	Detection	Size	Catalog Number
CytoSelect™ 24-Well Cell Migration Assay	3 µm	Fluorometric	12 Assays	CBA-103
			5 x 12 Assays	CBA-103-5
	5 µm	Fluorometric	12 Assays	CBA-102
			5 x 12 Assays	CBA-102-5
	8 µm	Colorimetric	12 Assays	CBA-100
			5 x 12 Assays	CBA-100-5
		Fluorometric	12 Assays	CBA-101
			5 x 12 Assays	CBA-101-5
12 µm	Colorimetric	12 Assays	CBA-107	
	Fluorometric	12 Assays	CBA-108	
CytoSelect™ 96-Well Cell Migration Assay	3 µm	Fluorometric	96 Assays	CBA-104
			5 x 96 Assays	CBA-104-5
	5 µm	Fluorometric	96 Assays	CBA-105
			5 x 96 Assays	CBA-105-5
	8 µm	Fluorometric	96 Assays	CBA-106
			5 x 96 Assays	CBA-106-5

CytoSelect™ Cell Migration Assays—Haptotaxis

Haptotaxis describes the migration of cells toward a gradient of immobilized extracellular matrix. The CytoSelect™ Cell Haptotaxis Assays are ideal for determining the migratory properties of cells. The kits utilize polycarbonate membrane inserts with an 8 µm pore size in a 24-well plate.

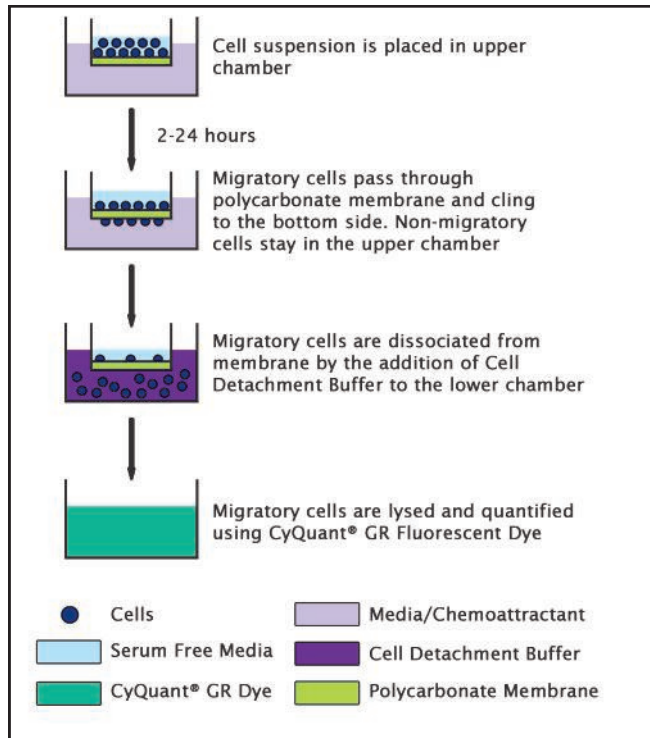
The undersides of the inserts are coated with either Collagen or Fibronectin. The 8 µm pore size in the membrane inserts is ideal for epithelial cells, endothelial cells, fibroblasts, and other cells of similar size. The membrane serves as a barrier that allows discrimination of migratory cells from non-migratory cells.

- **Fast Results:** Visualize cell haptotaxis in less than 6 hours with most cell types
- **Convenient:** Membrane inserts pre-coated on the underside with either Collagen I or Fibronectin
- **Versatile:** Useful with a variety of cell types including epithelial cells, endothelial cells, and fibroblasts*

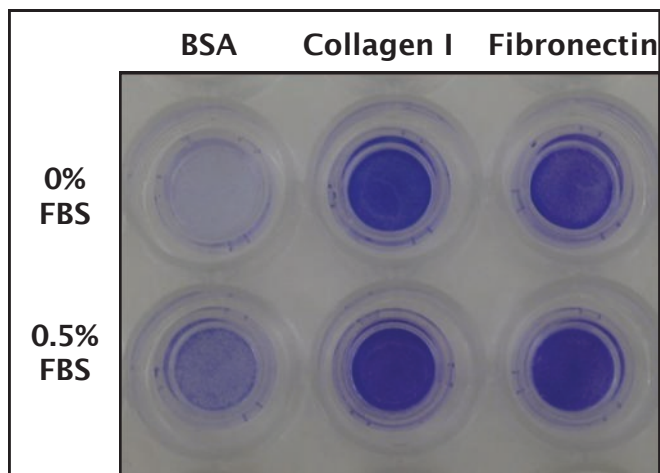
*For leukocyte migration a 3 µm pore size is recommended. See our CytoSelect™ Chemotaxis Assays (previous page) or the CytoSelect™ Leukocyte Transmigration Assay (next page).

Recent Product Citations

1. Herrera, I. et al. (2013). Matrix metalloproteinase (MMP)-1 induces lung alveolar epithelial cell migration and proliferation, protects from apoptosis, and represses mitochondrial oxygen consumption. *J. Biol. Chem.* **288**:25964-25975. (CBA-100-COL)
2. Niccoli, S. et al. (2012). The Asian-American E6 variant protein of human papillomavirus 16 alone is sufficient to promote immortalization, transformation, and migration of primary human foreskin keratinocytes. *J. Virol.* **86**:12384-12396. (CBA-110-COL)
3. Kamiya, K. et al. (2007). Protein Kinase C delta activated adhesion regulates vascular smooth muscle cell migration. *J. Surg. Res.* **141**:91-96. (CBA-100-COL)
4. Singh, D.R. et al. (2015). EphA2 unliganded dimers suppress EphA2 pro-tumorigenic signaling. *J. Biol. Chem.* 10.1074/jbc.M115.676866. (CBA-101-COL)



Assay Principle for the CytoSelect™ Cell Haptotaxis Assay.

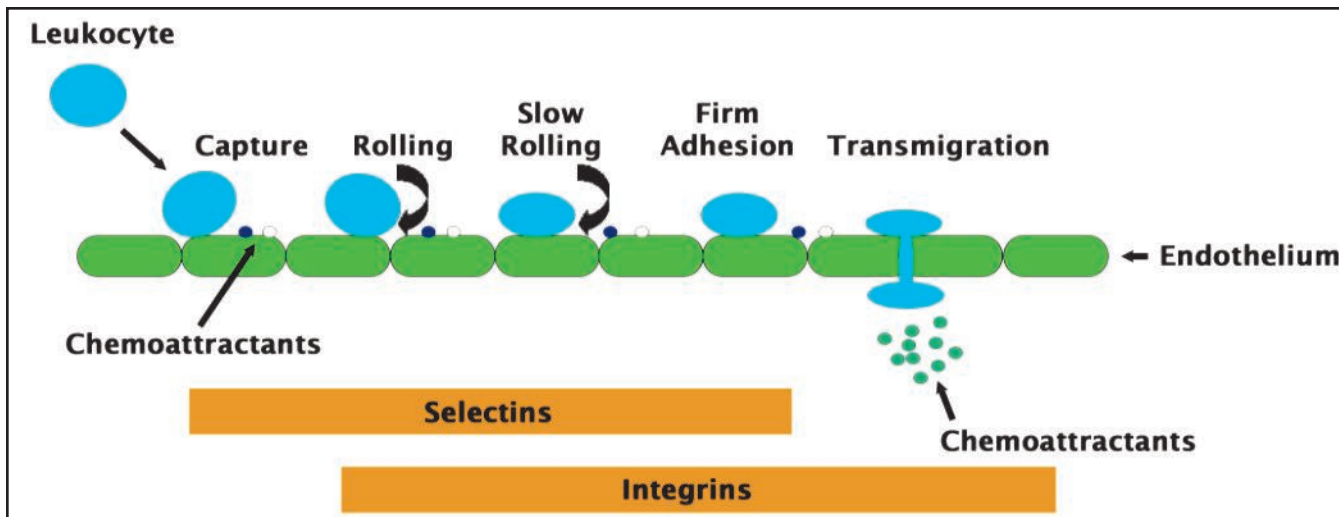


CytoSelect™ 24-well Cell Haptotaxis Assay. MDA-231 cells were seeded at 150,000 cells/well and allowed to migrate toward FBS for 4 hrs. Migratory cells, found on the bottom of the migration membrane, were stained according to the assay protocol.

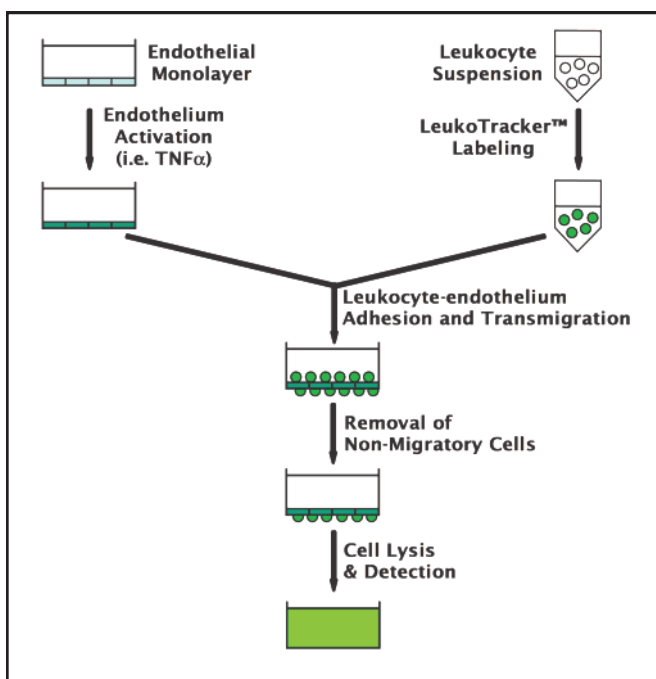
Product Name	Detection	Size	Catalog Number
CytoSelect™ 24-Well Cell Haptotaxis Assay, Collagen I-coated	Colorimetric	12 Assays	CBA-100-COL
	Fluorometric	12 Assays	CBA-101-COL
CytoSelect™ 24-Well Cell Haptotaxis Assay, Fibronectin-coated	Colorimetric	12 Assays	CBA-100-FN
	Fluorometric	12 Assays	CBA-101-FN

CytoSelect™ Cell Migration Assays—Transmigration

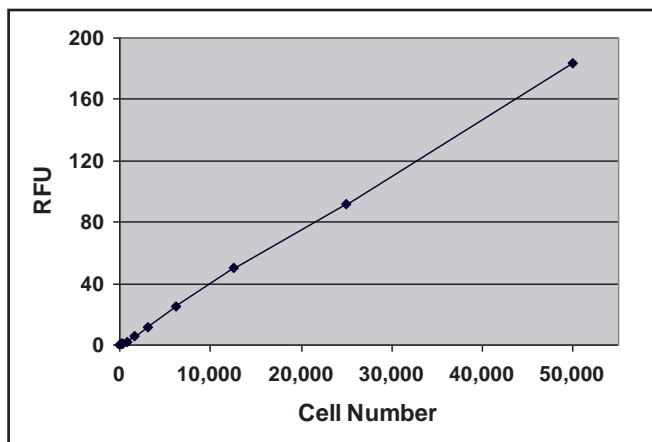
Cancer cell transmigration, particularly extravasation, is an important step in cancer metastasis. The CytoSelect™ Cell Transmigration Assays provide a robust system for the quantitation of trans migrations and interactions between endothelium and cancer cells. Migratory cells are quantified via fluorometer.



The Leukocyte Adhesion and Transmigration Cascade.



Assay Principle for the CytoSelect™ Leukocyte Transmigration Assay.



Quantitation of Human Monocytic THP-1. LeukoTracker™ labeled THP-1 cells were titrated in 1X PBS, then lysed with 2X lysis buffer. Fluorescence was quantified as described in the assay protocol.

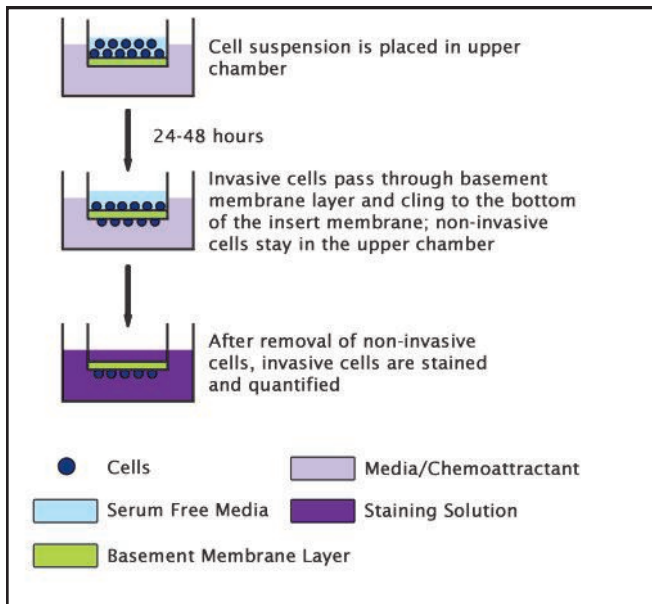
Recent Product Citations

- Giunzioni, I. et al. (2015). Cigarette smoke condensate affects monocyte interaction with endothelium. *Atherosclerosis* **234**:383-390. (CBA-212)
- Park, G.B. et al. (2014). The Epstein-Barr Virus causes epithelial-mesenchymal transition in human corneal epithelial cells via Syk/Src and Akt/ERK signaling pathways. *Invest. Ophthalmol. Vis. Sci.* **55**:1770-1779. (CBA-216)
- Choi, S.H. et al. (2014). MMP9 processing of HSPB1 regulates tumor progression. *PLoS One* **9**:e85509. (CBA-216)

Product Name	Pore Size	Detection	Size	Catalog Number
CytoSelect™ Leukocyte Transmigration Assay	3 μm	Fluorometric	24 Assays	CBA-212
CytoSelect™ Tumor Transendothelial Migration Assay	8 μm	Fluorometric	24 Assays	CBA-216

CytoSelect™ Cell Invasion Assays

Tumor cell invasion into surrounding normal tissue contributes to the morbidity of cancers. The CytoSelect™ Cell Invasion Assays use pre-coated inserts to assay invasive properties of tumor cells in 24-well or 96-well plates. The coated layer serves to distinguish invasive cells from non-invasive cells. Plates are pre-coated with either basement membrane matrix (from EHS mouse sarcoma cells), Collagen I or Laminin I.

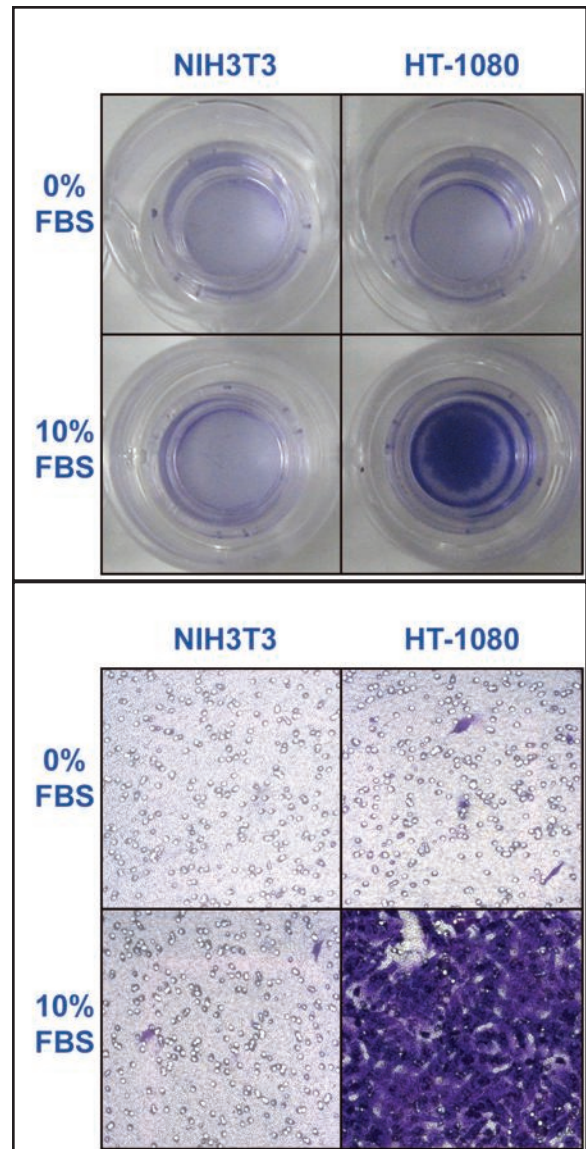


CytoSelect™ Cell Invasion Assay Principle.

Recent Product Citations

- Osawa, Y. et al. (2015). Decreased expression of carbonyl reductase 1 promotes ovarian cancer growth and proliferation. *Int. J. Oncol.* **46**:1252-1258. (CBA-110)
- Hirata, H. et al. (2015). Long noncoding RNA MALAT1 promotes aggressive renal cell carcinoma through Ezh2 and interacts with miR-205. *Cancer Res.* **75**:1322-1331. (CBA-110)
- Cheng X. et al. (2015). LAPTM4B-35, a cancer-related gene, is associated with poor prognosis in TNM stages I-III gastric cancer patients. *PLoS One* **10**:e0121559. (CBA-110)
- Chen, R. et al. (2015). The acetate/ACSS2 switch regulates HIF-2 stress signaling in the tumor cell microenvironment. *PLoS One* **10**:e0116515. (CBA-110)
- Djuzenova, C.S. et al (2015). Actin cytoskeleton organization, cell surface modification and invasion rate of 5 glioblastoma cell lines differing in PTEN and p53 status. *Exp. Cell Res.* **330**:346-357. (CBA-110-COL)
- Adam, M.G.. et al. (2015). SIAH ubiquitin ligases regulate breast cancer cell migration and invasion independent of the oxygen status. *Cell Cycle* **14**:3734-3747. (CBA-112)
- Yamamoto, K. et al. (2014). miR-379/411 cluster regulates IL-18 and contributes to drug resistance in malignant pleural mesothelioma. *Oncol. Rep.* **32**:2365-2372. (CBA-112)
- Takeuchi, S. et al. (2014). Significance of osteopontin in the sensitivity of malignant pleural mesothelioma to pemetrexed. *Int. J. Oncol.* **44**:1886-1894. (CBA-112)
- Ho, P.W. et al. (2015). Knockdown of PTHR1 in osteosarcoma cells decreases invasion and growth and increases tumor differentiation in vivo. *Oncogene* **34**:2922-2933. (CBA-112-COL)

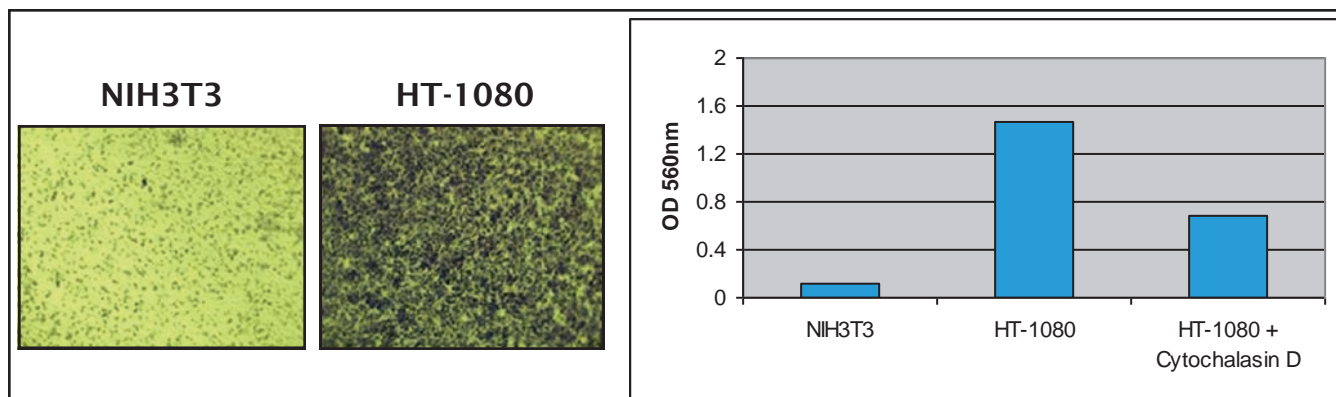
- **Quantitative:** Measure results in a colorimetric or fluorescence plate reader
- **Flexible:** Uniform protein matrix layer of your choice of basement membrane (from mouse tumor cells), Collagen I, or Laminin I
- **Versatile:** Characterize both the invasive and migratory properties of your cells with a Cell Migration / Invasion Combo Kit (next page)



Human Fibrosarcoma HT-1080 Laminin I Cell Invasion.

HT-1080 and NIH3T3 (negative control) were seeded at 200,000 cells/well and allowed to invade toward FBS for 24 hrs. Invasive cells on the membrane bottom were stained (top and center) and quantified at OD 560nm after extraction (data not shown).

CytoSelect™ Cell Invasion Assays, continued



Effects of Cytochalasin D on Invading Cells using the CytoSelect™ 24-well Cell Invasion Assay (CBA-110). HT-1080 and NIH3T3 cells (negative control) were seeded at 300,000 cells/well and allowed to invade toward 10% FBS for 24 hrs, in the presence or absence of 2 μ M Cytochalasin D. Invasive cells, on the bottom of the invasion membrane, were stained (left) and then quantified at OD 560 nm after extraction using a standard plate reader (right).

Product Name	Detection	Size	Catalog Number
CytoSelect™ 24-Well Cell Invasion Assay, Basement Membrane	Colorimetric	12 Assays	CBA-110
	Fluorometric	12 Assays	CBA-111
CytoSelect™ 24-Well Cell Invasion Assay, Collagen I	Colorimetric	12 Assays	CBA-110-COL
	Fluorometric	12 Assays	CBA-111-COL
CytoSelect™ 24-Well Cell Invasion Assay, Laminin I	Colorimetric	12 Assays	CBA-110-LN
	Fluorometric	12 Assays	CBA-111-LN
CytoSelect™ 96-Well Cell Invasion Assay, Basement Membrane	Fluorometric	96 Assays	CBA-112
CytoSelect™ 96-Well Cell Invasion Assay, Collagen I	Fluorometric	96 Assays	CBA-112-COL
CytoSelect™ 96-Well Cell Invasion Assay, Laminin I	Fluorometric	96 Assays	CBA-112-LN

CytoSelect™ Cell Migration / Invasion Assay Combo Kits

Our CytoSelect™ Cell Migration / Invasion Assay Combo Kits allow you to characterize both the migratory and invasive properties of your cells. Each 24-well combo kit provides sufficient reagents to perform 12 migration plus 12 invasion assays, while the 96-well combo kit allows you to perform 96 migration plus 96 invasion assays. The invasion plate provided contains basement membrane-coated inserts.

Recent Product Citations

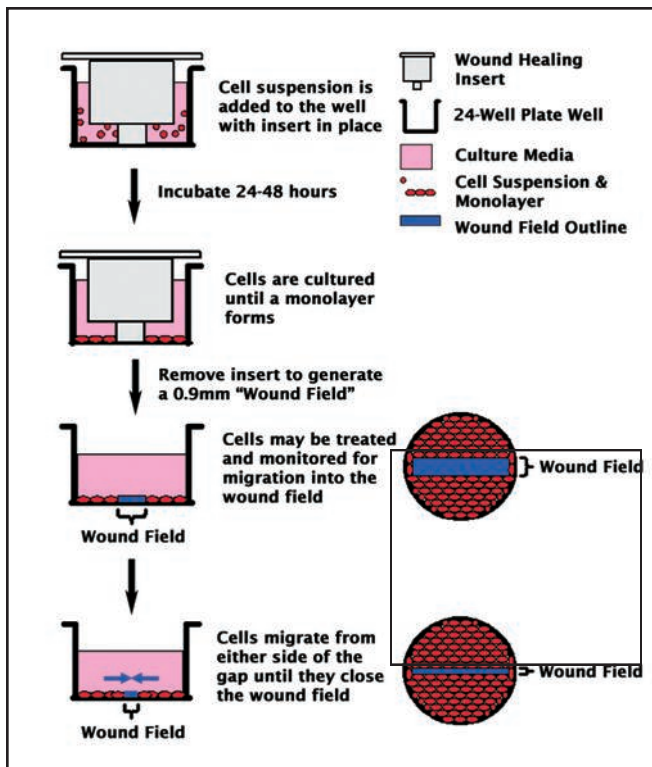
1. Yoo, B. et al. (2015). Combining miR-10b-targeted nanotherapy with low-dose doxorubicin elicits durable regressions of metastatic breast cancer. *Cancer Res.* **75**:4407-4415. (CBA-100-C)
2. Bhansali, M. et al. (2015). TM4SF3 and AR: A nuclear complex that stabilizes both proteins. *Mol. Endocrinol.* 10.1210/me.2015-1075. (CBA-101-C)
3. Zecchini, V. et al. (2015). Nuclear ARRB1 induces pseudohypoxia and cellular metabolism reprogramming in prostate cancer. *EMBO J.* **33**:1365-1382. (CBA-106-C)

Product Name	Pore Size	Detection	Size	Catalog Number
CytoSelect™ 24-Well Cell Migration / Invasion Combo Kit	8 μ m	Colorimetric	2 x 12 Assays	CBA-100-C
			2 x 60 Assays	CBA-100-C-5
		Fluorometric	2 x 12 Assays	CBA-101-C
CytoSelect™ 96-Well Cell Migration / Invasion Combo Kit	8 μ m	Fluorometric	2 x 96 Assays	CBA-106-C

CytoSelect™ 24-Well Wound Healing / Cell Migration Assay

Compared to traditional scratch assays, our CytoSelect™ 24-Well Wound Healing Assay provides a more consistent method to measure cell migration across a “wound field” gap *in vitro*. Proprietary treated inserts generate a consistently defined 0.9mm gap between the cells. Cells can then be treated and monitored for proliferation or migration across the wound field by imaging samples at fixed time points or time-lapse microscopy.

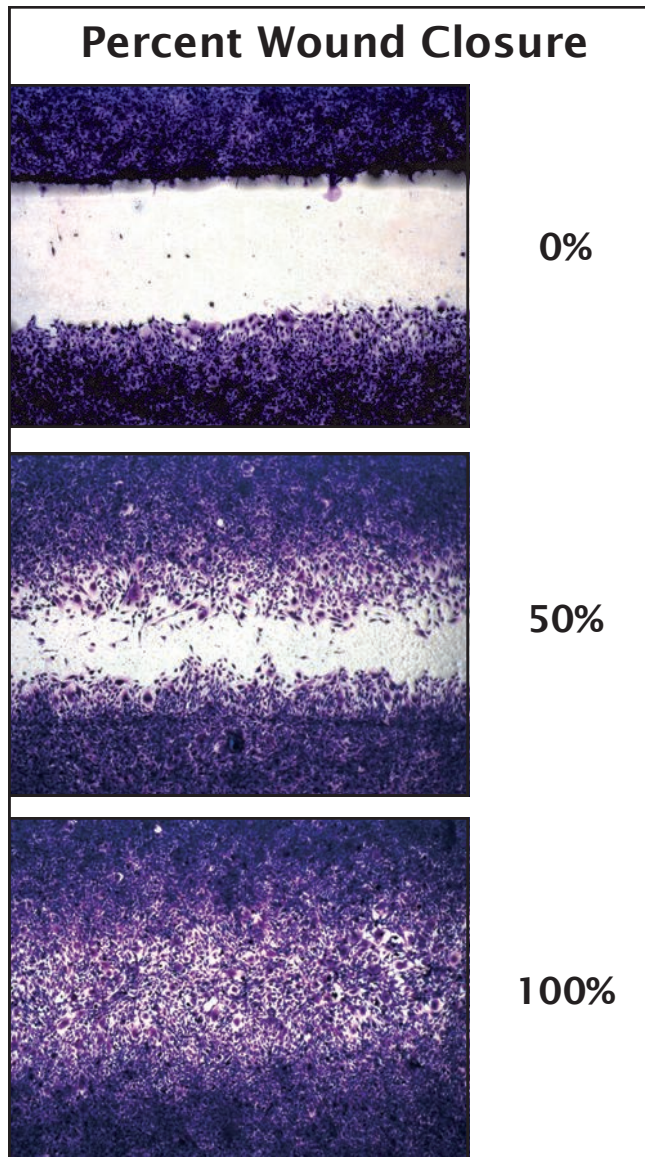
- **Highly Accurate:** More consistent results well-to-well compared to homemade scratch assays
- **Versatile:** Measure cell migration, cell proliferation, and wound closure
- **Inert Material:** No residues from inserts to impede cell migration or proliferation



CytoSelect™ 24-well Wound Healing Assay Principle.

Recent Product Citations

1. Mazumder, A. et al. (2015). In vitro wound healing and cytotoxic effects of sinigrin-phytosome complex. *Int. J. Pharm.* **498**:283-293.
2. Widhe, M. et al. (2015). A fibronectin mimetic motif improves integrin mediated cell binding to recombinant spider silk matrices. *Biomaterials* **74**:256-266.
3. Delalande, A. et al. (2015). Enhanced Achilles tendon healing by fibromodulin gene transfer. *Nanomedicine* **11**:1735-1744.
4. Latifi-Pupovci, H. et al. (2015). In vitro migration and proliferation (“wound healing”) potential of mesenchymal stromal cells generated from human CD271+ bone marrow mononuclear cells. *J. Transl. Med.* **13**:315.
5. Lakatos, K. et al. (2015). Mesenchymal stem cells respond to hypoxia by increasing diacylglycerols. *J. Cell Biochem.* 10.1002/jcb.25292.



Wound Closure of STO Cells. STO cells (mouse MEF) were cultured in the provided plate with inserts in place for 24 hours until a monolayer formed. Inserts were then removed to begin the assay. Cells were monitored at various time points and stained according to the assay protocol.

Product Name	Detection	Size	Catalog Number
CytoSelect™ 24-Well Wound Healing Assay	Microscopy	24 Assays	CBA-120
		5 x 24 Assays	CBA-120-5

CytoSelect™ 24-Well Cell Co-Culture System

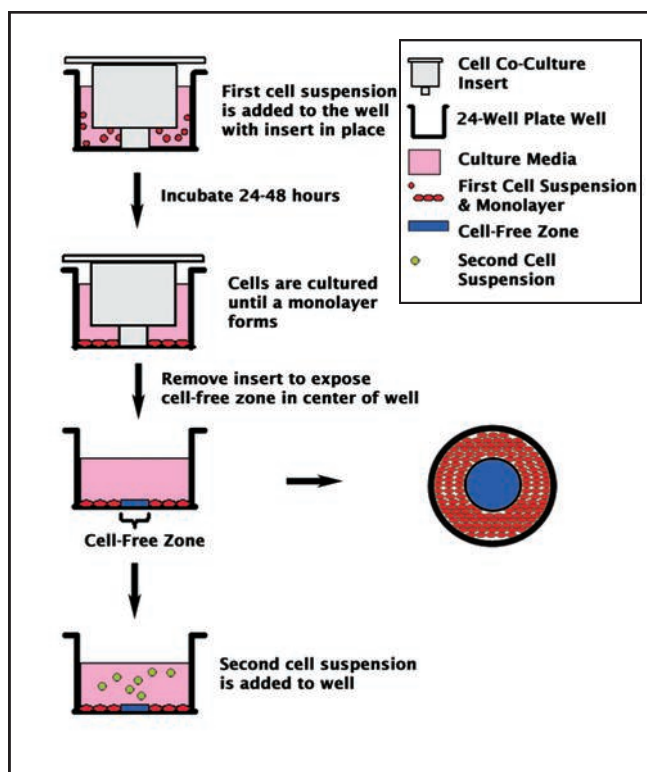
The culture of two cell lines together is advantageous for studying a variety of applications:

- Cell-cell interactions
- Cell activation
- Cellular differentiation
- Maintaining stem cell pluripotency
- Various effects of secreted factors from one cell type on a second cell type

Traditional methods of co-culture usually involve one of the following methods:

1. One cell type is cultured to form a monolayer, followed by seeding of a second cell type directly over the monolayer. This is a common method when feeder cells are used to maintain stem cells in an undifferentiated state. However, it is not useful when studying the effects of one cell on the other because the first cell is obscured from view by the second.
2. A Boyden Chamber (see page 12 for details) is used to culture one cell type above the membrane and a second cell type below the membrane. This system allows a separation between the two cells, but does not allow for direct cell-to-cell contact which may reduce its efficacy for certain applications.

The CytoSelect™ Cell Co-Culture System provides a unique platform for direct contact between two cell types in one well. A proprietary molded plastic insert creates a cell-free zone in the center of a 24-well cell culture-treated plate. The first cell type is seeded in the area around the insert. Once the cells form a monolayer, the insert is removed and the second cell is seeded.



Protocol for the CytoSelect™ 24-Well Co-Culture System. Cell type #1 is seeded with the Co-Culture insert in place. After cells form a monolayer, the insert is removed and cell type #2 is seeded.

Product Name	Detection	Size	Catalog Number
CytoSelect™ 24-Well Cell Co-Culture System	Microscopy	24 Assays	CBA-160
		5 x 24 Assays	CBA-160-5

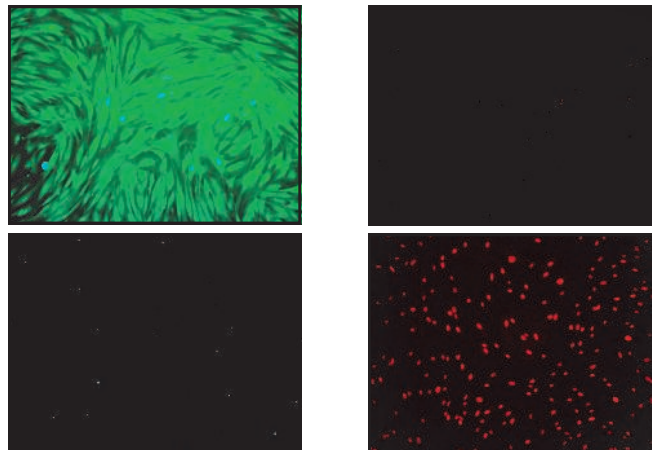
CytoSelect™ Cell Viability and Cytotoxicity Assay (Live/Dead Cells)

Cell viability characteristics include cellular metabolic activity and cell membrane integrity. Our CytoSelect™ Cell Viability and Cytotoxicity Assay provides both a colorimetric and fluorometric format for monitoring cell viability via metabolic activity. Live cells are detected with MTT (colorimetric detection) or Calcein AM (fluorometric); dead cells are detected with EthD-1 reagent (fluorometric). All 3 detection reagents are included, as well as Saponin, a cell death initiator. Cells may be treated with compounds or agents that affect cell viability. This kit is suitable for eukaryotic cells, not bacteria or yeast.

Recent Product Citations

- Hermann, D.M. et al. (2015). Sustained neurological recovery induced by resveratrol is associated with angiogenesis rather than neuroprotection after focal cerebral ischemia. *Neurobiol. Dis.* **83**:16-25.
- Maity, G. et al. (2015). Aspirin blocks growth of breast tumor cells and tumor-initiating cells and induces reprogramming factors of mesenchymal to epithelial transition. *Lab Invest.* 10.1038/labinvest.2015.49.
- Wu, M.Y. et al (2015). MiR-34a regulates therapy resistance by targeting HDAC1 and HDAC7 in breast cancer. *Cancer Lett.* **354**:311-319.

- Versatile:** Detect by microscopy, colorimetric or fluorescence plate reader, or flow cytometry
- Quantitative:** Quantify cells on a colorimetric or fluorescence plate reader



Viability of Human Foreskin Fibroblasts. BJ-TERT cells were allowed to culture for 24 hours, and then treated with and without Saponin. All cells were then stained with Calcein AM and EthD-1. **Top:** Cells without Saponin treatment. **Bottom:** Cells with Saponin treatment. **Left:** Calcein AM staining. **Right:** EthD-1 staining.

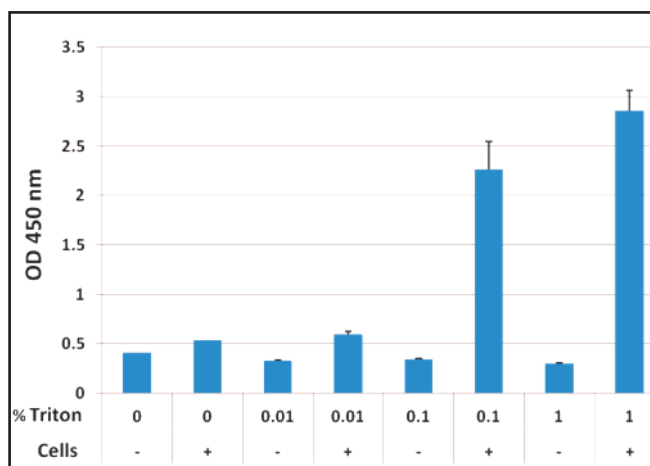
Product Name	Detection	Size	Catalog Number
CytoSelect™ Cell Viability and Cytotoxicity Assay Kit	Colorimetric / Fluorometric	96 Assays	CBA-240

CytoSelect™ LDH Cytotoxicity Assay

Loss of cell membrane integrity is one of the hallmarks of cytotoxicity. Upon cell death, lactate dehydrogenase (LDH) is released from the cytoplasm through the damaged membrane. Our CytoSelect™ LDH Cytotoxicity Assay provides a convenient plate-based method for testing cytotoxicity based on LDH release. In this assay, cells are cultured in a 96-well plate with and without the compound to be tested. LDH released into the media from cells converts a lactate substrate to pyruvate and generates NADH. In the presence of NADH, the colorimetric dye WST-1 is converted to a formazan that generates an orange color which is detected in a colorimetric plate reader.

Recent Product Citations

- Chu, J. et al. (2015). Gamma secretase-activating protein is a substrate for caspase-3: implications for Alzheimer's disease. *Biol. Psychiatry* **77**:720-728.
- Li, J.G. et al. (2014). Homocysteine exacerbates β -amyloid pathology, tau pathology, and cognitive deficit in a mouse model of Alzheimer's disease with plaques and tangles. *Ann. Neurol.* **75**:851-863.



LDH Release from HEK 293 Cells. 20,000 cells/well were cultured for 24 hours. After adding various concentrations of Triton X-100, the LDH Cytotoxicity Assay Reagent was added followed by a 30 minute incubation at 37°C and 5% CO₂.

Product Name	Detection	Size	Catalog Number
CytoSelect™ LDH Cytotoxicity Assay Kit	Colorimetric	960 Assays	CBA-241

Cellular Senescence Assays

Senescence Associated β -galactosidase is a common biochemical marker of cellular senescence. SA β -Gal produces a blue color in senescent cells. We offer three kit formats to test cellular senescence via SA- β -galactosidase activity:

- Our **β -Gal Staining Kit** allows you to visualize senescence by standard light microscope.
- Our **Quantitative Cellular Senescence Assay** measures senescence in cells cultured in a 35mm dish by either flow cytometry or fluorescence microscopy
- Our **96-Well Cellular Senescence Assay** provides a higher throughput assay in a fluorescence plate reader.

Recent Product Citations

1. Gan, W. et al. (2015). ERK5/HDAC5-mediated, resveratrol-, and pterostilbene-induced expression of MnSOD in human endothelial cells. *Mol. Nutr. Food Res.* 10.1002/mnfr.201500466. (CBA-230)
2. Lee, D. H. et al. (2014). Synergistic effect of JQ1 and rapamycin for treatment of human osteosarcoma. *Int. J. Cancer* **136**:2055-2064. (CBA-230)
3. Chang, Z. et al. (2015). Ascorbic acid provides protection for human chondrocytes against oxidative stress. *Mol. Med. Rep.* 10.3892/mmr.2015.4231. (CBA-231)
4. Hu, W. et al (2015). Mechanistic investigation of bone marrow suppression associated with palbociclib and its differentiation from cytotoxic chemotherapies. *Clin. Cancer Res.* 10.1158/1078-0432.CCR-15-1421. (CBA-231 and CBA-232)
5. Kim, J. et al. (2014). p53 induces skin aging by depleting Blimp1+ sebaceous gland cells. *Cell Death Dis.* 5:e1141. (CBA-232)

Product Name	Detection	Size	Catalog Number
Cellular Senescence Assay Kit (SA β -gal Staining)	Light Microscopy	50 Assays	CBA-230
		5 x 50 Assays	CBA-230-5
96-Well Cellular Senescence Assay (SA β -gal Activity)	Fluorometric Plate Reader	120 Assays	CBA-231
		5 x 120 Assays	CBA-231-5
Quantitative Cellular Senescence Assay (SA β -gal)	Flow Cytometry / Fluorescence Microscopy	10 Assays	CBA-232
		5 x 10 Assays	CBA-232-5

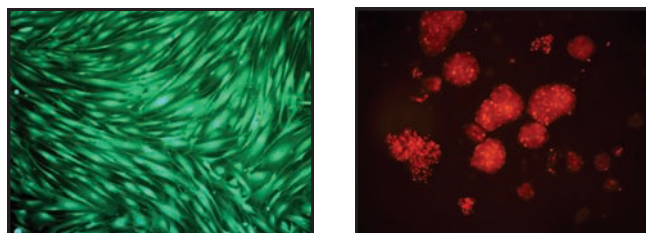
CytoSelect™ Anoikis Assays

Anoikis is defined as death of adherent cells due to loss of adhesion to the extracellular matrix. Our Anoikis Assays allow you to quantify and monitor anchorage-dependent cell death using a precoated plate. Live cells can be viewed under a microscope and quantified on a plate reader by MTT (colorimetric) or Calcein AM (fluorometric), both included with the kit. Dead cells are detected with an EthD-1 reagent.

Recent Product Citations

1. Lee, H.W. et al. (2013). Tpl2 kinase impacts tumor growth and metastasis of clear cell renal cell carcinoma. *Mol. Cancer Res.* **11**:1375-1386. (CBA-080)
2. Sisto, M. et al. (2009). Fibulin-6 expression and anoikis in human salivary gland epithelial cells: implications in Sjogren's syndrome. *Int. Immunol.* **21**:303-311. (CBA-080)
3. Liu, H. et al (2008). Cysteine-rich protein 61 and connective tissue growth factor induce de-adhesion and anoikis of retinal pericytes. *Endocrinology* **149**:1666-1677. (CBA-080)

- **Versatile:** Detect live and dead cells by microscopy, fluorescence, or flow cytometry
- **Quantitative:** Measure live and dead cells on a fluorescence plate reader; live cells may also be quantified on a standard microplate reader



Anoikis of Human Fibroblast BJ-TERT Cells. 50,000 cells/well were seeded in a control plate (left) and a Poly-HEMA coated plate (right) and cultured for 24 hours. Cells on the control plate were stained with Calcein AM. Cells on the Poly-HEMA coated plate were stained with EthD-1.

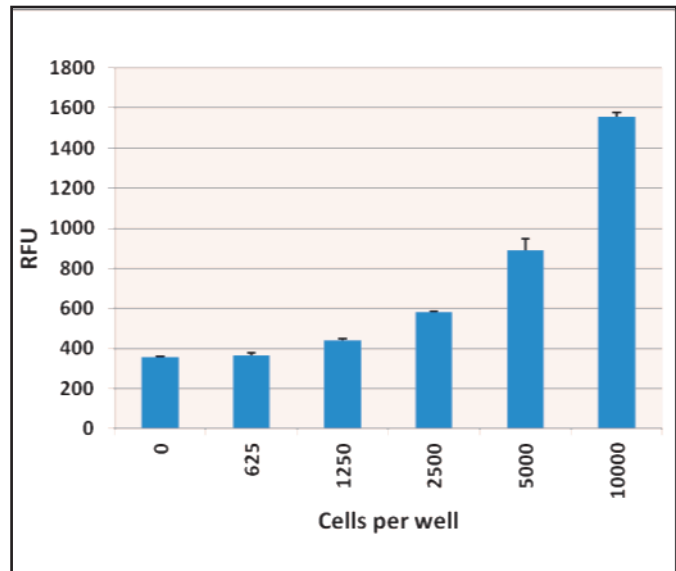
Product Name	Detection	Size	Catalog Number
CytoSelect™ 24-Well Anoikis Assay	Colorimetric / Fluorometric	24 Assays	CBA-080
CytoSelect™ 96-Well Anoikis Assay	Colorimetric / Fluorometric	96 Assays	CBA-081

CytoSelect™ Fluorometric Cell Proliferation Assay Reagent

Cell proliferation is easily measured by the addition of a variety of dyes that can be correlated with the number of cells. Various dyes producing a visible color are available to measure proliferation rates, but fluorometric dyes are often more sensitive and may be a superior choice for researchers with access to a fluorescence-based microplate reader.

Our CytoSelect™ Cell Proliferation Assay Reagent (Fluorometric) provides a simple, single reagent method to measure proliferation of cells. The fluorometric dye is added directly to cultured cells. Upon entering metabolically active live cells, the non-fluorescent dye is converted to a bright red fluorescent form. Quantitation is performed using a fluorescence plate reader with excitation at 560 nm and emission at 590-600 nm.

This reagent is versatile and can be used with a wide variety of cell types including cultured mammalian and piscine cells, bacteria, yeast, fungi, and protozoa.



Human HEK 293 Cell Density. Cells were seeded at various densities in triplicate and allowed to culture for 24 hours. Cells were then treated with the CytoSelect™ Cell Proliferation Assay Reagent for 6 hours at 37°C and 5% CO₂.

Product Name	Detection	Size	Catalog Number
CytoSelect™ Cell Proliferation Assay Reagent, Fluorometric	Fluorometric	960 Assays	CBA-250

CytoSelect™ MTT Cell Proliferation Assay

Cell proliferation is easily measured by the addition of a variety of dyes that produce a visible color that can be correlated with the number of cells. Our CytoSelect™ MTT Cell Proliferation Assay provides a simple method to measure proliferation of cells. The cell-permeable MTT dye is added directly to cultured cells followed by a detergent solution. Quantitation is performed using a standard microplate reader at 540-570 nm.

Recent Product Citations

- Dogan, M. et al. (2015). Are the leading drugs against *Staphylococcus aureus* really toxic to cartilage? *J. Infect. Public Health* 10.1016/j.jiph.2015.10.004.
- Wu, H. et al. (2015). MicroRNA-21 is a potential link between non-alcoholic fatty liver disease and hepatocellular carcinoma via modulation of the HBP1-p53-Srebp1c pathway. *Gut* 10.1136/gutjnl-2014-308430.
- Ren, Z. et al. (2014). Anti-tumor effect of a novel soluble recombinant human endostatin: administered as a single agent or in combination with chemotherapy agents in mouse tumor models. *PLoS One* 9:e107823.

Product Name	Detection	Size	Catalog Number
CytoSelect™ MTT Cell Proliferation Assay	Colorimetric	960 Assays	CBA-252

CytoSelect™ WST-1 Cell Proliferation Assay Reagent

Our CytoSelect™ WST-1 Cell Proliferation Assay provides a similar method to our MTT Cell Proliferation Assay, but with a single reagent format that does not require a detergent solubilization step. Quantitation is performed using a standard microplate reader at 450 nm.

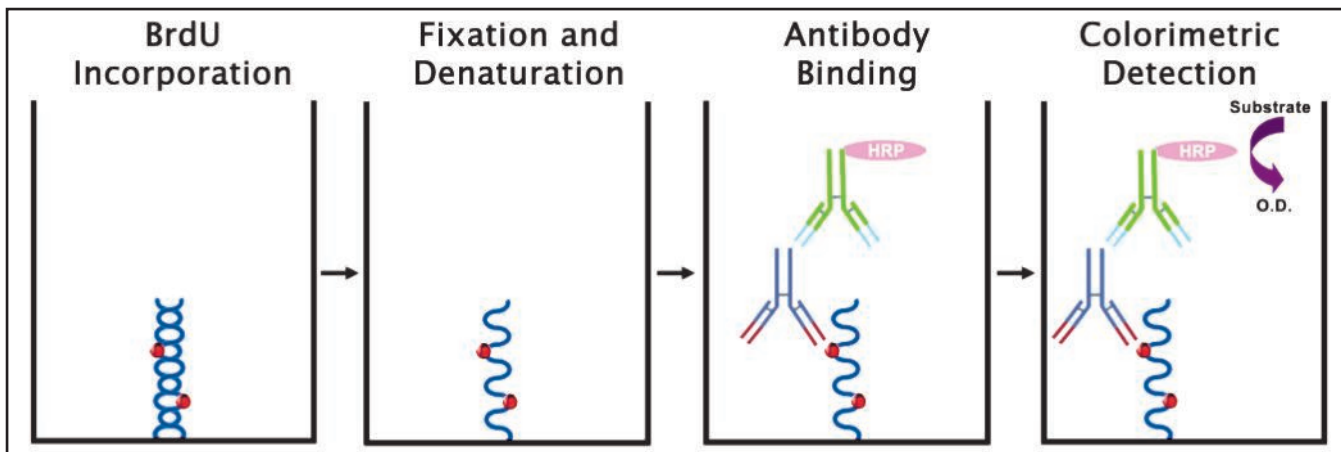
Product Name	Detection	Size	Catalog Number
CytoSelect™ WST-1 Cell Proliferation Assay Reagent	Colorimetric	960 Assays	CBA-253

CytoSelect™ BrdU Cell Proliferation ELISA Kit

BrdU is a thymidine analog that can incorporate into newly synthesized DNA strands of actively proliferating cells. Our CytoSelect™ BrdU Cell Proliferation ELISA Kit provides a convenient plate-based method to measure this incorporation. Once the BrdU is incorporated into the DNA, cells are fixed and DNA is denatured. Incorporated BrdU can be quantified in the denatured DNA by an anti-BrdU antibody.

Recent Product Citations

1. Kreiseder, B. et al. (2015). Alpha-catulin contributes to drug-resistance of melanoma by activating NF-kappaB and AP-1. *PLoS One* **10**:e0119402.
2. Hatzis, C. et al. (2014). Enhancing reproducibility in cancer drug screening: how do we move forward? *Cancer Res.* **74**:4016-4023.



Assay Principle for the CytoSelect™ BrdU Cell Proliferation ELISA Kit.

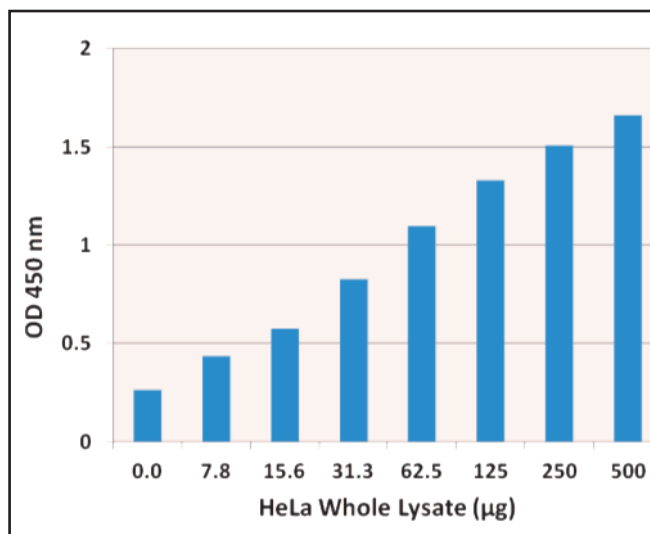
Product Name	Detection	Size	Catalog Number
CytoSelect™ BrdU Cell Proliferation ELISA Kit	Colorimetric	96 Assays	CBA-251

CytoSelect™ Proliferating Cell Nuclear Antigen (PCNA) ELISA Kit

Proliferating Cell Nuclear Antigen (PCNA) acts as a processivity factor for DNA polymerase by associating with various proteins involved in DNA replication. It is also associated with chromatin remodeling and cell cycle control, and it is often used as a marker of cell proliferation.

Our CytoSelect™ PCNA ELISA Kit provides a convenient plate-based method to quantify PCNA levels in nuclear or whole cell extracts.

- **Sensitive:** Detect PCNA as low as 12.5 ng/mL
- **Versatile:** Measure PCNA levels from human, mouse, or rat whole cell lysates or nuclear extracts
- **Quantitative:** Measure results in a colorimetric plate reader against a provided PCNA standard



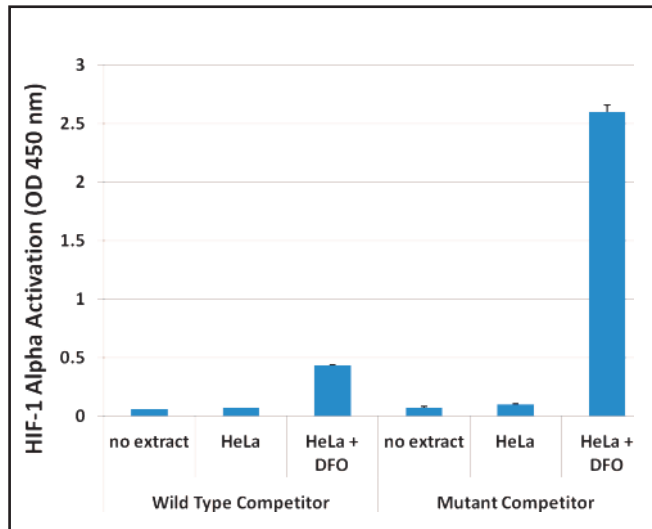
PCNA Detection in HeLa Whole Cell Lysates. Whole cell lysates were prepared in a RIPA lysis buffer. Protein concentrations were determined by BCA protein assay.

Product Name	Detection	Size	Catalog Number
CytoSelect™ Proliferating Cell Nuclear Antigen (PCNA) ELISA Kit	Colorimetric	96 Assays	CBA-254

HIF-1 Alpha DNA Binding Activity Assay Kit

Cell hypoxia, or low oxygen condition, is a normal physiological response to certain body stressors such as high altitudes, but it can also be a symptom of pathological conditions and is often used as a marker for tumor cells. In response to hypoxic conditions, the hypoxia-inducible factor 1 transcriptional activator complex (HIF-1) plays a role in activating several hypoxia-responsive genes such as erythropoietin and VEGF. During hypoxia, the alpha subunit of HIF-1 accumulates and translocates from the cytosol to the nucleus, where it dimerizes with the beta subunit and becomes transcriptionally active. It then binds transcriptional coactivators to induce gene expression.

The HIF-1 Alpha DNA Binding Activity Assay Kit detects activated HIF-1 in an ELISA format. Active HIF-1 complex is captured on a double-stranded oligo containing a hypoxic response element (HRE) that is attached to the plate. Detection is then performed with a primary antibody followed by an HRP-conjugated secondary antibody. The assay will detect HIF-1 complexes from human, mouse or rat protein samples.



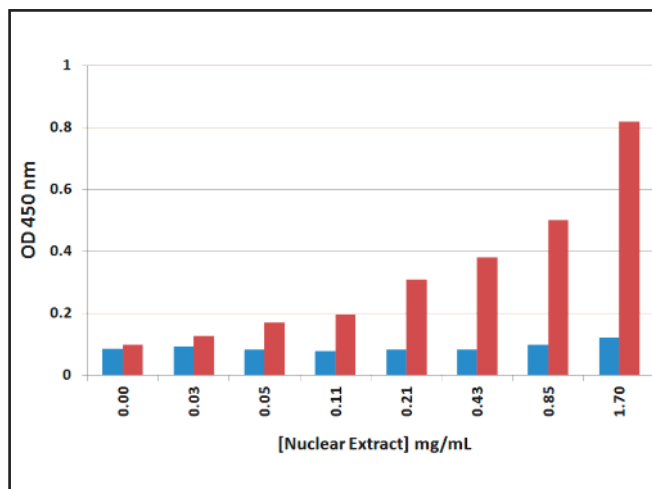
Detection Specificity of HIF-1 Alpha. HeLa cells were incubated in the presence or absence of 0.2 mM deferoxamine mesylate (DFO) for 4 hours at 37°C. Nuclear extracts were prepared using the Nuclear/Cytosolic Fractionation Kit (#AKR-171). 100 pmol of non-biotinylated wild type or mutated HRE double stranded competitor oligos were added to the Complete DNA Binding Buffer just prior to inclusion in the assay.

Product Name	Detection	Size	Catalog Number
HIF-1 Alpha DNA Binding Activity Assay Kit	Colorimetric	96 Assays	CBA-282

HIF-1 Alpha ELISA Kits

Our HIF-1 Alpha ELISA Kits provide a convenient method for detection and quantitation of human, mouse, or rat HIF-1 Alpha in cells or tissues. Two ELISA kit formats are available:

- The HIF-1 Alpha Sandwich ELISA Kit detects HIF-1 Alpha in any protein sample including tissue homogenates, whole cell lysates, or nuclear extracts. Samples are added to an anti-HIF-1 Alpha antibody coated plate. Quantitation of unknown samples is performed by comparison of the OD values to those of a known standard.
- The HIF-1 Alpha Cell Based ELISA Kit allows the detection of HIF-1 Alpha levels in intact cells. Cells are seeded in a tissue culture treated plate suitable for reading in a 96-well plate-based luminescence meter. Cells are fixed and permeabilized to allow detection with the anti-HIF-1 antibody. Detection is performed by chemiluminescence.



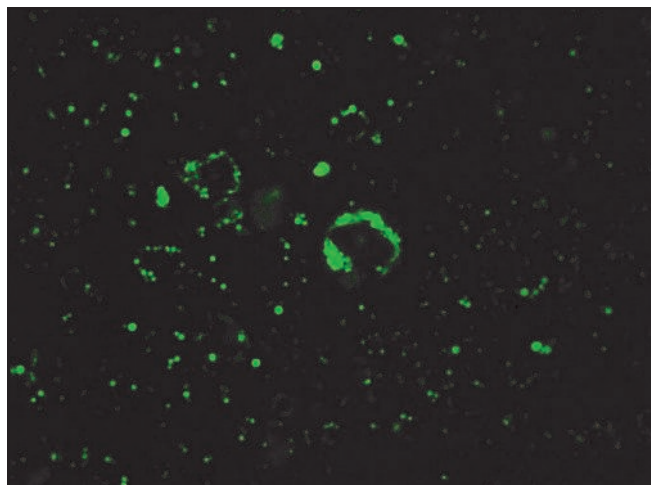
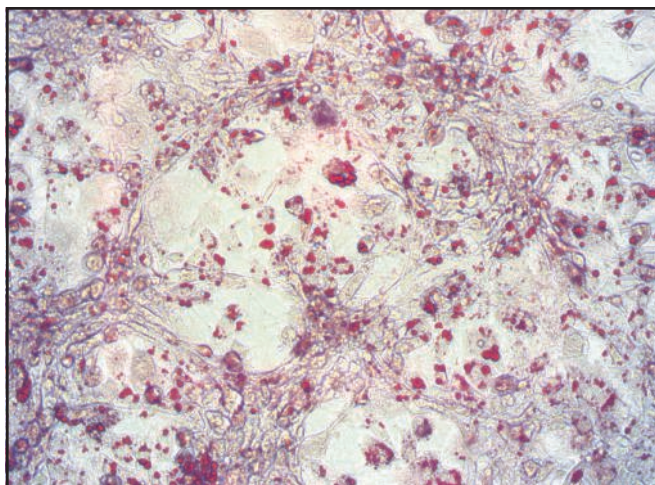
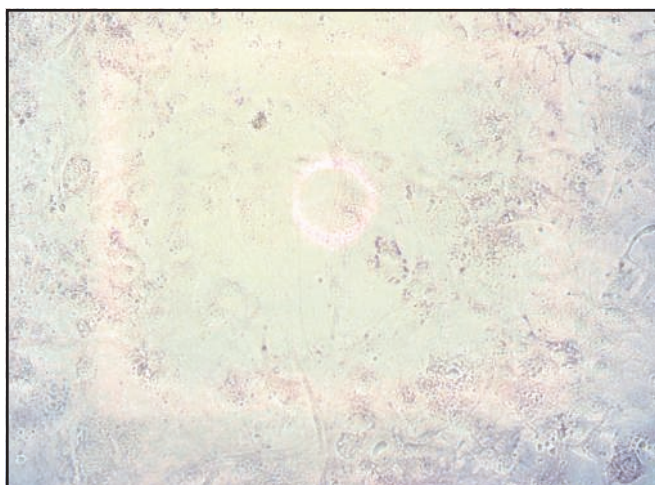
Detection of Nuclear HIF-1 Alpha with the HIF-1 Alpha Sandwich ELISA Kit. HeLa cells were incubated in the presence or absence of 0.2 mM DFO for 4 hours at 37°C. HIF-1 Alpha levels were measured in untreated (blue bars) and treated (red bars) nuclear extracts according to the Assay Protocol.

Product Name	Detection	Size	Catalog Number
HIF-1 Alpha Sandwich ELISA Kit	Colorimetric	96 Assays	CBA-280
HIF-1 Alpha Cell Based ELISA Kit	Chemiluminescent	96 Assays	CBA-281

CytoSelect™ 96-well Adipogenesis Assay Kit

The ability to regulate the cell cycle and differentiation of adipocytes is important to the understanding of obesity. Adipogenesis is the process in which preadipocytes develop into mature adipocytes in a multistep process that requires the sequential activation of numerous transcription factors. The 3T3-L1 cell line is the best characterized model for adipogenesis *in vitro*. 3T3-L1 cells display a fibroblast-like phenotype when grown under normal conditions. However, when treated with a combination of IBMX, insulin, and dexamethasone, these cells undergo terminal differentiation resulting in a more rounded phenotype and the formation of intracellular lipid droplets.

The CytoSelect™ 96-Well Adipogenesis Assay quantitatively measures lipid droplet accumulation in cultured cells of the 3T3-L1 model. Quantitation is performed either in a standard colorimetric plate reader with Oil Red O stain, or in a fluorescence plate reader with Nile Red fluorometric stain.



Staining of 3T3-L1 Cells with Oil Red O. 20,000 cells/well of preadipocyte 3T3-L1 cells were seeded overnight in a 96-well plate. Cells were uninduced (top) or induced (bottom) for 7 days and stained with Oil Red O colorimetric stain according to the Assay Protocol.

Staining of 3T3-L1 Cells with Nile Red Fluorescent Stain. 20,000 cells/well of preadipocyte 3T3-L1 cells were seeded overnight in a 96-well plate. Cells were uninduced (top) or induced (bottom) for 7 days and stained with Nile Red Fluorescent Stain according to the Assay Protocol.

Product Name	Detection	Size	Catalog Number
CytoSelect™ 96-Well Adipogenesis Assay Kit	Colorimetric / Fluorometric	200 Assays	CBA-290

CytoSelect™ 96-Well Phagocytosis Assays

Phagocytosis may be assayed by measuring the engulfing of a cell “substrate” such as an erythrocyte (RBC) or Zymosan particle. Traditional phagocytosis assays involve manually counting the engulfed substrates under a microscope. This process is tedious and time-consuming, can be somewhat inaccurate, and is not amenable to high throughput.

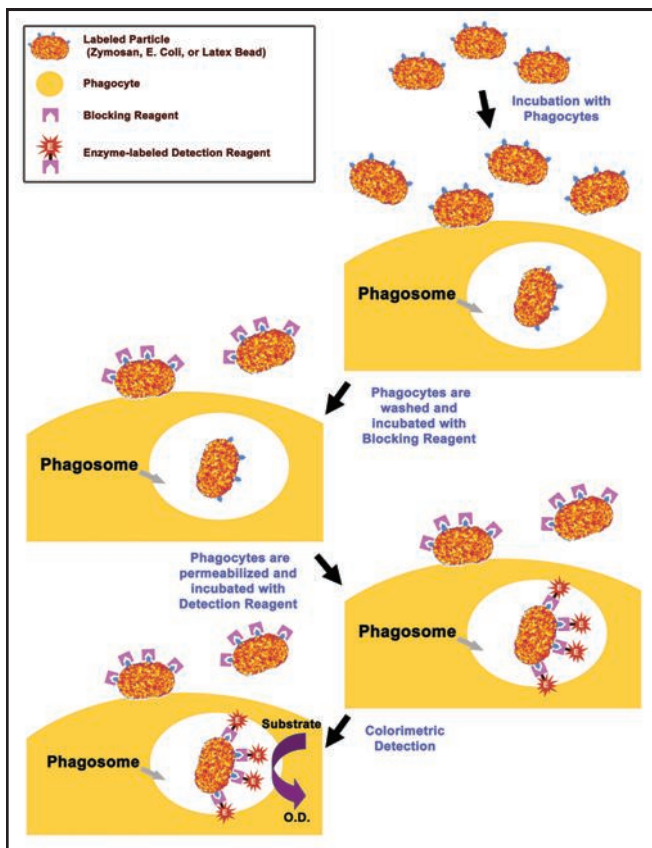
CytoSelect™ 96-Well Phagocytosis Assays are more accurate, high-throughput alternatives to the standard phagocytosis assay. The assays may be adapted for use in 48-well and 24-well plates if desired.

- **Highly Accurate:** Eliminates manual counting
- **High Throughput:** 96-well plate format
- **Quantitative:** Measure OD in a standard microplate reader
- **Flexible:** Choose from 3 substrates: E. coli, Zymosan particles, or red blood cells*

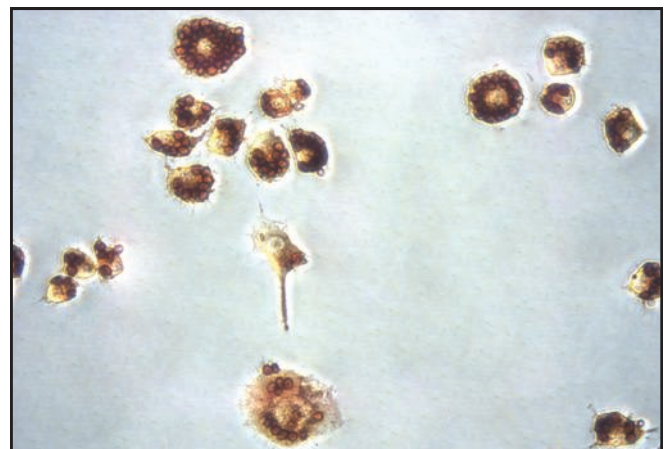
*Red blood cells are not provided in the kit. Fresh RBCs should be obtained immediately prior to running the assay. E. coli and Zymosan particles are provided in their respective kits.

Recent Product Citations

1. Yu, Z. et al. (2015). Therapeutic concentration of lithium stimulates complement C3 production in dendritic cells and microglia via GSK-3 inhibition. *Glia* **63**:257-270. (CBA-220)
2. Park, S.Y. et al. (2014). Immunostimulatory effect of fermented red ginseng in the mouse model. *Prev. Nutr. Food Sci.* **19**:10-18. (CBA-220)
3. Martin, I. et al. (2015). Fasciola hepatica fatty acid binding protein inhibits TLR4 activation and suppresses the inflammatory cytokines induced by lipopolysaccharide in vitro and in vivo. *J. Immunol.* 10.4049/jimmunol.1401182. (CBA-222)
4. Zhu, X. et al. (2014). Deletion of class A scavenger receptor deteriorates obesity-induced insulin resistance in adipose tissue. *Diabetes* **63**:562-577. (CBA-222)
5. Lee, S.G. et al. (2015). Immunostimulatory polysaccharide isolated from the leaves of Diospyros kaki Thumb modulate macrophage via TLR2. *Int. J. Biol. Macromol.* **79**:971-982. (CBA-224)
6. Zhang, H. et al. (2015). Functional analysis and transcriptomic profiling of iPSC-derived macrophages and their application in modeling Mendelian disease. *Circ. Res.* 10.1161/CIRCRESAHA.117.305860. (CBA-224)



Assay Principle for the CytoSelect™ 96-Well Phagocytosis Assay (Zymosan).



Particle Engulfment with the CytoSelect™ 96-Well Phagocytosis Assay (Zymosan).

Product Name	Detection	Size	Catalog Number
CytoSelect™ 96-Well Phagocytosis Assay (E. coli)	Colorimetric	96 Assays	CBA-222
CytoSelect™ 96-Well Phagocytosis Assay (Red Blood Cell)	Colorimetric	96 Assays	CBA-220
CytoSelect™ 96-Well Phagocytosis Assay (Zymosan)	Colorimetric	96 Assays	CBA-224
		5 x 96 Assays	CBA-224-5

CytoSelect™ Cell Contraction Assay Kits (Floating Matrix Model)

The wound healing process is comprised of epithelialization, connective tissue deposition, and contraction. The contraction process is believed to be mediated by specialized fibroblasts (myofibroblasts). 3D collagen gels have been widely used in fibroblast contraction studies.

Various culture models are available to study the ability of fibroblasts to reorganize and contract collagen matrices in vitro. In the floating matrix model, a freshly polymerized collagen matrix containing cells is released from the culture dish and allowed to float in culture medium. Contraction occurs in the absence of external mechanical load and without appearance of stress fibers in the cells.

The CytoSelect™ Cell Contraction Assay Kits (Floating Matrix Model) provide a simple system to assess cell contractivity and to screen for cell contraction mediators. The proprietary Cell Contraction Plate eliminates the matrix releasing step of the conventional attached model assay, providing a faster, higher-throughput method to assess cell contraction. Kits are available in 24-well and 48-well formats.



Contraction Inhibition by BDM. 5×10^5 COS-7 cells in 0.5 mL collagen gel lattice were cultured for two days according to the Assay Protocol. Dashed lines indicate the gel edges.

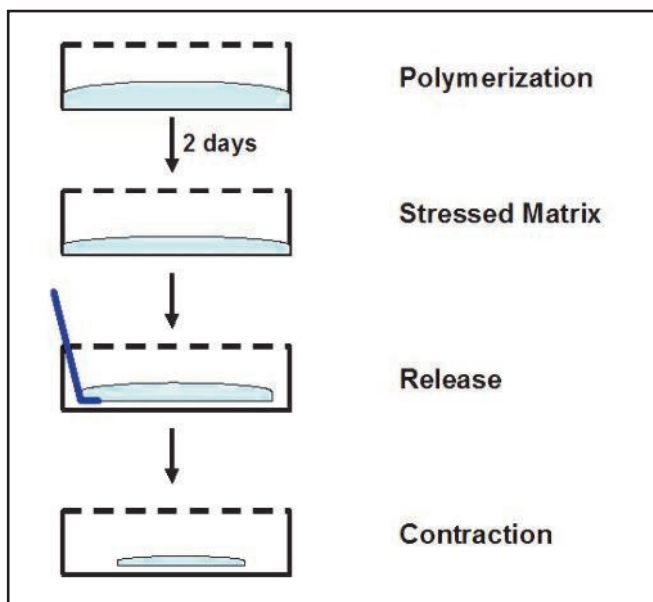
Product Name	Detection	Size	Catalog Number
CytoSelect™ 24-Well Cell Contraction Assay	Light Microscopy	24 Assays	CBA-5020
CytoSelect™ 48-Well Cell Contraction Assay	Light Microscopy	48 Assays	CBA-5021

Collagen-Based Cell Contraction Assay (Two-Step Attached Model)

Our Cell Contraction Assay (Attached Model) provides a simple system to assess cell contractivity and to screen for cell contraction mediators. The system uses a 3D collagen matrix to measure changes in the collagen gel size. An optional contraction inhibitor is provided.

Recent Product Citations

- Ye, Y. et al. (2016). Down-regulation of 14-3-3 Zeta inhibits TGF- β 1-induced actomyosin contraction in human trabecular meshwork cells through RhoA signaling pathway. *Invest. Ophthalmol. Vis. Sci.* **57**:71.
- Rinella, L. et al. (2016). Extracorporeal shockwaves modulate myofibroblast differentiation of adipose-derived stem cells. *Wound Repair Regen.* 10.1111/wrr.12410.
- Halim, D. et al. (2015). ACTG2 variants impair actin polymerization in sporadic Megacystis Microcolon Intestinal Hypoperistalsis Syndrome. *Hum. Mol. Genet.* 10.1093/hmg/ddv497.
- Li, H.Y. et al. (2015). Activation of TGF- β 1-CD147 positive feedback loop in hepatic stellate cells promotes liver fibrosis. *Sci. Rep.* **5**:16552.
- Duru, N. et al. (2015). NRF2/miR-140 signaling confers radio-protection to human lung fibroblasts. *Cancer Lett.* 10.1016/j.canlet.2015.08.011.
- Gutierrez, J. et al. (2015). RECK-mediated β 1-integrin regulation by TGF- β 1 is critical for wound contraction in mice. *PLoS One* **10**:e0135005.



Assay Principle for the Collagen-Based Cell Contraction Assay (Attached Model).

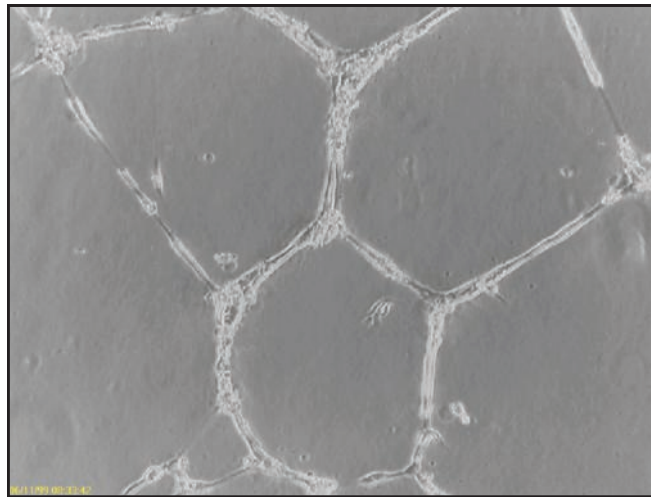
Product Name	Detection	Size	Catalog Number
Cell Contraction Assay	Light Microscopy	24 Assays	CBA-201

Endothelial Tube Formation (*In Vitro* Angiogenesis) Assay

For angiogenesis to occur, endothelial cells must escape their stable location and break through the basement membrane. These cells proliferate to form new blood vessels. Our Endothelial Tube Formation Assay provides an easy, robust system to assess angiogenesis *in vitro*. The assay uses an ECM gel matrix derived from mouse sarcoma cells; this matrix very closely resembles an *in vivo* basement membrane environment.

Recent Product Citations

- Zheng, D. et al. (2015). Silencing of miR-195 reduces diabetic cardiomyopathy in C57BL/6 mice. *Diabetologia* 10.1007/s00125-015-3622-8.
- Bae, W. J. et al. (2015). Effects of sodium tri- and hexameta-phosphate on proliferation, differentiation, and angiogenic potential of human dental pulp cells. *J. Endod.* 10.1016/j.joen.2015.01.038.
- Zhang, J. et al. (2015). Effects of bioactive cements incorporating zinc-bioglass nanoparticles on odontogenic and angiogenic potential of human dental pulp cells. *J. Biomater. Appl.* 29:954-964.
- Yamanegi, K. et al. (2015). Sodium valproate, a histone deacetylase inhibitor, modulates the vascular endothelial growth inhibitor-mediated cell death in human osteosarcoma and vascular endothelial cells. *Int. J. Oncol.* 10.3892/ijo.2015.2924.



HUVEC Tube Formation on ECM Gel. HUVEC cells from a standard tissue culture plate were incubated on an ECM gel. After several hours tube formation can be visualized under a light microscope.

Product Name	Detection	Size	Catalog Number
Endothelial Tube Formation Assay (<i>In Vitro</i> Angiogenesis)	Light Microscopy	50 Assays	CBA-200

GFP-LC3 Expression Vectors

Our GFP-LC3 expression vectors are convenient tools for the study of autophagy. These vectors are available in three formats: mammalian, lentiviral, and retroviral expression vectors. Each vector contains a GFP reporter gene. A GFP control plasmid is provided at no additional charge.

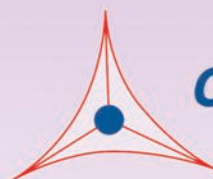
Recent Product Citations

- Yao, F. et al. (2015). Apelin-13 impedes foam cell formation by activating class III PI3K/Beclin-1-mediated autophagic pathway. *Biochem. Biophys. Res. Commun.* 10.1016/j.bbrc.2015.09.045. (CBA-401)
- Pi, H. et al. (2015). SIRT3-SOD2-mROS-dependent autophagy in cadmium-induced hepatotoxicity and salvage by melatonin. *Autophagy* 11:1037-1051. (CBA-401)
- He, Z. et al. (2015). Atorvastatin induces autophagic cell death in prostate cancer cells in vitro. *Mol. Med. Rep.* 10.3892/mmr.2015.3334. (CBA-401)
- Li, B.H. et al. (2014). TRPV1 activation impedes foam cell formation by inducing autophagy in oxLDL-treated vascular smooth muscle cells. *Cell Death Dis.* 5:e1182. (CBA-401)
- Meng, X. et al. (2014). Attenuation of A β 254-35-induced parallel autophagic and apoptotic cell death by gypenoside XVII through the estrogen receptor-dependent activation of Nrf2/ARE pathways. *Toxicol. Appl. Pharmacol.* 279:63-75. (CBA-401)
- Chen, W. et al. (2012). Andrographolide induces autophagic cell death in human liver cancer cells through cyclophilin D-mediated mitochondrial permeability transition pore. *Carcinogenesis* 10.1093/carcin/bgs264. (CBA-401)
- Cina, D.P. et al. (2012). Inhibition of MTOR disrupts autophagic flux in podocytes. *J. Am. Soc. Nephrol.* 23:412-420. (CBA-401)
- Tu, S.P. et al. (2011). IFN-gamma inhibits gastric carcinogenesis by inducing epithelial cell autophagy and T-cell apoptosis. *Cancer Res.* 71:4247-4259. (CBA-401)

Product Name	Size	Catalog Number
pCMV-GFP-LC3 Expression Vector	100 μ L	CBA-401
pSMPUW-GFP-LC3 Lentiviral Expression Vector	10 μ g	LTV-801
pMXs-GFP-LC3 Retroviral Expression Vector	10 μ g	RTV-801

Stem Cell Research

iPS Cell Reprogramming	32
Retroviral Expression Systems for Gene Delivery into Stem Cells	34
Stem Cell Feeders	35
Hematopoietic Colony Forming Cell Assay	36
Stem Cell Colony Formation Assay	37
Alkaline Phosphatase Assays	38
Stem Cell PCR Primer Set	38



CELL BIOLABS, INC.

Creating Solutions for Life Science Research

iPS Cell Reprogramming

Reprogramming of adult cells into induced pluripotent stem cells (iPS) has provided an important new vehicle to facilitate stem cell research. Recent studies have shown that this may be accomplished by the introduction of key genes into somatic cells by transduction with various viral vectors or transfection of plasmids.

Retroviral and lentiviral vectors appear to achieve among the highest levels of efficiency of iPS cell generation. We offer an extensive collection of vectors for iPS cell reprogramming.

Retroviral Vectors and Packaging Cells for iPS Cell Generation

Our iPS retroviral vectors are constructed from the pMXs vector backbone developed by Dr. Toshio Kitamura at the University of Tokyo.* Each vector contains one of 6 factors shown to help reprogram adult fibroblasts into iPS cells. Both human and mouse genes are available individually or in sets. Separate retroviral vectors are available for p53 shRNA, which has been shown to potentially increase the efficiency of iPS cell generation.

Platinum Retroviral Packaging Cells provide an easy way to produce high-titer retroviruses from these stem cell plasmids. For additional information on these cell lines please see [p. 63](#).

*Kitamura, T. et al. (2003). *Exp. Hematol.* 31:1007-1014.

Human iPS Vectors

Target Name	Vector Backbone	Catalog Number
Oct-3/4	pMXs	RTV-701
Sox2	pMXs	RTV-702
c-Myc	pMXs	RTV-703
Klf4	pMXs	RTV-704
NANOG	pMXs	RTV-709
Lin28	pMXs	RTV-710
Set of 4 vectors (Oct-3-4, Sox2, c-Myc, Klf4)	pMXs	RTV-701-C
Set of 6 vectors (Oct-3-4, Sox2, c-Myc, Klf4, NANOG, Lin28)	pMXs	RTV-709-C
p53 shRNA	pRetro	RTV-410

Mouse iPS Vectors

Target Name	Vector Backbone	Catalog Number
Oct-3/4	pMXs	RTV-705
Sox2	pMXs	RTV-706
c-Myc	pMXs	RTV-707
Klf4	pMXs	RTV-708
NANOG	pMXs	RTV-711
Lin28	pMXs	RTV-712
Set of 4 vectors (Oct-3-4, Sox2, c-Myc, Klf4)	pMXs	RTV-705-C
Set of 6 vectors (Oct-3-4, Sox2, c-Myc, Klf4, NANOG, Lin28)	pMXs	RTV-711-C
p53 shRNA	pRetro	RTV-400

Retroviral Packaging Cell Lines

Product Name	Size	Catalog Number
Platinum-E Retroviral Packaging Cell Line, Ecotropic	$\geq 3 \times 10^6$ cells	RV-101
Platinum-A Retroviral Packaging Cell Line, Amphotropic	$\geq 3 \times 10^6$ cells	RV-102
Platinum-GP Retroviral Packaging Cell Line, Pantropic	$\geq 3 \times 10^6$ cells	RV-103
pCMV-VSV-G Packaging Vector (for use with Platinum-GP cells)	10 μ g	RV-110

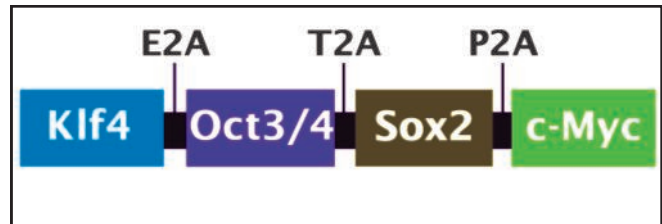
Polycistronic Vectors for iPS Cell Generation

Our Polycistronic Viral Vectors provide a convenient way to generate iPS cells. The defined stem cell factors Klf4, Oct-3/4, Sox2 and c-Myc are in-frame fused into a single open reading frame (ORF) by self-cleaving 2A peptides. The transcription factor ORF is followed by IRES-GFP as a reporter to verify viral transduction into your target cell. Efficiencies of iPS generation are typically higher compared to transduction of four separate viruses each containing a single gene.

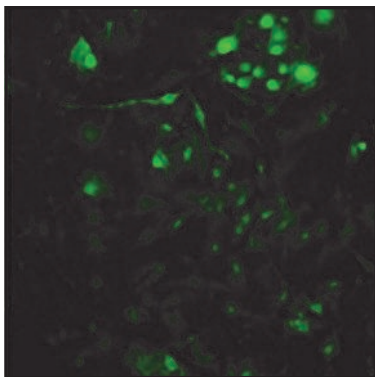
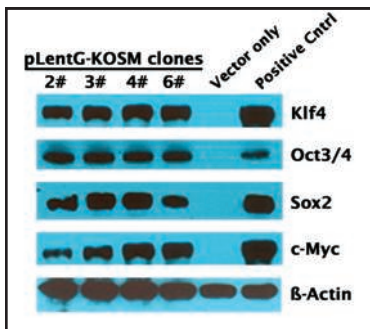
Two vectors are available:

- pLentG-KOSM is a lentiviral vector containing mouse sequences
- pRetroG-OKSM is a retroviral vector containing human sequences

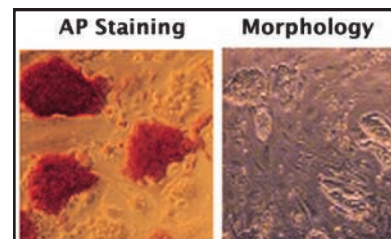
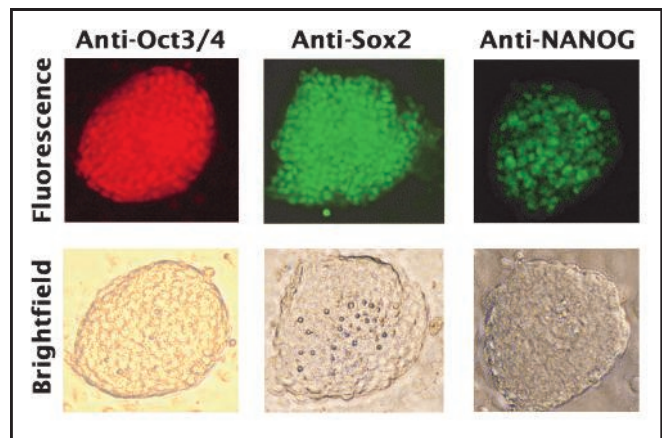
- **More Efficient:** Up to 10-fold higher efficiency compared to multi-virus transduction, and 500-fold compared to non-viral methods
- **Reporter Convenience:** GFP reporter gene helps to monitor viral transduction



Open Reading Frame of pLentG-KOSM Lentiviral Vector.



Expression of Stem Cell Factors and GFP. **Top:** Transient expression of KOSM fusion gene in 293T cells confirmed by Western blot. **Bottom:** GFP fluorescence in MEF cells 3 days after infection with lentivirus containing KOSM fusion.



Characterization of iPS Cell Colonies Generated from MEFs Infected with Lentivirus Containing the KOSM Fusion. **Top:** Staining of pluripotency markers in induced cell colonies at 200x magnification. **Bottom:** AP staining at 100x magnification and morphology at 40x magnification in induced cell colonies.

Product Name	Size	Catalog Number
pLentG-KOSM Polycistronic Lentiviral Vector (Mouse genes)	100 μ L	LTV-700
pRetroG-OKSM Polycistronic Retroviral Vector (Human genes)	100 μ L	RTV-700

For efficient packaging of your virus, please see our Lentiviral Packaging Systems on **p. 58** and Retroviral Packaging Cell Lines on **p. 63 and 66**.

Platinum Retroviral Expression Systems for Stem Cells

Retroviral vectors are useful for delivering genes of interest into a host cell where integration into the genome is desired. However, traditional retroviral expression technologies usually result in low viral titers which make gene expression studies difficult.

Our Platinum Retroviral Expression Systems incorporate superior packaging cell lines and vector technologies to produce high-titer virus with a single plasmid transfection. The Platinum Expression Systems include one of our exclusive Platinum Packaging Cell Lines which already contain the gag and pol genes; the Ecotropic and Amphotropic cells also contain an envelope protein. Simply clone your gene of interest into the vector provided and transfect into the Platinum cells. If you choose a Pantropic system, simply co-transfect with the VSV-G plasmid provided.

The Platinum Expression Systems below are specially designed for superior expression with either ES/EC cells or hematopoietic stem cells. For more information on our Platinum Expression Systems for a variety of cells, please see **page 64**.

- **Higher Viral Yields:** Average titer 10^7 infectious units/mL with transient transfection
- **Versatile:** 3 Packaging cell lines for use with nearly any target host species
- **Optimized for Stem Cell Studies:** Specially designed expression systems for ES/EC cells or hematopoietic stem cells

	Amphotropic	Ecotropic	Pantropic
Human	+++	N.S.	+++
Mouse	+++	+++	+++
Rat	+++	+++	+++
Monkey	+++	N.S.	+++
Cat	+++	N.S.	+++
Dog	+++	N.S.	+++
Hamster	+	N.S.	+++
Bird	N.S.	N.S.	+++
Fish	N.S.	N.S.	+++
Frog	N.S.	N.S.	+++
Insect	N.S.	N.S.	+++
Mollusk	N.S.	N.S.	+++

*Virus must be packaged with a pantropic envelope protein such as VSVG.
N.S. = Not Suitable

Suitability of Platinum Retroviral Expression Systems by Host Species.

Recent Product Citation

Kishida, T. et al (2015). Reprogrammed functional brown adipocytes ameliorate insulin resistance and dyslipidemia in diet-induced obesity and type 2 diabetes. *Stem Cell Reports* 10.1016/j.stemcr.2015.08.007. (VPK-303 and VPK-305)

Catalog Number	Packaging Cell Line	Transfer Vector	Envelope Vector	Control Vector
VPK-303	Plat-E (Ecotropic)	pMCs-Puro	————	pMCs-GFP
VPK-304	Plat-A (Amphotropic)	pMCs-Puro	————	pMCs-GFP
VPK-305	Plat-GP (Pantropic)	pMCs-Puro	pCMV-VSV-G	pMCs-GFP
VPK-306	Plat-E (Ecotropic)	pMYs-Puro	————	pMYs-GFP
VPK-307	Plat-A (Amphotropic)	pMYs-Puro	————	pMYs-GFP
VPK-308	Plat-GP (Pantropic)	pMYs-Puro	pCMV-VSV-G	pMYs-GFP

Components of the Platinum Retroviral Expression Systems for Stem Cells.

Product Name	Size	Catalog Number
Platinum ES/EC Retroviral Expression System, Ecotropic	1 kit	VPK-303
Platinum ES/EC Retroviral Expression System, Amphotropic	1 kit	VPK-304
Platinum ES/EC Retroviral Expression System, Pantropic	1 kit	VPK-305
Platinum HSC Retroviral Expression System, Ecotropic	1 kit	VPK-306
Platinum HSC Retroviral Expression System, Amphotropic	1 kit	VPK-307
Platinum HSC Retroviral Expression System, Pantropic	1 kit	VPK-308

Stem Cell Feeders

Leukemia inhibitory factor (LIF) is useful for maintaining the undifferentiated state of mouse embryonic stem (mES) cells. However, LIF does not have the same effect on human embryonic stem (hES) cells. Therefore, hES cells require the use of feeder cells for both derivation and maintenance. We offer a variety of feeder cells for stem cell culture. All feeder cells must be mitotically inactivated prior to use.

SNL 76/7 Passage-Independent Feeder Cells for iPS Culture

The SNL 76/7 is an immortalized cell line derived from mouse fibroblast STO cells which have been transformed with murine LIF and neomycin resistance genes.

- **Superior Culture:** Transformed with LIF gene for better maintenance of undifferentiated state
- **Versatile:** Useful for culture of human and mouse iPS cells and as a feeder for ES cells
- **Passage-Independent:** Immortalized cell line

Recent Product Citations

1. Arai, Y. et al. (2015). Spectral fingerprinting of individual cells visualized by cavity-reflection-enhanced light-absorption microscopy. *PLoS One* **10**:e0125733.
2. Wu, D.T. and Roth, M.J. (2014). MLV based viral-like particles for delivery of toxic proteins and nuclear transcription factors. *Biomaterials* **35**:8416-8426.
3. Takenaka-Ninagawa, N. et al. (2014). Generation of rat-induced pluripotent stem cells from a new model of metabolic syndrome. *PLoS One* **9**:e104462.
4. Pioyan, C. et al. (2014). Generation of mouse lines conditionally over-expressing microRNA using the Rosa26-Lox-Stop-Lox system. *Methods Mol. Biol.* **1194**:2103-224.

Product Name	Size	Catalog Number
SNL Feeder Cells	3 x 10 ⁶ cells	CBA-316

JK1 Passage-Independent Feeder Cells

JK1 is an immortalized CD34+ stromal cell line that supports long-term proliferation of stem cells. It has been shown to maintain capacity for stem cell renewal after serial passaging for over one year. JK1 may be used to culture a variety of cell types including pluripotent ES cells, germ-line derived stem cells, and primordial germ cell-derived EG cells.

Recent Product Citations

1. Burnight, E.R. et al (2014). CEP290 gene transfer rescued Leber congenital amaurosis cellular phenotype. *Gene Ther.* **21**:662-672.
2. Martin, L.A. et al. (2013). Serial enrichment of spermatogonial stem and progenitor cells (SSCs) in culture for derivation of long-term adult mouse SSC lines. *J. Vid. Exp.* **72**:e50017.

Product Name	Size	Catalog Number
JK1 Feeder Cells	1 x 10 ⁶ cells	CBA-315

MEF Feeder Cells

Our murine embryonic fibroblast (MEF) feeder cells are useful for the maintenance of human or mouse ES cells in their undifferentiated state. Cells must be mitotically inactivated prior to use.

Product Name	Size	Catalog Number
MEF Feeder Cells	5 x 10 ⁶ cells	CBA-310
MEF Feeder Cells, Hygromycin-resistant	5 x 10 ⁶ cells	CBA-313
MEF Feeder Cells, Neomycin-resistant	5 x 10 ⁶ cells	CBA-311
MEF Feeder Cells, Puromycin-resistant	5 x 10 ⁶ cells	CBA-312

CytoSelect™ 96-Well Hematopoietic Colony Forming Cell Assay

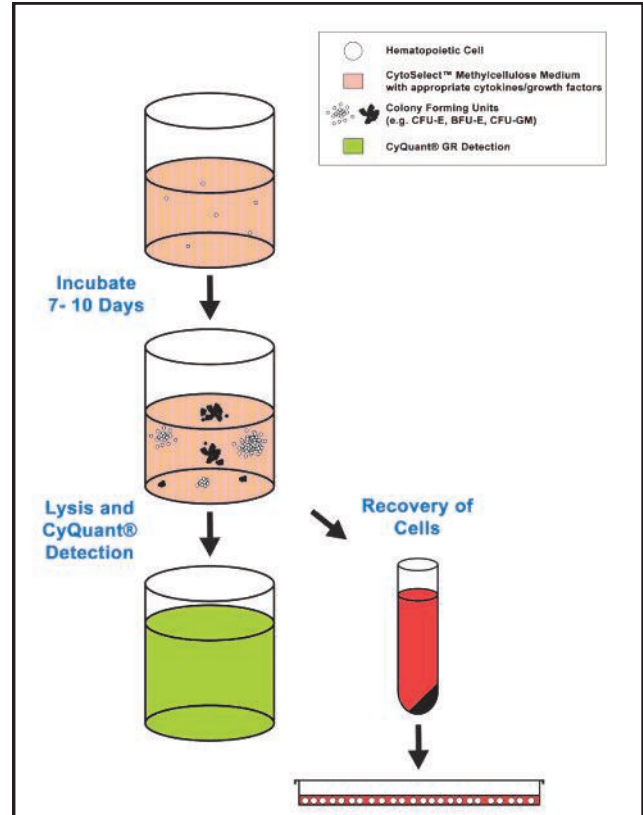
Hematopoietic stem cells (HSCs), when cultured in a suitable semisolid matrix such as methylcellulose supplemented with cytokines & nutrients, proliferate to form discrete cell clusters or colonies. Such HSCs or hematopoietic progenitors are known as colony-forming cells (CFCs). In classic CFC assays, cells are cultured in a 35mm dish for 14-21 days so the colonies can reach a certain size for manual counting, which can be tedious and subjective.

The CytoSelect™ 96-Well Hematopoietic Colony Forming Cell Assay provides a high-throughput method to quantify CFCs in just 7-10 days with no manual cell counting required. Cells are lysed, solubilized, and quantified using a fluorescent dye included in the kit. Alternatively, cells may be recovered for further culture and analysis.

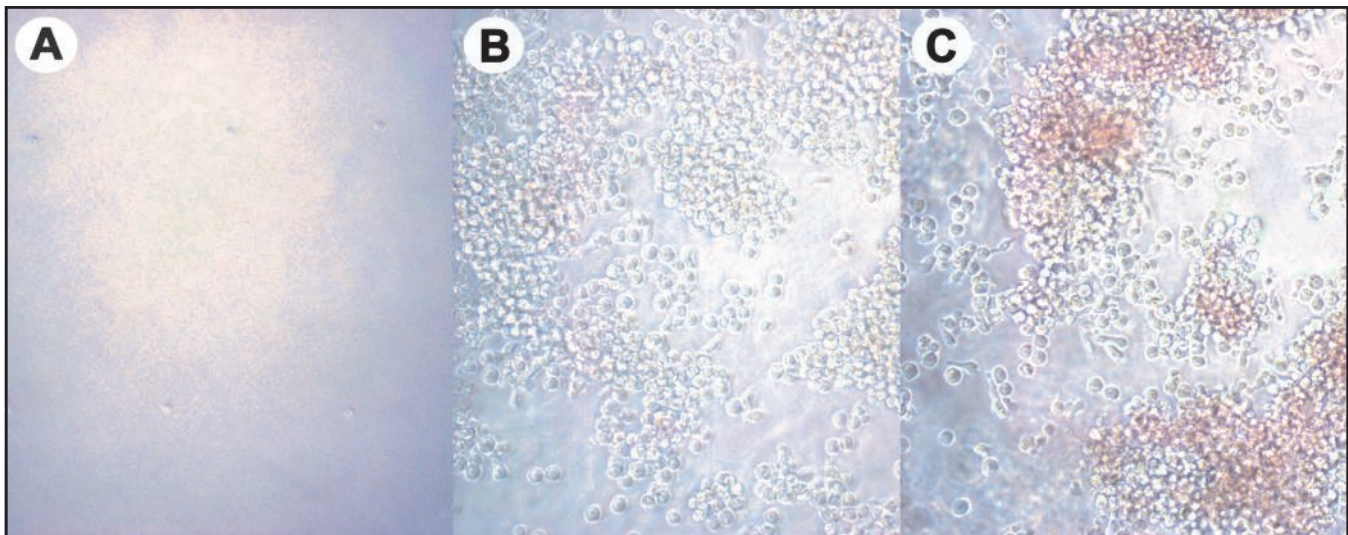
- **Fast Results:** 7-10 days vs. 2-3 weeks
- **Convenient:** Eliminates manual counting
- **Easier Reagent Handling:** Methylcellulose media can be handled using a pipet instead of a syringe

Recent Product Citations

1. Chiba, H. et al. (2013). Diabetes impairs the interactions between long-term hematopoietic stem cells and osteopontin-positive cells in the endosteal niche of mouse bone marrow. *Am. J. Physiol. Cell Physiol.* **305**:C693-C703.
2. Neri, P. et al. (2011). Bortezomib-induced "BRCAness" sensitizes multiple myeloma cells to PARP inhibitors. *Blood* **118**:6368-6379.



Assay Principle for the CytoSelect™ 96-Well Hematopoietic Colony Forming Cell Assay.



HSC Colony Formation. Human bone marrow derived CD34+ Hematopoietic Progenitor Cells were seeded at 3000 cells/well and cultured for 7-10 days in the absence or presence of growth factors/cytokines. Colonies were quantified according to the assay protocol. **A:** After 7 days without cytokines. **B:** After 7 days in presence of cytokines. **C:** After 10 days in presence of cytokines (hemoglobin visible).

Product Name	Detection	Size	Catalog Number
CytoSelect™ 96-Well Hematopoietic Colony Forming Cell Assay	Fluorometric	96 Assays	CBA-320
		5 x 96 Assays	CBA-320-5

StemTAG™ 96-Well Stem Cell Colony Formation Assay

Our StemTAG™ 96-Well Stem Cell Colony Formation Assay provides a high-throughput method to quantify ES cells in just 7-10 days with no manual cell counting required.

After colonies are formed, stem cells may be analyzed in 3 ways:

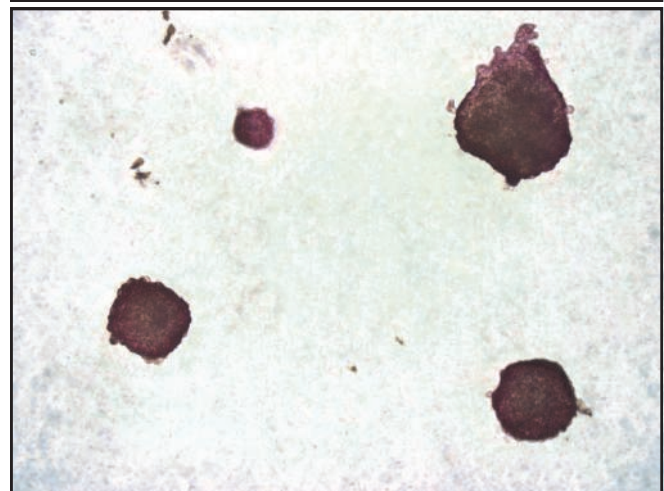
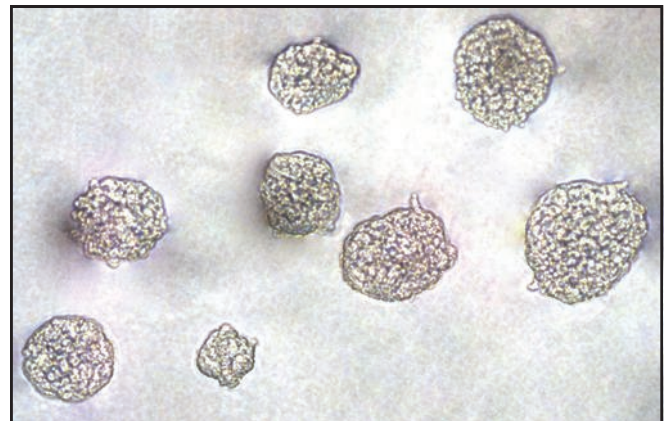
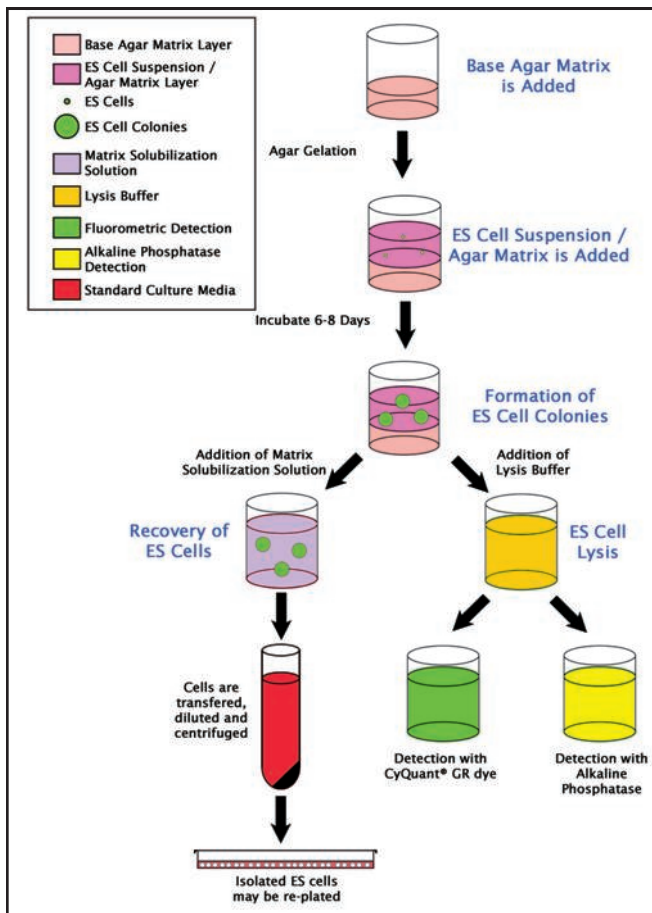
1. Lyse cells, then quantify using a fluorescent dye included in the kit.
2. Lyse cells, then measure alkaline phosphatase activity using reagents provided.
3. Recover colonies for further culture and analysis.

This assay may be of particular interest for the study of tumor stem cells.

- **Fast Results:** 7-10 days vs. 2-3 weeks using conventional methods
- **Versatile:** Quantify cells using fluorescent dye, measure alkaline phosphatase activity, or recover cells for further analysis
- **Plate Reader Convenience:** No manual cell counting required

Recent Product Citation

Shin, M.R. et al (2015). Isocudraxanthone K induces growth inhibition and apoptosis in oral cancer cells via hypoxia inducible factor-1 α . *Biomed. Res. Int.* **2014**:934691.



StemTAG™ Stem Cell Colony Formation Assay Principle.

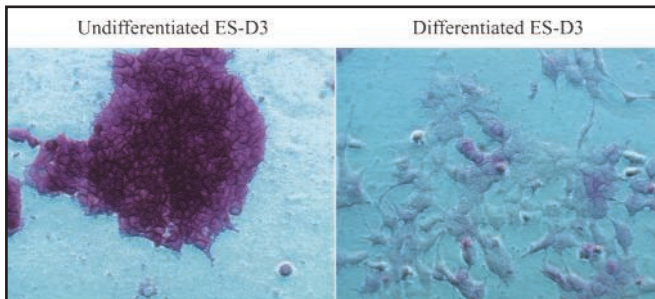
Anchorage-Independent Growth of Mouse ES-D3 Cells.
Top: Phase Contrast. **Bottom:** Alkaline Phosphatase Staining.

Product Name	Detection	Size	Catalog Number
StemTAG™ 96-Well Stem Cell Colony Formation Assay	Fluorometric	96 Assays	CBA-325
		5 x 96 Assays	CBA-325-5

StemTAG™ Alkaline Phosphatase Assay Kits

The StemTAG™ Alkaline Phosphatase Staining and Activity Assay Kits monitor AP activity via both immunocytochemistry staining and a colorimetric 96-well plate-based activity assay. The staining and activity assay kits are also sold separately.

- **Fast Results:** Staining and Activity Assay protocols each take less than 1 hour
- **Versatile:** Useful for human ES, EG and EC cells, as well as mouse ES and EG cells



StemTAG™ Alkaline Phosphatase Staining Kit. Murine embryonic stem cells (ES-D3) were maintained in an undifferentiated state with LIF. To induce differentiation, LIF was withdrawn over several days. Various differentiation events were observed: cells became flattened and enlarged with reduced proliferation. On day 5, cells were stained according to the assay protocol.

Recent Product Citations

1. Lee, K.H. et al. (2015). Subculture of germ cell-derived colonies with GATA4-positive feeder cells from neonatal pig testes. *Stem Cells Int.* 6029271. (CBA-300)
2. Jacinto, F.V. et al. (2015). The nucleoporin Nup153 regulates embryonic stem cell pluripotency through gene silencing. *Genes Dev.* 29:1224-1238. (CBA-300)
3. Langlois, T. et al. (2014). TET2 deficiency inhibits mesoderm and hematopoietic differentiation in human embryonic stem cells. *Stem Cells* 32:2084-2097. (CBA-300)
4. Lee, K.H. et al. (2014). Identification and in vitro derivation of spermatogonia in beagle testis. *PLoS One* 9:e109963. (CBA-300)
5. Manukyan, M. and Singh, P.B. (2014). Epigenome rejuvenation: HP18 mobility as a measure of pluripotent and senescent chromatin ground states. *Sci. Rep.* 4:4789. (CBA-300)
6. Yue, Y. et al. (2015). Safe and bodywide muscle transduction in young adult Duchenne muscular dystrophy dogs with adeno-associated virus. *Hum. Mol. Genet.* 10.1093/hmg/ddv310. (CBA-310)
7. Pino-Barrio, M.J. et al. (2015). V-myc immortalizes human neural stem cells in the absence of pluripotency-associated traits. *PLoS One* 10:e0118499. (CBA-301)
8. Pan, X. et al. (2015). AAV-8 is more efficient than AAV-9 in transducing neonatal dog heart. *Hum. Gene Ther. Methods* 10.1089/hgtb.2014.128. (CBA-301)
9. Dong, Y. et al. (2014). NOTCH-mediated maintenance and expansion of human bone marrow stromal/stem cells: a technology designed for orthopedic regenerative medicine. *Stem Cells Trans. Med.* 3:1456-1466. (CBA-301)
10. Dixon, J.E. et al. (2014). Combined hydrogels that switch human pluripotent stem cells from self-renewal to differentiation. *PNAS* 111:5580-5585. (CBA-301)
11. Guo, L. et al. (2014). Effects of erythropoietin on osteoblast proliferation and function. *Clin. Exp. Med.* 14:69-76. (CBA-301)

Product Name	Detection	Size	Catalog Number
StemTAG™ Alkaline Phosphatase Staining and Activity Assay Kit	ICC & Colorimetric	2 x 100 Assays	CBA-302
	ICC & Fluorometric	2 x 100 Assays	CBA-308
StemTAG™ Alkaline Phosphatase Activity Assay Kit	Colorimetric	100 Assays	CBA-301
	Fluorometric	100 Assays	CBA-307
StemTAG™ Alkaline Phosphatase Staining Kit (Purple)	ICC	100 Assays	CBA-306
StemTAG™ Alkaline Phosphatase Staining Kit (Red)	ICC	100 Assays	CBA-300

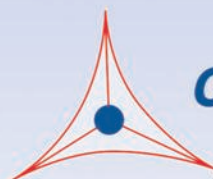
StemTAG™ PCR Primer Set for Stem Cell Characterization

Pluripotent stem cells can differentiate into cells derived from all three embryonic germ layers: endoderm, mesoderm and ectoderm. Our StemTAG™ PCR Primer Set provides an efficient system for monitoring ES cell differentiation/undifferentiation. Seven primer sets are included: primers for two widely studied stem cell markers (Oct-4 and NANOG), one marker for each embryonic germ layer (AFP/Endoderm, Flk-1/Mesoderm and NCAM/Ectoderm), and two controls (GAPDH and β -Actin). Primers are suitable for either end-point or real-time (quantitative) PCR.

Product Name	Size	Catalog Number
StemTAG™ PCR Primer Set for Stem Cell Characterization	50 Reactions	CBA-303

Viral Expression

Overview of Viral Gene Delivery	40
AAV (Adeno-Associated Virus) Expression	41
Adenoviral Expression	50
Lentiviral Expression	57
Retroviral Expression	63



CELL BIOLABS, INC.

Creating Solutions for Life Science Research

Recombinant Viral Gene Delivery

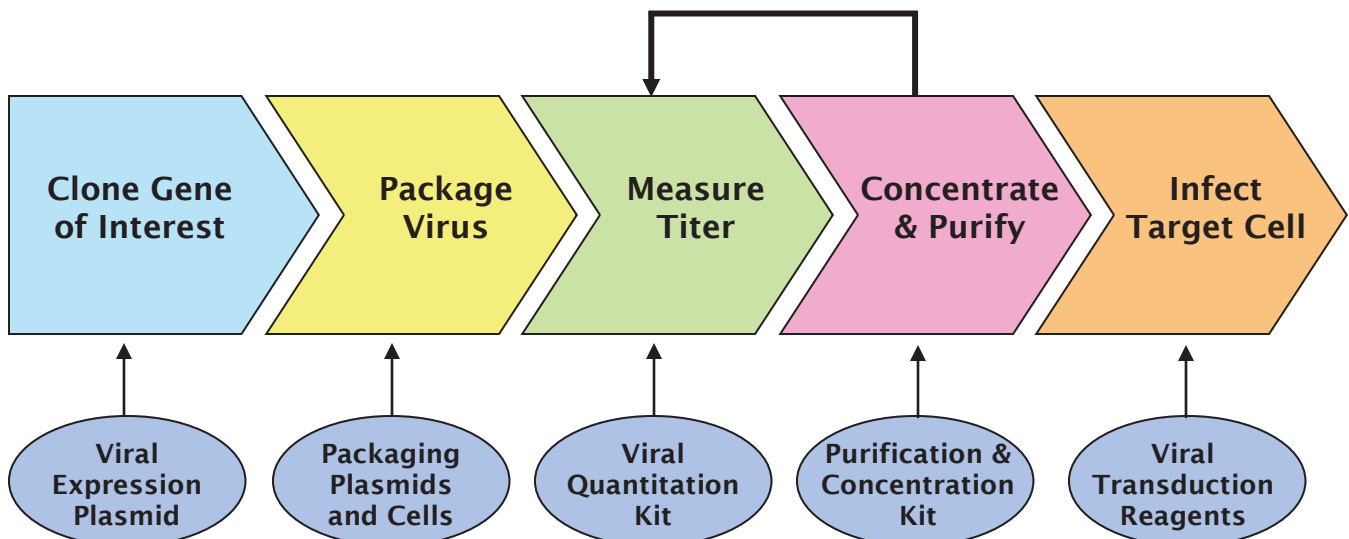
Recombinant viral vectors provide a powerful means of delivering a gene into a target cell. There are many viral vectors available, and there are pros and cons to each. Use the following table to select the best viral vector for your research.

Comparison of Viral Vectors for Gene Delivery

	Adeno-Associated Virus (AAV) (p. 41-49)	Adenovirus (p. 50-56)	Lentivirus (HIV-1, FIV, SIV) (p. 57-62)	Retrovirus (MMLV) (p. 63-70)
Gene Expression	Transient or Stable	Transient	Transient or Stable	Stable
Will Infect Dividing Cells	Yes	Yes	Yes	Yes
Will Infect Non-Dividing Cells	Yes	Yes	Yes	No
Integrates into Target Cell Genome	No*	No	Yes	Yes
Immune Response in Target Cells	Very Low	High	Low	Moderate
Relative Viral Titer	XXX	XXXX	XXX	XX
Relative Transduction Efficiency	XXX	XXXX	XXX	XX

*Native AAV can integrate, but recombinant AAV rarely does.

Typical Workflow for Viral Gene Delivery



Cell Biolabs offers kits and reagents for every step in your workflow.

Adeno-Associated Virus Kits & Reagents

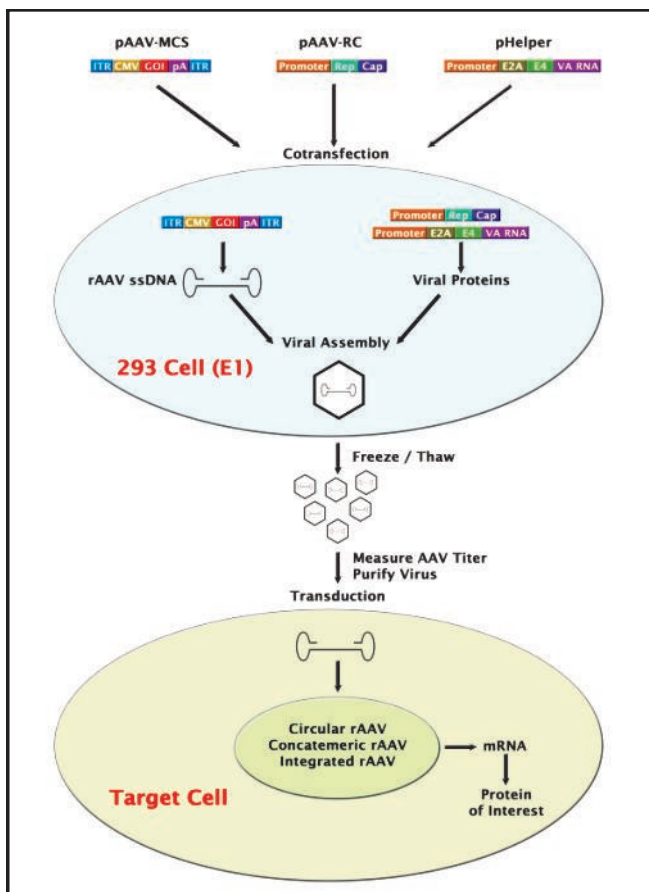
Adeno-associated virus (AAV) is less immunogenic than adenovirus or retrovirus. We offer a comprehensive line of AAV kits and reagents to ensure you get the best expression from your AAV expression studies:

- Helper Free Expression Systems
- Helper Free Packaging Systems
- Expression & Control Vectors
- Viral Packaging Cell Line
- Premade AAV Controls
- Purification Kits
- Quantitation / Titer Kit
- Transduction Kits

AAV Helper Free Systems

Production of recombinant AAV requires certain genes from the adenovirus genome, which means that an adenovirus usually needs to be present. The AAV Helper Free System eliminates the need for a helper adenovirus. Most of the required adenoviral genes (E2A, E4 and VA RNA) are provided in a pHelper plasmid, while the required E1 gene is provided by the 293 packaging cells.

- **Safer:** pHelper plasmid eliminates the need for a helper virus
- **Flexible:** Packaging vectors and expression vectors available separately or as one complete system, so you only order what you need
- **Expandable:** All plasmids are provided individually, not in a mixture, so you can amplify in competent cells



Gene Delivery using the AAV Helper Free System.

AAV Helper Free Systems are available for a variety of formats and serotypes:

- **AAV Complete Expression Systems** contain all packaging plasmids plus an expression vector and a GFP control vector: **p. 42-45**
- **AAV Packaging Systems** contain the pHelper plasmid and a serotype-specific Rep-Cap plasmid for use with your own expression construct: **p. 45**
- If you have an AAV packaging system for one serotype and want to try another, choose one of 8 different **AAV Rep-Cap Plasmids** from native serotypes 1 through 6 plus AAV-DJ and AAV-DJ/8: **p. 46**
- If you already have an AAV packaging system and need a cloning vector, choose one of 10 different **AAV Expression Vectors** available individually: **p. 46**
- Want to make a control virus? Choose one of our **AAV Control Vectors**: **p. 47**

AAV Helper Free Complete Expression Systems

AAV Helper Free Complete Expression Systems contain everything you need to produce high-titer recombinant adeno-associated virus:

- pHelper Plasmid
- Rep-Cap Plasmid (serotype specific)
- GFP Control Vector
- Choice of 10 AAV Expression Vectors:
 - Gene Expression (CMV or no promoter)
 - shRNA (U6 promoter)
 - Self complementary (scAAV)

AAV Helper Free Expression Systems are available for the following serotypes:

- Native serotypes 1-6
- AAV-DJ, engineered by DNA family shuffling to form a hybrid capsid from 8 different native serotypes; provides significantly higher infectivity rates *in vitro* (see table below)
- AAV-DJ/8, a mutant of AAV-DJ that exhibits increased uptake in brain and other tissues *in vivo*, similar to serotypes 8 and 9

Cell Line	Cell or Tissue Source	AAV-1	AAV-2	AAV-3	AAV-4	AAV-5	AAV-6	AAV-8	AAV-9	AAV-DJ	AAV-DJ/8
HEK293	Hu Kidney	25	100	2.5	0.1	0.1	5	0.7	0.1	500	0.3
HeLa	Hu Cervix	3	100	2.0	0.1	3.7	1.0	0.2	0.1	667	0.2
HepG2	Hu Liver	3	100	16.7	0.3	1.7	5	0.3	ND	1250	0.5
Hep1A	Ms Liver	20	100	0.2	1.0	0.1	1.0	0.2	0.0	400	0.1
911	Hu Retina	17	100	11.1	0.2	0.1	17	0.1	ND	500	0.0
CHO	Hm Ovary	100	100	14.3	1.4	333	50	10.0	1.0	25000	5.0
COS	Si Kidney	33	100	33	3.3	5.0	14	2.0	0.5	500	0.3
MeWo	Hu Skin	10	100	20	0.3	6.7	10	1.0	0.2	2857	1.0
NIH3T3	Ms Fibroblasts	10	100	2.9	2.9	0.3	10	0.3	ND	500	0.1
A549	Hu Lung	14	100	20	ND	0.5	10	0.5	0.1	1000	0.1
HT1180	Hu Fibroblasts	20	100	10.0	0.1	0.3	33	0.5	0.1	333	0.2

Relative Infectivity Rates of AAV Serotypes. Normalized to AAV-2 = 100. ND = Not determined.

Recent Product Citations

1. Altemeier, W.A. et al. (2012). Transmembrane and extracellular domains of syndecan-1 have distinct functions in regulating lung epithelial migration and adhesion. *J. Biol. Chem.* **287**:34927-34935. (VPK-410-DJ)
2. Zhao, H. et al. (2014). SCAMP5 plays a critical role in synaptic vesicle endocytosis during high neuronal activity. *J. Neurosci.* **34**:10085-10095. (VPK-410-SER1)
3. Moshiri, F. et al. (2014). Inhibiting the oncogenic mir-221 by microRNA sponge: toward microRNA-based therapeutics for hepatocellular carcinoma. *Gastroenterol. Hepatol. Bed Bench* **7**:43-54. (VPK-418-DJ)

AAV-DJ Helper Free Complete Expression Systems

Product Name	Size	Catalog Number
AAV-DJ Helper Free Expression System	1 kit	VPK-410-DJ
AAV-DJ Helper Free Bicistronic Expression System (Puro)	1 kit	VPK-415-DJ
AAV-DJ Helper Free Bicistronic Expression System (Neo)	1 kit	VPK-416-DJ
AAV-DJ Helper Free Bicistronic Expression System (Hygro)	1 kit	VPK-417-DJ
AAV-DJ Helper Free Bicistronic Expression System (GFP)	1 kit	VPK-418-DJ
AAV-DJ Helper Free Bicistronic Expression System (Blasticidin)	1 kit	VPK-419-DJ
AAV-DJ Helper Free Promoterless Expression System	1 kit	VPK-411-DJ
AAV-DJ Helper Free shRNA Expression System (Puro)	1 kit	VPK-412-DJ
AAV-DJ/Helper Free shRNA Expression System (GFP)	1 kit	VPK-413-DJ
scAAV-DJ Helper Free Expression System	1 kit	VPK-430-DJ

AAV-DJ/8 Helper Free Complete Expression Systems

Product Name	Size	Catalog Number
AAV-DJ/8 Helper Free Expression System	1 kit	VPK-410-DJ-8
AAV-DJ/8 Helper Free Bicistronic Expression System (Puro)	1 kit	VPK-415-DJ-8
AAV-DJ/8 Helper Free Bicistronic Expression System (Neo)	1 kit	VPK-416-DJ-8
AAV-DJ/8 Helper Free Bicistronic Expression System (Hygro)	1 kit	VPK-417-DJ-8
AAV-DJ/8 Helper Free Bicistronic Expression System (GFP)	1 kit	VPK-418-DJ-8
AAV-DJ/8 Helper Free Bicistronic Expression System (Blasticidin)	1 kit	VPK-419-DJ-8
AAV-DJ/8 Helper Free Promoterless Expression System	1 kit	VPK-411-DJ-8
AAV-DJ/8 Helper Free shRNA Expression System (Puro)	1 kit	VPK-412-DJ-8
AAV-DJ/8 Helper Free shRNA Expression System (GFP)	1 kit	VPK-413-DJ-8
scAAV-DJ/8 Helper Free Expression System	1 kit	VPK-430-DJ-8

AAV-1 Helper Free Complete Expression Systems

Product Name	Size	Catalog Number
AAV-1 Helper Free Expression System	1 kit	VPK-410-SER1
AAV-1 Helper Free Bicistronic Expression System (Puro)	1 kit	VPK-415-SER1
AAV-1 Helper Free Bicistronic Expression System (Neo)	1 kit	VPK-416-SER1
AAV-1 Helper Free Bicistronic Expression System (Hygro)	1 kit	VPK-417-SER1
AAV-1 Helper Free Bicistronic Expression System (GFP)	1 kit	VPK-418-SER1
AAV-1 Helper Free Bicistronic Expression System (Blasticidin)	1 kit	VPK-419-SER1
AAV-1 Helper Free Promoterless Expression System	1 kit	VPK-411-SER1
AAV-1 Helper Free shRNA Expression System (Puro)	1 kit	VPK-412-SER1
AAV-1 Helper Free shRNA Expression System (GFP)	1 kit	VPK-413-SER1
scAAV-1 Helper Free Expression System	1 kit	VPK-430-SER1

AAV-2 Helper Free Complete Expression Systems

Product Name	Size	Catalog Number
AAV-2 Helper Free Expression System	1 kit	VPK-410-SER2
AAV-2 Helper Free Bicistronic Expression System (Puro)	1 kit	VPK-415-SER2
AAV-2 Helper Free Bicistronic Expression System (Neo)	1 kit	VPK-416-SER2
AAV-2 Helper Free Bicistronic Expression System (Hygro)	1 kit	VPK-417-SER2
AAV-2 Helper Free Bicistronic Expression System (GFP)	1 kit	VPK-418-SER2
AAV-2 Helper Free Bicistronic Expression System (Blasticidin)	1 kit	VPK-419-SER2
AAV-2 Helper Free Promoterless Expression System	1 kit	VPK-411-SER2
AAV-2 Helper Free shRNA Expression System (Puro)	1 kit	VPK-412-SER2
AAV-2 Helper Free shRNA Expression System (GFP)	1 kit	VPK-413-SER2
scAAV-2 Helper Free Expression System	1 kit	VPK-430-SER2

AAV-3 Helper Free Complete Expression Systems

Product Name	Size	Catalog Number
AAV-3 Helper Free Expression System	1 kit	VPK-410-SER3
AAV-3 Helper Free Bicistronic Expression System (Puro)	1 kit	VPK-415-SER3
AAV-3 Helper Free Bicistronic Expression System (Neo)	1 kit	VPK-416-SER3
AAV-3 Helper Free Bicistronic Expression System (Hygro)	1 kit	VPK-417-SER3
AAV-3 Helper Free Bicistronic Expression System (GFP)	1 kit	VPK-418-SER3
AAV-3 Helper Free Bicistronic Expression System (Blasticidin)	1 kit	VPK-419-SER3
AAV-3 Helper Free Promoterless Expression System	1 kit	VPK-411-SER3
AAV-3 Helper Free shRNA Expression System (Puro)	1 kit	VPK-412-SER3
AAV-3 Helper Free shRNA Expression System (GFP)	1 kit	VPK-413-SER3
scAAV-3 Helper Free Expression System	1 kit	VPK-430-SER3

AAV-4 Helper Free Complete Expression Systems

Product Name	Size	Catalog Number
AAV-4 Helper Free Expression System	1 kit	VPK-410-SER4
AAV-4 Helper Free Bicistronic Expression System (Puro)	1 kit	VPK-415-SER4
AAV-4 Helper Free Bicistronic Expression System (Neo)	1 kit	VPK-416-SER4
AAV-4 Helper Free Bicistronic Expression System (Hygro)	1 kit	VPK-417-SER4
AAV-4 Helper Free Bicistronic Expression System (GFP)	1 kit	VPK-418-SER4
AAV-4 Helper Free Bicistronic Expression System (Blasticidin)	1 kit	VPK-419-SER4
AAV-4 Helper Free Promoterless Expression System	1 kit	VPK-411-SER4
AAV-4 Helper Free shRNA Expression System (Puro)	1 kit	VPK-412-SER4
AAV-4 Helper Free shRNA Expression System (GFP)	1 kit	VPK-413-SER4
scAAV-4 Helper Free Expression System	1 kit	VPK-430-SER4

AAV-5 Helper Free Complete Expression Systems

Product Name	Size	Catalog Number
AAV-5 Helper Free Expression System	1 kit	VPK-410-SER5
AAV-5 Helper Free Bicistronic Expression System (Puro)	1 kit	VPK-415-SER5
AAV-5 Helper Free Bicistronic Expression System (Neo)	1 kit	VPK-416-SER5
AAV-5 Helper Free Bicistronic Expression System (Hygro)	1 kit	VPK-417-SER5
AAV-5 Helper Free Bicistronic Expression System (GFP)	1 kit	VPK-418-SER5
AAV-5 Helper Free Bicistronic Expression System (Blasticidin)	1 kit	VPK-419-SER5
AAV-5 Helper Free Promoterless Expression System	1 kit	VPK-411-SER5
AAV-5 Helper Free shRNA Expression System (Puro)	1 kit	VPK-412-SER5
AAV-5 Helper Free shRNA Expression System (GFP)	1 kit	VPK-413-SER5
scAAV-5 Helper Free Expression System	1 kit	VPK-430-SER5

AAV-6 Helper Free Complete Expression Systems

Product Name	Size	Catalog Number
AAV-6 Helper Free Expression System	1 kit	VPK-410-SER6
AAV-6 Helper Free Bicistronic Expression System (Puro)	1 kit	VPK-415-SER6
AAV-6 Helper Free Bicistronic Expression System (Neo)	1 kit	VPK-416-SER6
AAV-6 Helper Free Bicistronic Expression System (Hygro)	1 kit	VPK-417-SER6
AAV-6 Helper Free Bicistronic Expression System (GFP)	1 kit	VPK-418-SER6
AAV-6 Helper Free Bicistronic Expression System (Blasticidin)	1 kit	VPK-419-SER6
AAV-6 Helper Free Promoterless Expression System	1 kit	VPK-411-SER6
AAV-6 Helper Free shRNA Expression System (Puro)	1 kit	VPK-412-SER6
AAV-6 Helper Free shRNA Expression System (GFP)	1 kit	VPK-413-SER6
scAAV-6 Helper Free Expression System	1 kit	VPK-430-SER6

AAV Helper Free Packaging Systems

AAV Helper Free Packaging Systems contain everything found in the Complete Expression Systems, with the exception of the AAV expression vector. This is an ideal choice if you already have an AAV construct containing your gene of interest.

The following vectors are included with each AAV Helper Free Packaging System:

- pHelper Plasmid
- Rep-Cap Plasmid (serotype specific)
- GFP Control Vector

All plasmids are provided individually, not as a packaging mixture.

Recent Product Citations

1. Iwata, R. et al. (2015). Developmental RacGAP α 2-chimaerin signaling is a determinant of the morphological features of dendritic spines in adulthood. *J. Neurosci.* **35**:13728-13744. (VPK-400-DJ-8)
2. Friedland, A.E. et al. (2015). Characterization of *Staphylococcus aureus* Cas9: a smaller Cas9 for all-in-one adeno-associated virus delivery and paired nickase applications. *Genome Biol.* **16**:257. (VPK-402)

- If you need an AAV expression vector as well as an AAV packaging system, choose one of our **AAV Complete Expression Systems: p. 42-45**
- If you want to make AAV from more than one serotype but don't want to order multiple packaging systems, choose one AAV Packaging System from this list and then add additional **AAV Rep-Cap Plasmids: p. 46**

Product Name	Size	Catalog Number
AAV-DJ Helper Free Packaging System	1 kit	VPK-400-DJ
AAV-DJ/8 Helper Free Packaging System	1 kit	VPK-400-DJ-8
AAV-1 Helper Free Packaging System	1 kit	VPK-401
AAV-2 Helper Free Packaging System	1 kit	VPK-402
AAV-3 Helper Free Packaging System	1 kit	VPK-403
AAV-4 Helper Free Packaging System	1 kit	VPK-404
AAV-5 Helper Free Packaging System	1 kit	VPK-405
AAV-6 Helper Free Packaging System	1 kit	VPK-406

AAV Rep-Cap Plasmids (Serotype-Specific)

AAV Rep-Cap plasmids allow you to make recombinant AAV of a specific serotype. These plasmids are ideal if you already have an AAV packaging system for a different serotype. Just substitute one of these plasmids into your AAV Helper Free Packaging System or Expression System.

Recent Product Citations

- Blackburn, J. et al. (2015). Damage-inducible intragenic demethylation of the human TP53 tumor suppressor gene is associated with transcription from an alternative intronic promoter. *Mol. Carcinog.* 10.1002/mc.22441. (VPK-420-DJ)
- Kato, H.E. et al. (2015). Atomistic design of microbial opsin-based blue-shifted optogenetics tools. *Nat. Commun.* 6:7177. (VPK-420-DJ)
- Holehonur, R. et al. (2014). Adeno-associated viral serotypes produce differing titers and differentially transduce neurons within the rat basal and lateral amygdala. *BMC Neurosci.* 15:28. (VPK-420-DJ, VPK-420-DJ-8)

Product Name	Catalog Number
pAAV-DJ Vector	VPK-420-DJ
pAAV-DJ/8 Vector	VPK-420-DJ-8
pAAV-RC1 Vector	VPK-421
pAAV-RC2 Vector	VPK-422

Product Name	Catalog Number
pAAV-RC3 Vector	VPK-423
pAAV-RC4 Vector	VPK-424
pAAV-RC5 Vector	VPK-425
pAAV-RC6 Vector	VPK-426

AAV Expression Vectors

Each of our AAV Expression Vectors may be used with any of our AAV Helper Free Systems, regardless of AAV serotype. Choose one of these vectors when you already have an AAV Packaging System but may want to use a different promoter or selection marker.

Recent Product Citations

- Tang, F.L. et al. (2015). VPS35 deficiency or mutation causes dopaminergic neuronal loss by impairing mitochondrial fusion and function. *Cell Rep.* 12:1631-1643. (VPK-410, VPK-413)
- Orabi, A.I. et al. (2015). Dynamic imaging of pancreatic NF- κ B activation in live mice using AAV infusion and bioluminescence. *J. Biol. Chem.* 10.1074/jbc.M115.647933. (VPK-410)
- Fyk-Kolodziej, B. et al. (2014). Marking cells with infrared fluorescent proteins to preserve photoresponsiveness in the retina. *Biotechniques* 57:245-253. (VPK-410)
- Lutz, D. et al. (2014). Myelin basic protein cleaves cell adhesion molecule L1 and promotes neuritogenesis and cell survival. *J. Biol. Chem.* 289:13503-13518. (VPK-410)
- Xiang, J. et al. (2015). Postnatal loss of Hap1 reduces hippocampal neurogenesis and causes adult depressive-like behavior in mice. *PLoS Genet.* 11:e1005175. (VPK-411)
- Nishikawa, T. et al. (2015). Resetting the transcription factor network reverses terminal chronic hepatic failure. *J. Clin. Invest.* 10.1172/JCI73137. (VPK-418)
- Huckstepp, R.T. et al. (2015). Role of parafacial nuclei in control of breathing in adult rats. *J. Neurosci.* 35:1052-1067. (VPK-418)
- Krol, J. et al. (2015). A network comprising short and long noncoding RNAs and RNA helicase controls mouse retina architecture. *Nat. Commun.* 6:7305. (VPK-430)

Product Name	Cloning Capacity	Size	Catalog Number
pAAV-MCS Expression Vector	3 kb	10 μ g	VPK-410
pAAV-IRES-Puro Expression Vector	1.8 kb	10 μ g	VPK-415
pAAV-IRES-Neo Expression Vector	1.6 kb	10 μ g	VPK-416
pAAV-IRES-Hygro Expression Vector	1.4 kb	10 μ g	VPK-417
pAAV-IRES-GFP Expression Vector	1.7 kb	10 μ g	VPK-418
pAAV-IRES-Bsd Expression Vector	2 kb	10 μ g	VPK-419
pAAV-MCS Promoterless Expression Vector	3.9 kb	10 μ g	VPK-411
pAAV-U6-Puro Expression Vector	2.2 kb	10 μ g	VPK-412
pAAV-U6-GFP Expression Vector	2.1 kb	10 μ g	VPK-413
pscAAV-MCS Expression Vector	1.5 kb	10 μ g	VPK-430

AAV Control Plasmids

Our AAV control plasmids are useful for making a transduction control virus. Choose one of these constructs to pair with an AAV Packaging System. The vectors are provided as purified DNA.

Product Name	Size	Catalog Number
pAAV-GFP Control Vector	10 µg	AAV-400
pAAV-Cre Control Vector	10 µg	AAV-401
pAAV-LacZ Control Vector	10 µg	AAV-402
pscAAV-GFP Control Vector	10 µg	AAV-410

AAV Premade Control Viruses

Our AAV premade control viruses provide a convenient tool for measuring transduction efficiency into a target cell. Each virus contains a reporter gene, with the exception of the Null Control virus.

All AAV premade viruses are provided at a concentration of 1×10^{12} GC/mL.

Product Name	Size	Catalog Number
AAV1-GFP Control Virus	50 µL	AAV-301
AAV2 Null Control Virus	50 µL	AAV-300
AAV2-Cre Control Virus	50 µL	AAV-310
AAV2-GFP Control Virus	50 µL	AAV-302
AAV2-Luc Control Virus	50 µL	AAV-320
AAV3-GFP Control Virus	50 µL	AAV-303
AAV5-GFP Control Virus	50 µL	AAV-305
AAV6-GFP Control Virus	50 µL	AAV-306

293AAV Cell Line

Our 293AAV cell line is selected from the parental 293 cell line for larger surface area, flattened morphology, and firmer attachment to culture plates, resulting in production of higher yields of AAV.

Recent Product Citation

Lutz, D. et al. (2014). Myelin basic protein cleaves cell adhesion molecule L1 and promotes neuritogenesis and cell survival. *J. Biol. Chem.* **289**:13503-13518.

Product Name	Size	Catalog Number
293AAV Cell Line	1×10^6 cells	AAV-100

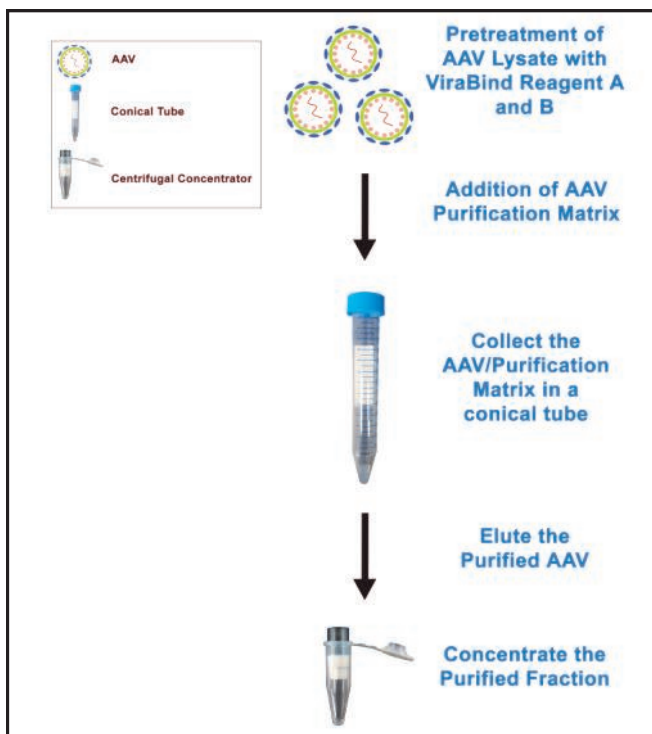
ViraBind™ AAV Purification Kits

Purification of AAV via ultracentrifugation can be tedious and time-consuming, and may result in low yields. ViraBind™ AAV Purification Kits use a one-step proprietary matrix followed by further purification and concentration using a centrifugal concentrator. The result is a higher AAV yield with high purity in a fraction of the time. Kits are available in two sizes:

- The Standard kit can purify up to two 10cm dishes per prep
- The Mega kit can purify up to ten 15cm dishes per prep

ViraBind™ Kits are suitable for AAV-2 or AAV-DJ; they are not compatible with other AAV serotypes.

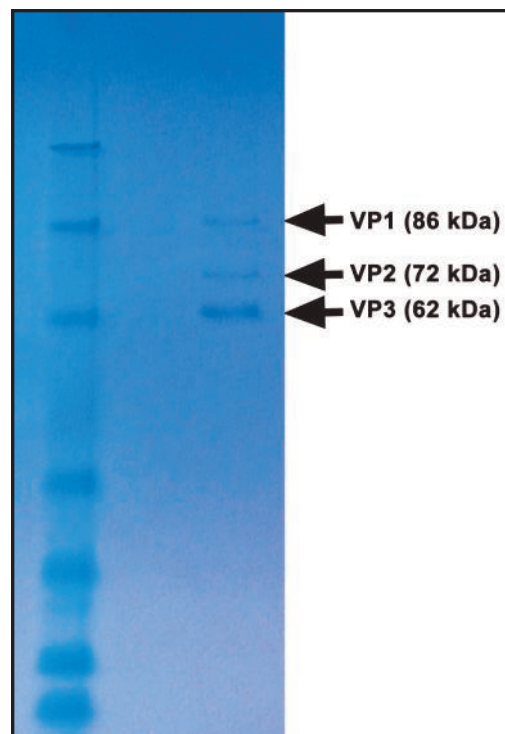
- **High Purity:** No contamination bands as seen on SDS gel
- **Fast Results:** Obtain purified virus in about 3 hours
- **High Yields:** Recovery rate >60%



Purification Procedure for the ViraBind™ AAV Purification Kit.

Recent Product Citations

1. Tsuneoka, Y. et al. (2015). Distinct preoptic-BST nuclei dissociate paternal and infanticidal behavior in mice. *EMBO J.* 10.15252/embj.201591942. (VPK-140)
2. Nishikawa, T. et al. (2015). Resetting the transcription factor network reverses terminal chronic hepatic failure. *J. Clin. Invest.* 10.1172/JCI73137. (VPK-140)
3. Stankowska, D.L. et al. (2015). Neuroprotective effects of transcription factor Brn3b in an ocular hypertension rat model of glaucoma. *Invest. Ophthalmol. Vis. Sci.* 56:893-907. (VPK-140)
4. Moshiri, F. et al. (2014). Inhibiting the oncogenic mir-221 by microRNA sponge: toward microRNA-based therapeutics for hepatocellular carcinoma. *Gastroenterol. Hepatol. Bed Bench* 7:43-54. (VPK-140)
5. Inaba, Y. et al. (2014). Gadd34 regulates liver regeneration in hepatic steatosis. *Hepatology* 6:1343-1356. (VPK-140)
6. Rodriguez, J.P. et al. (2014). Abrogation of β -catenin signaling in oligodendrocyte precursor cells reduces glial scarring and promotes axon in the medial prefrontal cortex of rodents. *J. Neurosci.* 30:15007-15018. (VPK-140)
7. Uchida, S. et al. (2010). Early life stress enhances behavioral vulnerability to stress through the activation of REST4-mediated gene transcription in the medial prefrontal cortex of rodents. *J. Neurosci.* 30:15007-15018. (VPK-140)
8. Nazari, M. et al. (2014). AAV2-mediated follistatin overexpression induces ovine primary myoblasts proliferation. *BMC Biotechnol.* 14:87. (VPK-141)

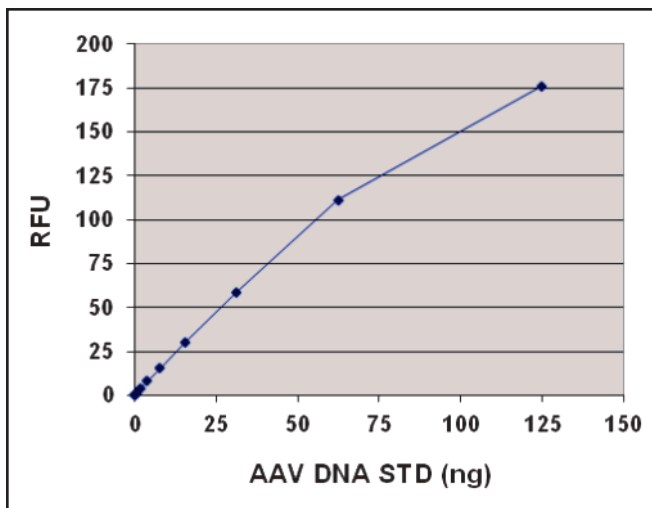


Electrophoretic Profile of Purified AAV2-GFP.

Product Name	Capacity/Prep	Size	Catalog Number
ViraBind™ AAV Purification Kit	Two 10-cm dishes	10 Preps	VPK-140
ViraBind™ AAV Purification Mega Kit	Ten 15-cm dishes	2 Preps	VPK-141
		10 Preps	VPK-141-5

QuickTiter™ AAV Quantitation Kit

Traditional AAV Quantitation by dot blot can be tedious, time consuming, and suffer from high inter-assay variability. Our QuickTiter™ AAV Quantitation Kit uses a proprietary technology to quantify AAV nucleic acid content of unpurified AAV-2 or AAV-DJ, or from purified AAV of any serotype.



AAV-2 DNA Standard Curve. The QuickTiter™ AAV-2 DNA Standard was diluted as described in the assay protocol. Fluorescence was measured on a SpectraMax Gemini XS Fluorometer (Molecular Devices) with a 485/538 nm filter set and 530 nm cutoff.

- **Fast Results:** Obtain purified virus in less than 2 hours
- **High Sensitivity:** Limit of detection 1×10^9 GC/mL from unpurified supernatant or 5×10^{10} GC/mL from purified AAV

Recent Product Citations

1. Orabi, A.I. et al. (2015). Dynamic imaging of pancreatic NF- κ B activation in live mice using AAV infusion and bioluminescence. *J. Biol. Chem.* 10.1074/jbc.M115.647933.
2. Oh, S.M. et al. (2015). Combined Nurr1 and Foxa2 roles in the therapy of Parkinson's disease. *EMBO Mol. Med.* 10.15252/emmm.201404610.
3. Stankowska, D.L. et al. (2015). Neuroprotective effects of transcription factor Brn3b in an ocular hypertension rat model of glaucoma. *Invest. Ophthalmol. Vis. Sci.* 56:893-907.
4. Li, Y. et al. (2014). Assembly and validation of versatile transcription activator-like effector libraries. *Sci. Rep.* 4:4857.
5. Paydar, A. et al. (2014). Extrasynaptic GABAA receptors in mediodorsal thalamic nucleus modulate fear extinction learning. *Mol. Brain* 7:39.
6. Vinnikov, I.A. et al. (2014). Hypothalamic miR-103 protects from hyperphagic obesity in mice. *J. Neurosci.* 34:10659-10674.
7. Ma, J. et al. (2013). RNA interference-mediated silencing of Atp6i prevents both periapical bone erosion and inflammation in the mouse model of endodontic disease. *Infect. Immun.* 81:1021-1030.
8. Tao, P. et al. (2013). In vitro and in vivo delivery of genes and proteins using the bacteriophage T4 DNA packaging machine. *PNAS* 10.1073/pnas.1300867110.

Product Name	Capacity/Prep	Size	Catalog Number
QuickTiter™ AAV Quantitation Kit	Fluorometric	20 Assays	VPK-145

ViraDuctin™ AAV Transduction Reagent

Successful gene expression studies using AAV depend on high transduction efficiencies into host cells. Infection rates appear to be highest in S-phase cells, which can account for a very small fraction of a cell population.

Our ViraDuctin™ AAV Transduction Reagent can significantly increase the transduction efficiency of AAV vectors in both dividing and non-dividing cells. Increases are greatest in non-dividing cells, but even cells in S-phase show a noticeable increase in transduction efficiencies.

- **Higher Efficiencies:** Significantly increase rate of infection of host cells
- **Low Toxicity:** No noticeable effect on cell viability
- **Universal:** Suitable for use with both dividing and non-dividing cells

Recent Product Citation

Nazari, M. et al. (2014). AAV2-mediated follistatin overexpression induces ovine primary myoblasts proliferation. *BMC Biotechnol.* 14:87.

Product Name	Size*	Catalog Number
ViraDuctin™ AAV Transduction Reagent	10 Transductions	AAV-200
	50 Transductions	AAV-201

*Number of transductions performed in 35mm culture dishes. May be modified for use in culture plates or larger dishes. See product insert.

Adenoviral Expression Kits & Reagents

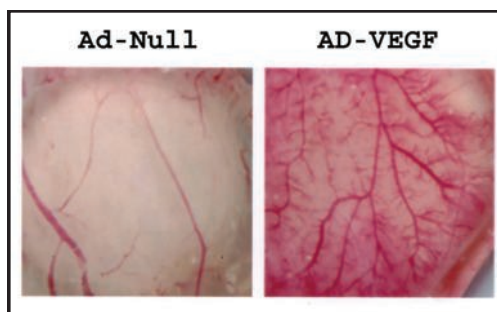
Recombinant adenoviruses are excellent tools for introducing genetic material into host cells, since they can infect a variety of mammalian cell types with high efficiency. They remain epichromosomal upon infection, so they are only suitable for transient gene expression. We offer a complete workflow solution to your adenoviral expression studies:

- Premade Recombinant Adenoviruses
- Viral Expression Systems
- Viral Packaging Cell Line
- Purification Kits
- Quantitation / Titer Kits
- Transduction Reagents

Premade Recombinant Adenoviruses

Don't have time to make your own adenovirus? Are you studying the expression of multiple genes? Rely on our premade recombinant adenoviruses that already contain a gene of interest. All of Cell Biolabs' premade recombinant adenoviruses are provided as 50 μ l aliquots at a concentration of 1×10^{11} viral particles/mL in TBS with 10% glycerol.

Angiogenesis



Blood Vessel Formation After 3 Days. Purified Ad-Null or Ad-VEGF viruses were applied to a 10-day old CAM (chick chorioallantoic membrane). Results were visualized by stereomicroscope.

Recent Product Citations

1. Jiang, Y.Z. et al. (2014). Distinct roles of HIF1A in endothelial adaptations to physiological and ambient oxygen. *Mol. Cell Endocrinol.* **391**:60-67. (ADV-100)
2. Kelber, J.A. et al. (2012). KRas induces a Src/PEAK1/ErbB2 kinase amplification loop that drives metastatic growth and therapy resistance in pancreatic cancer. *Cancer Res.* **72**:2554-2564. (ADV-101)
3. Qiu, X. et al. (2012). Combined strategy of mesenchymal stem cell injection with vascular endothelial growth factor gene therapy for the treatment of diabetes-associated erectile dysfunction. *J. Androl.* **33**:37-44. (ADV-101)
4. Stoletov, K. et al. (2010). Visualizing extravasation dynamics of metastatic tumor cells. *J. Cell Sci.* **123**:2332-2341. (ADV-101)

Target Name	Catalog Number
HIF-1 α	ADV-100
VEGF	ADV-101

Controls and Reporter Genes

Recent Product Citations

1. Wang, Y. et al. (2015). MiR-31 downregulation protects against cardiac ischemia/reperfusion injury by targeting protein kinase C epsilon (PKC ϵ) directly. *Cell Physiol. Biochem.* **36**:179-190. (ADV-001)
2. Haidari, M. et al. (2014). Disruption of endothelial adherens junctions by high glucose is mediated by protein kinase C- β -dependent vascular endothelial cadherin tyrosine phosphorylation. *Circulation.* **130**:112. (ADV-001 and ADV-004)
3. Kaneshiro, S. et al. (2015). MEK5 suppresses osteoblastic differentiation. *Biochem. Biophys. Res. Commun.* **463**:1016-1019. (ADV-002)
4. Choi, J.M. et al. (2015). HepG2 cells as an in vitro model for evaluation of cytochrome P450 induction by xenobiotics. *Arch. Pharm. Res.* **38**:691-704. (ADV-002 and ADV-005)
5. Lampert, F.M. et al. (2015). Overexpression of Hif-1a in mesenchymal stem cells affects cell-autonomous angiogenic and osteogenic parameters. *J. Cell Biochem.* **120**:25361. (ADV-004)
6. Jiang, Y.Z. et al. (2014). Distinct roles of HIF1A in endothelial adaptations to physiological and ambient oxygen. *Mol. Cell Endocrinol.* **391**:60-67. (ADV-004)
7. Salvati, E. et al. (2014). Evidence for G-quadruplex in the promoter of VEGFR-2 and its targeting to inhibit tumor angiogenesis. *Nucleic Acids Res.* **42**:2945-2957. (ADV-004)
8. Wu, Y. et al. (2012). ERK5 regulates glucose-induced increased fibronectin production in the endothelial cells and in the retina in diabetes. *Invest. Ophthalmol. Vis. Sci.* **53**:8405-8413. (ADV-004)
9. Choi, S. et al. (2014). MMP9 processing of HSPB1 regulates tumor progression. *PLoS One* **9**:e85509. (ADV-005)
10. Kato, H. et al. (2011). Wnt/ β -Catenin pathway in podocytes integrates cell adhesion, differentiation and survival. *J. Biol. Chem.* **286**:26003-26015. (ADV-005)

Target Name	Catalog Number
Null Control (No gene)	ADV-001
β -Galactosidase	ADV-002
Cre	ADV-005
Firefly Luciferase	ADV-008
GFP	ADV-004
SEAP (Secretory Alkaline Phosphatase)	ADV-003

Premade Recombinant Adenoviruses, continued

MAP Kinase Signaling

Recent Product Citations

1. Harbrecht, B.G. et al. (2012). Insulin inhibits hepatocyte iNOS expression induced by cytokines by an Akt-dependent mechanism. *Am. J. Physiol. Gastrointest. Liver Physiol* **302**:G116-G122. (ADV-105)
2. Monick, M. et al. (2008). Constitutive ERK MAPK activity regulates macrophage ATP production and mitochondrial integrity. *J. Immunol.* **180**:7485-7496. (ADV-112, ADV-113, ADV-118, ADV-119)
3. Li, M.Y. et al. (2014). Curcumin inhibits 19-kDa lipoprotein of *Mycobacterium tuberculosis* induced macrophage apoptosis via regulation of the JNK pathway. *Biochem. Biophys. Res. Commun.* **446**:626-632. (ADV-115)
4. Jiang, S. et al. (2014). Regulation of hepatic insulin receptor activity following injury. *Am. J. Physiol. Gastrointest. Liver Physiol.* **306**:G886-G892. (ADV-115)
5. Jiang, S. et al. (2011). Role of inhibitory kB kinase and c-Jun NH2-terminal kinase in the development of hepatic insulin resistance in critical illness diabetes. *Am. J. Physiol. Gastrointest. Liver Physiol.* **301**:G454-G463. (ADV-115)
6. Zhao, P. et al. (2015). Filamin A (FLNA) modulates chemosensitivity to docetaxel in triple-negative breast cancer through the MAPK/ERK pathway. *Tumor Biol.* 10.1007/s13277-015-4357-3. (ADV-118)
7. Aissaoui, H. et al. (2015). MDA-9/syntenin is essential for factor VIIa-induced signaling, migration, and metastasis in melanoma cells. *J. Biol. Chem.* **290**:3333-3348. (ADV-118)
8. Zhang, Z. et al. (2013). MEK inhibition leads to lysosome-mediated Na⁺/I⁻ symporter protein degradation in human breast cancer cells. *Endocr. Relat. Cancer* **20**:241-250. (ADV-118)
9. Goc, A. et al. (2015). p70 S6-kinase mediates the cooperation between Akt1 and MEK1 pathways in fibroblast-mediated extracellular matrix remodeling. *Biochim. Biophys. Acta.* **1853**:1626-1635. (ADV-118 and ADV-119)
10. Matsushita, T. et al. (2009). FGFR3 promotes synchondrosis closure and fusion of ossification centers through the MAPK pathway. *Hum. Mol. Genet.* **18**:227-240. (ADV-119)
11. Tan, S.H. et al. (2009). Regulation of cell proliferation and migration by TAK1 via transcriptional control of von Hippel-Lindau tumor suppressor. *J. Biol. Chem.* **284**:18047-18058. (ADV-128)
12. Kaneshiro, S. et al (2015). MEK5 suppresses osteoblastic differentiation. *Biochem. Biophys. Res. Commun.* 10.1016/j.bbrc.2015.05.035. (ADV-129)
13. Stankiewicz, T.R. et al. (2015). Neuronal apoptosis induced by selective inhibition of Rac GTPase versus global suppression of Rho family GTPases is mediated by alterations in distinct mitogen-activated protein kinase signaling cascades. *J. Biol. Chem.* **290**:9363-9376. (ADV-129 and ADV-131)
14. Wu, Y. et al. (2012). ERK5 regulates glucose-induced increased fibronectin production in the endothelial cells and in the retina in diabetes. *Invest. Ophthalmol. Vis. Sci.* **53**:8405-8413. (ADV-130)
15. Zuo, Y. et al. (2015). Modulation fo ERK5 is a novel mechanism by which Cdc42 regulates migration of breast cancer cells. *J. Cell Biochem.* **116**:124-132. (ADV-131)
16. Ozcan, L. et al. (2015). Treatment of obese insulin-resistant mice with an allosteric MAPKAPK2/3 inhibitor lowers blood glucose and improves insulin sensitivity. *Diabetes* **64**:3396-3405. (ADV-138)
17. Taniguchi, C. et al. (2007). The p85a regulatory subunit of phosphoinositide 3-kinase potentiates c-Jun N-terminal kinase-mediated insulin resistance. *Mol. Cell Biol.* **27**:2830-2840. (ADV-161)

Target Name	Catalog Number
ERK2	ADV-112
ERK2 (Dominant Negative)	ADV-113
Interferon- γ	ADV-103
JNK1	ADV-114
JNK1 (Dominant Negative)	ADV-115
MAPKAPK2	ADV-137
MAPKAPK2 (Dominant Negative)	ADV-138
MAPKAPK2 (Constitutively Active)	ADV-139
MEK1 (Dominant Negative)	ADV-118
MEK1 (Constitutively Active)	ADV-119
MEK5	ADV-129
MEK5 (Dominant Negative)	ADV-130
MEK5 (Constitutively Active)	ADV-131
MEKK1	ADV-135
MEKK1 (Dominant Negative)	ADV-136
MKK3	ADV-120
MKK3 (Dominant Negative)	ADV-121
MKK3 (Constitutively Active)	ADV-122
MKK4 (Dominant Negative)	ADV-160
MKK4 (Constitutively Active)	ADV-161
MKK6	ADV-123
MKK6 (Dominant Negative)	ADV-124
MKK6 (Constitutively Active)	ADV-125
MKK7	ADV-126
MKK7 (Dominant Negative)	ADV-127
MKK7 (Constitutively Active)	ADV-128
p38 α	ADV-104
p38 α (Dominant Negative)	ADV-105
Raf1	ADV-132
Raf1 (Dominant Negative)	ADV-133
Raf1 (Constitutively Active)	ADV-134

Premade Recombinant Adenoviruses, continued

Cytoskeleton Regulation / Small GTPase

Recent Product Citations

1. Aissaoui, H. et al. (2015). MDA-9/syntenin is essential for factor VIIa-induced signaling, migration, and metastasis in melanoma cells. *J. Biol. Chem.* **290**:3333-3348. (ADV-149, ADV-152)
2. Mao, Y. et al. (2012). Essential diurnal Rac1 activation during retinal phagocytosis requires $\alpha\text{v}\beta 5$ integrin but not tyrosine kinases focal adhesion kinase or Mer tyrosine kinase. *Mol. Cell Biol.* **23**:1104-1114. (ADV-150)
3. Thomas, M.A. et al. (2009). E4orf1 limits the oncolytic potential of the E1B-55K-deleted adenovirus. *J. Virol.* **83**:2406-2416. (ADV-150)
4. Yu, W.-M. et al. (2009). Laminin is required for Schwann cell morphogenesis. *J. Cell Sci.* **122**:929-936. (ADV-150, ADV-153, ADV-154)
5. Salvati, E. et al. (2014). Evidence for G-quadruplex in the promoter of VEGFR-2 and its targeting to inhibit tumor angiogenesis. *Nucleic Acids Res.* **42**:2945-2957. (ADV-151, ADV-157)
6. Cheng, Z.-J. et al. (2010). Co-regulation of caveolar and Cdc42-dependent fluid phase endocytosis by phosphocaveolin-1. *J. Biol. Chem.* **285**:15119-15125. (ADV-153)
7. Neal M. et al. (2013). A critical role for TLR4 induction of autophagy in the regulation of enterocyte migration and the pathogenesis of necrotizing enterocolitis. *J. Immunol.* **190**:3541-3551. (ADV-156, ADV-157)

Target Name	Catalog Number
Cdc42	ADV-152
Cdc42 L61 (Constitutively Active)	ADV-154
Cdc42 N17 (Dominant Negative)	ADV-153
Rac1	ADV-149
Rac1 L61 (Constitutively Active)	ADV-151
Rac1 N17 (Dominant Negative)	ADV-150
Ras N17 (Dominant Negative)	ADV-145
Ras V12 (Constitutively Active)	ADV-146
Ras V12C40	ADV-148
Ras V12S35	ADV-147
Rho L63 (Constitutively Active)	ADV-157
Rho N19 (Dominant Negative)	ADV-156
SDF-1 α	ADV-210

Cell Cycle & Transcription Regulation

Recent Product Citation

Nguyen, N. et al. (2014). Mitsugumin 53 (MG53) ligase ubiquitinates focal adhesion kinase during skeletal myogenesis. *J. Biol. Chem.* **289**:3209-3216. (ADV-508)

Target Name	Catalog Number
MyoD	ADV-508
p53	ADV-501
p53 (Temperature Sensitive Mutant)	ADV-502

NF κ B Signaling**Recent Product Citation**

Wang, Y. et al. (2015). MiR-31 downregulation protects against cardiac ischemia/reperfusion injury by targeting protein kinase C epsilon (PKC ϵ) directly. *Cell Physiol. Biochem.* **36**:179-190. (ADV-302)

Target Name	Catalog Number
I κ B- α S32A (Dominant Negative)	ADV-302
IKK- β	ADV-305
IKK- β (Dominant Negative)	ADV-303

293AD Cell Line for Adenoviral Packaging and Amplification

The 293AD cell line is ideal for packaging and amplifying adenovirus. The cell line is derived from the parental 293 cell line, but has been specifically selected for adenovirus applications and offers advantages over conventional 293 cells: flattened morphology, firm attachment to culture plates, and a larger surface area for superior transfection and greater viral yields.

Recent Product Citations

1. Bae, E.J. et al. (2015). Cell models to study cell-to-cell transmission of α -synuclein. *Methods Mol. Biol.* **1345**:291-298.
2. Sugiyama, K. et al. (2014). Expression of the miR200 family of microRNAs in mesothelial cells suppresses the dissemination of ovarian cancer cells. *Mol. Cancer Ther.* **13**:2081-2091.
3. Peng, D. et al. (2014). Glutathione peroxidase 7 has potential tumour suppressor functions that are silenced by location-specific methylation in oesophageal adenocarcinoma. *Gut* **63**:540-551.

Product Name	Size	Catalog Number
293AD Cell Line	1 x 10 ⁶ Cells	AD-100

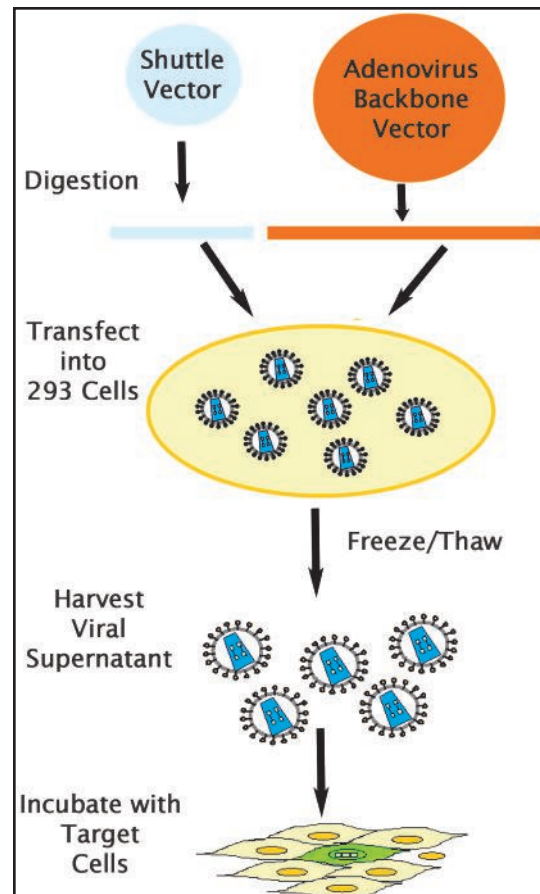
RAPAd® Adenoviral Expression Systems

Compared to other adenoviral expression systems, RAPAd® Adenoviral Expression Systems produce recombinant adenovirus in a much shorter time (about 2-3 weeks) with a substantial reduction in wild-type adenovirus. The RAPAd systems use a backbone vector from which the 5' ITR, packaging signal and E1 sequences have been removed. Additionally, serial amplification of the recombinant adenovirus does not increase the level of replication-competent adenovirus.

Recent Product Citations

- Li, P. et al. (2013). MicroRNA-663 regulates human vascular smooth muscle cell phenotypic switch and vascular neointimal formation. *Circ. Res.* **113**:1117-1127. (VPK-250)
- Bae, E.J. et al. (2015). Cell models to study cell-to-cell transmission of α -synuclein. *Methods Mol. Biol.* **1345**:291-298. (VPK-252)
- Suchanek, A.L. and Salati, L.M. (2015). Construction and evaluation of an adenoviral vector for the liver-specific expression of the serine/arginine rich splicing factor, SRSF3. *Plasmid* 10.1016/j.plasmid.2015.07.004. (VPK-252)
- Li, M. et al. (2014). Bisphenol AF-induced endogenous transcription is mediated by ER α and ERK1/2 activation in human breast cancer cells. *PLoS One* **9**:e94725. (VPK-252)
- Kim, S.C. et al. (2014). All-trans-retinoic acid ameliorates hepatic steatosis in mice by a novel transcriptional cascade. *Hepatology* **59**:1750-1760. (VPK-252)
- Mohan, R. et al. (2015). Differentially expressed microRNA-483 confers distinct functions in pancreatic beta- and alpha-cells. *J. Biol. Chem.* 10.1074/jbc.M115.650705. (VPK-253)
- Sugiyama, K. et al. (2014). Expression of the miR200 family of microRNAs in mesothelial cells suppresses the dissemination of ovarian cancer cells. *Mol. Cancer Ther.* **13**:2081-2091. (VPK-253)
- Feng, J. et al. (2015). SIRT6 suppresses glioma cell growth via induction of apoptosis, inhibition of oxidative stress and suppression of JAK2/STAT3 signaling pathway activation. *Oncol Rep.* 10.3892/or.2015.4477. (VPK-254)
- Lozic, M. et al. (2015). Overexpression of oxytocin receptors in the hypothalamic PVN increases baroreceptor reflex sensitivity and buffers BP variability in conscious rats. *Br. J. Pharmacol.* **171**:4385-4398. (VPK-254)
- Brunton, P.J. et al. (2015). 5 α -reduced neurosteroids sex-dependently reverse central prenatal programming of neuroendocrine stress responses in rats. *J. Neurosci.* **35**:666-677. (VPK-254)

- Virtually No Wild-Type Virus:** Backbone vector engineered to produce <300 wild-type plaques per 10^9 particles, compared with 10^4 - 10^6 WT plaques per 10^9 VP with most other methods
- Faster Production:** Virus generated in 2-3 weeks compared to a few months with traditional methods
- 7 Complete Systems:** Choose CMV or RSV for gene expression, EF-1 for miRNA expression, U6 for shRNA, or clone your own promoter along with your gene of interest using our Universal system



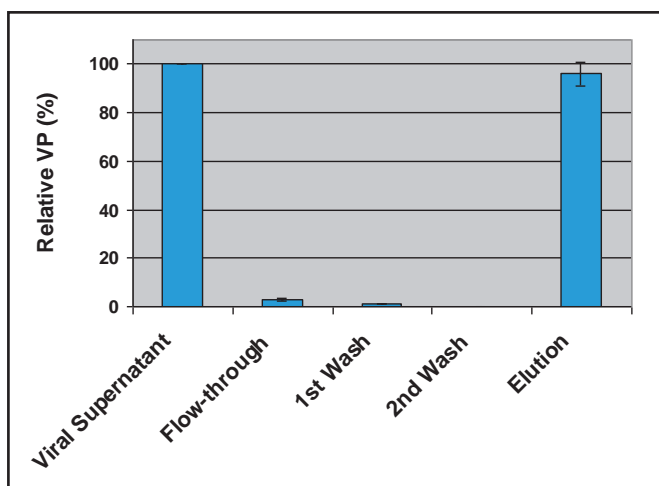
Adenovirus Production using the RAPAd® Adenoviral Expression System.

Product Name	Promoter	Size	Catalog Number
RAPAd® Universal Adenoviral Expression System	None	1 Kit	VPK-250
RAPAd® RSV Adenoviral Expression System	RSV	1 Kit	VPK-251
RAPAd® CMV Adenoviral Expression System	CMV	1 Kit	VPK-252
RAPAd® Bicistronic Adenoviral Expression System (GFP)	CMV	1 Kit	VPK-254
RAPAd® miRNA Adenoviral Expression System	EF-1	1 Kit	VPK-253
RAPAd® shRNA Adenoviral Expression System (Puro)	U6	1 Kit	VPK-255
RAPAd® shRNA Adenoviral Expression System (GFP)	U6	1 Kit	VPK-256

ViraBind™ Adenovirus Purification Kits

Purification of viruses via cesium chloride (CsCl) ultracentrifugation procedures can be tedious and time-consuming. ViraBind™ Adenovirus Purification Kits use an efficient system for quick adenoviral purification with high recovery. No ultracentrifugation is required. Kits use either a spin column or syringe filter for high purity adenovirus (see selection guide).

- **High Viral Yield:** >90% recovery
- **High Quality:** Provides quality of CsCl procedures, but in much less time
- **Faster Results:** 30 minutes (1-2 hrs for Mega kit)
- **User-Friendly Protocol:** No gradient preparation or ultracentrifugation steps



Purification of Recombinant Ad-β-Gal with the ViraBind™ Adenovirus Purification Kit. Ad-β-Gal was purified according to the assay protocol. Each purification fraction was used to infect A549 cells in a 12-well plate. After 48 hr, cells were scored using our β-Galactosidase Staining Kit (p. 114).

Recent Product Citations

1. Morris, S.J. et al. (2015). Laboratory-scale production of replication-deficient adenovirus vectored vaccines. *Vaccine Technol. Vet Viral Disease* 10.1007/978-1-4939-3008-1_8. (VPK-099)
2. Muller, J. et al. (2015). TROM21, a negative modulator of LFG in breast carcinoma MDA-MB-231 cells in vitro. *Int. J. Oncol.* 47:1634-1646. (VPK-099)
3. Zhu, L. et al. (2015). Inhibition of porcine reproductive and respiratory syndrome virus replication with exosome-transferred artificial microRNA targeting the 3' untranslated region. *J. Virol. Methods* 223:61-68. (VPK-099)
4. Boehme, P. et al. (2015). Standard free droplet digital polymerase chain reaction as a new tool for the quality control of high-capacity adenoviral vectors in small-scale preparations. *Hum. Gene Ther. Methods* 26:25-34. (VPK-099)
5. Kumar, A. et al. (2015). Immune responses against hepatitis C virus genotype 3a virus-like particles in mice: a novel VLP prime-adenovirus boost strategy. *Vaccine* 10.1016/j.vaccine.2015.11.061. (VPK-100)
6. Gibot, L. et al. (2015). Cell-based approach for 3D reconstruction of lymphatic capillaries in vitro reveals distinct functions of HGF and VEGF-C in lymphangiogenesis. *Biomaterials* 10.1016/j.biomaterials.2015.11.027. (VPK-100)
7. Betz, V.M. et al. (2015). Gene-activated fat grafts for the repair of spinal cord injury: a pilot study. *Acta Neurochir.* 10.1007/s00701-0154-2626-y. (VPK-100)
8. Garcia-Pascual, C.M. et al. (2015). Evaluation of the potential therapeutic effects of a double-stranded RNA mimic complexed with polycations in an experimental mouse model of endometriosis. *Fertil. Steril.* 10.1016/j.fertnstert.2015.07.1147. (VPK-100)
9. Tu, X. et al. (2015). microRNA-30 protect against CCl4-induced liver fibrosis by attenuating TGF-β signaling in hepatic stellate cells. *Toxicol. Sci.* 10.1093/toxsci/kfv081. (VPK-100)
10. Miklavc, P. et al. (2015). Actin depolymerisation and crosslinking joint forces with myosin II to contract actin coats on fused secretory vesicles. *J. Cell Sci.* 128:1193-1203. (VPK-100)
11. Westermeier, F. et al. (2015). Insulin requires normal expression and signaling of insulin receptor A to a reverse gestational diabetes-reduced adenosine transport in human umbilical vein endothelium. *FASEB J.* 29:37-49. (VPK-100)

Selection Guide for ViraBind™ Adenovirus Purification Kits

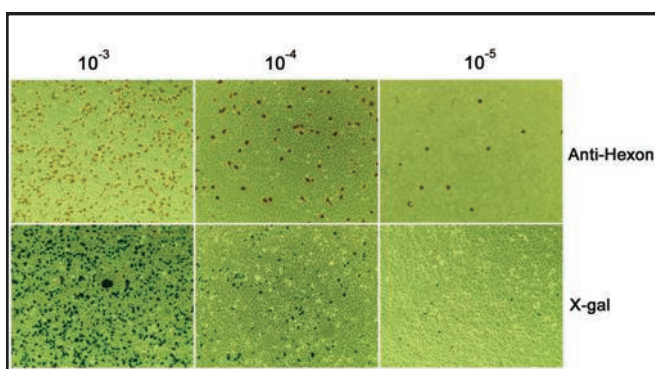
	ViraBind™ Adenovirus Miniprep Kit	ViraBind™ Adenovirus Purification Kit
Purification Method	Spin column	Syringe filter
Purification Time	30 minutes	30 minutes
Capacity/Prep (Viral Particles)	1 x 10 ¹¹ VP	2.5 x 10 ¹² VP
Capacity/Prep (Supernatant)	One T75 flask or one 10cm dish	Four T75 flasks

Product Name	Capacity/Prep	Size	Catalog Number
ViraBind™ Adenovirus Miniprep Kit	1 x 10 ¹¹ VP	10 Preps	VPK-099
ViraBind™ Adenovirus Purification Kit	2.5 x 10 ¹² VP	10 Preps	VPK-100

QuickTiter™ Adenoviral Titer & Quantitation Kits

Accurate measurement of virus titer is critical for viral gene delivery. Traditional plaque-forming unit (PFU) assays are long and have high inter-assay variability. The QuickTiter™ Adenovirus Titer Kits provide a complete system to functionally titer virus infectivity with greater accuracy in a fraction of the time. The assays may be used with any adenovirus system that can amplify in 293 cells. Assays are available for ICC staining or 96-well ELISA.

For a quick test of physical titer, our QuickTiter™ Adenovirus Quantitation Kit measures the concentration of your adenovirus prep in about one hour.



QuickTiter™ Adenovirus Titer Immunoassay Kit. 293AD cells (p. 42) were infected with different dilutions of purified Ad-β-Gal for 48 hours. Immunostaining was performed according to the assay protocol. X-gal staining was performed with β-Galactosidase Staining Kit (p. 106).

- **Faster, More Accurate and Precise:** Compared to traditional plaque-forming unit assays
- **User-Friendly Protocol:** No agar overlay steps
- **Versatile:** Recognize all 41 adenovirus serotypes

Recent Product Citations

1. Nuche-Berenguer, B. et al. (2015). Elucidation of the roles of the Src kinases in pancreatic acinar cell signaling. *J. Cell Biochem.* **116**:22-36. (VPK-106)
2. Sanchez-Lugo, Y.E. et al. (2014). CXCL10/XCL1 fusokine elicits in vitro and in vivo chemotaxis. *Biotechnol. Lett.* **10.1007/s10529-014-1746-1.** (VPK-106)
3. Gibot, L. et al. (2015). Cell-based approach for 3D reconstruction of lymphatic capillaries in vitro reveals distinct functions of HGF and VEGF-C in lymphangiogenesis. *Biomaterials* **10.1016/j.biomaterials.2015.11.027.** (VPK-109)
4. Herath, S. et al. (2015). Analysis of T cell responses to chimpanzee adenovirus vectors encoding HIV gag-pol-nef antigen. *Vaccine* **10.1016/j.vaccine.2015.10.111.** (VPK-109)
5. Yang, Y. et al. (2015). RGD-modified oncolytic adenovirus exhibited potent cytotoxic effect on CAR-negative bladder cancer-initiating cells. *Cell Death Dis.* **6**:e1760. (VPK-109)
6. Nakao, S. et al. (2015). Stimulus-dependent regulation of nuclear Ca²⁺ signaling in cardiomyocytes: a role of neuronal calcium sensor-1. *PLoS One* **10**:e0125050. (VPK-109)
7. Patsouris, D. et al. (2014). Insulin resistance is associated with MCP1-mediated macrophage accumulation in skeletal muscle in mice and humans. *PLoS One* **9**:e110653. (VPK-109)
8. Barrett, A. et al. (2014). A crucial role for DOK1 in PDGF-BB-stimulated glioma cell invasion through p130Cas and Rap1 signalling. *J. Cell Sci.* **127**:2647-2658. (VPK-109)
9. Garcia-Pascual, C.M. et al. (2015). Evaluation of the potential therapeutic effects of a double-stranded RNA mimic complexed with polycations in an experimental mouse model of endometriosis. *Fertil. Steril.* **10.1016/j.fertnstert.2015.07.1147.** (VPK-110)
10. Gibson, H. et al. (2015). Immunotherapeutic intervention with oncolytic adenovirus in mouse mammary tumors. *Oncol Immunology* **4**:e984523. (VPK-110)

Selection Guide for QuickTiter™ Adenoviral Quantitation Kits

	QuickTiter™ Adenovirus Titer Immunoassay Kit	QuickTiter™ Adenovirus Titer ELISA Kit	QuickTiter™ Adenovirus Quantitation Kit
Functional or Physical Titer	Functional (Infectious units)	Functional (Infectious units)	Physical (Viral particles)
Assay Time	2.5 days	2.5 days	45-60 minutes
Assay Principle	Antibody-based	Antibody-based	Total nucleic acid content
Detection Method	Immunocytochemical staining	Colorimetric (ELISA) plate reader	Fluorescence plate reader
Key Benefit	Accuracy	Accuracy	Speed

Product Name	Detection	Size	Catalog Number
QuickTiter™ Adenovirus Titer Immunoassay Kit	ICC Staining	100 Assays	VPK-109
QuickTiter™ Adenovirus Titer ELISA Kit	Colorimetric	2 x 96 Assays	VPK-110
QuickTiter™ Adenovirus Quantitation Kit	Fluorometric	20 Assays	VPK-106

Rapid Replication Competent Adenovirus (RCA) Assay Kit

Traditionally RCA (replication competent adenovirus) is measured in permissive cells by a plaque-forming unit (PFU) assay which takes 10-14 days. This kit uses the assay principles of the QuickTiter™ Adenovirus Titer Immunoassay Kit (see [page 55](#)), but is designed specifically to measure the level of replication-competent virus in your adenoviral prep.

- **Faster Results:** 2.5 days vs. 10 days with the traditional plaque assay
- **Versatile:** Recognizes all 41 adenovirus serotypes

Recent Product Citation

Dubuisson, O. et al. (2015). Accurate identification of neutralizing antibodies to adenovirus Ad36, a putative contributor of obesity in humans. *J. Diabetes Complications* 29:83-87.

Product Name	Detection	Size	Catalog Number
Rapid RCA Assay Kit	ICC Staining	30 Assays	VPK-111
		5 x 30 Assays	VPK-111-5

ViraDuctin™ Adenovirus Transduction Reagent, CAR-Independent

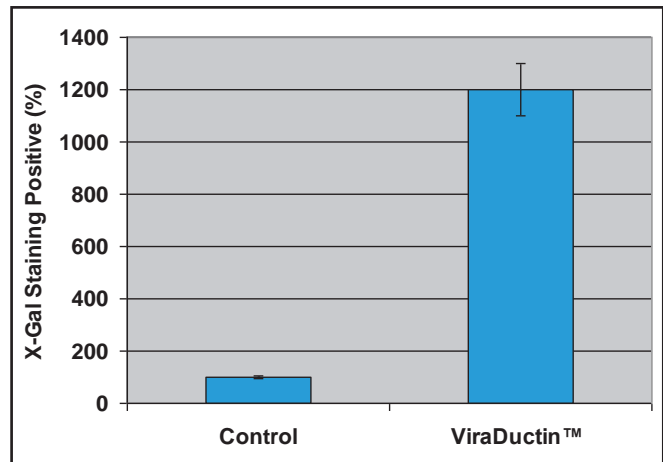
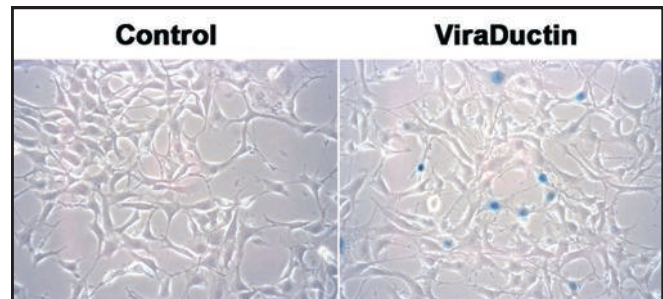
Adenovirus infection of target cells is mediated largely by the coxsackievirus-adenovirus receptor (CAR). Generally adenoviral transduction of many immortalized cell lines proceeds with a high level of efficiency. However, in many primary cells this receptor is either absent or present at extremely low-levels. This can reduce the efficiency of adenovirus transduction into your cell of choice.

ViraDuctin™ Adenovirus Transduction Reagent is designed specifically to increase the efficiency of adenoviral transduction, without regard to the level of CAR expression on the surface of the target cells.

- **Higher Transduction Efficiency:** Up to 12-fold increase in adenoviral uptake
- **User-Friendly:** Short incubation step prior to host cell infection
- **Versatile:** Ideal for target cells expressing little or no CAR, but may also improve transduction efficiency for CAR-expressing cells

Recent Product Citations

1. Haidari, M. et al. (2014). Disruption of endothelial adherens junctions by high glucose is mediated by protein kinase C- β -dependent vascular endothelial cadherin tyrosine phosphorylation. *Cardiovasc. Diabetol.* 13:112.
2. Haidari, M. et al. (2012). Integrin α 2 β 1 mediates tyrosine phosphorylation of vascular endothelial cadherin induced by invasive breast cancer cells. *J. Biol. Chem.* 287:32981-32992.
3. Ackerman, W. et al (2008). Nuclear Factor-kappa B regulates inducible prostaglandin E synthase expression in human amnion mesenchymal cells. *Biol. Reprod.* 78:68-76.



Enhanced Transduction using ViraDuctin™ Adenovirus Transduction Reagent. Infection of NIH3T3 cells with recombinant Ad- β -gal (ADV-002). **Top:** X-gal staining under microscope. **Bottom:** scoring of infection with ViraDuctin™ reagent as a percentage of infection with control.

Product Name	Size*	Catalog Number
ViraDuctin™ Adenovirus Transduction Reagent (CAR-Independent)	10 Transductions	AD-200
	50 Transductions	AD-201

*Based on using 6-well plates or 35mm culture dishes; may also be used with 96-,24- or 12-well plates or 60mm or 100mm dishes.

Lentiviral Expression Kits & Reagents

As a sub-class of retroviruses, lentiviruses based on HIV-1 have the unique advantage of being able to infect both proliferating and non-proliferating cells, and they can be used for both transient and stable gene expression.

We offer a complete workflow solution to your lentiviral expression studies:

- Expression Systems & Vectors
- Premade Controls
- Viral Host Cell Line
- Purification Kits
- Quantitation / Titer Kits
- Transduction Reagents

ViraSafe™ Lentiviral Expression Systems

Lentiviruses based on HIV-1 may infect both dividing and non-dividing cells. Recently developed third-generation lentiviral expression systems have reduced the risk of creating replication-competent virus upon recombination, but the risk is still present.

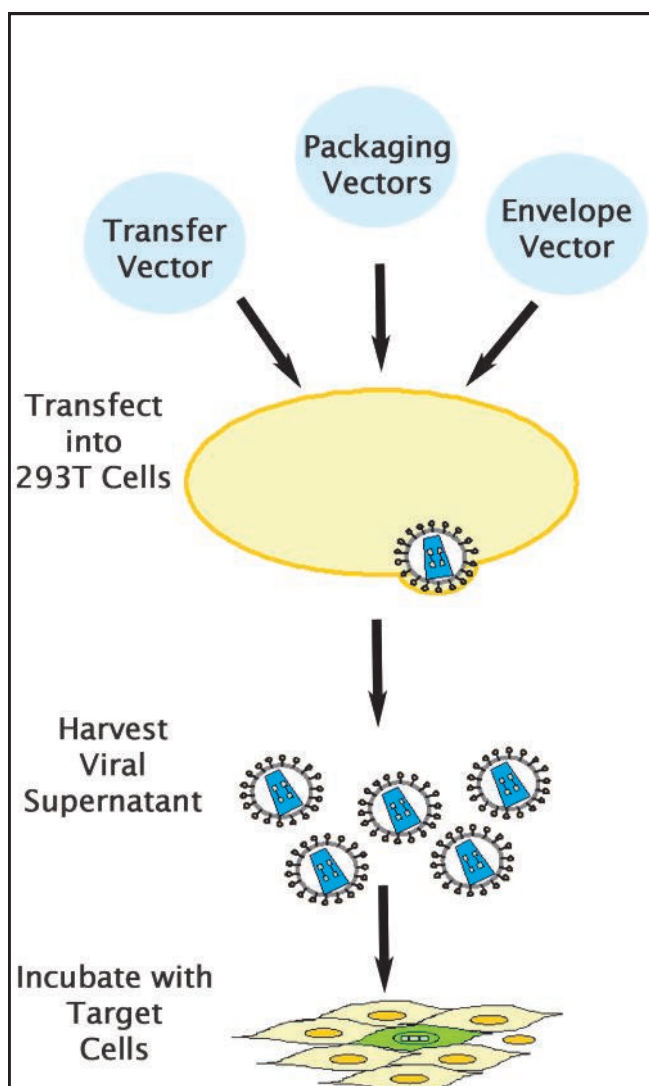
Our ViraSafe™ Lentiviral Expression Systems provide a safer and more flexible method to package your lentivirus, even compared to other third-generation lentivirus systems.

- **Safer:** 80-90% less sequence homology compared to other 3rd-generation lentiviral systems; ecotropic systems provide even more safety*
- **High Titters:** Incorporates elements that provide titers comparable to other 3rd-generation systems
- **Flexible:** Packaging vectors provided separately for increased safety and optimization of vector ratios

*Lentiviruses made with a ViraSafe™ Ecotropic Expression System will only readily infect mouse and rat cells. Pantropic lentiviruses are VSVG-pseudotyped and may infect cells of any species.

ViraSafe™ Lentiviral Technology is available in three formats (see next two pages for ordering information):

- **Complete Expression Systems:** Include 3 packaging plasmids, expression vector and control vector
- **Packaging Systems:** Include the 3 individual packaging plasmids; ideal if you already have a 3rd-generation lentiviral expression construct
- **Expression Vectors:** 11 cloning vectors to choose from; compatible with any 2nd or 3rd generation packaging system, but produce the highest titers with the ViraSafe™ packaging system



Lentivirus Production using the ViraSafe™ Lentiviral Expression System.

ViraSafe™ Lentiviral Expression Systems, continued

Complete ViraSafe™ Expression Systems include three individual packaging plasmids, an expression vector, and a control vector. Choose an ecotropic system for infection of mouse or rat cells, or a pan-tropic system to produce VSVG-pseudotyped lentivirus for infection of cells from any species.

Recent Product Citation

Davis, M. et al. (2013). RAC1P29S is a spontaneously activating cancer-associated GTPase. *PNAS* **110**:912-917. (VPK-214-PAN)

Product Name	Envelope	Size	Catalog Number
ViraSafe™ Universal Lentiviral Expression System (Promoterless)	Ecotropic	1 Kit	VPK-211-ECO
	Pantropic (VSVG)	1 Kit	VPK-211-PAN
ViraSafe™ Lentiviral Expression System (Puro)	Ecotropic	1 Kit	VPK-212-ECO
	Pantropic (VSVG)	1 Kit	VPK-212-PAN
ViraSafe™ Lentiviral Expression System (Neo)	Ecotropic	1 Kit	VPK-213-ECO
	Pantropic (VSVG)	1 Kit	VPK-213-PAN
ViraSafe™ Lentiviral Expression System (Hygro)	Ecotropic	1 Kit	VPK-214-ECO
	Pantropic (VSVG)	1 Kit	VPK-214-PAN
ViraSafe™ Lentiviral Bicistronic Expression System (Puro)	Ecotropic	1 Kit	VPK-215-ECO
	Pantropic (VSVG)	1 Kit	VPK-215-PAN
ViraSafe™ Lentiviral Bicistronic Expression System (Neo)	Ecotropic	1 Kit	VPK-216-ECO
	Pantropic (VSVG)	1 Kit	VPK-216-PAN
ViraSafe™ Lentiviral Bicistronic Expression System (Hygro)	Ecotropic	1 Kit	VPK-217-ECO
	Pantropic (VSVG)	1 Kit	VPK-217-PAN
ViraSafe™ Lentiviral Bicistronic Expression System (Blasticidin)	Ecotropic	1 Kit	VPK-219-ECO
	Pantropic (VSVG)	1 Kit	VPK-219-PAN
ViraSafe™ shRNA Lentiviral Expression System (Puro)	Ecotropic	1 Kit	VPK-221-ECO
	Pantropic (VSVG)	1 Kit	VPK-221-PAN
ViraSafe™ shRNA Lentiviral Expression System (GFP)	Ecotropic	1 Kit	VPK-222-ECO
	Pantropic (VSVG)	1 Kit	VPK-222-PAN

ViraSafe™ Lentiviral Packaging Systems

ViraSafe™ Packaging Systems contain 3 packaging plasmids for use with any 3rd-generation lentiviral expression vector. These systems are perfect if you already have a lentiviral construct containing your gene of interest.

Recent Product Citation

Vogt, J. et al. (2014). Protein associated with SMAD1 (PAWS1/FAM83G) is a substrate for type I bone morphogenetic protein receptors and modulates bone morphogenetic protein signaling. *Open Bio.* **4**:130210. (VPK-206)

Product Name	Envelope	Size	Catalog Number
ViraSafe™ Lentiviral Packaging System	Ecotropic	1 Kit	VPK-205
	Pantropic (VSVG)	1 Kit	VPK-206

ViraSafe™ Lentiviral Expression Vectors

These lentiviral expression vectors may be used with any 2nd or 3rd generation lentiviral packaging system, but best results are achieved when used with our ViraSafe™ Lentiviral Packaging Systems.

Recent Product Citations

1. Wang, Z. et al. (2015). Elabela-apelin receptor signaling pathway is functional in mammalian systems. *Sci. Rep.* **5**:8170. (VPK-211)
2. Meyer, A.E. (2014). Role of TGF- β receptor III localization in polarity and breast cancer progression. *Mol. Biol. Cell* **25**:2291. (VPK-213)
3. Davis, M. et al. (2013). RAC1P29S is a spontaneously activating cancer-associated GTPase. *PNAS* **110**:912-917. (VPK-214)
4. Belin, B. et al. (2013). Visualization of actin filaments and monomers in somatic cell nuclei. *Mol. Biol. Cell* **24**:982-994. (VPK-219)

Product Name	Cloning Capacity	Size	Catalog Number
pSMPUW Universal Lentiviral Expression Vector (Promoterless)	9.4 kb	10 μ g	VPK-211
pSMPUW-Puro Lentiviral Expression Vector	7.9 kb	10 μ g	VPK-212
pSMPUW-Neo Lentiviral Expression Vector	7.7 kb	10 μ g	VPK-213
pSMPUW-Hygro Lentiviral Expression Vector	7.4 kb	10 μ g	VPK-214
pSMPUW-IRES-Puro Lentiviral Expression Vector	7.8 kb	10 μ g	VPK-215
pSMPUW-IRES-Neo Lentiviral Expression Vector	7.5 kb	10 μ g	VPK-216
pSMPUW-IRES-Hygro Lentiviral Expression Vector	7.3 kb	10 μ g	VPK-217
pSMPUW-IRES-Bsd Lentiviral Expression Vector	7.9 kb	10 μ g	VPK-219
pSMPUW-U6-Puro Lentiviral Expression Vector	7.7 kb	10 μ g	VPK-221
pSMPUW-U6-GFP Lentiviral Expression Vector	7.6 kb	10 μ g	VPK-222

Lentiviral Control Plasmids

Product Name	Size	Catalog Number
pLenti-GFP Lentiviral Control Vector	10 μ g	LTV-400
pSMPUW-GFP-Puro Lentiviral Control Vector	10 μ g	LTV-401
pSMPUW-MNDnLacZ Lentiviral Control Vector	10 μ g	LTV-402
pLenti-RFP-Puro Lentiviral Control Vector	100 μ L	LTV-403

Premade Reporter Lentivirus Controls

Product Name	Concentration	Size	Catalog Number
GFP Lentivirus Control	1 x 10 ⁶ TU/mL	200 μ L	LTV-300
RFP Lentivirus Control	1 x 10 ⁶ TU/mL	200 μ L	LTV-301

293LTV Lentiviral Cell Line

Our 293LTV cell line was selected from the parental 293T cell line for firmer attachment to culture plates and larger, rounder morphology for greater lentiviral production.

Recent Product Citations

1. Billcliff, P.G. et al. (2015). OCRL1 engages with the F-BAR protein pacsin 2 to promote biogenesis of membrane trafficking intermediates. *Mol. Biol. Cell* **10**.1091/mbc.E15-06-0329.
2. Latta, C.H. et al. (2015). Determining the role of IL-4 induced neuroinflammation in microglial activity and amyloid- β using BV2 microglial cells and APP/PS1 transgenic mice. *J. Neuroinflamm.* **12**:41.

Product Name	Size	Catalog Number
293LTV Cell Line	1 x 10 ⁶ Cells	LTV-100

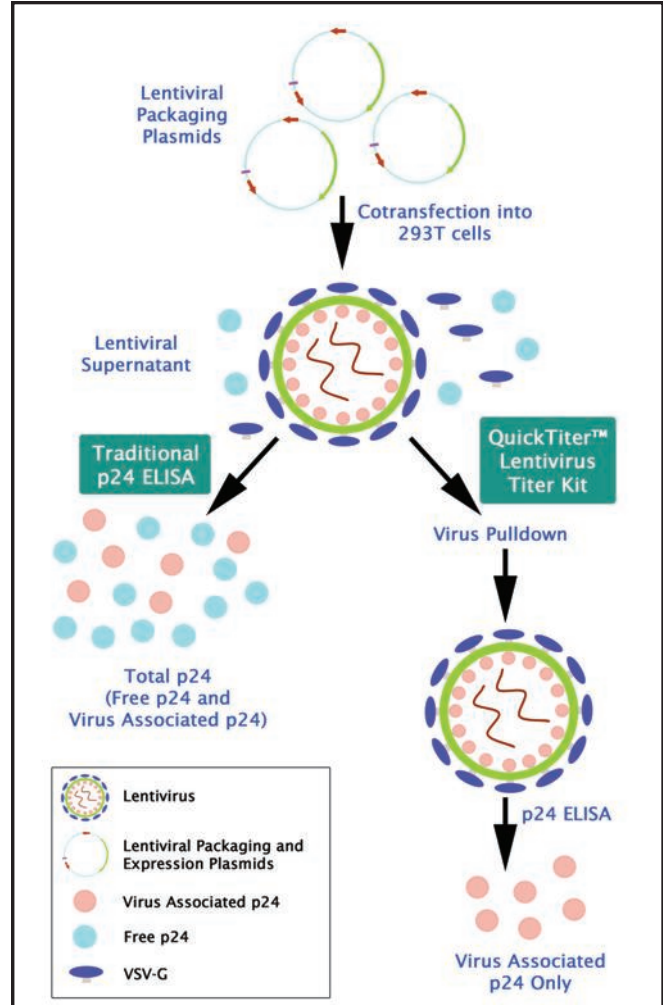
QuickTiter™ Lentivirus Titer / Quantitation Kits

Measuring lentiviral titer is important prior to infection of your target cells, and one of the most published methods is the p24 ELISA. Our traditional p24 ELISA kit provides a quick, convenient way to quantify the concentration of your HIV-1 based lentivirus.

One disadvantage of using a traditional p24 ELISA to quantify lentivirus is the overexpression of p24 during lentiviral packaging. Free p24 protein may account for a substantial portion of total p24 in lentiviral supernatant. The traditional p24 ELISA detects both virus-associated p24 and free p24 generated by 293T cells during transient transfection. Our QuickTiter™ Lentivirus Titer Kit minimizes the overestimation of p24 in lentivirus supernatant. Our proprietary technology separates the lentivirus-associated p24 from free p24 protein prior to performing the ELISA.

If you need a very quick estimate of your lentiviral concentration, try the QuickTiter™ Lentivirus Quantitation Kit. This kit specifically measures the viral nucleic acid content of purified virus or unpurified viral supernatant. This method is ideal for a quick measurement of viral titer, either before or after purification of your lentivirus.

- **More Accurate:** Exclusive technology in QuickTiter™ Lentivirus Titer Kit minimizes overestimation of virus titer
- **User-Friendly:** Read results on a standard microplate reader

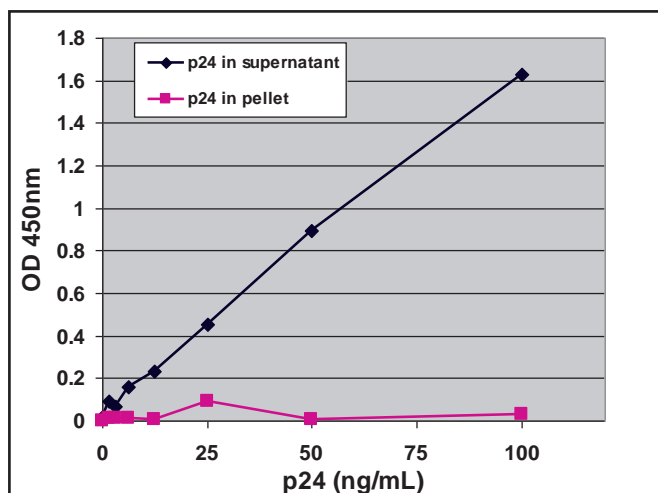


Assay Principle for the QuickTiter™ Lentivirus Titer Kit. Lentivirus particles are packaged with p24 protein, but additional free p24 protein is present in viral supernatant. A traditional p24 ELISA detects both sources of p24 which overestimates viral titer. The QuickTiter™ Lentivirus Titer Kit uses technology to pull the virus out of solution prior to quantitation for a more accurate viral titer.

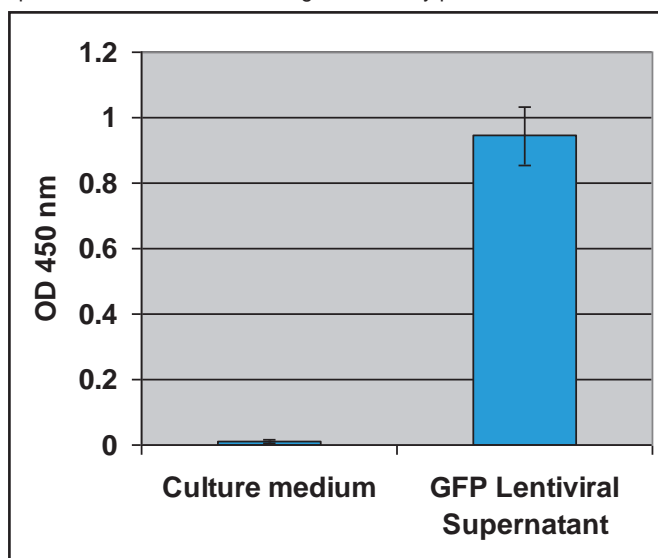
Selection Guide for QuickTiter™ Lentivirus Quantitation & Titer Kits

	QuickTiter™ Lentivirus Titer Kit (Lentivirus-Associated p24 ELISA)	QuickTiter™ Lentivirus Quantitation Kits (Traditional p24 ELISA)	QuickTiter™ Lentivirus Quantitation Kit
Assay Principle	p24 ELISA with proprietary technology to separate free p24 from viral p24	p24 ELISA	Measures nucleic acid content
Suitable Viruses	Recombinant HIV-1	Recombinant or native HIV-1	HIV-1, FIV, SIV
Detection Method	Colorimetric (ELISA) plate reader	Colorimetric (ELISA) plate reader	Fluorescence plate reader
Key Benefit	Accuracy	Most Published	Speed (45-60 min.)

QuickTiter™ Lentivirus Titer / Quantitation Kits, continued



Free p24 Does not Complex with ViraBind™ Reagents. Recombinant p24 was diluted in culture medium and treated with ViraBind™ Lentivirus Reagents A and B found in the QuickTiter™ Lentivirus Titer Kit. The amount of p24 in the supernatant and the pellet was measured according to the assay protocol.



p24 Titer of GFP Lentiviral Supernatant. GFP lentiviral construct was cotransfected with a packaging mix into 293 cells. The conditioned medium was harvested 48 hrs after transfection and used to further infect 293 cells. The p24 level of the diluted lentiviral supernatant (1:10 dilution) was determined as described in the assay protocol.

Recent Product Citations

- Loperfido, M. et al. (2015). piggyBac transposons expressing full-length human dystrophin enable genetic correction of dystrophic mesoangioblasts. *Nucleic Acids Res.* 10.1093/nar/gkv1464. (VPK-107)
- Chen, P.Y. et al. (2015). Endothelial-to-mesenchymal transition drives atherosclerosis progression. *J. Clin. Invest.* 10.1172/JCI82719. (VPK-107)
- Feng, Y. et al. (2015). Natural polymorphisms and oligomerization of human APOBEC3H contribute to single-stranded DNA scanning ability. *J. Biol. Chem.* 10.1074/jbc.M115.666065. (VPK-107)
- Noh, K.M. et al. (2015). ATX tolerates activity dependent histone H3 methyl/phos switching to maintain repetitive element silencing in neurons. *PNAS* 112:6820-6827. (VPK-107)
- Chaubaud, M. et al. (2015). Cell migration and antigen capture are antagonistic processes coupled by myosin II in dendritic cells. *Nat. Commun.* 6:7526. (VPK-107)
- Li, L. et al. (2015). Mammalian target of rapamycin overexpression antagonizes chronic hypoxia-triggered pulmonary arterial hypertension via the autophagic pathway. *Int. J. Mol. Med.* 36:316-322. (VPK-107)
- Zhao, S. et al. (2015). The DEAD-box RNA helicase 5 positively regulates the replication of porcine reproductive and respiratory syndrome virus by interacting with viral Nsp9 in vitro. *Virus Res.* 195:217-224. (VPK-107)
- Haggani, A.A. et al. (2015). Central memory DE4+ cells are preferential targets of double infection by HIV-1. *Viral. J.* 12:184. (VPK-108-H)
- Oh, S.M. et al. (2015). Combined Nurr1 and Foxa2 roles in the therapy of Parkinson's disease. *EMBO Mol. Med.* 10.15252/emmm.201404610. (VPK-108-H)
- Tilton, C.A. et al. (2015). A combination HIV reporter virus system for measuring post-entry event efficiency and viral outcome in primary CD4+ T cell subsets. *J. Virol. Methods* 195:164-169. (VPK-108-H)
- Lucera, M.B. et al. (2014). The histone deacetylase inhibitor Vorinostat (SAHA) increases the susceptibility of uninfected CD4+ T cells to HIV by increasing the kinetics and efficiency of postentry viral events. *J. Virol.* 88:10803-10812. (VPK-108-H)
- Lambert, M.P. et al. (2015). Intramedullary megakaryocytes internalize released platelet factor 4 (PF4) and store it in alpha granules. *J. Thromb. Haemost.* 10.1111/jth.13069. (VPK-112)
- Yadavilli, S. et al. (2015). The emerging role of NG2 in pediatric diffuse intrinsic pontine glioma. *Oncotarget* 6:12141-12155. (VPK-112)
- Ahmad, M.A. et al. (2015). Label-free capacitance-based identification of viruses. *Sci. Rep.* 5:9809. (VPK-112)
- Tang, X. et al. (2015). The advantages of PD1 activating chimeric receptor (PD1-ACR) engineered lymphocytes for PDL1+ cancer therapy. *Am. J. Transl. Res.* 7:460-473. (VPK-112)
- Shin, H.S. et al. (2015). Crosstalk among IL-23 and DNAX activating protein of 2 kDa-dependent pathways promotes osteoclastogenesis. *J. Immunol.* 194:316-324. (VPK-112)

Product Name	Detection	Size	Catalog Number
QuickTiter™ Lentivirus Titer Kit (Lentivirus-Associated HIV p24 ELISA)	Colorimetric	96 Assays	VPK-107
		5 x 96 Assays	VPK-107-5
QuickTiter™ Lentivirus Quantitation Kit (HIV-1 p24 ELISA)	Colorimetric	96 Assays	VPK-108-H
		5 x 96 Assays	VPK-108-H-5
QuickTiter™ Lentivirus Quantitation Kit	Fluorometric	20 Assays	VPK-112

ViraBind™ Lentivirus Purification Kit

Ultracentrifugation methods used for lentiviral supernatants are tedious and time-consuming and usually only partially purify your virus.

The ViraBind™ Lentivirus Purification Kit produces purified lentivirus with extremely high titer without the need for ultracentrifugation. The kit uses a proprietary syringe filter for highly pure lentivirus preps.

- **High Viral Yield:** >90% recovery
- **High Quality:** Provides quality of CsCl procedures,
- **Faster Results:** Quick 2 hour protocol

Recent Product Citation

Zhou, C. et al. (2015). Lhx8 mediated Wnt and TGFβ pathways in tooth development and regeneration. *Biomaterials* 10.1016/j.biomaterials.2015.06.004.

Product Name	Capacity/Prep	Size	Catalog Number
ViraBind™ Lentivirus Purification Kit	2 x 10 ⁸ IFU	10 Preps	VPK-104

ViraDuctin™ Lentivirus Transduction Kit

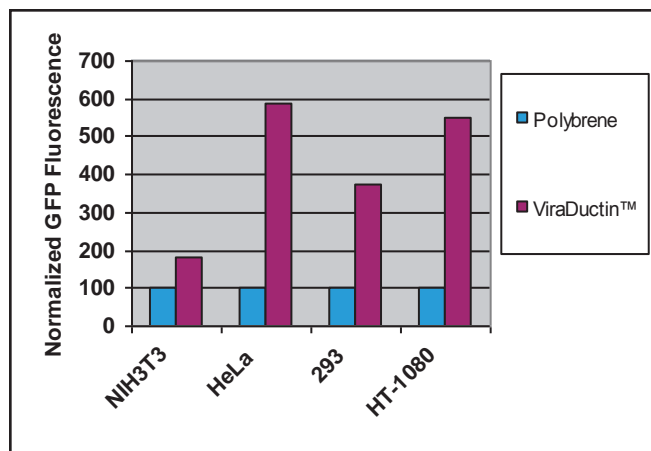
Lentivirus transduction efficiency is typically low. Additives such as Polybrene® can boost transduction efficiencies, but even then only a small fraction of lentiviral vectors can transduce many target cell lines.

Our ViraDuctin™ Lentivirus Transduction Kit provides superior transduction efficiencies in a variety of cell lines, even when compared to transductions in the presence of Polybrene®.

Recent Product Citations

1. Osorio, L.A. et al. (2015). SNAIL transcription factor increases the motility and invasive capacity of prostate cancer cells. *Mol. Med. Rep.* 13:778-786.
2. Kandasamy, K. et al. (2015). Changes in endothelial Cx43 expression inversely correlates with microvessel permeability and VE-cadherin expression in endotoxin challenged lungs. *Am. J. Physiol. Lung Cell Mol. Physiol.* 10.1152/ajplung.00211.2014.
3. Abel, E.V. et al. (2014). The Notch pathway is important in maintaining the cancer stem cell population in pancreatic cancer. *PLoS One* 9:e91983.
4. Ozelo, M.C. et al. (2014). Omental implantation of BOECs in hemophilia dogs results in circulating FVIII antigen and a complex immune response. *Blood* 123:4045-4053.
5. Rossello, R.A. et al. (2013). Mammalian genes induce partially reprogrammed pluripotent stem cells in non-mammalian vertebrate and invertebrate species. *eLife Sci.* 2:e00036.
6. McEachron, T.A. et al. (2010). Protease-activated receptors mediate crosstalk between coagulation and fibrinolysis. *Blood* 116:5037-5044.
7. Zemskova, M. et al. (2010). p53-dependent induction of prostate cancer cell senescence by the PIM1 protein kinase. *Mol. Cancer Res.* 8:1126-1141.

- **Higher Transduction Efficiency:** 2-6x higher in many cell lines compared to Polybrene
- **More Robust:** Useful for transduction of nonpermissive cells, including primary cells and stem cells



Transduction Efficiencies in Various Cell Lines. NIH3T3 cells, HeLa cells, our own 293AD cells (page 36) and HT-1080 cells were each seeded at 50,000 cells/well in a 24-well plate overnight. Cells were infected with GFP lentivirus for 48 hours in the presence of Polybrene® or ViraDuctin™ Lentivirus Transduction Kit. For each cell line, fluorescence levels using the ViraDuctin™ system are depicted relative to a normalized fluorescence of 100 for Polybrene®.

Polybrene is a registered trademark of Abbott Laboratories.

Product Name	Size*	Catalog Number
ViraDuctin™ Lentivirus Transduction Kit	40 Transductions	LTV-200
	200 Transductions	LTV-201

*Based on a 24-well plate. Can also be used with 96-well, 12-well or 6-well plates, as well as 60mm or 100mm dishes. See product insert.

Retroviral Expression Kits & Reagents

Traditional retroviral vectors based on MMLV are useful for integrating genetic material into the host cell genome. However, retrovirus titer tends to be significantly lower than that of adenovirus, which can lead to a lower infection efficiency.

Our retroviral reagents and kits incorporate technologies that increase your chances of successful retroviral expression. We offer a comprehensive solution from start to finish:

- Retroviral Expression Systems
- Retroviral Packaging Cell Lines
- Retroviral Cloning & Expression Vectors
- Gene-Specific Retroviral Vectors
- Concentration / Purification Kits
- Quantitation / Titer Kits
- Transduction Reagents

Platinum Retroviral Packaging Cell Lines

Generate high titers of recombinant retrovirus with a single plasmid transfection* using these extremely powerful, stable cell lines. Platinum Retroviral Packaging Cells are based on the 293T cell line and exhibit greater stability and produce higher yields of retroviral structure proteins, resulting in higher retroviral titers.

The Platinum cell lines were invented in the laboratory of Dr. Toshio Kitamura at the University of Tokyo and are available exclusively from Cell Biolabs. They were first described in the following paper:

Morita, S. et al. (2000). *Gene Therapy* 7:1063-1066.

Recent Product Citations

- Jani, R.A. et al. (2015). STX13 regulates cargo delivery from recycling endosomes during melanosome biogenesis. *J. Cell Sci.* 128:3263-3276. (RV-101)
- Song, A. et al. (2015). Molecular changes associated with acquired resistance to crizotinib in ros1-rearranged non-small cell lung cancer. *Clin. Cancer Res.* 21:2379-2387. (RV-101)
- Ogi, H. et al. (2015). The oncogenic role of the cochaperone Sgt1. *Oncogenesis* 4:e149. (RV-101)
- Chinyengetere, F. et al. (2015). Mice null for the deubiquitinase USP18 spontaneously develop leiomyosarcomas. *BMC Cancer* 15:886. (RV-102)
- Fuerstenau-Sharp, M. et al. (2015). Generation of highly purified human cardiomyocytes from peripheral blood mononuclear cell-derived induced pluripotent stem cells. *PLoS One* 10:e0126596. (RV-102)
- Kuroda, M. et al. (2015). Interaction between TIM-1 and NPC1 is important for cellular entry of Ebola virus. *J. Virol.* 89:6481-6493. (RV-103)

Not sure which Platinum Expression System is right for you? See the table below for a selection guide based on the host species of your target cell.

	Plat-A Cells (Amphotropic)	Plat-E Cells (Ecotropic)	Plat-GP Cells (Pantropic*)
Human	+++	N.S.	+++
Mouse	+++	+++	+++
Rat	+++	+++	+++
Monkey	+++	N.S.	+++
Cat	+++	N.S.	+++
Dog	+++	N.S.	+++
Hamster	+	N.S.	+++
Bird	N.S.	N.S.	+++
Fish	N.S.	N.S.	+++
Frog	N.S.	N.S.	+++
Insect	N.S.	N.S.	+++
Mollusk	N.S.	N.S.	+++

*Plat-GP cells must be co-transfected with a pantropic envelope protein such as VSV-G.
N.S. = Not Suitable

Suitability of Platinum Retroviral Packaging Cell Lines by Host Species.

Product Name	Size	Catalog Number
Platinum-E Retroviral Packaging Cell Line, Ecotropic	$\geq 3 \times 10^6$ cells	RV-101
Platinum-A Retroviral Packaging Cell Line, Amphotropic	$\geq 3 \times 10^6$ cells	RV-102
Platinum-GP Retroviral Packaging Cell Line, Pantropic	$\geq 3 \times 10^6$ cells	RV-103
pVSV-G Packaging Vector	10 μ g	RV-110

Platinum Retroviral Packaging Cells and Expression Systems

Our Platinum Retroviral Expression Systems incorporate superior packaging cell lines and vector technologies to produce high-titer virus with a single plasmid transfection. Each Platinum Expression System includes one of our exclusive Platinum Packaging Cell Lines which stably express the gag and pol genes. In the Ecotropic and Amphotropic systems, the packaging cells also express the envelope protein.* Simply clone your gene of interest into the vector provided and transfect into the Platinum cells.

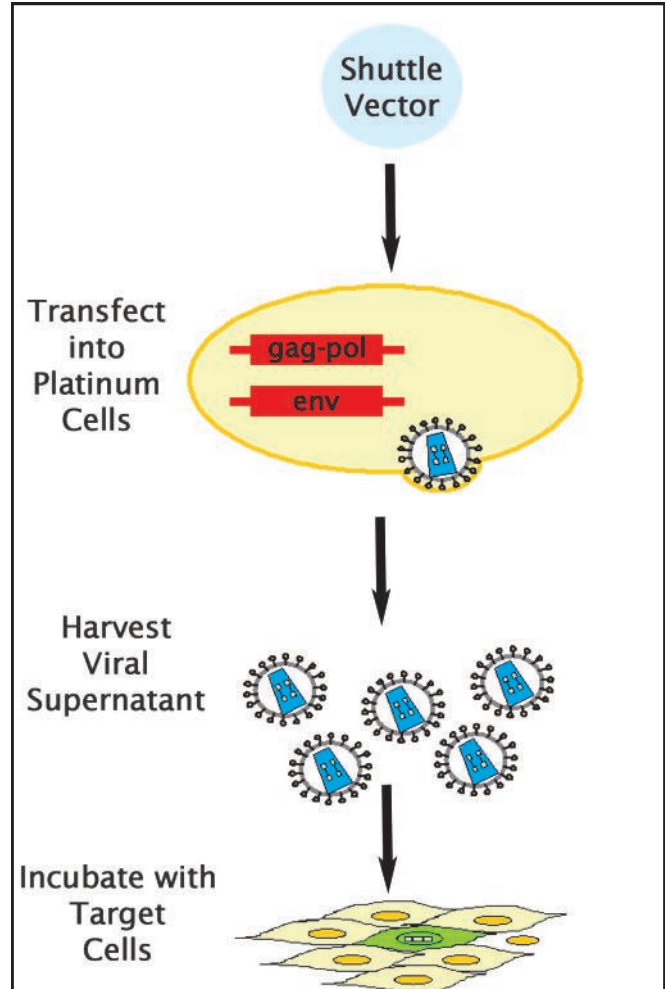
- **Higher Viral Yields:** Average titer 10^7 infectious units/mL with transient transfection
- **Longer Stability:** Expression up to 4 months in the presence of drug selection
- **Optimized Systems:** 3 packaging cell lines for infection of various species; 3 vector backbones (two specifically for infection of stem cells)
- **Flexible:** Order complete systems or cells and vectors separately

*Pantropic systems require co-transfection with the provided VSVG envelope vector.

Recent Product Citations

1. Aoi, N. et al. (2012). 1 α ,25-dihydroxyvitamin D3 modulates the hair-inductive capacity of dermal papilla cells: therapeutic potential for hair regeneration. *Stem Cells Trans Med.* 1:615-626. (VPK-301)
2. Saito, Y. et al. (2015). Enhancement of spontaneous activity by HCN4 overexpression in mouse embryonic stem cell-derived cardiomyocytes—a possible biological pacemaker. *PLoS One* 10:e0138193. (VPK-302)
3. Yamaguchi, J. et al. (2015). Inflammation and hypoxia linked to renal injury by CCATT/enhancer-binding protein δ . *Kidney Int.* 10.1038/ki.2015.21. (VPK-302)
4. Wang, N. et al. (2013). Lacritin rescues stressed epithelia via rapid forkhead box O3 (FOXO3)-associated autophagy that restores metabolism. *J. Biol. Chem.* 288:18146-18161. (VPK-302)
5. Kishida, T. et al. (2015). Reprogrammed functional brown adipocytes ameliorate insulin resistance and dyslipidemia in diet-induced obesity and type 2 diabetes. *Stem Cell Reports* 10.1016/j.stemcr.2015.08.007. (VPK-303, VPK-305)

Each system contains a packaging cell line, an expression vector, and GFP control vector. Our pantropic systems also contain a VSVG envelope vector.



Retrovirus Production Using the Platinum Expression Systems (Ecotropic and Amphotropic).

Product Name	Expression Vector	Packaging Cell	Catalog Number
Platinum Retroviral Expression System, Ecotropic	pMXs-Puro	Plat-E	VPK-300
Platinum Retroviral Expression System, Amphotropic	pMXs-Puro	Plat-A	VPK-301
Platinum Retroviral Expression System, Pantropic	pMXs-Puro	Plat-GP	VPK-302
Platinum ES/EC Retroviral Expression System, Ecotropic	pMCs-Puro	Plat-E	VPK-303
Platinum ES/EC Retroviral Expression System, Amphotropic	pMCs-Puro	Plat-A	VPK-304
Platinum ES/EC Retroviral Expression System, Pantropic	pMCs-Puro	Plat-GP	VPK-305
Platinum HSC Retroviral Expression System, Ecotropic	pMYs-Puro	Plat-E	VPK-306
Platinum HSC Retroviral Expression System, Amphotropic	pMYs-Puro	Plat-A	VPK-307
Platinum HSC Retroviral Expression System, Pantropic	pMYs-Puro	Plat-GP	VPK-308

Retroviral Cloning & Expression Vectors

Our Retroviral Expression Vectors are based on backbones derived from Moloney murine leukemia virus (MMLV). We offer the traditional pBABE system and the novel pMXs system, which has been shown to be useful in induced pluripotent stem cell (iPS) studies. pMYs vectors are optimal for use with hematopoietic stem cells, and pMCs vectors are optimal for ES and EC cells. All cloning vectors are supplied as 10 µg in TE buffer.

Retroviral Cloning Vectors for General Gene Expression (driven by 5' LTR)

Recent Product Citations

- Diep, C.M. et al. (2015). Retroviral expression of human cystatin genes in HeLa cells. *Methods Mol. Bio.* **1249**:121-131. (RTV-001-PURO)
- Nakamura, H. et al. (2015). Genomic spectra of biliary tract cancer. *Nat. Genet.* **47**:1003-1010. (RTV-010)
- Yeon, J.T. et al. (2015). Arginase 1 is a negative regulator of osteoclast differentiation. *Amino Acids* **10.1007/s00726-015-2112-0**. (RTV-012)
- Kageyama-Yahara, N. et al. (2014). Gli regulates MUC5AC transcription in human gastrointestinal cells. *PLoS One* **9**:e106106. (RTV-013)
- Koso, H. et al. (2014). Identification of FoxR2 as an oncogene in medulloblastoma. *Cancer Res.* **74**:2351-2361. (RTV-014, RTV-015)

Vector Name	Cloning Capacity	Catalog Number
pBABEhygro	5.6 kb	RTV-001-HYGRO
pBABEneo	5.9 kb	RTV-003
pBABEpuro	6 kb	RTV-001-PURO
pBABEzeo	6.3 kb	RTV-004
pMXs	5.4 kb	RTV-010
pMXs-IRES-Bsd	5.6 kb	RTV-016
pMXs-IRES-GFP	5.3 kb	RTV-013
pMXs-IRES-Neo	5.2 kb	RTV-015
pMXs-IRES-Puro	5.4 kb	RTV-014
pMXs-Neo	3.8 kb	RTV-011
pMXs-Puro	4.4 kb	RTV-012
pMZs	5.3 kb	RTV-030

Retroviral Cloning Vector for miRNA

Recent Product Citation

Mansour, M. et al. (2013). The TAL1 complex targets the FBXW7 tumor suppressor by activating miR-223 in human T cell acute lymphoblastic leukemia. *J. Exp. Med.* **210**:1545-1557. (RTV-017)

Vector Name	Cloning Capacity	Catalog Number
pMXs-miR-GFP/Puro	4.2 kb	RTV-017

Retroviral Cloning Vectors with Strong Promoters for Overexpression

Vector Name	Cloning Capacity	Catalog Number
pMXs-CAG	5.2 kb	RTV-064
pMXs-CMV	5.5 kb	RTV-065
pMXs-EF1 α	5.5 kb	RTV-063
pMXs-EF1-Bsd	4.2 kb	RTV-062
pMXs-EF1-GFP	3.9 kb	RTV-061
pMXs-EF1-Puro	4 kb	RTV-060
pMXs-SR α	5.4 kb	RTV-066

Retroviral Cloning Vectors for use with ES/EC Cells

Recent Product Citation

Mochizunki, Y. et al. (2013). Phosphatidylinositol 3-phosphate myotubularin-related protein 6 (MTMR6) is regulated by small GTPase Rab1b in the early secretory and autophagic pathways. *J. Biol. Chem.* **288**:1009-1021. (RTV-041)

Vector Name	Cloning Capacity	Catalog Number
pMCs-IRES-GFP	5.2 kb	RTV-040
pMCs-Puro	4.3 kb	RTV-041

Retroviral Cloning Vectors for use with Hematopoietic Cells

Recent Product Citation

Xiao, X. et al. (2015). GITR subverts Foxp3+ Tregs to boost Th9 immunity through regulation of histone acetylation. *Nat. Commun.* **6**:8266. (RTV-021)

Vector Name	Cloning Capacity	Catalog Number
pMYs	5.2 kb	RTV-020
pMYs-IRES-GFP	5.2 kb	RTV-021
pMYs-IRES-Neo	5.2 kb	RTV-023
pMYs-IRES-Puro	5.4 kb	RTV-022
pMYs-Puro	4.3 kb	RTV-024

Retroviral Cloning Vectors for shRNA

Vector Name	Cloning Capacity	Catalog Number
pMXs-U6-GFP	5 kb	RTV-071
pMXs-U6-Puro	5.1 kb	RTV-070
pMXs-U6-Puro-shGFP		RTV-055
pMXs-U6-Puro-shLuc		RTV-056

Retroviral Packaging Vectors and Cells

Recent Product Citations

- Amagai, Y. et al. (2015). A point mutation in the extracellular domain of KIT promotes tumorigenesis of mast cells via ligand-independent auto-dimerization. *Sci. Rep.* **5**:9775. (RV-110)
- Zhang, T. et al. (2015). Homoharringtonine binds to and increases myosin-9 in myeloid leukemia. *Br. J. Pharmacol.* 10.1111/bph.13359. (RV-110)
- Okamoto, K. et al. (2012). Dengue virus strain DEN2 16681 utilizes a specific glycochain of syndecan-2 proteoglycan as a receptor. *J. Gen. Virol.* **93**:761-770. (RV-110, RV-111)
- Ng, A.J. et al. (2015). The DNA helicase Recq14 is required for normal osteoblast expansion and osteosarcoma formation. *PLoS Genet.* 10:e1005160. (RV-112)

Product Name	Size	Catalog Number
pCMV-10A1 Envelope Vector	100 µL	RV-114
pCMV-Ampho Envelope Vector	100 µL	RV-113
pCMV-Eco Envelope Vector	100 µL	RV-112
pCMV-Gag-Pol Retroviral Vector	10 µg	RV-111
pCMV-VSV-G Envelope Vector	10 µg	RV-110

293RTV Cell Line

Our 293RTV cells are derived from the 293 parental cell line, but are selected for firmer attachment to culture plates, faster growth and higher yields of retrovirus produced.

Product Name	Size	Catalog Number
293RTV Cell Line	≥1 x 10 ⁶ cells	RV-100

Gene-Specific Recombinant Retroviral Vectors

These constructs are based on backbones derived from MMLV. Vectors with GFP or stem cell factors are supplied as 10 µg of plasmid in TE buffer. All other vectors are supplied as 100 µL of bacterial glycerol stock. Product listing continues on the following pages.

Cell Cycle

Recent Product Citation

Huang, J. et al. (2009). Regulation of the leucocyte chemoattractant receptor FPR in glioblastoma cells by cell differentiation. *Carcinogenesis* **30**(2):348-355. (RTV-401)

Target Name	Vector Backbone	Catalog Number
c-Abl	pBABEpuro	RTV-402
c-Abl-TM	pBABEpuro	RTV-403
c-Abl (1-565)	pBABEpuro	RTV-404
c-Abl (1-958)	pBABEpuro	RTV-405
hTERT	pBABEhygro	RTV-007
	pBABEneo	RTV-005
	pBABEpuro	RTV-006
p53	pBABEpuro	RTV-401

Autophagy

This vector is supplied with a separate pMXs-GFP control vector at no additional cost.

Target Name	Vector Backbone	Catalog Number
GFP-LC3	pMXs	RTV-801

Reporter Genes

Recent Product Citations

- Hrdlickova, R. et al. (2012). Alternatively spliced telomerase reverse transcriptase variants lacking telomerase activity stimulate cell proliferation. *Mol. Cell Biol.* **32**:4283-4296. (RTV-002)
- Malaver-Ortega, L.F. et al. (2013). Inducing pluripotency in cattle. *Methods Mol. Biol.* 10.1007/978-1-4939-2848-4_6. (RTV-050)

Target Name	Vector Backbone	Catalog Number
GFP	pBABE	RTV-002
GFP	pMCs	RTV-051
GFP	pMX	RTV-050
GFP	pMYs	RTV-052
GFP-Puro	pMX	RTV-053

Gene-Specific Recombinant Retroviral Vectors, continued

Cytoskeleton Regulation

Recent Product Citation

Zhao, B. et al. (2012). TNF-induced osteoclastogenesis and inflammatory bone resorption are inhibited by transcription factor RBP-J. *J. Exp. Med.* **209**:2467-2483. (RTV-101)

Target Name	Vector Backbone	Mutation State	Catalog Number
Cdc42	pBABEhygro	L61	RTV-203
K-Ras	pBABEpuro	N/A	RTV-220
	pWZLhygro	Q61	RTV-221
myr-Rac1	pBABEpuro	N/A	RTV-201
		V12	RTV-206
Rac1	pBABEhygro	V12	RTV-202
N-Ras	pBABEpuro	K61	RTV-222
Rac3	pBABEhygro	V12	RTV-205
Ras	pBABEpuro	V12	RTV-101
	pBABEpuro	V12C40	RTV-104
	pBABEpuro	V12G37	RTV-103
	pBABEpuro	V12S35	RTV-102
RhoA	pBABEhygro	L63	RTV-204

iPS / Stem Cell Factors

Human iPS Genes

Target Name	Vector Backbone	Catalog Number
4-Vector Set*	pMXs	RTV-701-C
6-Vector Set**	pMXs	RTV-709-C
c-Myc	pMXs	RTV-703
Klf4	pMXs	RTV-704
Lin-28	pMXs	RTV-710
NANOG	pMXs	RTV-709
Oct-3/4	pMXs	RTV-701
Sox2	pMXs	RTV-702
p53 shRNA	pRetro	RTV-410

Mouse iPS Genes

Target Name	Vector Backbone	Catalog Number
4-Vector Set*	pMXs	RTV-705-C
6-Vector Set**	pMXs	RTV-711-C
c-Myc	pMXs	RTV-707
Klf4	pMXs	RTV-708
Lin-28	pMXs	RTV-712
NANOG	pMXs	RTV-711
Oct-3/4	pMXs	RTV-705
Sox2	pMXs	RTV-706
p53 shRNA	pRetro	RTV-400

*4-Vector sets contain individual constructs with the following genes: c-Myc, Klf4, Oct-3/4 and Sox2.

**6-Vector sets contain individual constructs with the following genes: c-Myc, Klf4, Oct-3/4, Sox2, Lin-28 and NANOG.

Proteases and Related Molecules

Target Name	Vector Backbone	Catalog Number
uPA	pBABEpuro	RTV-501
uPAR	pBABEhygro	RTV-502

Recent Product Citation

Gutova, M. et al (2008). Urokinase plasminogen activator and urokinase plasminogen activator receptor mediate human stem cell tropism to malignant solid tumors. *Stem Cells* **26**:1406-1413. (RTV-501, RTV-502)

Gene-Specific Recombinant Retroviral Vectors, continued

MAP Kinase Signaling

Vector Name	Vector Backbone	Mutation State	Catalog Number
ERK2	pBABEhygro	Dominant Negative	RTV-109
JNK1	pBABEpuro	Dominant Negative	RTV-110
MAPKAPK2	pBABEpuro	Constitutively Active	RTV-118
	pBABEpuro	Dominant Negative	RTV-119
MAPKAPK3	pBABEpuro	Constitutively Active	RTV-120
	pBABEpuro	Dominant Negative	RTV-121
MEK1	pBABEhygro	Constitutively Active	RTV-112
	pBABEhygro	Dominant Negative	RTV-111
MKK3	pBABEpuro	Constitutively Active	RTV-114
	pBABEhygro	Dominant Negative	RTV-115
MKK6	pBABEpuro	Constitutively Active	RTV-116
	pBABEhygro	Dominant Negative	RTV-117
myr-Akt1	pWZLneo	Constitutively Active	RTV-125
p38 α	pBABEhygro	Dominant Negative	RTV-105
p38 β	pBABEhygro	Dominant Negative	RTV-106
p38 γ	pBABEhygro	Dominant Negative	RTV-107
p38 δ	pBABEhygro	Wild Type	RTV-128
PI3K p110 α -CAAX	pWZLneo	Constitutively Active	RTV-124
PRAK	pBABEpuro	Constitutively Active	RTV-122
	pBABEpuro	Dominant Negative	RTV-123
Raf1-CAAX	pWZLneo	Constitutively Active	RTV-113

Transcription Regulation

Target Name	Vector Backbone	Catalog Number
AUF1	pBABEpuro	RTV-305
hnRNPA0	pBABEpuro	RTV-310
hnRNP-A2	pBABEpuro	RTV-340
HuB	pBABEpuro	RTV-302
HuC	pBABEpuro	RTV-303
HuD	pBABEpuro	RTV-301
HuR	pBABEpuro	RTV-304
PABP	pBABEpuro	RTV-307
Stat5A	pMXs	RTV-330
Stat5A(1*6)	pMXs	RTV-331

Recent Product Citation

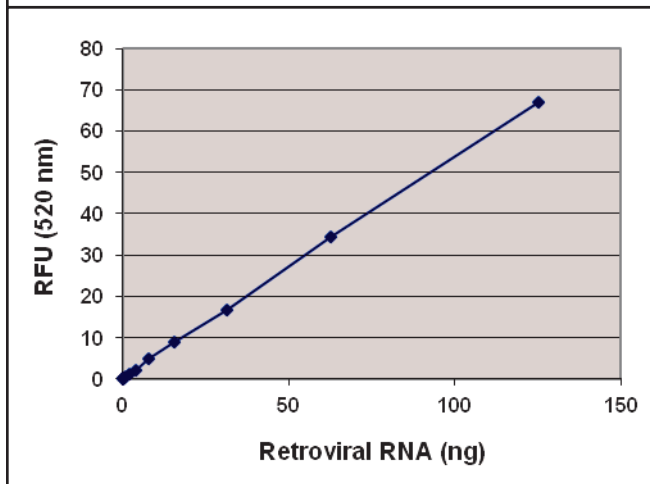
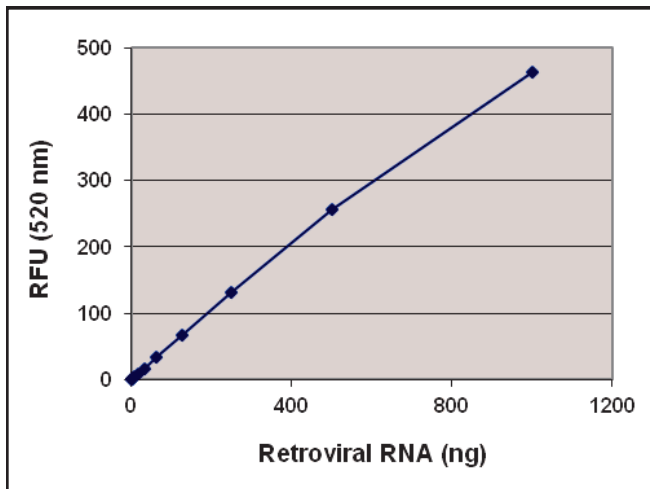
Yu, Y. et al. (2012). Bcl11a is essential for lymphoid development and negatively regulates p53. *J. Exp. Med.* **209**:2467-2483. (RTV-331)

Target Name	Vector Backbone	Catalog Number
Stat5A-IRES-GFP	pMXs	RTV-332
Stat5A(1*6)-IRES-GFP	pMXs	RTV-333
Stat5B	pMXs	RTV-334
Stat5B(1*6)	pMXs	RTV-335
TIA-1	pBABEpuro	RTV-309
TIAR	pBABEpuro	RTV-308
TTP	pBABEpuro	RTV-306

QuickTiter™ Retrovirus Rapid Quantitation Kit

This kit specifically measures the viral nucleic acid content of purified virus or unpurified viral supernatant. This method is ideal for a quick measurement of viral titer, either before or after purification of your retrovirus.

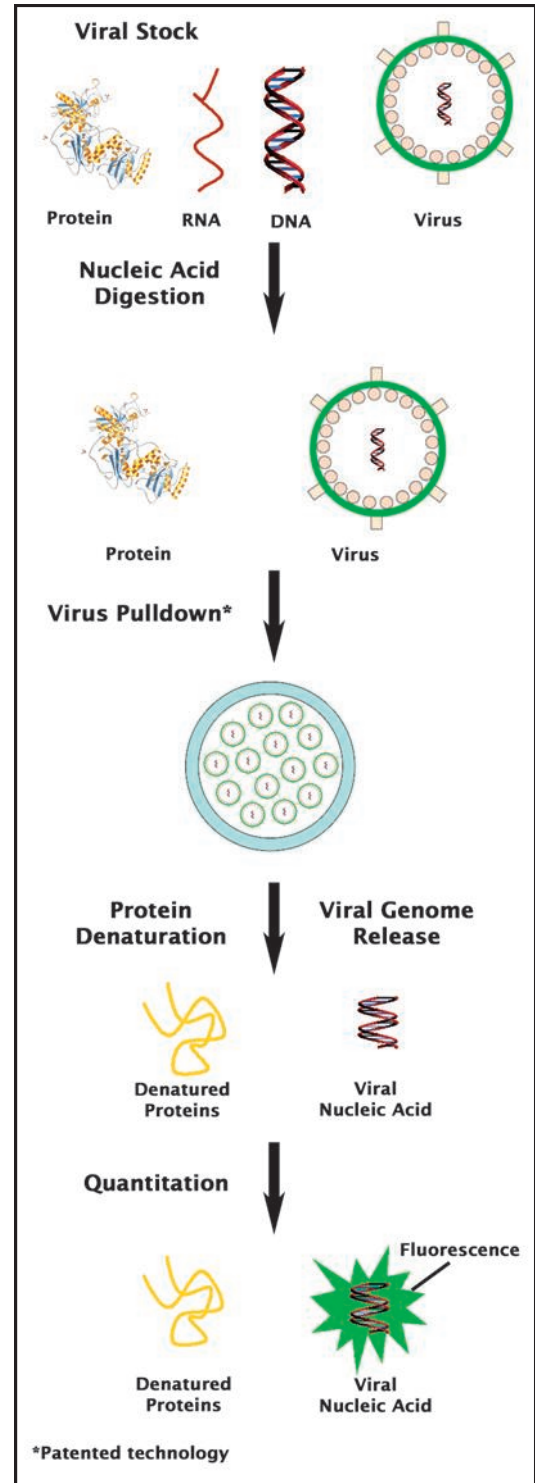
- **Ultra-fast Results:** 45-60 minute procedure
- **Sensitive:** Limit of detection = 1.5×10^9 VP/mL from 2 mL of retroviral supernatant



Retrovirus RNA Standard Curve. The QuickTiter™ Retrovirus RNA Standard was diluted according to the assay protocol. Fluorescence was measured on a SpectraMax Gemini XS Fluorometer.

Recent Product Citations

1. Manian, K.V. et al. (2015). Understanding the molecular basis of heterogeneity in induced pluripotent stem cells. *Cell Rerogram.* 17:427-440.
2. Ito, T. et al. (2012). Stem cell factor programs the mast cell activation phenotype. *J. Immunol.* 188:5428-5437.



Assay Procedure for the QuickTiter™ Retrovirus Quantitation Kit.

Product Name	Detection	Size	Catalog Number
QuickTiter™ Retrovirus Quantitation Kit	Fluorometric	20 Assays	VPK-120

ViraDuctin™ Retrovirus Transduction Kit

The efficiency of retrovirus transduction can be low compared to other viruses. The rate at which retroviral vectors bind to cells is controlled mostly by diffusion. Additionally, the presence of transduction inhibitors such as proteoglycans and glycosaminoglycans in retroviral supernatants can lead to poor gene transfer. Additives such as Polybrene® can boost transduction efficiencies, but they do not eliminate these transduction inhibitors.

Our ViraDuctin™ Retrovirus Transduction Kit provides superior transduction efficiencies even when compared to transductions in the presence of Polybrene®. A proprietary reagent cocktail forms a supercomplex with the retrovirus which is pelleted away from the supernatant, removing detrimental transduction inhibitors that decrease infection efficiency.

- **More Robust:** Removes harmful transduction inhibitors from retroviral supernatant
- **Higher Transduction Efficiencies:** Compared to infections in the presence of Polybrene or no additives
- **Versatile:** Particularly useful for nonpermissive cells including primary cells and stem cells, but may boost transduction rates in a wide variety of cells

Recent Product Citations

1. Gandhi, M. et al. (2012). Homologous chromosomes make contact at the sites of double-strand breaks in genes in somatic G0/G1-phase human cells. *PNAS* **109**:9454-9459.
2. Miyoshi, N. et al. (2010). Defined factors induce reprogramming of gastrointestinal cancer cells. *PNAS* **107**:40-45.

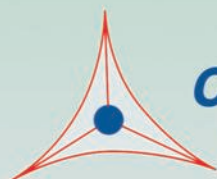
Product Name	Size*	Catalog Number
ViraDuctin™ Retrovirus Transduction Kit	40 Transductions	RV-200
	200 Transductions	RV-201

*Number of transductions shown is based on use in a 24-well plate. This product may also be used with 96-well, 12-well or 6-well plates, as well as 60mm or 100mm dishes. See product insert for specific details.

Polybrene is a registered trademark of Abbott Laboratories.

Oxidative Stress / Damage

Choose Oxidative Stress Assays by Sample Type	72
Oxidative Protein Damage	73
Lipid Peroxidation	79
DNA / RNA Damage	84
Hypoxia Assays	91
Reactive Oxygen Species (ROS) Assays	92
Antioxidant Assays	96
Oxidase / Peroxidase Assays	102



CELL BIOLABS, INC.

Creating Solutions for Life Science Research

Measuring Oxidative Stress

Oxidative stress may be measured using one of three primary methods:

- Measure the reactive oxygen species (ROS) directly
- Measure the presence of antioxidants
- Measure the resulting damage to proteins, lipids, DNA or RNA (most reliable)

Use the following table to determine the best oxidative stress assays for your samples.

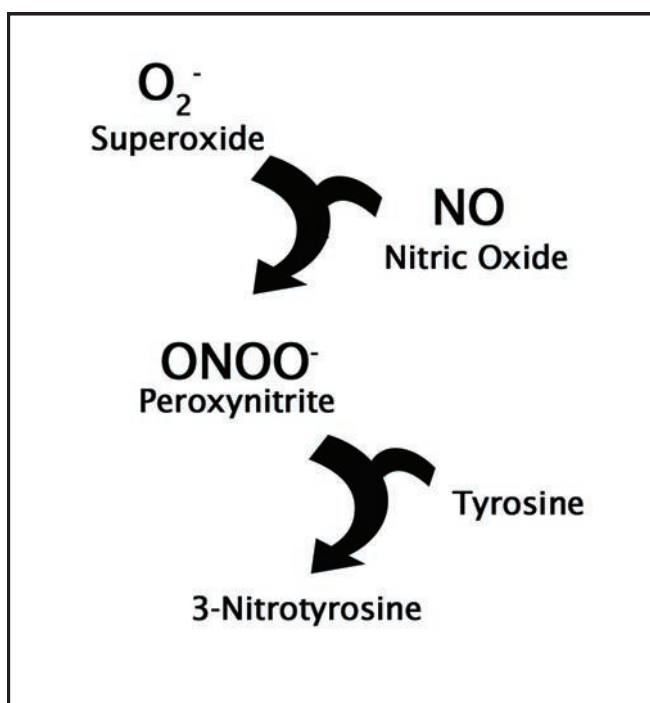
	Marker or Type of Damage	Sample Type				
		Cells	Tissues	Blood	Urine	Other
Protein Damage (p. 73-78)	Protein carbonyl content (PCC)	X	X	X		
	3-Nitrotyrosine	X	X	X		
	BPDE Protein Adduct	X	X	X		
	Advanced Glycation End Products (AGE)	X	X	X		
	Advanced Oxidation Protein Products (AOPP)	X	X	X		
	Protein Radicals	X	X	X		
	S-Glutathione Protein Adduct	X	X	X		
Lipid Peroxidation (p. 79-83)	4-Hydroxynonenal (4-HNE)	X	X	X		
	Malondialdehyde (MDA)	X	X	X	X	
	8-iso-Prostaglandin F _{2α} (8-Isoprostane)	X	X	X	X	
	Oxidized LDL and HDL (OxLDL & OxHDL)			X		
DNA / RNA Damage and Repair (p. 84-90)	8-hydroxyguanosine (8-OHG)	X	X	X	X	Cerebrospinal Fluid
	8-hydroxydeoxyguanosine (8-OHdG)	X	X	X	X	
	Abasic (AP) sites	X	X			
	Aldehyde DNA Damage (Etheno adducts)	X	X			
	BPDE DNA Adduct	X	X			
	Comet Assay	X				
	Double-strand DNA breaks	X				
UV DNA Damage (CPD and 6-4PP)	X					
Reactive Oxygen Species (p. 92-95)	Universal ROS	X	X	X	X	
	Hydrogen Peroxide	X	X	X	X	
	Nitric Oxide	X	X	X	X	Saliva
Antioxidants & Antioxidant Capacity (p. 96-101)	Superoxide Dismutase	X	X	X	X	
	Catalase	X	X	X		
	Glutathione	X	X	X	X	
	Ascorbic Acid	X	X	X		Food
	Total Antioxidant Capacity (TAC & FRAP)	X	X	X		Food
	Oxygen Radical Antioxidant Capacity (ORAC)	X	X	X		Food
	Hydroxyl Radical Antioxidant Capacity (HORAC)	X	X	X		
	Cellular Antioxidant Capacity (CAA)					Antioxidant compounds

Assays and Reagents for Protein Damage

Cellular proteins are subject to damage in the presence of reactive oxygen species (ROS). The resulting protein damage may take the form of nitration or oxidation of various amino acid residues, or may result in formation of advanced glycation end products (AGE) or advanced oxidation protein products (AOPP). We have developed unique assays to detect protein damage with higher sensitivity and more user-friendly protocols.

OxiSelect™ Nitrotyrosine Assay Kits and Antibodies

Our OxiSelect™ Nitrotyrosine Assay Kits provide a simple method to measure the formation of 3-nitrotyrosine in proteins. This assay is available in two formats: a 96-well competitive ELISA and an immunoblot kit. The ELISA format can detect the presence of 3-nitrotyrosine as low as 10 nM. Both kits can detect nitrotyrosine in protein from any species.



Formation of 3-Nitrotyrosine During Oxidative Stress.

Recent Product Citations

- Shivanna, B. et al. (2015). Omeprazole attenuates pulmonary aryl hydrocarbon receptor activation and potentiates hyperoxia-induced developmental lung injury in newborn mice. *Toxicol. Sci.* 10.1093/toxsci/kfv183. (STA-303)
- Capo, X. et al. (2015). Diet supplementation with DHA-enriched food in football players during training season enhances the mitochondrial antioxidant capabilities in blood mononuclear cells. *Eur. J. Nutr.* 54:35-49. (STA-303)
- Zhang, Z.Y. et al. (2015). Enhanced therapeutic potential of nano-curcumin against subarachnoid hemorrhage-induced blood-brain barrier disruption through inhibition of inflammatory response and oxidative stress. *Mol. Neurobiol.* 10.1007/s12035-015-9635. (STA-305)
- Yoshioka, K. et al. (2015). Sepsia prevents left ventricular hypertrophy and dilatory remodeling induced by pressure overload in rats. *Am J. Physiol. Heart Circ. Physiol.* 10.1152/ajpheart.00417.2015.
- Peh, H.Y. et al. (2015). Vitamin E isoform ψ -tocotrienol down-regulates house dust mite-induced asthma. *J. Immunol.* 195:437-444. (STA-305)
- Toth, P. et al. (2015) IGF-1 deficiency impairs neurovascular coupling in mice: implications for cerebrovascular aging. *Aging Cell* 10.1111/ace1.12372. (STA-305)
- Maingrette, F. et al. (2015). Psychological stress impairs ischemia-induced neovascularization: protective effect of fluoxetine. *Atherosclerosis* 241:569-578. (STA-305)
- Wang, Y.N. et al. (2015). Protein interacting with C-kinase deficiency impairs glutathione synthesis and increases oxidative stress via reduction of surface excitatory amino acid carrier 1. *J. Neurosci.* 35:6429-6443. (STA-305)
- Sataranatarajan, K. et al. (2015). Neuron specific reduction in CuZnSOD is not sufficient to initiate a full sarcopenia phenotype. *Redox Biol.* 10.1016/j.redox.2015.04.005. (STA-305)
- Stonehouse, W. et al. (2015). Palmolein and olive oil consumed within a high protein test meal have similar effects on postprandial endothelial function in overweight and obese men: a randomized controlled trial. *Atherosclerosis* 239:178-185. (STA-305)

Product Name	Detection	Size	Catalog Number
Nitrotyrosine ELISA Kit	Colorimetric	96 Assays	STA-305
		5 x 96 Assays	STA-305-5
Nitrotyrosine Immunoblot Kit	Immunoblot/ECL	10 Blots	STA-303
Goat Anti-Nitrotyrosine Polyclonal Antibody	Immunoblot/ELISA	100 μ g	STA-003
Rabbit Anti-Nitrotyrosine Polyclonal Antibody	Immunoblot/ELISA	100 μ g	STA-004
Protein Tyrosine Nitration Control (Nitrotyrosine-BSA)	Immunoblot/ECL	10 μ g	STA-304

OxiSelect™ Protein Carbonyl Assay Kits

The most common products of protein oxidation in biological samples are the carbonyl derivatives of Pro, Arg, Lys and Thr residues. Such derivatives are chemically stable and serve as markers for oxidative stress in most types of reactive oxygen species.

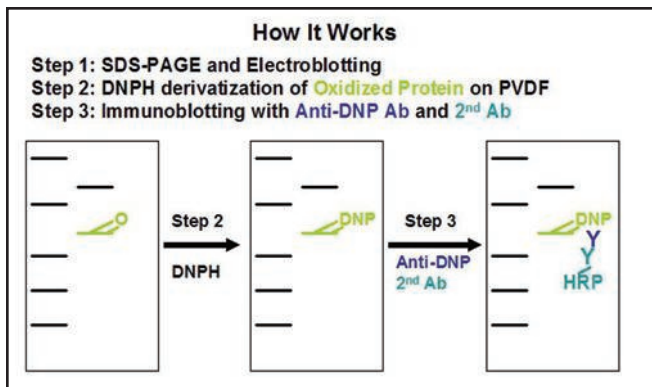
Our OxiSelect™ Protein Carbonyl Assay Kits provide rapid, efficient methods for detection of protein carbonyls. Four assay formats are available: immunoblot, ELISA, fluorometric and spectrophotometric. All formats are suitable for use with purified protein, plasma, serum, or cell lysate samples from any species.

Protein Carbonyl ELISA Kit

- **Sensitive:** Detects samples as low as 10 µg/ml
- **Greater Sample Retention:** No concentration or TCA precipitation steps that contribute to sample loss

Protein Carbonyl Immunoblot Kit

- **No Molecular Weight Shift:** DNPH derivatization after immunoblotting allows direct comparison of oxidized and non-oxidized protein fingerprints



Assay Principle for the OxiSelect™ Protein Oxidation Immunoblot Kit (STA-308).

Recent Product Citations

1. Lauritzen, K.H. et al. (2015). Impaired dynamics and function of mitochondria caused by mtDNA toxicity leads to heart failure. *Am. J. Physiol. Heart Circ. Physiol.* **309**:H434-H449. (STA-307)
2. Tong, M. et al. (2014). Therapeutic reversal of chronic alcohol-related steatohepatitis with the ceramide inhibitor myricin. *Int. J. Exp. Pathol.* **95**:49-63. (STA-307)
3. Zhou, J. et al. (2015). Correlations between photodegradation of bisretinoid constituents of retina and dicarbonyl adduct deposition. *J. Biol. Chem.* **290**:27215-27227. (STA-308)
4. Martorell, M. et al. (2015). Docosahexaenoic acid supplementation promotes erythrocyte antioxidant defense and reduces protein nitrosative damage in male athletes. *Lipids* **50**:131-148. (STA-308)
5. Cui, Z. et al. (2014). Identification of the immunoproteasome as a novel regulator of skeletal muscle differentiation. *Mol. Cell Biol.* **34**:96-109. (STA-308)
6. Kim, K.C. et al. (2015). Non-thermal dielectric-barrier discharge plasma damages human keratinocytes by inducing oxidative stress. *Int. J. Mol. Med.* **347**:29-38. (STA-310)
7. Ahn, M.Y. et al. (2015). Gene expression profiling and inhibition of adipose tissue accumulation of G. bimaculatus extract in rats on high fat diet. *Lipids Health Dis.* **14**:116. (STA-310)
8. Kim, H.K. et al. (2015). The link between mitochondrial complex I and brain-derived neurotrophic factor in SH-SY5Y cells—the potential of JNX1001 as a therapeutic agent. *Eur. J. Pharmacol.* **764**:379-384. (STA-310)
9. Seo, S.W. et al. (2015). Differential tissue-specific function of Adora2b in cardioprotection. *J. Immunol.* 10.4049/jimmunol.1402288. (STA-310)
10. Williams, A.S. et al. (2015). Innate and ozone-induced airway hyperresponsiveness in obese mice: role of TNF α . *Am. J. Physiol. Lung Cell Mol. Physiol.* **308**:L1168-L1177. (STA-310)
11. Westenbrink, B.D. et al. (2015). Mitochondrial reprogramming induced by CaMKII δ mediates hypertrophy decompensation. *Circ. Res.* **116**:e28-e39. (STA-310)
12. Alway, S.E. et al. (2015). Green tea extract attenuates muscle loss and improves muscle function during disuse, but fails to improve muscle recovery following unloading in aged rats. *J. Appl. Physiol.* **118**:319-330. (STA-310)
13. Zhu, X. et al. (2015). Role of spermidine in overwintering of cyanobacteria. *J. Bacteriol.* **197**:2325-2334. (STA-315)
14. Cai, H. et al. (2015). Cancer chemoprevention: evidence of a nonlinear dose response for the protective effects of resveratrol in humans and mice. *Sci. Transl. Med.* **7**:298ra117. (STA-315)
15. Dupre-Aucouturier, S. et al. (2015). Trichostatin A, a histone deacetylase inhibitor, modulates unloaded-induced skeletal muscle atrophy. *J. Appl. Phys.* 10.1152/jappphysiol.01031.2014. (STA-315)
16. Tanase, M. et al. (2015). Hydrodynamic size-based separation and characterization of protein aggregates from total cell lysates. *Nat. Protoc.* **10**:134-148. (STA-315)

Product Name	Detection	Size	Catalog Number
OxiSelect™ Protein Carbonyl ELISA Kit	Colorimetric	96 Assays	STA-310
		5 x 96 Assays	STA-310-5
OxiSelect™ Protein Carbonyl Fluorometric Assay	Fluorometric	100 Assays	STA-307
OxiSelect™ Protein Carbonyl Spectrophotometric Assay	Spectrophotometric	40 Assays	STA-315
OxiSelect™ Protein Carbonyl Immunoblot Kit	Immunoblot/ECL	10 Blots	STA-308
Oxidized Protein Immunoblot Control (Carbonyl-BSA)	Immunoblot/ECL	10 µg	STA-309

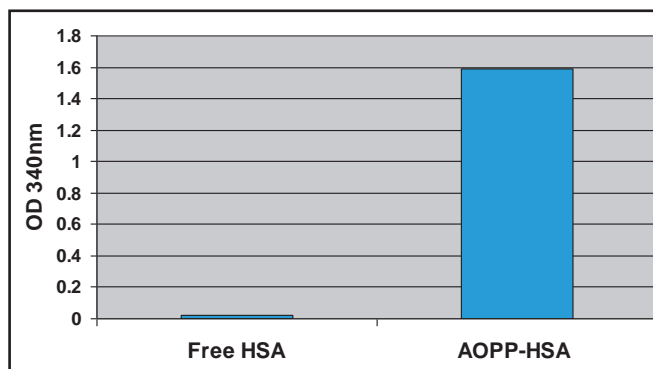
OxiSelect™ AOPP Assay Kit

Advanced oxidation protein products are toxins created during oxidative stress in patients with diabetes mellitus, atherosclerosis, renal complications, and HIV. Our OxiSelect™ AOPP Assay Kit provides a quick, easy method for assessing AOPP levels.

Recent Product Citations

- Jung, E. et al. (2015). Gemigliptin improves renal function and attenuates podocyte injury in mice with diabetic nephropathy. *Eur. J. Pharmacol.* 10.1016/j.ejphar.2015.04.055.
- Bloomer, R.J. et al. (2015). Comparison of a restricted and unrestricted vegan diet plan with a restricted omnivorous diet plan on health-specific measures. *Healthcare* 3:544-555.
- Witthaus, M.W. et al. (2014). Bladder oxidative stress in sleep apnea contributes to detrusor instability and nocturia. *J. Urol.* 10.1016/j.juro.2014.11.055.
- Zhang, Q. et al. (2014). Effects of ischemia and oxidative stress on bladder purinoceptors expression. *Urology* 84:e1-e7.

- **Fast:** Obtain results in <30 minutes
- **Sensitive:** Detect concentrations as low as 5 μ M



Untreated Human Serum Albumin and AOPP-HSA Positive Control Tested with the OxiSelect™ AOPP Assay Kit.

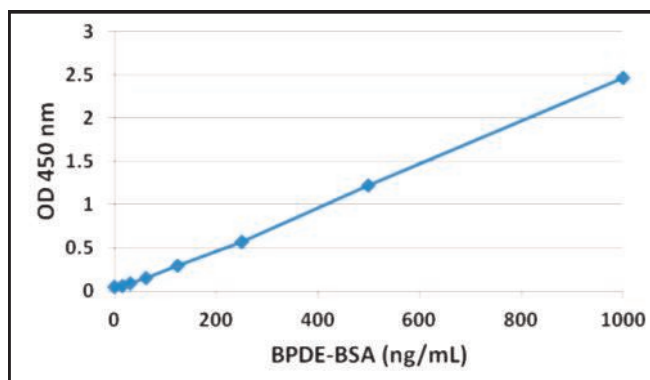
Product Name	Detection	Size	Catalog Number
OxiSelect™ AOPP Assay Kit	Colorimetric	200 Assays	STA-318
AOPP-Human Serum Albumin	N/A	50 μ L	STA-319

OxiSelect™ BPDE Protein Adduct ELISA Kit

Polycyclic aromatic hydrocarbons (PAH) are potent carcinogenic pollutants commonly associated with oil, cigarette smoke, and automotive exhaust. They may also be found in some cooked foods. One PAH, benzo(a)pyrene, was the first chemical carcinogen to be discovered. Through a series of enzymatic reactions, benzo(a)pyrene is converted to benzo(a)pyrene 7,8 diol-9,10 epoxide (BPDE) which attacks both proteins and DNA.

Our OxiSelect™ BPDE Protein Adduct ELISA Kit provides a convenient method to measure the modification of proteins by BPDE.

- **Sensitive:** Detect concentrations as low as 60 ng/mL
- **Convenient:** Quantify on a standard microplate reader
- **Versatile:** Suitable for use with cell lysates, tissue homogenates, plasma or serum



BPDE-BSA Standard Curve Generated Using the OxiSelect™ BPDE Protein Adduct ELISA Kit.

Recent Product Citation

Feng, P.H. et al. (2015). Dysfunction of methionine sulfoxide reductases to repair damaged proteins by nickel nanoparticles. *Chem. Biol. Interact.* 10.1016/j.cbi.2015.05.003.

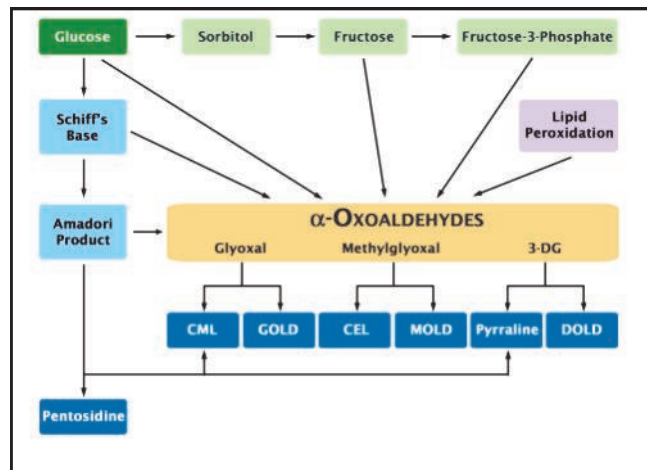
For information on our BPDE DNA Adduct ELISA Kit, please see **page 89**.

Product Name	Detection	Size	Catalog Number
OxiSelect™ BPDE Protein Adduct ELISA Kit	Colorimetric	96 Assays	STA-301

OxiSelect™ Advanced Glycation End Product Kits & Antibodies

Advanced glycation end products (AGE) are formed during the Maillard reaction where reducing carbohydrates react with lysine side chains and N-terminal amino groups of various macromolecules, particularly proteins. These AGE products can adversely affect the function of the affected proteins and play a role in atherosclerosis, diabetes, aging and renal disease.

Our OxiSelect™ Advanced Glycation End Product Kits are designed for the rapid detection of AGE protein adducts. We offer assays to study generic AGE formation or specific AGE structures including N^ε-(Carboxyethyl) lysine (CEL), N^ε-(Carboxymethyl) lysine (CML), and methylglyoxal (MG). All kits will detect AGE structures from protein of any species.



Advanced Glycation End Products (AGE) Pathways.

OxiSelect™ Advanced Glycation End Product (AGE) Competitive ELISA Kit

Our OxiSelect™ Advanced Glycation End Product (AGE) Competitive ELISA Kit detects a variety of AGE structures including CML and pentosidine. It does not detect CEL or methylglyoxal (MG).

Samples are added to a plate coated with an AGE-protein conjugate. AGE-protein adducts in the sample compete with the AGE-coated plate for antibody binding. High AGE adduct content in a sample results in less binding of the antibody to the plate, producing a low signal. Conversely, low AGE content in a sample results in most antibody binding to the plate, producing a higher signal.

- **Sensitive:** Detect levels as low as 1 µg/mL of AGE-protein adduct
- **Versatile:** Compatible with cell lysates, plasma, serum, or purified proteins

Recent Product Citations

1. Martins, L.S. et al. (2015). Advanced Glycation Endproducts (AGE) evolution after pancreas-kidney transplantation: plasmatic and cutaneous assessments. *Oxid. Med. Cell Longev.* 2189582.
2. Chen, S.J. et al. (2015). Methylglyoxal-derived hydroimidazolone residue of plasma protein can behave as a predictor of prediabetes in Spontaneously Diabetic Torii rats. *Physiol. Rep.* 3:e12477.
3. Song, Y. et al. (2014). Ferulic acid alleviates the symptoms of diabetes in obese rats. *J. Funct. Foods* 9:141-147.
4. Foster, D. et al. (2014). AGE metabolites: a biomarker linked to cancer disparity? *Cancer Epidemiol. Biomarkers Prev.* 23:2186-2191.

Product Name	Detection	Size	Catalog Number
OxiSelect™ Advanced Glycation End Product (AGE) Competitive ELISA Kit	Colorimetric	96 Assays	STA-817
		5 x 96 Assays	STA-817-5
Glycoaldehyde-AGE-BSA	N/A	100 µg	STA-348

OxiSelect™ N^ε-(Carboxyethyl) Lysine (CEL) Competitive ELISA Kit

The OxiSelect™ N^ε-(Carboxyethyl) Lysine (CEL) Competitive ELISA Kit detects CEL protein adducts in a variety of samples including cell lysates, blood samples, and other protein sources.

- **Sensitive:** Detect levels as low as 100 ng/mL of CEL-protein adduct
- **Versatile:** Compatible with cell lysates, plasma, serum, or purified proteins

Recent Product Citation

Morgan, P.E. et al. (2014). Perturbation of human coronary artery endothelial cell redox state and NADPH generation by methylglyoxal. *PLoS One* 9:e86564.

Product Name	Detection	Size	Catalog Number
OxiSelect™ N ^ε -(Carboxyethyl) Lysine (CEL) Competitive ELISA Kit	Colorimetric	96 Assays	STA-813
CEL-BSA	N/A	100 µg	STA-302

OxiSelect™ N^ε-(Carboxymethyl) Lysine (CML) Assays and Antibodies

The OxiSelect™ N^ε-(Carboxymethyl) Lysine (CML) Competitive ELISA Kit detects CML protein adducts in a variety of samples including cell lysates, blood samples, and other protein sources.

- **Sensitive:** Detect levels as low as 3 ng/mL of CML-protein adduct with the ELISA kit
- **Versatile:** Compatible with cell lysates, plasma, serum, or purified proteins

Recent Product Citations

1. Martins, L.S. et al. (2015). Advanced Glycation Endproducts (AGE) evolution after pancreas-kidney transplantation: plasmatic and cutaneous assessments. *Oxid. Med. Cell Longev.* 2189582.
2. Niquet-Leridon, C. et al. (2015). The rehabilitation of raw and brown butters by the measurement of two of the major Maillard products, N^ε-Carboxymethyl-Lysine and 5-hydroxymethylfurfural, with validated chromatographic methods. *Food Chemistry* **177**:361-368.
3. Huang, T.C. et al. (2014). Increased renal semicarbazide-sensitive amine oxidase activity and methylglyoxal levels in aristolochic acid-induced nephrotoxicity. *Life Sci.* **114**:4-11.
4. Morgan, P.E. et al. (2014). Perturbation of human coronary artery endothelial cell redox state and NADPH generation by methylglyoxal. *PLoS One* **9**:e86564.

Product Name	Detection	Size	Catalog Number
OxiSelect™ N ^ε -(Carboxymethyl) Lysine (CML) Competitive ELISA Kit	Colorimetric	96 Assays	STA-816
		5 x 96 Assays	STA-816-5
OxiSelect™ N ^ε -(Carboxymethyl) Lysine (CML) Immunoblot Kit	Immunoblot	10 Blots	STA-313
Goat Anti-N ^ε -CML Polyclonal Antibody	Immunoblot/ELISA	100 µg	STA-013
Rabbit Anti-N ^ε -CML Polyclonal Antibody	Immunoblot/ELISA	100 µg	STA-014
CML-BSA Control	N/A	100 µg	STA-314

OxiSelect™ Methylglyoxal (MG) Assays and Antibodies

The OxiSelect™ Methylglyoxal (MG) Competitive ELISA Kit detects MG protein adducts in a variety of samples including cell lysates, blood samples, and other protein sources.

- **Sensitive:** Detect levels as low as 200 ng/mL of MG-protein adduct
- **Versatile:** Compatible with cell lysates, plasma, serum, or purified proteins

Recent Product Citation

Morgan, P.E. et al. (2014). Perturbation of human coronary artery endothelial cell redox state and NADPH generation by methylglyoxal. *PLoS One* **9**:e86564.

Product Name	Detection	Size	Catalog Number
OxiSelect™ Methylglyoxal (MG) Competitive ELISA Kit	Colorimetric	96 Assays	STA-811
		5 x 96 Assays	STA-811-5
Mouse Anti-Methylglyoxal Monoclonal Antibody	Immunoblot/ Immunohistochemistry	100 µg	STA-011
MG-BSA	N/A	100 µg	STA-306

Oxidized / Nitrated Proteins

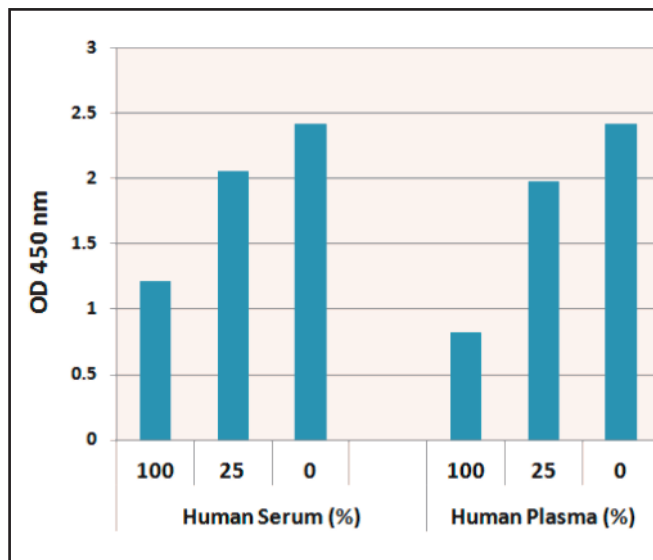
All proteins are provided at a concentration of 1.0 mg/mL.

Product Name	Size	Catalog Number
Copper (Cu ⁺⁺) Oxidized Human Low Density Lipoprotein (LDL)	100 µg	STA-214
Malondialdehyde (MDA) Modified Human Albumin	100 µg	STA-210
Malondialdehyde (MDA) Modified Human Apolipoprotein B-100	100 µg	STA-211
Malondialdehyde (MDA) Modified Human Low Density Lipoprotein (LDL)	100 µg	STA-212
Nitrated Human Low Density Lipoprotein (LDL)	100 µg	STA-213

OxiSelect™ s-Glutathione Adduct ELISA Kit

While glutathione protects cells from free radical damage as an antioxidant, it can also covalently attach to proteins through its sulfhydryl moiety upon derivatization by reactive oxygen species. Glutathione protein adducts can therefore serve as a marker of oxidative stress.

Our OxiSelect™ s-Glutathione Adduct Competitive ELISA Kit quantifies the glutathionylation of proteins in a standard 96-well plate. Protein standards and unknown samples are added to a plate precoated with an s-glutathione protein conjugate. A primary anti-s-glutathione antibody is added and competes for binding between the protein adduct in the sample and the protein adduct bound to the plate. High concentrations of adduct in samples leave little antibody to bind to the plate, resulting in a low O.D. value.



S-Glutathione Protein Adducts in Human Plasma and Serum.

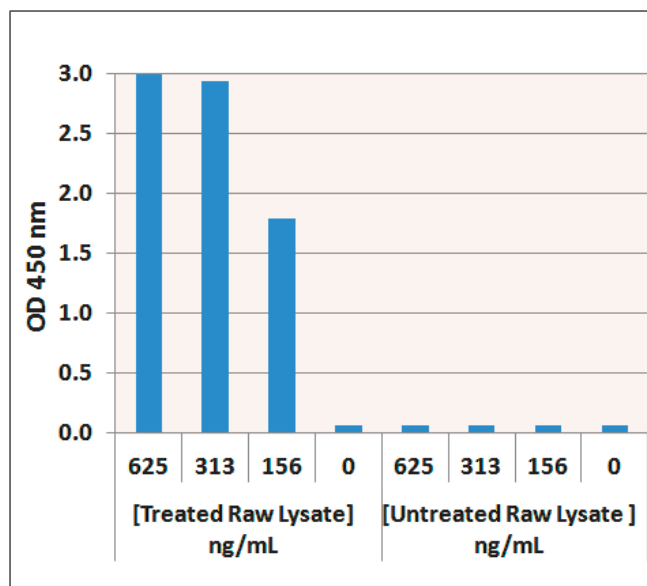
Product Name	Detection	Size	Catalog Number
OxiSelect™ s-Glutathione Adduct Competitive ELISA Kit	Colorimetric	96 Assays	STA-814

OxiSelect™ Protein Radical ELISA Kit

Protein radicals form from electron transfer from various reactive oxygen and reactive nitrogen species. Protein radicals have been linked to various disorders including amyotrophic lateral sclerosis, Huntington's Disease, and Alzheimer's Disease.

Our OxiSelect™ Protein Radical ELISA Kit quantifies free radicals in a standard 96-well plate. The kit employs electron spin resonance (ESO) technology, using the molecule DMPO as a spin trap to bind to the protein radical and create an adduct which can be detected with an anti-DMPO Nitron Adduct Antibody.

The protein radical content in unknown samples is determined by comparing the optical density with a standard curve generated from predetermined DMPO Nitron Adduct-HSA (human serum albumin) standards.



Detection of Protein Radicals in Raw 264.7 Cell Lysate. Raw 264.7 macrophages were trypsinized, washed, subjected to three freeze thaw cycles, and centrifuged. Lysates were subjected to 100 mM DMPO in the presence (left) or absence (right) of 4.4 mM H₂O₂ and 50 μM CuSO₄.

Product Name	Detection	Size	Catalog Number
OxiSelect™ Protein Radical ELISA Kit	Colorimetric	96 Assays	STA-810

Assays and Reagents for Lipid Peroxidation

Lipid peroxidation is a well-defined mechanism of cellular damage in both animals and plants that occurs during aging and in some disease states. Our OxiSelect™ Lipid Peroxidation Assays allow you to quickly and easily quantify the most common markers and by-products of lipid peroxidation.

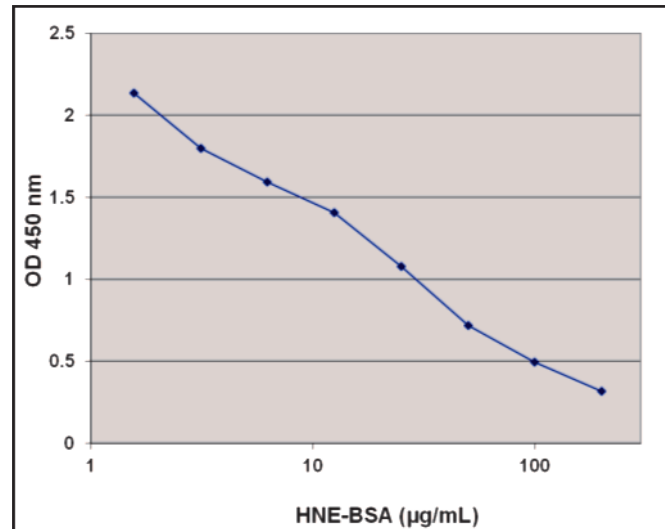
OxiSelect™ HNE ELISA Kits and Antibodies

4-hydroxynonenal (4-HNE) is a well-known by-product of lipid peroxidation and is widely accepted as a stable marker for oxidative stress. HNE protein adducts are typically stable when frozen for up to 6 months or more. Our OxiSelect™ HNE Adduct Competitive ELISA Kit provides a simple, user-friendly way to assess HNE adduct formation on lysine, histidine and/or cysteine.

- **Sensitive:** ELISA kit detects protein adducts as low as 2 µg/mL
- **Versatile:** Suitable for use with serum, plasma, cell lysates or tissue homogenates

Recent Product Citations

1. Hollis, F. et al. (2015). Mitochondrial function in the brain links anxiety with social subordination. *PNAS* **112**:15486-15491.
2. DuPont, J.J. et al. (2014). NADPH oxidase-derived reactive oxygen species contribute to impaired cutaneous microvascular function in chronic kidney disease. *Am. J. Physiol. Renal Physiol.* **306**:F1499-F1506.
3. Kador, P.F. et al. (2014). Topical nutraceutical Optixcare EH ameliorates experimental ocular oxidative stress in rats. *J. Ocul. Pharmacol. Ther.* **30**:593-602.



Standard Curve Generated with the OxiSelect™ HNE Adduct Competitive ELISA Kit.

Product Name	Detection	Size	Catalog Number
OxiSelect™ HNE Adduct Competitive ELISA Kit	Colorimetric	96 Assays	STA-838
		5 x 96 Assays	STA-838-5
Goat Anti-4-Hydroxynonenal (HNE) Polyclonal Antibody	Immunoblot/ELISA	100 µg	STA-034
Rabbit Anti-4-Hydroxynonenal (HNE) Polyclonal Antibody	Immunoblot/ELISA	100 µg	STA-035
HNE-BSA	N/A	100 µg	STA-335

OxiSelect™ 8-iso-Prostaglandin F2α ELISA Kit (8-isoprostane)

The OxiSelect™ 8-iso-Prostaglandin F2α ELISA Kit provides rapid, sensitive detection of 8-iso-PGF2α as low as 50 pg/mL. The assay is suitable for quantitation of 8-isoprostane in a variety of sample types including cell and tissue lysates, plasma, serum, and urine.

Recent Product Citations

1. Wang, Z. et al. (2015). Mechanistic investigation of toxaphene induced mouse liver tumors. *Toxicol. Sci.* 10.1093/toxsci/kfv151.
2. Pereira, S. et al. (2015). Effect of N-acetyl-L-cysteine on insulin resistance caused by prolonged FFA elevation. *J. Endocrinol* 10.1530/JOE-14-0676.

Product Name	Detection	Size	Catalog Number
OxiSelect™ 8-iso-Prostaglandin F2α ELISA Kit	Colorimetric	96 Assays	STA-337
		5 x 96 Assays	STA-337-5

OxiSelect™ MDA (Malondialdehyde) Assays and Antibodies

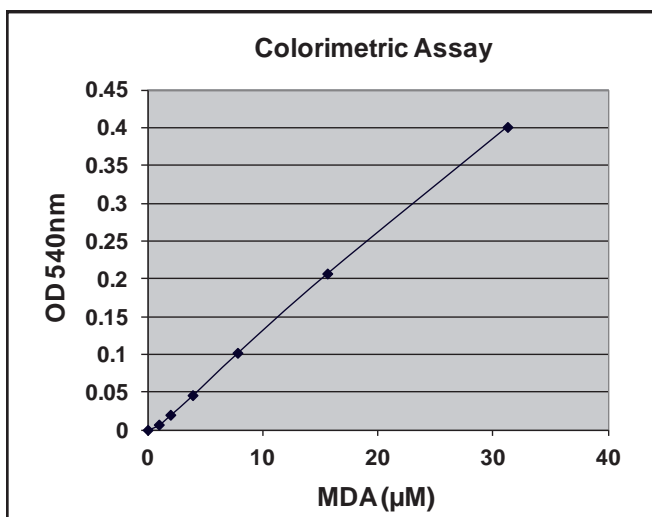
As a common by-product of lipid peroxidation, malondialdehyde (MDA) is a well-accepted marker of oxidative stress. Modification of proteins by MDA can cause structural and functional changes in oxidized proteins. We offer assays and antibodies to measure MDA in a variety of formats. Kits are available to measure total MDA as well as MDA protein adducts specifically.

OxiSelect™ TBARS Assay Kit

The TBARS assay is a well-established method for screening and monitoring lipid peroxidation via the by-product malondialdehyde (MDA). MDA forms a 1:2 adduct with thiobarbituric acid.

Our OxiSelect™ TBARS Assay Kit provides a more user-friendly protocol for quantitation of the MDA-TBA adduct compared to other commercial assays. This assay detects total MDA, both free and in protein adducts, in a variety of samples including cell and tissue lysates, plasma, and urine.

- **Fast:** Obtain results in 30 minutes
- **Sensitive:** Smaller reaction volumes require less sample; detect as little as 2 μM
- **Convenient:** 96-well format; no glass tubes are required



MDA-TBA Standard Curve Using a Standard Plate Reader.

Note: MDA is most reliably detected in fresh samples, or in samples that have been frozen for a maximum of 1-2 months. For samples stored for longer periods, consider testing other markers of lipid peroxidation such as 4-HNE or 8-isoprostane.

Recent Product Citations

1. Mohamed, R.A. et al. (2015). Role of adenosine A_{2A} receptor in cerebral ischemia reperfusion injury: signaling to phosphorylated extracellular signal regulated protein kinase (pERK1/2). *Neuroscience* 10.1016/j.neuroscience.2015.11.059.
2. Dugbartey, G.J. et al. (2015). Dopamine treatment attenuates acute kidney injury in a rat model of deep hypothermia and rewarming—the role of renal H₂S-producing enzymes. *Eur. J. Pharmacol.* **769**:225-233.
3. Pettersen, K. et al. (2015). DHA-induced stress response in human colon cancer cells—focus on oxidative stress and autophagy. *Free Radic. Biol. Med.* **90**:158-172.
4. Songstad, N.T. et al. (2015). Effects of high intensity interval training on pregnant rats, and the placenta, heart and liver of their fetuses. *PLoS One* **10**:e0143095.
5. Brand, R.M. et al. (2015). Skin immunization obviates alcohol-related immune dysfunction. *Biomolecules* **5**:3009-3028.
6. Afify, H. et al. (2015). Molecular mechanisms of the modulatory effect of vitamin E on tacrolimus (FK506)-induced renal injury in rats. *Br. J. Pharm. Res.* **9**:1-9.
7. Palipoch, S. et al. (2015). Heme oxygenase-1 alleviates alcoholic liver steatosis: histopathological study. *J. Toxicol. Pathol.* 10.1293/tox.2015-0035.
8. Galougahi, K.K. et al. (2015). β 3-adrenoceptor activation relieves oxidative inhibition of the cardiac Na⁺-K⁺ pump in hyperglycemia induced by insulin receptor blockade. *Am. J. Physiol. Cell Physiol.* **309**:C286-C295.
9. Dal, S. et al. (2015). Oxidative stress status and liver tissue defenses in diabetic rats during intensive subcutaneous insulin therapy. *Exp. Biol. Med.* 10.1177/1535370215603837.
10. Lee, J.Y. et al. (2015). Effects of non-thermal plasma on the electrical properties of an erythrocyte membrane. *Appl. Phys. Lett.* **107**:113701.
11. Sun, Y. et al. (2015). Impacts of low level aflatoxin in feed and the use of yeast cell wall based feed additive on growth and health of nursery pigs. *Anim. Nutr.* 10.1016/j.aninu.2015.08.012.
12. Rangel-Huerta, O.D. et al. (2015). Normal or high polyphenol concentration in orange juice affects antioxidant activity, blood pressure, and body weight in obese or overweight adults. *J. Nutr.* **145**:1808-1816.
13. Sosa, R.A. et al. (2015). IFN- γ ameliorates autoimmune encephalomyelitis by limiting myelin lipid peroxidation. *PNAS USA* **112**:E5038-E5047.
14. Dhall, S. et al. (2015). Release of insulin from PLGA-alginate dressing stimulates regenerative healing of burn wounds in rats. *Clin. Sci. (Lond.)* **129**:1115-1129.

Product Name	Detection	Size	Catalog Number
OxiSelect™ TBARS Assay Kit (MDA Quantitation)	Colorimetric or Fluorometric	200 Assays	STA-330
		5 x 200 Assays	STA-330-5

OxiSelect™ MDA Adduct Assay Kits

Our MDA Adduct Assay Kits provide simple methods to measuring these protein adducts in a variety of sample types.

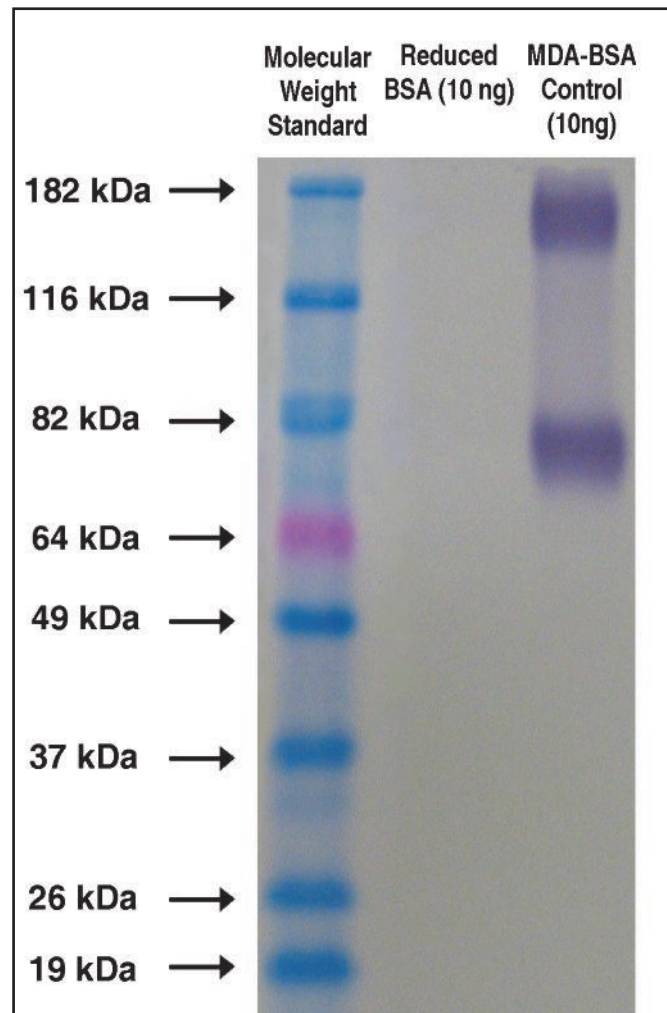
The MDA Adduct Competitive ELISA Kit is a sensitive method for the quantitation of MDA in proteins from cells, tissues, or blood. Samples are added to a malondialdehyde protein conjugate-coated plate. The MDA in the sample competes with the MDA on the plate for binding to the primary anti-MDA antibody. A high concentration of MDA in the sample results in little to no antibody binding to the plate, producing a low signal.

Our MDA Immunoblot is a convenient method for qualitative measurement of MDA protein adducts.

- **Sensitive:** ELISA kit detects MDA protein adducts as low as 6 pmol/mL
- **Versatile:** Suitable for use with serum, plasma, cell lysates or tissue homogenates

Recent Product Citations

1. Shivanna, B. et al. (2015). Omeprazole attenuates pulmonary aryl hydrocarbon receptor activation and potentiates hyperoxia induced developmental lung injury in newborn mice. *Toxicol. Sci.* 10.1093/toxsci/kfv183. (STA-331)
2. Maccarinelli, F. et al. (2014). A novel neuroferritinopathy mouse model (FTL 498InsTC) shows progressive brain iron dysregulation, morphological signs of early neurodegeneration and motor coordination deficits. *Neurobiol. Dis.* 10.1016/j.nbd.2014.10.023. (STA-331)
3. Galay, R.L. et al. (2014). Two kinds of ferritin protect iron overload and consequent oxidative stress. *PLoS One* 9:e90661. (STA-331)
4. Montez, P. et al. (2012). Angiotensin receptor blockade recovers hepatic UCP2 expression and aconitase and SDH activities and ameliorates hepatic oxidative damage in insulin resistant rats. *Endocrinology* 153:5845-5856. (STA-331)
5. De Souza, P.C. et al. (2015). OKN-007 decreases free radical levels in a preclinical F98 rat glioma model. *Free Radic. Biol. Med.* 10.1016/j.freeradbiomed.2015.06.026. (STA-832)



Immunoblot of MDA-BSA Control Using the OxiSelect™ MDA Immunoblot Kit. Immunoblot control was electroblotted onto a nitrocellulose membrane, followed by detection with the provided anti-MDA antibody.

Product Name	Detection	Size	Catalog Number
OxiSelect™ MDA Immunoblot Kit	Immunoblot	10 Blots	STA-331
OxiSelect™ MDA Adduct Competitive ELISA Kit	Colorimetric	96 Assays	STA-832
		5 x 96 Assays	STA-832-5
MDA-BSA	N/A	100 µg	STA-333

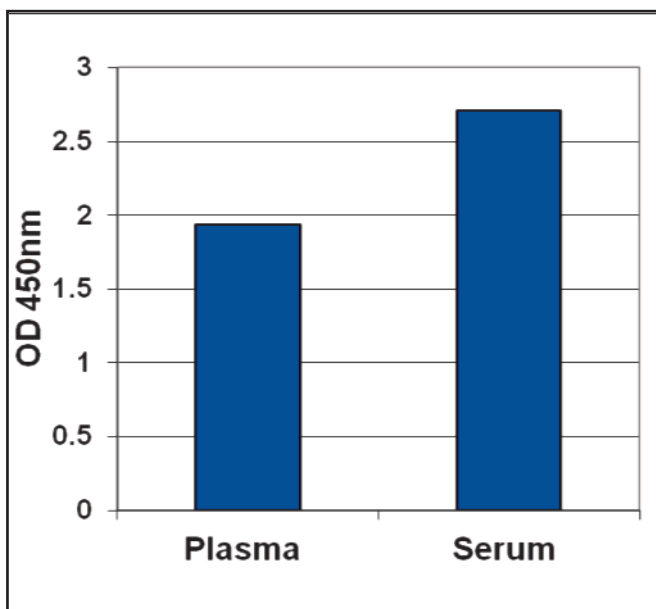
OxiSelect™ MDA Polyclonal Antibodies

Product Name	Detection	Size	Catalog Number
Goat Anti-Malondialdehyde (MDA) Polyclonal Antibody	Immunoblot/ELISA	100 µg	STA-031
Rabbit Anti-Malondialdehyde (MDA) Polyclonal Antibody	Immunoblot/ELISA	100 µg	STA-032

OxiSelect™ Human Oxidized LDL ELISA Kits

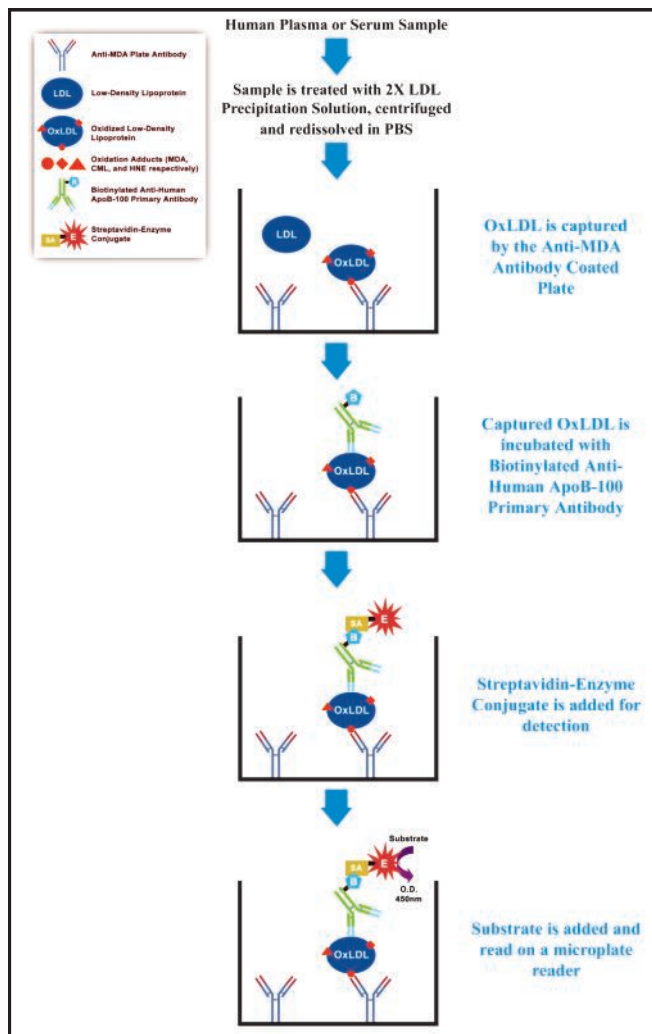
LDL contains a hydrophobic core of various lipids surrounded by one molecule of Apolipoprotein B-100 (ApoB-100), which promotes solubility of the LDL in blood. LDL, often described as “bad” cholesterol, is even more dangerous when it becomes oxidized. Oxidized LDL (OxLDL) is more reactive with surrounding tissues and can collect within the inner lining of arteries.

Our OxiSelect™ Human Oxidized LDL ELISA Kits are designed for the detection and quantitation of modified LDL in human plasma or serum. Kits are available to detect MDA-LDL, CML-LDL, or HNE-LDL in either the protein or lipid component of LDL. Our OxPL-LDL kit specifically detects oxidation in the phospholipid component of LDL.



Quantitation of MDA-LDL in Serum and Plasma Samples. Serum and plasma samples were treated with LDL Precipitation Solution. Precipitated LDL pellets were resuspended in 1.6 mL of PBS before further diluting 1:160 in Assay Diluent according to the Assay Protocol.

- **Sensitive:** Detect as little as 50 ng/mL of MDA-LDL, 150 ng/mL of CML-LDL, 150 ng/mL of HNE-LDL, or 100 ng/mL of OxPL-LDL
- **Quantitative:** Compare unknown samples with provided copper oxidized LDL standard



OxiSelect™ Human Oxidized LDL ELISA Assay Principle.

MDA is the most commonly found damage marker in oxidized LDL, but it can degrade in frozen samples after 1-2 months. CML and HNE, while less commonly found in OxLDL, may be more reliably detectable in samples that have been frozen for several months.

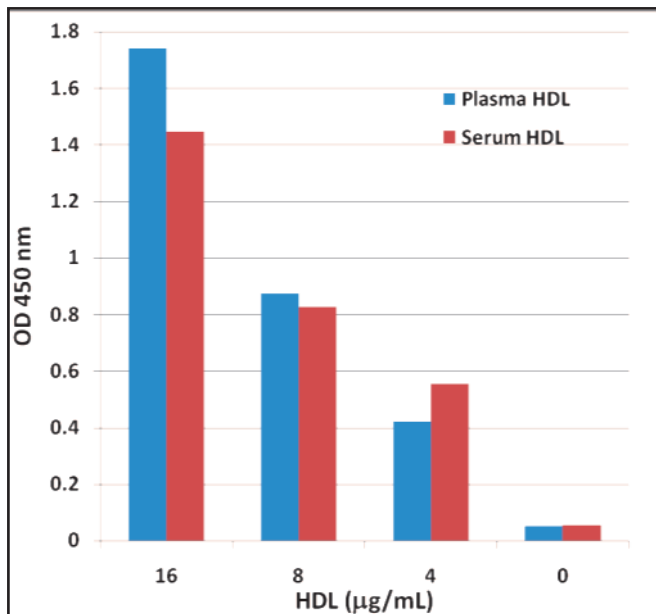
Product Name	Detection	Size	Catalog Number
OxiSelect™ Human Oxidized LDL ELISA Kit (CML-LDL Quantitation)	Colorimetric	96 Assays	STA-388
OxiSelect™ Human Oxidized LDL ELISA Kit (HNE-LDL Quantitation)	Colorimetric	96 Assays	STA-389
OxiSelect™ Human Oxidized LDL ELISA Kit (MDA-LDL Quantitation)	Colorimetric	96 Assays	STA-369
OxiSelect™ Human Oxidized LDL ELISA Kit (OxPL-LDL Quantitation)	Colorimetric	96 Assays	STA-358

OxiSelect™ Human Oxidized HDL ELISA Kits

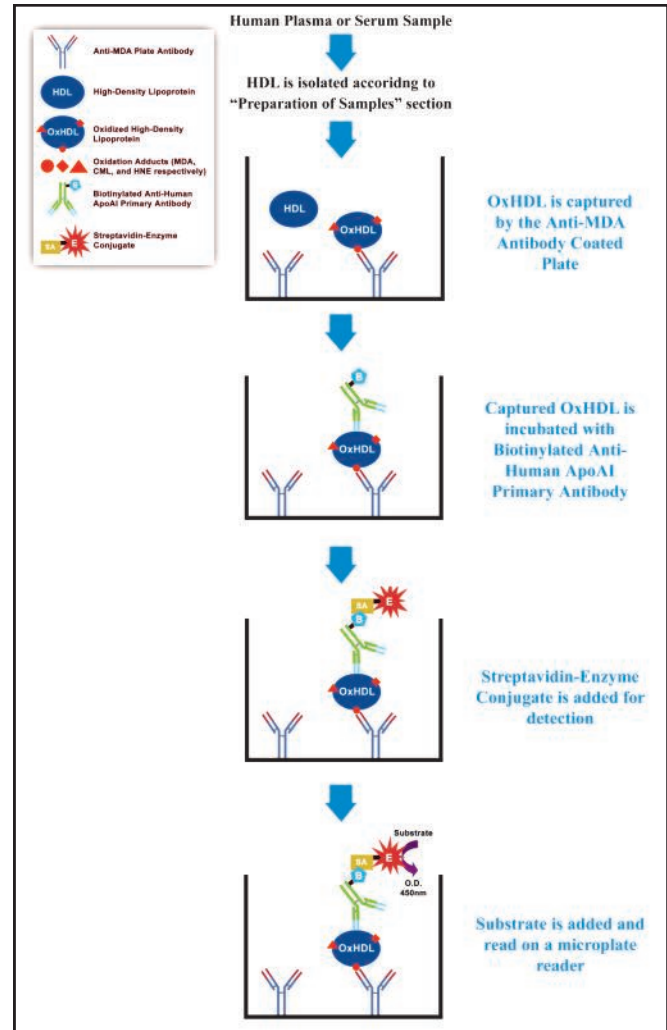
Like LDL, HDL (high density lipoprotein) can become oxidized in either the protein or lipid component. While HDL is often described as “good” cholesterol, oxidation of HDL can cause it to lose its usual cardioprotective properties and cause it to be more dangerous than helpful.

Our OxiSelect™ Human Oxidized HDL ELISA Kits are designed for the detection and quantitation of modified HDL in human plasma or serum. Kits are available to detect MDA-HDL, CML-HDL or HNE-HDL.

- **Sensitive:** Detect as low as 1 ng/mL of MDA-HDL, 1 ng/mL of CML-HDL, or 2 ng/mL of HNE-HDL
- **Quantitative:** Compare unknown samples with provided copper oxidized HDL standard



Quantitation of HNE-HDL in Serum and Plasma Samples. Serum and plasma samples were isolated and diluted in Assay Diluent.



Assay Principle for the OxiSelect™ Human Oxidized HDL ELISA (MDA-HDL Quantitation).

MDA is the most commonly found damage marker in oxidized HDL, but it can degrade in frozen samples after 1-2 months. CML and HNE, while less commonly found in OxHDL, may be more reliably detectable in samples that have been frozen for several months.

Product Name	Detection	Size	Catalog Number
OxiSelect™ Human Oxidized HDL ELISA Kit (CML-HDL Quantitation)	Colorimetric	96 Assays	STA-888
OxiSelect™ Human Oxidized HDL ELISA Kit (HNE-HDL Quantitation)	Colorimetric	96 Assays	STA-889
OxiSelect™ Human Oxidized HDL ELISA Kit (MDA-HDL Quantitation)	Colorimetric	96 Assays	STA-869

Assays for DNA & RNA Damage and Repair

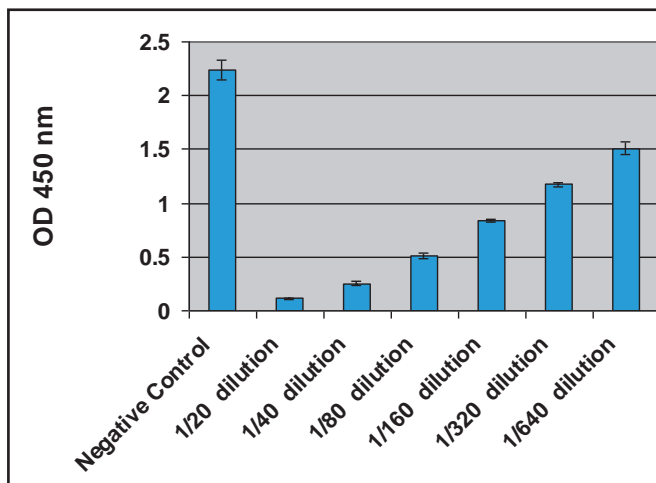
DNA is arguably the most biologically significant target of oxidative and cellular stress. Continuous DNA damage has been implicated in age-related development of various cancers. More recently, RNA damage has been described in conjunction with various neurological diseases including Alzheimer's and Parkinson's diseases. We offer a wide range of assays to measure the most common types of DNA and RNA damage in cells.

OxiSelect™ Oxidative DNA Damage ELISA Kit (8-OHdG Quantitation)

Among the various types of oxidative DNA damage, 8-hydroxydeoxyguanosine (8-OHdG) is a ubiquitous marker of oxidative stress. 8-OHdG, one of the by-products of DNA oxidative damage, is physiologically formed and enhanced by chemical carcinogens.

Our OxiSelect™ Oxidative DNA Damage ELISA Kit provides a powerful method for rapid quantitation of 8-OHdG in DNA samples. 8-OHdG is easily detectable directly in serum and urine samples, after it is excised and secreted during the DNA repair process. It also may be detected in DNA extracted from cells or tissues of any species, following full DNA digestion into single bases.

- **Highly Sensitive:** Detect as little as 100 pg/mL of 8-OHdG
- **Versatile:** Suitable for use with urine, serum, and DNA extracted from cells or tissues



8-OHdG Levels in a Human Urine Sample.

Recent Product Citations

1. Chaiprasongsuk, A. et al. (2015). Photoprotection by dietary phenolics against melanogenesis induced by UVA through Nrf2-dependent antioxidant responses. *Redox Biol.* 10.1016/j.redox.2015.12.006.
2. Zhang, Z.Y. et al. (2015). Enhanced therapeutic potential of nano-curcumin against subarachnoid hemorrhage-induced blood-brain barrier disruption through inhibition of inflammatory response and oxidative stress. *Mol. Neurobiol.* 10.1007/s12035-015-9635.
3. Huang, Y.T. et al. (2015). Resveratrol alleviates the cytotoxicity induced by the radiocontrast agent, ioxitalamate, by reducing the production of reactive oxygen species in HK-2 human renal proximal tubule epithelial cells in vitro. *Int. J. Mol. Med.* 37:83.
4. Belenky, P. et al. (2015). Bactericidal antibiotics induce toxic metabolic perturbations that lead to cellular damage. *Cell Rep.* 13:968-980.
5. Ren, J.D. et al. (2015). Molecular hydrogen inhibits lipopolysaccharide-triggered NLRP3 inflammasome activation in macrophages by targeting the mitochondrial reactive oxygen species. *Biochim. Biophys. Acta.* 1863:50-55.
6. Huang, Y.T. et al. (2015). Therapeutic potential of thalidomide for gemcitabine-resistant bladder cancer. *Int. J. Oncol.* 47:1711-1724.
7. Lim, S.W. et al. (2015). Inhibition of dipeptidyl peptidase IV protects tacrolimus-induced kidney injury. *Lab Invest.* 10.1038/labinvest.2015.93.
8. Dong, Y. et al. (2015). Alpha-lipoic acid attenuates cerebral ischemia and reperfusion injury via insulin receptor and PI3K/Akt-dependent inhibition of NADPH oxidase. *Int. J. Endocrinol.* 2015:903186.
9. Schweitzer, K.S. et al. (2015). Endothelial disruptive pro-inflammatory effects of nicotine and e-cigarette vapor exposures. *Am. J. Physiol. Lung Cell Mol. Physiol.* 309:L175-L187.
10. Ahn, M.Y. et al. (2015). Anti-aging effect and gene expression profiling of aged rats treated with *G. bimaculatus* extract. *Toxicol. Res.* 31:173.
11. Sheng, H. et al. (2015). Bactericidal effect of photolysis of H₂O₂ in combination with sonolysis of water via hydroxyl radical generation. *PLoS One* 10:e0132445.
12. Mu, H.N. et al. (2015). Caffeic acid attenuates rat liver reperfusion injury through Sirt3-dependent regulation of mitochondrial respiratory chain. *Free Radic. Biol. Med.* 10.1016/j.freeradbiomed.2015.04.033.
13. Glenn, D.J. et al. (2015). Cardiac steatosis potentiates angiotensin II effects in the heart. *Am. J. Physiol. Heart Circ. Physiol.* 308:H339-H350.

Product Name	Detection	Size	Catalog Number
OxiSelect™ Oxidative DNA Damage ELISA Kit (8-OHdG Quantitation)	Colorimetric	96 Assays	STA-320
		5 x 96 Assays	STA-320-5

OxiSelect™ Oxidative RNA Damage ELISA Kit (8-OHG Quantitation)

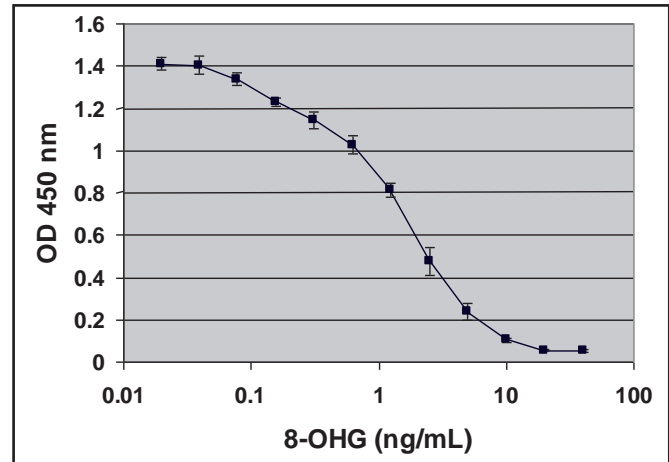
Similarly to 8-hydroxydeoxyguanosine (8-OHdG) forming during DNA oxidation, RNA can become oxidized resulting in 8-hydroxyguanosine (8-OHG). Oxidation of RNA has been implicated in a number of neurological diseases including Alzheimer's and Parkinson's diseases.

Our OxiSelect™ Oxidative RNA Damage ELISA Kit provides a powerful method for rapid quantitation of 8-OHG in urine, serum or cerebrospinal fluid. It also may be used to detect 8-OHG in RNA extracted from cells or tissues of any species.

Recent Product Citations

1. Belenky, P. et al. (2015). Bactericidal antibiotics induce toxic metabolic perturbations that lead to cellular damage. *Cell Rep.* **13**:968-980.
2. Tsai, C.H. et al. (2015). Transcriptional analysis of *Deinococcus radiodurans* reveal novel small RNAs that are differentially expressed under ionizing radiation. *Appl. Env. Microbiol.* **81**:1754.
3. Kannan, S. et al. (2012). Dendrimer-based postnatal therapy for neuroinflammation and cerebral palsy in a rabbit model. *Sci. Transl. Med.* **4**:130ra46.
4. Bazin, J. et al. (2011). Targeted mRNA oxidation regulates sunflower seed dormancy alleviation during dry after-ripening. *Plant Cell* **23**:2196-2208.

- **Highly Sensitive:** Detect as little as 150 pg/mL of 8-OHG
- **Versatile:** Suitable for use with urine, serum, cerebrospinal fluid, and DNA extracted from cells or tissues



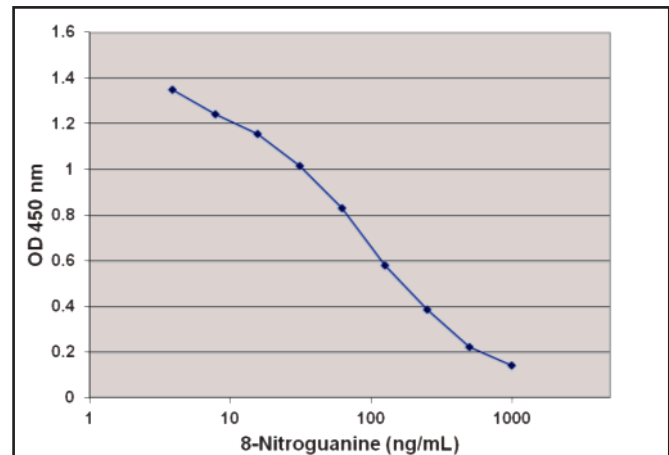
Standard Curve Generated with the OxiSelect™ Oxidative RNA Damage ELISA Kit (8-OHG).

Product Name	Detection	Size	Catalog Number
OxiSelect™ Oxidative RNA Damage ELISA Kit (8-OHG Quantitation)	Colorimetric	96 Assays	STA-325
		5 x 96 Assays	STA-325-5

OxiSelect™ Nitrosative DNA/RNA Damage ELISA Kit (8-Nitroguanine Quantitation)

Various reactive nitrogen species (RNS) including peroxynitrite and nitrogen oxides can form during pathophysiological conditions. These RNS can nitrate guanine bases to form 8-nitroguanine in both DNA and RNA. Nitrosative damage to DNA and RNA is a significant contributor to the age-related development of major inflammation-related diseases as well as colon, breast, and prostate cancers.

Our OxiSelect™ Nitrosative DNA/RNA Damage ELISA Kit provides a simple method for rapid quantitation of 8-nitroguanine in urine, serum or plasma samples. The assay measures total 8-nitroguanine from both DNA and RNA combined.



Standard Curve Generated with the OxiSelect™ Nitrosative DNA/RNA Damage ELISA Kit (8-Nitroguanine).

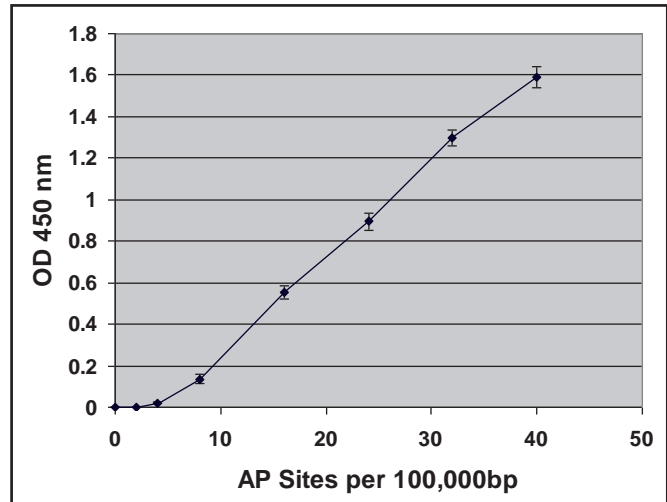
Product Name	Detection	Size	Catalog Number
OxiSelect™ Nitrosative DNA/RNA Damage ELISA Kit (8-Nitroguanine Quantitation)	Colorimetric	96 Assays	STA-825
		5 x 96 Assays	STA-825-5

OxiSelect™ Oxidative DNA Damage Quantitation Kit (AP Sites)

Oxidative DNA Damage can manifest in the formation of apurinic or apyrimidinic (AP) sites, also known as loss of bases. Spontaneous base loss, if unrepaired, can inhibit transcription and may be mutagenic.

Our OxiSelect™ Oxidative DNA Damage Quantitation Kit provides a simple, user-friendly method for measuring AP sites in DNA. The assay uses an aldehyde reactive probe (ARP) which specifically reacts with an aldehyde group on the open ring of the AP site, followed by labeling with Biotin and subsequent detection by Streptavidin-enzyme conjugate.

- **Highly Sensitive:** Detect as few as 4-40 AP sites in 10^5 bp of DNA
- **Versatile:** Suitable for use with genomic DNA from cells or tissues
- **Quantitative:** Kit includes both oxidized and reduced DNA standards for absolute quantitation



Standard Curve Generated with the OxiSelect™ Oxidative DNA Damage Quantitation Kit (STA-324).

Recent Product Citations

1. Ferreira, E. et al. (2015). Glyceraldehyde-3-phosphate dehydrogenase is required for efficient repair of cytotoxic DNA lesions in *Escherichia coli*. *Int. J. Biochem. Cell Biol.* **60**:202-212.
2. Zhao, K. et al. (2014). S-sulphydration of MEK1 leads to PARP1 activation and DNA damage repair. *EMBO Rep.* **15**:792-800.

Product Name	Detection	Size	Catalog Number
OxiSelect™ Oxidative DNA Damage Quantitation Kit (AP Sites)	Colorimetric	50 Assays	STA-324

OxiSelect™ DNA Double-Strand Break Assay

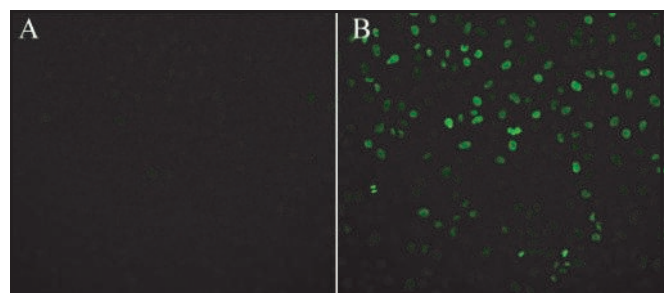
Double-strand breaks (DSB) are among the most dangerous types of DNA damage within cells. An early cellular response is phosphorylation of the histone variant H2AX at the site of the DSB. This triggers a cascade of events and appears to play a role in recruitment of repair factors to the damaged sites.

Our OxiSelect™ DNA Double-Strand Break Staining Kit provides an easy-to-use method for detecting DNA breaks. The kit utilizes simple immunofluorescence staining of the phosphorylated histone H2AX.

Recent Product Citations

1. Ohashi, S. et al. (2014). Preclinical validation of talaporfin sodium-mediated photodynamic therapy for esophageal squamous cell carcinoma. *PLoS One* **9**:e103126.
2. Matusda, S. et al. (2014). An easy-to-use genotoxicity assay using EGFP-MDC1-expressing human cells. *Gene Environ.* **36**:17-28.

- **Fast:** See staining results in about 3 hours
- **Positive Control:** DNA Double-strand break inducer included in kit



DNA Double-Strand Break Formation in A549 Cells. A549 cells were seeded at 50,000 cells/well overnight. Immunofluorescence staining was then performed according to the assay protocol. (A) Untreated cells. (B) Cells treated with 100 μ M etoposide for one hour.

Product Name	Detection	Size	Catalog Number
OxiSelect™ DNA Double-Strand Break Staining Kit	Immunofluorescence	100 Assays	STA-321

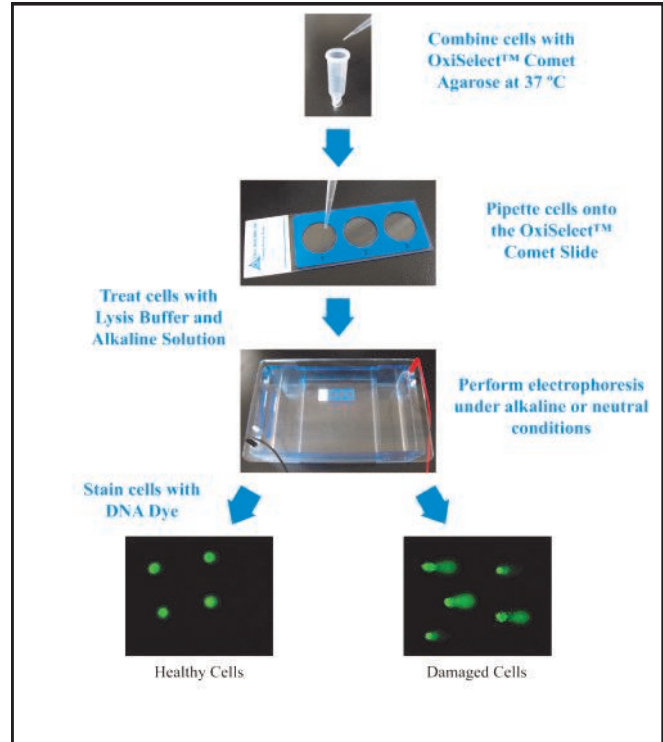
OxiSelect™ Comet Assays (Single Cell Gel Electrophoresis)

DNA damage can result from a variety of intracellular and extracellular stimuli, and can manifest in a variety of mutations to the DNA including base modifications, missing bases and single-stranded or double-stranded breaks. Traditionally the comet assay, or single cell gel electrophoresis (SCGE), has been used as a well-published, high-level screening tool to measure DNA damage in single cells.

Our OxiSelect™ Comet Assay Kits provide a quick, easy method to screen for DNA damage at a macro level. Our OxiSelect™ Comet Assay Slides have been specially treated for adhesion of low-melting agarose used in the assay. Damaged DNA moves farther in electrophoresis than intact DNA, causing a “tail” to form upon visualization under a fluorescence microscope.

Recent Product Citations

1. Ramy, N. et al. (2015). Jaundice, phototherapy and DNA damage in full-term neonates *J. Perinatol.* 10.1038/jp.2015.166. (STA-350, STA-351)
2. Wu, C.F. et al. (2015). Anticancer activity of cryptotanshinone on acute lymphoblastic leukemia cells. *Arch Toxicol.* 10.1007/s00204-015-1616-4. (STA-350, STA-351)
3. Singh, A.K. et al. (2012). Parental age affects somatic mutation rates in the progeny of flowering plants. *Plant Physiol.* **168**:247-257 (STA-350, STA-351)
4. Hou, W. et al. (2015). The protecting effect of deoxyschisandrin and schisandrin B on HaCaT cells against UVB-induced damage. *PLoS One* **10**:e0127177. (STA-350, STA-351)
5. Aydin, E. et al. (2014). The effect of carvacrol on healthy neurons and N2a cancer cells: some biochemical, anticarcinogenicity and genotoxicity studies. *Cytotechnology* **66**:149-157. (STA-355)
6. Jones, D.A. et al. (2014). Changes in markers of oxidative stress and DNA damage in human visceral adipose tissue from subjects with obesity and type 2 diabetes. *Diabetes Res. Clin. Pract.* **106**:627-633. (STA-355)



Assay Principle for the OxiSelect™ Comet Assay Kit.



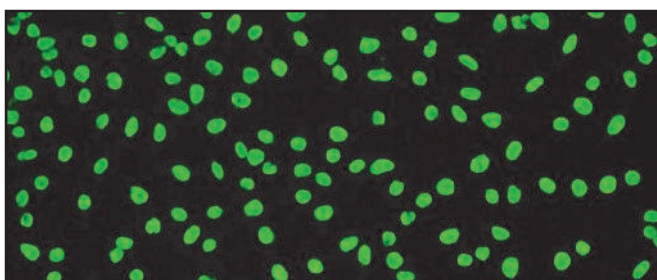
Etoposide Treatment of Jurkat Cells. Jurkat cells were either untreated (left) or treated with etoposide (right) prior to performing the OxiSelect™ Comet Assay.

Product Name	Detection	Size	Catalog Number
OxiSelect™ 3-Well Comet Assay Kit	Light Microscopy	15 Wells	STA-350
		75 Wells	STA-351
		5 x 75 Wells	STA-351-5
OxiSelect™ 3-Well Comet Assay Slides	Light Microscopy	5 Slides	STA-352
		25 Slides	STA-353
		125 Slides	STA-353-5
OxiSelect™ 96-Well Comet Assay Kit	Light Microscopy	96 Wells	STA-355
		5 x 96 Wells	STA-355-5
OxiSelect™ 96-Well Comet Assay Slides	Light Microscopy	1 Slide	STA-356
		5 Slides	STA-356-5
OxiSelect™ Comet Assay Control Cells (includes positive and negative controls)	N/A	1 Set	STA-354

OxiSelect™ UV-Induced DNA Damage Assays

Absorption of ultraviolet radiation can damage DNA by the formation of pyrimidine dimers. The two most common forms of pyrimidine dimers are cyclobutane pyrimidine dimers (CPD) and pyrimidine (6-4) pyrimidone photoproducts (6-4PP).

Our OxiSelect™ UV-Induced DNA Damage Assays conveniently measure the formation of either CPD or 6-4PP in intact cells. Kits for each marker are available in three formats: an ELISA for DNA extracted from cells or tissues, a Cell-Based ELISA, and a Cellular Immunostaining kit.



UV-Induced DNA Damage in HeLa Cells Treated with Ultraviolet Light for 30 Minutes and Visualized with the OxiSelect™ Cellular UV-Induced DNA Damage Staining Kit (CPD).

Recent Product Citations

1. Donniger, H. et al. (2015). The RASSF1A tumor suppressor regulates XPA-mediated DNA repair. *Mol. Cell Biol.* **35**:277-287. (STA-322)
2. Zirkin, S. et al. (2013). The PIN-2 kinase is an essential component of the ultraviolet damage response that acts upstream to E2F-1 and ATM. *J. Biol. Chem.* **288**:21770-21789. (STA-322)
3. Gao, L. et al. (2015). The tomato DDI2, a PCNA ortholog, associating with DDB1-CUL4 complex is required for UV-damaged DNA repair and plant tolerance to UV stress. *Plant Science* **235**:101-110. (STA-322-C)
4. Fujimori, N. et al. (2014). Plant DNA-damage repair/tolerance 100 protein repairs UV-B-induced DNA damage. *DNA Repair (Amst.)* **21**:171-176. (STA-322-C)
5. Akaike, Y. et al. (2014). Homeodomain-interacting protein kinase 2 regulates DNA damage response through interacting with heterochromatin protein 1 ψ . *Oncogene* **10.1038/onc.2014.278**. (STA-323)
6. Dai, W. et al. (2015). A functional single-nucleotide polymorphism in the ERCC1 gene alters the efficiency of NB-UVB therapy in active vitiligo patients in a Chinese population. *Br. J. Dermatol.* **10.1111/brj.13892**. (STA-326)
7. Shin, S. et al. (2014). Protective effects of a new phloretin derivative against UVB-induced damage in skin cell model and human volunteers. *Int. J. Mol. Sci.* **15**:18919-18940. (STA-326)
8. Nunez-Lozano, R. et al. (2015). Biocompatible films with tailored spectral response for prevention of DNA damage in skin cells. *Adv. Healthc. Mater.* **10.1002/adhm.201500223**. (STA-327)
9. Kuschal, C. et al. (2013). Repair of UV photolesions in Xeroderma pigmentosum group C cells induced by translational readthrough of premature termination codons. *PNAS* **110**:19483-19488. (STA-328)

OxiSelect™ UV-Induced DNA Damage ELISA Kits, for extracted DNA

Product Name	Detection	Size	Catalog Number
OxiSelect™ UV-Induced DNA Damage ELISA Combo Kit (CPD/6-4PP)	Colorimetric	96 Assays	STA-322-C
OxiSelect™ UV-Induced DNA Damage ELISA Kit (CPD Quantitation)	Colorimetric	96 Assays	STA-322
		5 x 96 Assays	STA-322-5
OxiSelect™ UV-Induced DNA Damage ELISA Kit (6-4PP Quantitation)	Colorimetric	96 Assays	STA-323
		5 x 96 Assays	STA-323-5

OxiSelect™ Cellular UV-Induced DNA Damage Staining Kits, for intact cells

Product Name	Detection	Size	Catalog Number
OxiSelect™ Cellular UV-Induced DNA Damage ELISA Kit (CPD)	Colorimetric	96 Assays	STA-326
		5 x 96 Assays	STA-326-5
OxiSelect™ Cellular UV-Induced DNA Damage ELISA Kit (6-4PP)	Colorimetric	96 Assays	STA-328

OxiSelect™ Cellular UV-Induced DNA Damage ELISA Kits, for intact cells

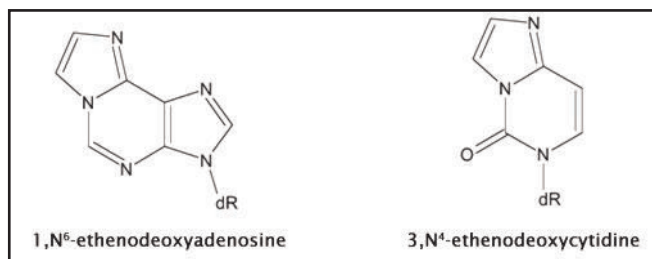
Product Name	Detection	Size	Catalog Number
OxiSelect™ Cellular UV-Induced DNA Damage Staining Kit (CPD)	Fluorescence Microscopy	96 Assays	STA-327
OxiSelect™ Cellular UV-Induced DNA Damage Staining Kit (6-4PP)	Fluorescence Microscopy	96 Assays	STA-329

OxiSelect™ Aldehyde-Induced DNA Damage Assays (Etheno Adducts)

Oxidation of phospholipids can lead to the formation of lipid hydroperoxides. These resulting short-lived hydroperoxides can either be converted to inert fatty acid alcohols, or can react with metals to form aldehydes such as malondialdehyde (MDA), 4-hydroxynonenal (HNE), acrolein, and crotonaldehyde. These aldehydes (which can also be formed through exposure to carcinogenic substances such as urethane or vinyl chloride) can damage DNA resulting in the formation of various etheno adducts, including 1,N⁶-ethenodeoxyadenosine and 3,N⁴-ethenodeoxycytidine. The presence of these bases can lead to base pair substitution mutations.

Our OxiSelect™ Aldehyde-Induced DNA Damage Assays conveniently measure the formation of either 1,N⁶-ethenodeoxyadenosine (ethenoadenosine) or 3,N⁴-ethenodeoxycytidine (ethenocytidine) in DNA extracted from cells or tissues.

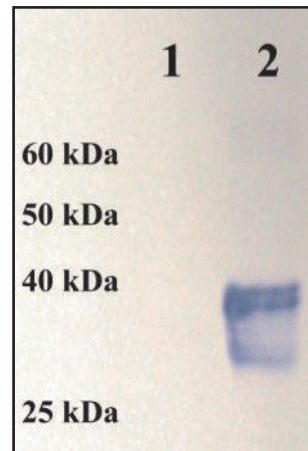
In addition, we offer a convenient combination kit that can measure both etheno bases in separate wells of the same plate.



Checkpoint Kinase Activity Assays

Checkpoint kinases, specifically CHK1 and CHK2, are activated in response to DNA damage to subsequently phosphorylate Cdc25C prior to mitosis, which prompts cell cycle arrest. Mutation of these checkpoint kinases can ultimately lead to decreased DNA repair.

Our Checkpoint Kinase Activity Assays allow you to conveniently measure the activity of CHK1 and CHK2. The assays use recombinant Cdc25C as a checkpoint kinase substrate. Phosphorylated Cdc25C (Ser216) is detected using a phospho-specific antibody. Assays are available in two formats: a Western blot assay and a 96-well plate-based activity assay.



CHK1 Activity Immunoblot Assay. 1X Kinase Buffer with 10 ng of Active CHK1 was incubated with 0.2 mM ATP and 8 µg of Cdc25C at 37°C for one hour. Kinase reaction was stopped by adding SDS-PAGE sample buffer. **Lane 1:** Without kinase (negative control). **Lane 2:** With kinase. Phosphorylation was detected by anti-phospho-Cdc25C antibody.

Product Name	Detection	Size	Catalog Number
Checkpoint Kinase Activity Immunoblot Kit	Immunoblot	20 Assays	STA-413
96-Well Checkpoint Kinase Activity Assay Kit	Colorimetric	96 Assays	STA-414
		5 x 96 Assays	STA-414-5

Global DNA Methylation ELISA Kit

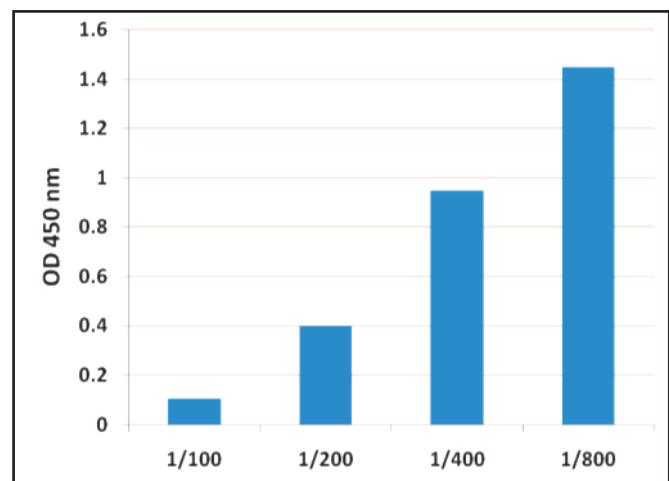
DNA methylation is an epigenetic change shown to be associated with nearly every biological process. In mammalian cells, DNA methylation is found predominantly at CpG dinucleotides; however, in certain cases such as embryonic stem cells it may also be found in non-CpG contexts. Due to the important role of DNA methylation in maintaining genomic stability, deregulation of DNA methylation is associated with various diseases including cancer.

Our Global DNA Methylation and Hydroxymethylation Assays provide a convenient, accurate way to quantify 5'-methyl-2'-deoxycytidine (5MedCyd) and 5-hydroxymethylcytosine respectively. Unknown samples are compared with a standard provided with each kit.

Recent Product Citations

- Shah, S. et al. (2015). Bone morphogenetic protein 4 (BMP4) induces buffalo (*Bubalus bubalis*) embryonic stem cell differentiation into germ cells. *Biochimie* **119**:113-124.
- Creppy, E.E. et al. (2014). Study of epigenetic properties of Poly(Hexamethylene Biguanide) hydrochloride (PHMB). *Int. J. Environ. Res. Public Health* **11**:8069-8092.
- Jefferson, W. et al. (2013). Persistently altered epigenetic marks in the mouse uterus after neonatal estrogen exposure. *Mol. Endocrinol.* **27**:1666-1677.

- **Sensitive:** Detect as little as 15 nM of 5MedCyd
- **Versatile:** Suitable for use with any isolated DNA as well as urine samples
- **Convenient:** Quantify on a standard microplate reader



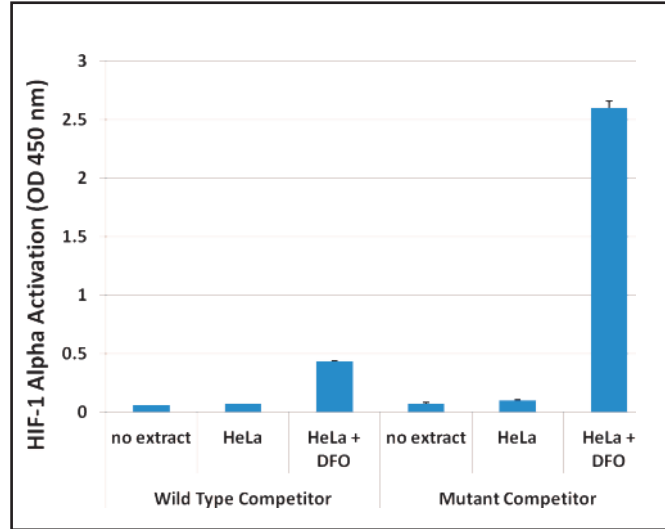
5MedCyd Levels in Human Urine Sample as Measured with the Global DNA Methylation ELISA Kit.

Product Name	Detection	Size	Catalog Number
Global DNA Methylation ELISA Kit (5'-methyl-2'-deoxycytidine Quantitation)	Colorimetric	96 Assays	STA-380
		5 x 96 Assays	STA-380-5

HIF-1 Alpha DNA Binding Activity Assay Kit

Cell hypoxia, or low oxygen condition, is a normal physiological response to certain body stressors such as high altitudes, but it also can be a symptom of pathological conditions. In some cases hypoxia may contribute to the induction of oxidative stress. In response to hypoxic conditions, the hypoxia-inducible factor 1 transcriptional activator complex (HIF-1) plays a role in activating several hypoxia-responsive genes such as erythropoietin and VEGF. During hypoxia, the alpha subunit of HIF-1 accumulates and translocates from the cytosol to the nucleus, where it dimerizes with the beta subunit and becomes transcriptionally active. It then binds transcriptional coactivators to induce gene expression.

The HIF-1 Alpha DNA Binding Activity Assay Kit is an ELISA-based assay to detect activated HIF-1. Active HIF-1 complex is captured on a double-stranded oligo containing a hypoxic response element (HRE) that is attached to the plate. Detection is then performed with a primary antibody followed by an HRP-conjugated secondary antibody. The assay will detect HIF-1 complexes from human, mouse or rat samples.



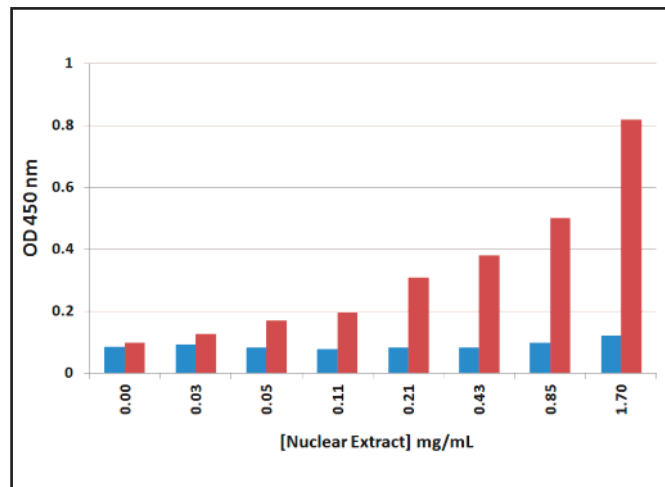
Detection Specificity of HIF-1 Alpha. HeLa cells were incubated in the presence or absence of 0.2 mM deferoxamine mesylate (DFO) for 4 hours at 37°C. Nuclear extracts were prepared using the Nuclear/Cytosolic Fractionation Kit (#AKR-171). 100 pmol of non-biotinylated wild type or mutated HRE double stranded competitor oligos were added to the Complete DNA Binding Buffer just prior to inclusion in the assay.

Product Name	Detection	Size	Catalog Number
HIF-1 Alpha DNA Binding Activity Assay Kit	Colorimetric	96 Assays	CBA-282

HIF-1 Alpha ELISA Kits

Our HIF-1 Alpha ELISA Kits provide a convenient method for detection and quantitation of human, mouse, or rat HIF-1 Alpha in cells or tissues. Two ELISA kit formats are available:

- The HIF-1 Alpha Sandwich ELISA Kit detects HIF-1 Alpha in any protein sample including tissue homogenates, whole cell lysates, or nuclear extracts. Samples are added to an anti-HIF-1 Alpha antibody coated plate. Quantitation of unknown samples is performed by comparison of the OD values to those of a known standard.
- The HIF-1 Alpha Cell Based ELISA Kit allows the detection of HIF-1 Alpha levels in intact cells. Cells are seeded in a tissue culture treated plate suitable for reading in a 96-well plate-based luminescence meter. Cells are fixed and permeabilized to allow detection with the anti-HIF-1 antibody. Detection is performed by chemiluminescence.



Detection of Nuclear HIF-1 Alpha. HeLa cells were incubated in the presence or absence of 0.2 mM DFO for 4 hours at 37°C. Nuclear extracts were prepared using the Nuclear/Cytosolic Fractionation Kit. HIF-1 Alpha levels were measured in untreated (blue bars) and treated (red bars) extracts according to the Assay Protocol.

Product Name	Detection	Size	Catalog Number
HIF-1 Alpha Sandwich ELISA Kit	Colorimetric	96 Assays	CBA-280
HIF-1 Alpha Cell Based ELISA Kit	Chemiluminescent	96 Assays	CBA-281

Reactive Oxygen Species Assays

Reactive oxygen species (ROS) such as superoxide and hydrogen peroxide are continually produced during metabolic processes. Excess ROS can lead to cellular injury in the form of damaged DNA, lipids and proteins. We offer assays for quantitation of various reactive oxygen species, in both *in vitro* and intracellular formats.

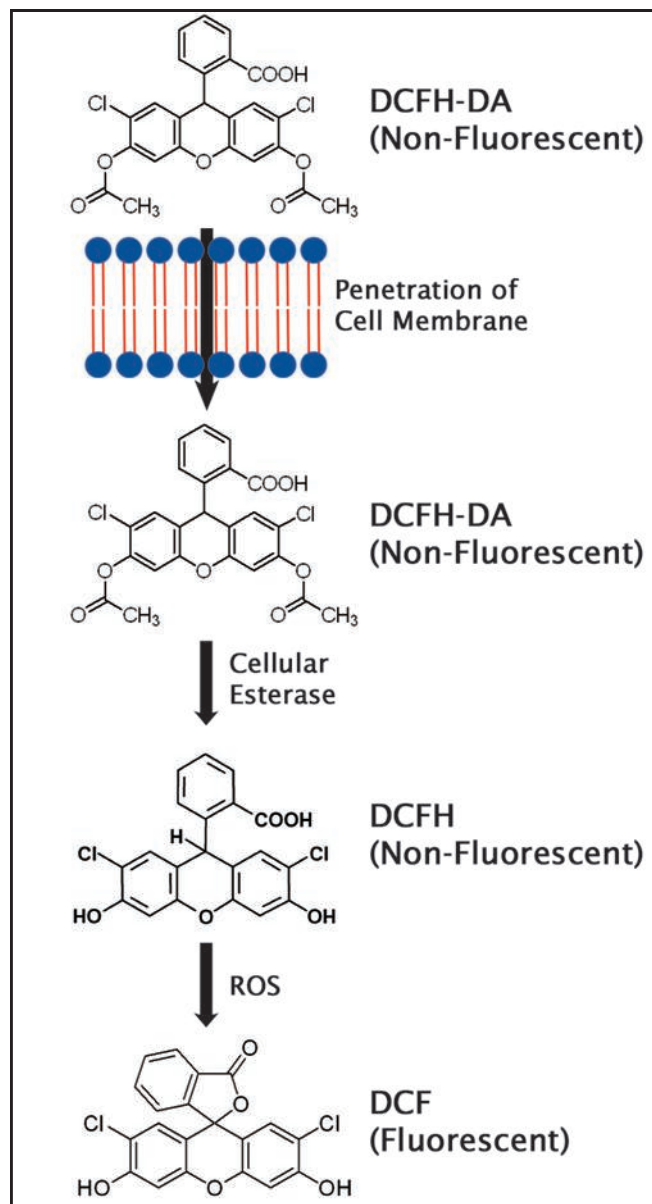
OxiSelect™ Intracellular ROS Assay Kit

The OxiSelect™ Intracellular ROS Assay Kit measures the activity of hydroxyl, peroxy, and other reactive oxygen species. The assay uses the cell-permeable fluorogenic probe DCFH-DA, which diffuses into cells and is deacetylated into the non-fluorescent DCFH. In the presence of ROS, the DCFH is oxidized into highly fluorescent DCF. Fluorescence is quantified on a fluorometric plate reader.

- **Sensitive:** Detect concentrations as little as 10 pM
- **Fast:** Entire protocol takes about one hour

Recent Product Citations

1. Zhelev, Z. et al. (2015). 2-deoxy-D-glucose sensitizes cancer cells to barasertib and everolimus by ROS-independent mechanism(s). *Anticancer Res.* **35**:6623-6632.
2. Gao, S. et al. (2015). Apoptotic effects of Photofrin-Diomed 630-PDT on SHEEC human esophageal squamous cancer cells. *Int. J. Clin. Exp. Med.* **8**:15098.
3. Wang, Y. et al. (2015). ROS-mediated activation of JNK/p38 contributes partially to the pro-apoptotic effect of ajoene on cells of lung adenocarcinoma. *Tumor Biol.* **10.1007-s13277-015-4181-9**.
4. Kim, K.A. and Yim, J.E. (2015). Antioxidative activity of onion peel extract in obese women: a randomized, double-blind, placebo controlled study. *J. Cancer Prev.* **20**:202-207.
5. Dong, H. et al. (2015). Paeoniflorin inhibition of 6-hydroxydopamine-induced apoptosis in PC12 cells via suppressing reactive oxygen species-mediated PKC δ /NF- κ B pathway. *Neuroscience* **285**:70-80.
6. Zou, Y. et al. (2015). Phytoestrogen β -ecdysterone protects PC12 cells against MPP $^{+}$ -induced neurotoxicity in vitro: involvement of PI3K-Nrf2-regulated pathway. *Toxicol. Sci.* **10.1093/toxsci/kfv111**.
7. Sun, L. et al. (2015). Tyrosol prevents ischemia/reperfusion-induced cardiac injury in H9c2 cells: involvement of ROS, Hsp70, JNK and ERK, and apoptosis. *Molecules* **20**:3758-3775.
8. Patlolla, A.K. et al. (2015). Cytogenetic evaluation of functionalized single-walled carbon nanotube in mice bone marrow cells. *Environ. Toxicol.* **10.1002/tox.22118**.
9. Lolicato, F. et al. (2015). The cumulus cell layer protects the bovine maturing oocyte against fatty acid-induced lipotoxicity. *Biol. Reprod.* **10.1095/biolreprod.114.120634**.
10. Li, C. et al. (2015). The interplay between autophagy and apoptosis induced by tanshinone IIA in prostate cancer cells. *Tumor Biol.* **10.1007/s13277-015-4602-9**.
11. Di, K. et al. (2015). Marizomib activity as a single agent in malignant gliomas: ability to cross the blood-brain barrier. *Neuro Oncol.* **10.1093/neuonc/nov299**.



Assay Principle for the OxiSelect™ Intracellular ROS Assay.

Product Name	Detection	Size	Catalog Number
OxiSelect™ Intracellular ROS Assay Kit	Fluorometric	96 Assays	STA-342
		5 x 96 Assays	STA-342-5

OxiSelect™ In Vitro ROS/RNS Assay Kit

Free radicals and related reactive oxygen species (ROS) and reactive nitrogen species (RNS) can appear in the body both inside and outside the cell. Until recently it has been difficult to detect ROS and RNS outside of intact cells.

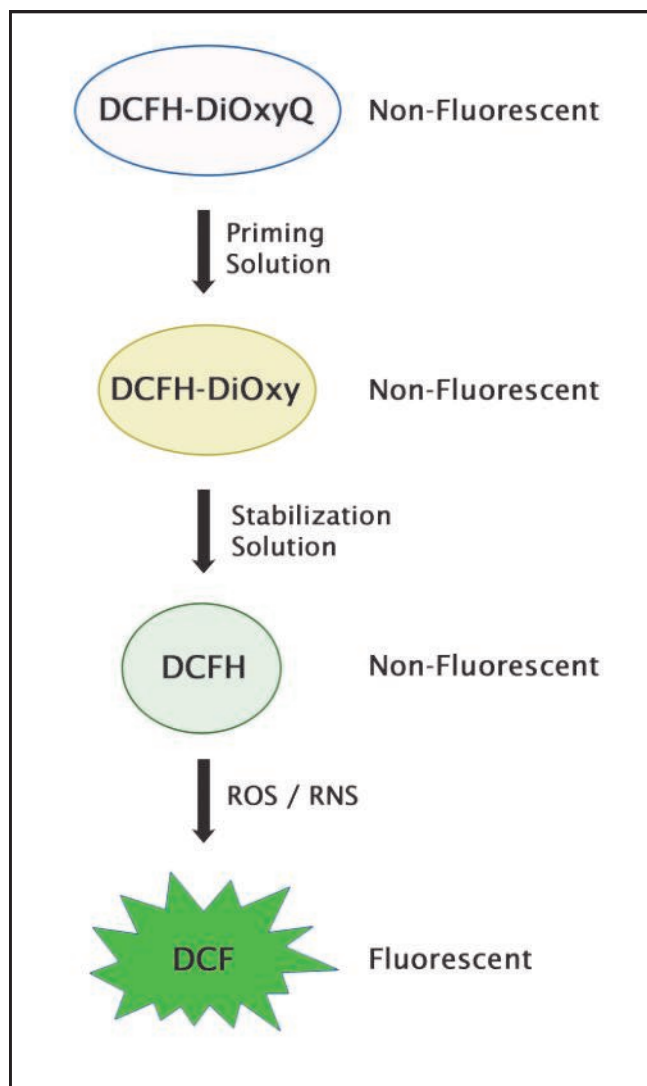
The OxiSelect™ In Vitro ROS/RNS Assay Kit allows you to measure ROS and RNS formation in various body fluids including urine, serum and plasma. It is also useful for testing cell lysates, tissue homogenates, and cell culture supernatants.

The assay universally measures reactive oxygen and reactive nitrogen species that may include hydrogen peroxide, nitric oxide, peroxynitrite, peroxy radicals, and others. The assay principle is similar to our Intracellular ROS Assay (previous page), except that the chemistry is modified to allow detection of ROS outside the cell. Fluorescence is quantified on a fluorometric plate reader.

Recent Product Citations

- Dong, W. et al. (2015). Enhancement of thiamin content in *Arabidopsis thaliana* by metabolic engineering. *Plant Cell Physiol.* **56**:2285-2296.
- Li, M. et al. (2015). Role of PKC δ in insulin sensitivity and skeletal muscle metabolism. *Diabetes* **64**:4023-4032.
- Zhelev, Z. et al. (2015). 2-deoxy-D-glucose sensitizes cancer cells to barasertib and everolimus by ROS-independent mechanism(s). *Anticancer Res.* **35**:6623-6632.
- Hiramoto, K. et al. (2015). The role of the active oxygen produced from gp91phox NADPH oxidase on the newborn weight of mouse pups. *Biol. Med.* **7**:259.
- Hu, X.Q. et al. (2015). Direct effect of chronic hypoxia in suppressing large conductance Ca²⁺-activated K⁺ channel activity in ovine uterine arteries via increasing oxidative stress. *J. Physiol.* **10.1113/JP271626**.
- Klaren, W.D. et al. (2015). Progression of micronutrient alternation and hepatotoxicity following acute PCB126 exposure. *Toxicology* **338**:1-7.
- Roche, J.R. et al. (2015). Effects of precalving body condition score and prepartum feeding level on production, reproduction, and health parameters in pasture-based transition dairy cows. *J. Dairy Sci.* **10.3168/jds.2014.9269**.
- Xiao, D. et al. (2015). Antenatal antioxidant prevents nicotine-mediated hypertensive response in rat adult offspring. *Biol. Reprod.* **10.1095/biolreprod.115.132381**.
- Barhwal, K. et al. (2015). Insulin receptor A and Sirtuin 1 synergistically improve learning and spatial memory following chronic salidroside treatment during hypoxia. *J. Neurochem.* **10.1111/jnc.13225**.
- Pawlak, M. et al. (2015). Ketone body therapy protects from lipotoxicity and acute liver failure upon PPAR α -deficiency. *Mol. Endocrinol.* **10.1210/me/20147-1383**.
- Jiao, S.S. et al. (2015). Edaravone alleviates Alzheimer's disease-type pathologies and cognitive deficits. *PNAS* **112**:5225.

- Sensitive:** Detect concentrations as little as 10 pM for DCF or 40 nM for hydrogen peroxide
- Fast:** Entire protocol takes about one hour
- Versatile:** Suitable for a wide variety of sample types including urine, serum, plasma, cell lysates, tissue homogenates and cell culture supernatants



Assay Principle for the OxiSelect™ In Vitro ROS/RNS Assay.

Product Name	Detection	Size	Catalog Number
OxiSelect™ In Vitro ROS/RNS Assay Kit	Fluorometric	96 Assays	STA-347
		5 x 96 Assays	STA-347-5

OxiSelect™ Hydrogen Peroxide Assay, Colorimetric

Hydrogen peroxide is one of the most prevalent and most stable of the various reactive oxygen species. The half-life of hydrogen peroxide is significantly longer than that of most ROS, making it easier to detect in many sample types.

Our OxiSelect™ Hydrogen Peroxide Assay Kit provides a simple method for quantitation of hydrogen peroxide. This colorimetric assay measures the oxidation of ferrous (Fe^{2+}) ions to ferric (Fe^{3+}) ions in the presence of peroxides. The ferric ions form a complex with a provided dye which may be read on a standard microplate reader. The assay may be run with either aqueous phase or lipid phase samples.

- **Sensitive:** Detect as little as 1 μM
- **Fast:** Easy 30-90 minute incubation, depending on sample type
- **Versatile:** Suitable for plasma, serum, urine, and cell culture supernatants (for cells and tissues, please use our OxiSelect™ Hydrogen Peroxide / Peroxidase assays below)

Recent Product Citations

1. Delijewski, M. et al. (2014). Effect of nicotine on melanogenesis and antioxidant status in HEMn-LP melanocytes. *Environ. Res.* **134**:309-314.
2. Chang, C.H. et al. (2014). Curcumin-protected PC12 cells against glutamate-induced oxidative toxicity. *Food Technol. Biotechnol.* **52**:468-478.
3. Di Cesare Mannelli, L. et al. (2014). PPAR- γ impairment alters peroxisome functionality in primary astrocyte cell cultures. *Biomed. Res. Int.* **10**.1155/2014/546453.

Product Name	Detection	Size	Catalog Number
OxiSelect™ Hydrogen Peroxide Assay Kit	Colorimetric	500 Assays	STA-343

OxiSelect™ Hydrogen Peroxide / Peroxidase Assays

Our OxiSelect™ Hydrogen Peroxide / Peroxidase Assay Kit provides a convenient plate-based method for quantitation of hydrogen peroxide or peroxidases in a wide variety of sample types.

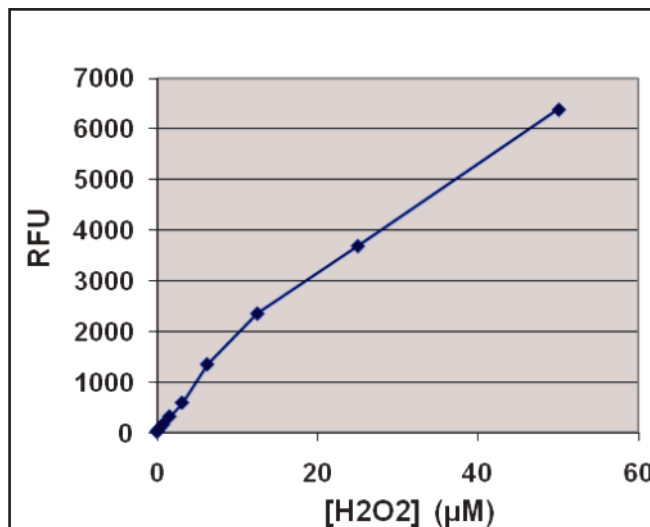
These kits uses either a colorimetric or a fluorogenic probe which provides a signal in the presence of peroxides and is catalyzed by peroxidases.

The kits include both a hydrogen peroxide standard and a peroxidase standard for quantitative results with either target.

Recent Product Citations

1. Zhao, X. et al. (2014). Cleaning up after ICH: the role of Nrf2 in modulating microglia function and hematoma clearance. *J. Neurochem.* **133**:144-152. (STA-344)
2. Ishida, T. et al. (2014). The effect of dihydropyrazines on human hepatoma HepG2 cells: a comparative study using 2,3-dihydro-5,6-dimethylpyrazine and 3-hydro-2, 2, 5, 6-tetramethylpyrazine. *J. Toxicol. Sci.* **39**:601-608. (STA-344)
3. Bak, J.S. (2014). Electron beam irradiation enhances the digestibility and fermentatino yield of water-soaked lignocellulosic biomass. *Biotechnology Reports* **4**:30-33. (STA-344)
4. Lara-Chavez, A. et al. (2015). Global gene expression profiling of two switchgrass cultivars following inoculation with *Burkholderia phytofirmans* strain PsJN. *J. Exp. Bot.* **10**.1093/jxb/erv096. (STA-344)

- **Sensitive:** Detect as little as 50 nM
- **Fast:** Easy 30 minute incubation
- **Versatile:** Measure either hydrogen peroxide or peroxidase in plasma, serum, urine, cell culture supernatants, cell lysates and tissue homogenates



Standard Curve Generated with the OxiSelect™ Hydrogen Peroxide/Peroxidase Assay (Fluorometric).

Product Name	Detection	Size	Catalog Number
OxiSelect™ Hydrogen Peroxide/Peroxidase Assay Kit	Colorimetric	500 Assays	STA-844
	Fluorometric	500 Assays	STA-344

OxiSelect™ Intracellular Nitric Oxide Assay Kit

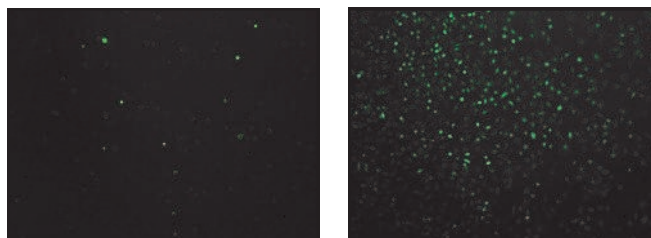
Nitric oxide (NO) is a progenitor of various reactive nitrogen species (RNS). Because of its short half-life, nitric oxide is often difficult to detect directly.

The OxiSelect™ Intracellular Nitric Oxide Assay Kit allows direct detection of NO in intact cells. A cell-permeable fluorogenic probe is added to cells; upon treatment to induce oxidative stress, nitric oxide generated within the cell binds to the probe and produces a bright fluorescent signal. Results may be visualized under a fluorescence microscope or quantified in a 96-well fluorescence plate reader.

Recent Product Citations

1. Nasrallah, R. et al. (2015). Endoglin potentiates nitric oxide synthesis to enhance definitive hematopoiesis. *Biology Open*. 4:819-829.
2. Syed, D.N.. et al. (2014). Involvement of ER stress and activation of apoptotic pathways in fisetin induced cytotoxicity in human melanoma. *Arch. Biochem. Biophys.* 563:108-117.

- **Direct detection:** Probe binds directly to nitric oxide, not to by-products such as nitrate and nitrite
- **Sensitive:** Detect as little as 3 nM
- **Versatile:** Read results as endpoint or time course (kinetic) in a fluorescence plate reader, or visualize under a fluorescence microscope



Induction of NOS in RAW 264.7 Cells. Cells were seeded in a 96-well plate at 100,000 cells/well. Cells were uninduced (left) or induced with 50 ng/mL LPS and 10 ng/mL IFN γ (right) for 20 hours at 37°C.

Product Name	Detection	Size	Catalog Number
OxiSelect™ Intracellular Nitric Oxide (NO) Assay Kit	Fluorometric	96 Assays	STA-800
		5 x 96 Assays	STA-800-5

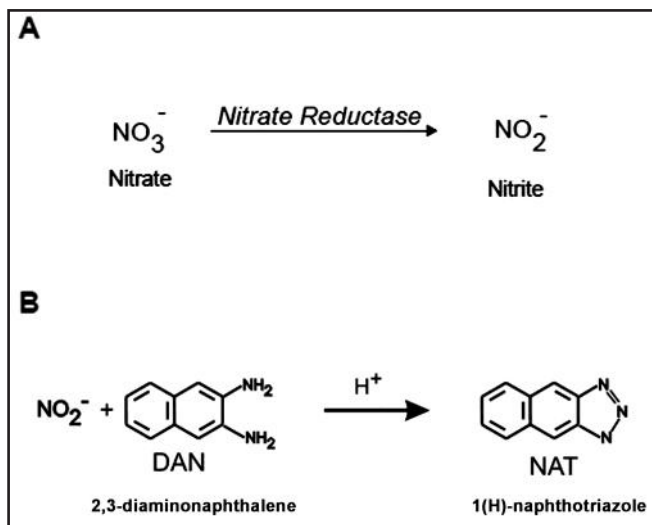
OxiSelect™ In Vitro Nitric Oxide Assay Kits

Nitric oxide (NO) is difficult to detect directly in vitro due to its short half-life. It is therefore common to measure nitric oxide formation by detection of its final oxidized products, nitrate and nitrite.

The OxiSelect™ In Vitro Nitric Oxide Assay Kits provide a convenient plate-based method for the quantitation of nitrate and nitrite in a variety of sample types. First, nitrate is reduced to nitrite. Then total nitrite is measured by the addition of a Griess Reagent (for colorimetric detection) or a fluorometric probe (for fluorescence detection). Results are then quantified in a 96-well plate reader. These kits are suitable for use with serum, plasma, urine, saliva, cell lysates, and culture media.

Recent Product Citation

Wang, Z. et al. (2015). Dual-microstructured porous, anisotropic film for biomimicking of endothelial basement membrane. *ACS Appl. Mater. Interfaces* 10.1021/acsami.5b02464.



Assay Principle for the OxiSelect™ In Vitro Nitric Oxide (Nitrite / Nitrate) Assay, Fluorometric Format.

Product Name	Detection	Size	Catalog Number
OxiSelect™ In Vitro Nitric Oxide (Nitrite / Nitrate) Assay Kit	Colorimetric	100 Assays	STA-802
		5 x 100 Assays	STA-802-5
	Fluorometric	100 Assays	STA-801
		5 x 100 Assays	STA-801-5

Antioxidant Assays

ROS generation is normally counterbalanced by the action of antioxidant enzymes and other redox molecules. We offer two types of assays for antioxidant quantitation:

- Assays to quantify the presence or activity of antioxidant molecules
- Assays to determine the antioxidant capacity of biomolecules

OxiSelect™ Catalase Activity Assay Kits

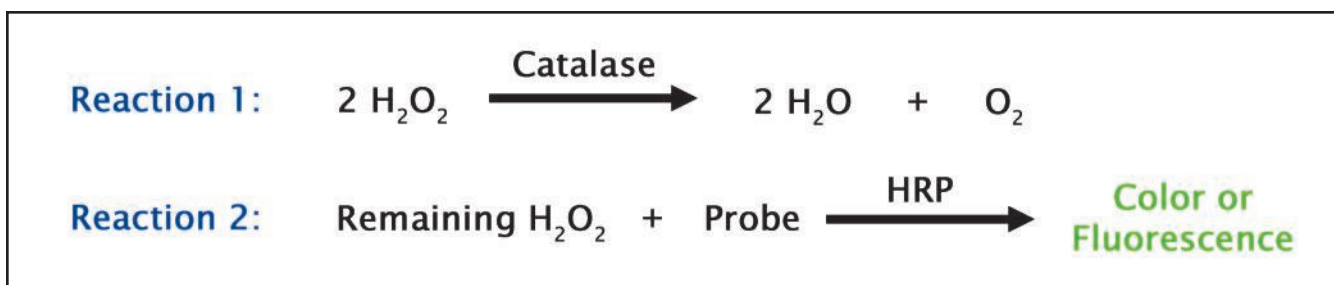
Catalase is a ubiquitous enzyme that destroys hydrogen peroxides formed during oxidative stress. Since hydrogen peroxides have a longer half-life than most free radicals and can make up a large portion of all reactive oxygen species, the ability to remove hydrogen peroxides can be extremely important at combating oxidative stress.

Our OxiSelect™ Catalase Activity Assay Kits provide a quick, user-friendly protocol to monitor catalase activity from a variety of sample types. Kits are available with either colorimetric or fluorometric detection.

- **Sensitive:** Detect as little as 1.25 units/mL (colorimetric) or 50 mU/mL (fluorometric)
- **Fast:** Obtain results in less than 30 minutes
- **Versatile:** Suitable for use with whole blood, plasma, serum, cell lysates or tissue homogenates
- **High Throughput:** 96-well format

Recent Product Citations

1. Iqbal, S. et al. (2015). Trehalose improves semen antioxidant enzymes activity, post-thaw quality, and fertility in Nili Ravi buffaloes (*Bubalus bubalis*). *Theriogenology* 10.1016/j.theriogenology.2015.11.004. (STA-339)
2. Cheng, Y.Y. et al. (2015). SIRT1-related inhibition of pro-inflammatory responses and oxidative stress are involved in the mechanism of nonspecific low back pain relief after exercise through modulation of Toll-like receptor 4. *J. Biochem.* **158**:299-308. (STA-341)
3. Yener, A.U. et al. (2015). Effects of kefir on ischemia-reperfusion injury. *Eur. Rev. Med. Pharmacol. Sci.* **19**:887-896. (STA-341)
4. Javanbakht, M.H. et al. (2015). Evaluation of antioxidant enzyme activity and antioxidant capacity in patients with newly diagnosed pemphigus vulgaris. *Clin. Exp. Dermatol.* 10.1111/ced.12489. (STA-341)
5. Mora, M. et al. (2015). Minocycline increases the activity of superoxide dismutase and reduces the concentration of nitric oxide, hydrogen peroxide, and mitochondrial malondialdehyde in manganese treated *Drosophila melanogaster*. *Neurochem. Res.* **39**:1270-1278. (STA-341)
6. Saikolappan, S. et al. (2015). Inactivation of the organic hydroperoxide stress resistance regulator OhrR enhances resistance to oxidative stress and isoniazid in *Mycobacterium smegmatis*. *J. Bacteriol.* **197**:51-62. (STA-341)
7. Torres, F. et al. (2015). Melatonin reduces oxidative stress and improves vascular function in pulmonary hypertensive newborn sheep. *J. Pineal Res.* 10.1111/jpi.12222. (STA-341)



Assay Principle for the OxiSelect™ Catalase Activity Assays. Catalase present in samples converts hydrogen peroxide into water and oxygen (Reaction 1). Any remaining hydrogen peroxide that is not converted reacts with a colorimetric or fluorometric probe in the presence of horseradish peroxidase (Reaction 2) to produce a color or fluorescence which is measured in a plate reader.

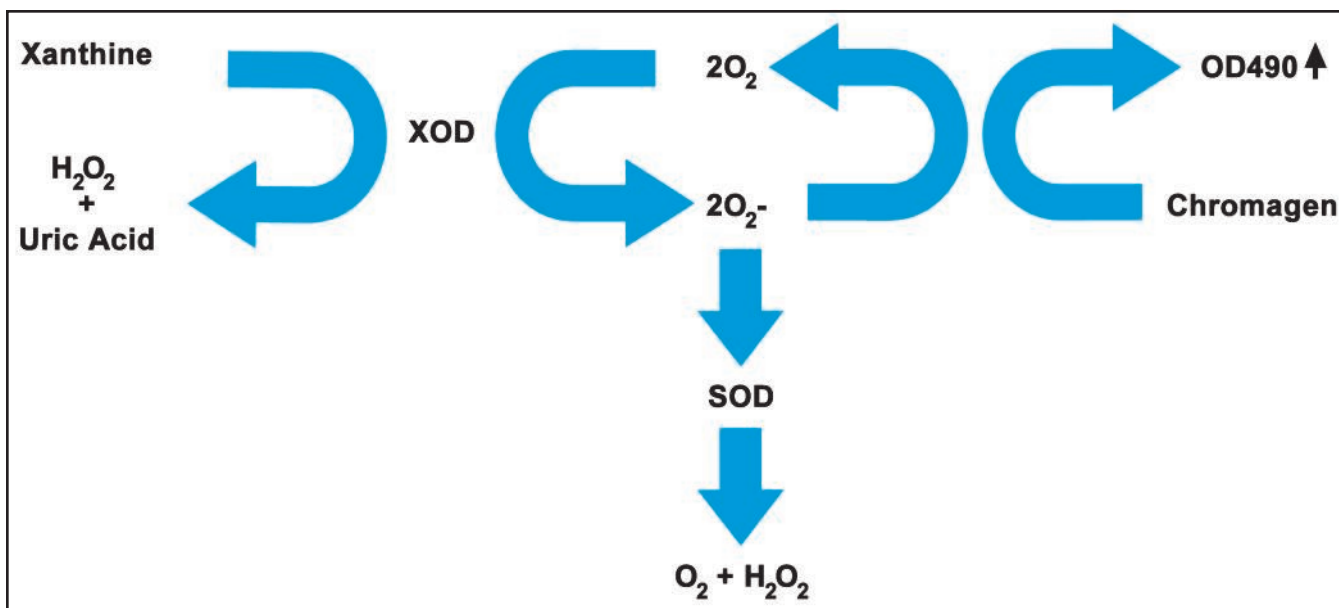
Product Name	Detection	Size	Catalog Number
OxiSelect™ Catalase Activity Assay Kit	Colorimetric	96 Assays	STA-341
	Fluorometric	96 Assays	STA-339

OxiSelect™ Superoxide Dismutase Activity Assay

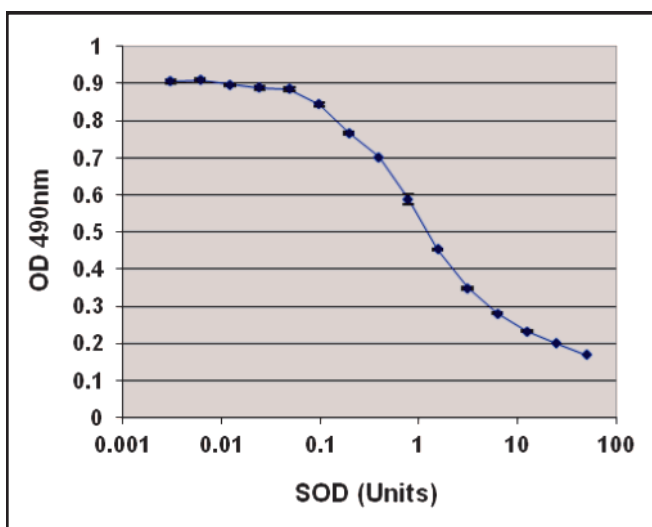
Superoxide dismutase (SOD), which catalyzes the dismutation of the superoxide anion into hydrogen peroxide and molecular oxygen, is one of the most important antioxidant enzymes.

The OxiSelect™ Superoxide Dismutase Activity Assay uses a xanthine/xanthine oxidase (XOD) system to generate superoxide anions and a chromagen to produce a water-soluble dye upon reduction by the superoxide anions.

- **Sensitive:** Detect as little as 0.6 units/mL
- **Fast:** Obtain results in about 2 hours
- **Versatile:** Suitable for use with urine, serum, cells or tissue samples



OxiSelect™ Superoxide Dismutase Activity Assay Principle. Superoxide anions generated by a Xanthine/Xanthine Oxidase system are detected with the provided chromagen. SOD reduces superoxide concentrations, so higher SOD concentrations result in a decreased signal.



Standard Curve Using the OxiSelect™ Superoxide Dismutase Activity Assay.

Recent Product Citations

1. Arumugam, A. et al. (2015). Desacetyl nimbinene inhibits breast cancer growth and metastasis through reactive oxygen species mediated mechanisms. *Tumor Biol.* 10.1007/s13277-015-4468-x.
2. Pandupuspitasari, N. S. (2015). Effects of diludine on the production, oxidative status, and biochemical parameters in transition cows. *J. Environ. Agric. Sci.* 6:3-9.
3. Hunter, J.P. et al. (2015). Ischaemic conditioning reduces kidney injury in an experimental large-animal model of warm renal ischaemia. *Br. J. Surg.* 10.1002/bjs.9909.
4. Tarhan, S. et al. (2015). Direct and protective effects of single or combined addition of vincristine and ε-viniferin on human HepG2 cellular oxidative stress markers in vitro. *Cytotechnology* 10.1007/s10616-015-69863-z.
5. Perez, E. et al. (2015). Improved antitumor effect of paclitaxel administered in vivo as pH and glutathione-sensitive nanohydrogels. *Int. J. Pharm.* 492:10-19.
6. Cheng, Y.Y. et al. (2015). SIRT1-related inhibition of pro-inflammatory responses and oxidative stress are involved in the mechanism of nonspecific low back pain relief after exercise through modulation of Toll-like receptor 4. *J. Biochem.* 158:299-308.

Product Name	Detection	Size	Catalog Number
OxiSelect™ Superoxide Dismutase Activity Assay	Colorimetric	100 Assays	STA-340

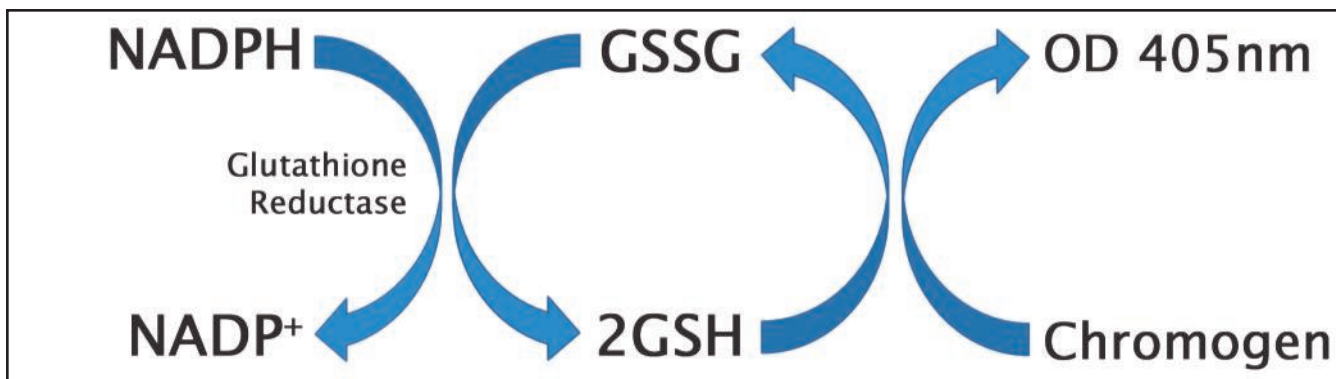
OxiSelect™ Total Glutathione (GSSG/GSH) Assay Kit

The OxiSelect™ Total Glutathione Assay Kit is a quantitative assay for measuring total combined reduced (GSH) and oxidized (GSSG) glutathione content in a variety of sample types. Oxidized glutathione is enzymatically reduced, followed by colorimetric detection in a microplate reader.

- **Sensitive:** Detect as little as 8 nM total glutathione
- **Fast:** Obtain results in less than 30 minutes
- **Versatile:** Suitable for use with saliva, urine, serum, plasma, and cell or tissue lysates

Recent Product Citations

1. Lee, Y.M. et al. (2015). Inhibition of glutamine utilization sensitizes lung cancer cells to apigenin-induced apoptosis resulting from metabolic and oxidative stress. *Int. J. Oncol.* **48**:399-408.
2. Yim, B. et al. (2015). Cadmium modulates the mRNA expression and activity of glutathione S-transferase in the monogonont Rotifer *Brachionus koreanus*. *Toxicol. Environ. Health Sci.* **7**:217-223.
3. Perez, E. et al. (2015). Improved antitumor effect of paclitaxel administered in vivo as pH and glutathione-sensitive nanohydrogels. *Int. J. Pharm.* **492**:10-19.
4. Nuora, A. et al. (2015). The impact of beef steak thermal processing on lipid oxidation and postprandial inflammation related responses. *Food Chem.* **184**:57-64.



Assay Principle for the OxiSelect™ Total Glutathione Assay Kit. In the presence of NADPH, glutathione reductase (provided) converts all glutathione into reduced form (GSH). The reduced glutathione then reacts with the provided chromogen to yield a color detectable at 405 nm.

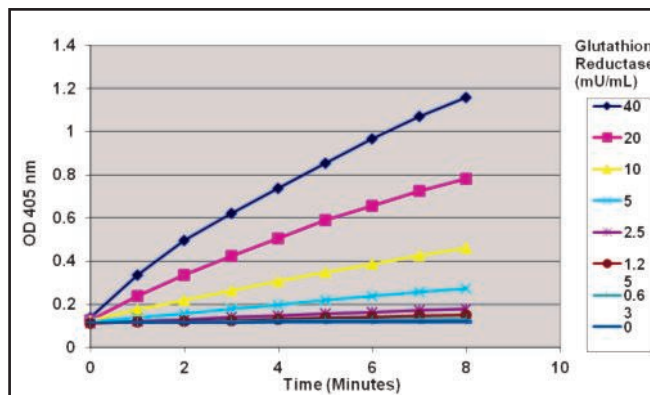
Product Name	Detection	Size	Catalog Number
OxiSelect™ Total Glutathione (GSSG/GSH) Assay Kit	Colorimetric	100 Assays	STA-312

OxiSelect™ Glutathione Reductase Assay Kit

The OxiSelect™ Glutathione Reductase Assay Kit is a quantitative assay for measuring the activity levels of glutathione reductase in a variety of sample types.

The assay principle is similar to that of our Total Glutathione Assay Kit above, except that endogenous levels of glutathione reductase drive the reduction of oxidized glutathione (GSSG) to reduced glutathione (GSH).

- **Sensitive:** Detect activity levels as low as 0.6 mU/mL
- **Fast:** Obtain results in less than 30 minutes
- **Versatile:** Suitable for use with erythrocytes, plasma, cell lysates, or tissue extracts



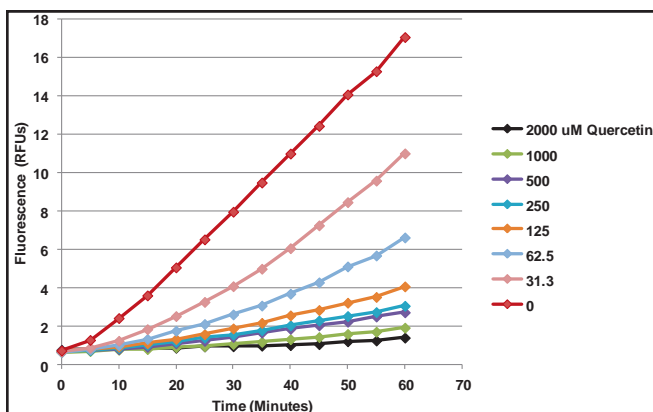
Standard Curve Generated with the OxiSelect™ Glutathione Reductase Assay Kit. Various concentrations of glutathione reductase standard were tested according to the Assay Protocol. OD values were read at 1 minute increments at 405 nm.

Product Name	Detection	Size	Catalog Number
OxiSelect™ Glutathione Reductase Assay Kit	Colorimetric	100 Assays	STA-812

OxiSelect™ Cellular Antioxidant Assay Kit, for *in vivo* Evaluation of Exogenous Antioxidants

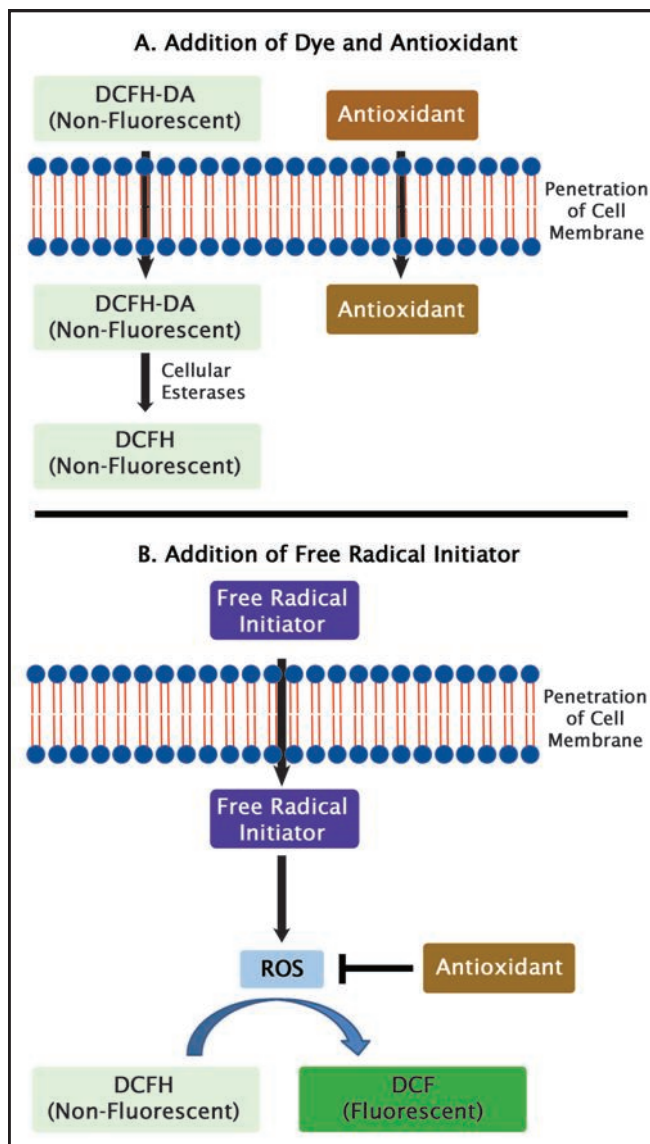
Measuring the effects of antioxidant compounds in an *in vitro* assay may not accurately reflect their efficacy because such assays do not account for physiological conditions such as pH, temperature, uptake, metabolism, or the bioavailability or efficacy of an antioxidant compound.

The OxiSelect™ Cellular Antioxidant Activity Assay Kit provides a mechanism to test exogenous antioxidants in a cell-based environment, delivering a more accurate measurement of the compound's true physiological efficacy. A cell-permeable fluorometric dye is added to intact cells; when free radicals are generated, they bind to the dye producing a bright fluorescent signal. When the exogenous antioxidant is added, it eliminates the free radicals resulting in decreased fluorescence.



Cellular Antioxidant Activity of Quercetin in HeLa Cells.

60,000 HeLa cells were seeded and cultured in a 96-well plate until confluent. Cells were then pretreated with DCFH-DA and Quercetin for 60 minutes at 37°C. Free Radical Initiator was then added to the cells to begin the assay. Fluorescence readings were taken every 5 minutes for one hour at 37°C.



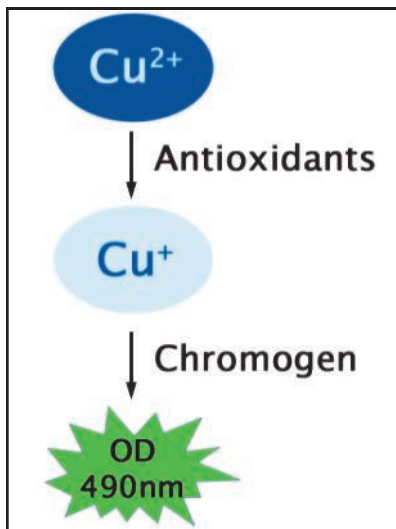
Assay Principle for the OxiSelect™ Cellular Antioxidant Activity Assay Kit.

An exogenous antioxidant compound is added to cells along with DCFH-DA dye. Upon entry into the cell, the DCFH-DA is cleaved to DCFH which can bind reactive oxygen species (ROS) generated within the cell by the addition of a free radical initiator. Binding of DCFH to ROS yields DCF which produces a bright fluorescence. The presence of the exogenous antioxidant compound reduces the ROS available to the DCFH dye, yielding a lower fluorescent signal.

Product Name	Detection	Size	Catalog Number
OxiSelect™ Cellular Antioxidant Activity Assay Kit	Fluorometric	192 Assays	STA-349

OxiSelect™ Total Antioxidant Capacity (TAC) Assay Kit

The OxiSelect™ Total Antioxidant Capacity (TAC) Assay Kit measures the total antioxidant capacity of biomolecules from a variety of sample types via a Single Electron Transfer (SET) mechanism. The assay works with a variety of antioxidants and is suitable for testing plasma, serum, urine, cell lysates, tissue homogenates and food extracts.



OxiSelect™ Total Antioxidant Capacity Assay Principle.

Recent Product Citations

- Dong, W. et al. (2015). Enhancement of Thiamin Content in *Arabidopsis thaliana* by metabolic engineering. *Plant Cell Physiol.* **56**:2285-2296.
- Padnupuspitasari, N.S. et al. (2015). Effects of diludine on the production, oxidative status, and biochemical parameters in transition cows. *J. Environ. Agric. Sci.* **6**:3-9.
- Ni, R. et al. (2015). Mitochondrial calpain-1 disrupts ATP synthase and induces superoxide generation in type-1 diabetic hearts: a novel mechanism contributing to diabetic cardiomyopathy. *Diabetes* **10.2337/db15-0963**.
- Liu, M. et al. (2015). Shen-Kang protects 5/6 nephrectomized rats against renal injury by reducing oxidative stress through the MAPK signaling pathways. *Int. J. Mol. Med.* **36**:975-984.
- Perez, E. et al. (2015). Improved antitumor effect of paclitaxel administered in vivo as pH and glutathione-sensitive nanohydrogels. *Int. J. Pharm.* **492**:10-19.
- Turkmenoglu, F.P. et al. (2015). Characterization of volatile compounds of eleven Achillea species from Turkey and biological activities of essential oil and methanol extract of *A. hamzaoglu* arabaci & budak. *Molecules* **20**:11432-11458.
- Park, S.Y. et al. (2015). Study on the health benefits of brown algae (*Sargassum muticum*) in volunteers. *J. Food Nutr. Res.* **3**:126-130.
- Youn, P. et al. (2015). Cytoprotection against Beta-Amyloid (A β) peptide-mediated oxidative damage and autophagy by Keap1 RNAi in human glioma U87MG cells. *Neurosci Res.* **10.1016/j.neures.2014.12.015**.
- Beretta, G.L. et al. (2015). Unravelling "off-target" effects of redox-active polymers and polymer multilayered capsules in prostate cancer cells. *Nanoscale* **10.1039/C4NR07240E**.

Product Name	Detection	Size	Catalog Number
OxiSelect™ Total Antioxidant Capacity (TAC) Assay Kit	Colorimetric	200 Assays	STA-360

OxiSelect™ ORAC and HORAC Activity Assay Kits

The ORAC (Oxygen Radical Antioxidant Capacity) and HORAC (Hydroxyl Radical Antioxidant Capacity) assays measure the antioxidant capacity of biomolecules against peroxy radicals and hydroxyl radicals, respectively. The assays are suitable for plasma, cell fractions, and tissue lysates, as well as solid and aqueous nutrition samples.

Recent Product Citations

- Nishikawa, Y. et al. (2015). Cytoprotective effects of lysophospholipids from sea cucumber *Holothuria atra*. *PLoS One* **10**:e0135701. (STA-345)
- Orena, S. et al. (2015). Extracts of fruits and vegetables activate the antioxidant response element in IMR-32 cells. *J. Nutr.* **145**:2006-2011. (STA-345)
- Okutsu, K. et al. (2015). Antioxidants in heat-processed koji and tea production mechanisms. *Food Chem.* **10.1016/j.foodchem.2015.04.004**. (STA-345)
- Wada, S.I. et al. (2015). Novel autophagy inducers leucotrehaloses A, B and C. *J. Antibiot. (Tokyo)* **10.1038/ja.2015.23**. (STA-345)
- Jeong, M.H. et al. (2015). In vitro evaluation of *Cordyceps militaris* as a potential radioprotective agent. *Int. J. Mol. Med.* **34**:1349-1357. (STA-346)
- Gardner, A.W. et al. (2014). Greater endothelial apoptosis and oxidative stress in patients with peripheral artery disease. *Int. J. Vasc. Med.* **10.1155/2014/160534**. (STA-346)

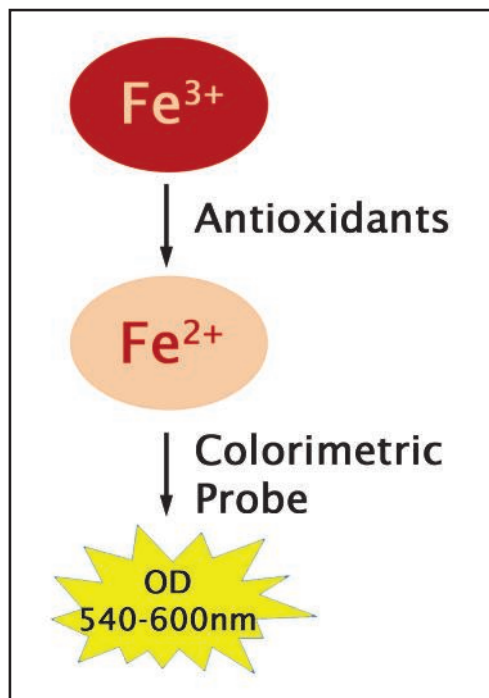
Product Name	Detection	Size	Catalog Number
OxiSelect™ ORAC Activity Assay Kit	Fluorometric	192 Assays	STA-345
		5 x 192 Assays	STA-345-5
OxiSelect™ HORAC Activity Assay Kit	Fluorometric	192 Assays	STA-346
		5 x 192 Assays	STA-346-5

OxiSelect™ Ferric Reducing Antioxidant Power (FRAP) Assay Kit

The OxiSelect™ Ferric Reducing Antioxidant Power (FRAP) Assay Kit is a quantitative assay for measuring the antioxidant potential within a variety of sample types. Following the reduction of ferric iron (Fe^{3+}) to ferrous iron (Fe^{2+}) by antioxidants present in the sample, the colorimetric probe provided in the kit develops a blue color that may be easily read in a standard plate reader at 540-600 nm.

The antioxidant potential of samples is determined by comparing their optical densities to an iron standard curve. Results are calculated as Fe^{2+} equivalents, or FRAP value.

- **Sensitive:** Detect as little as 2 μM of Fe^{2+} iron equivalents
- **Fast:** Quick 10 minute protocol
- **Versatile:** Suitable for use with serum, plasma, lysates, biological fluids, and purified food or drug extracts.



OxiSelect™ Ferric Reducing Antioxidant Power (FRAP) Assay Principle.

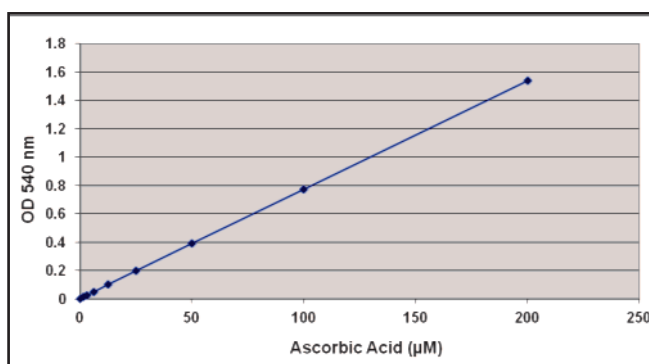
Product Name	Detection	Size	Catalog Number
OxiSelect™ Ferric Reducing Antioxidant Power (FRAP) Assay Kit	Colorimetric	200 Assays	STA-859

OxiSelect™ Ascorbic Acid Assay Kit (FRASC)

Ascorbic acid is a vital water-soluble antioxidant found in living organisms. Ascorbic acid is critical for a variety of functions related to tissue growth and wound healing, neurotransmitter formation, blood cholesterol levels, and free radical neutralization.

The OxiSelect™ Ascorbic Acid Assay Kit is a quantitative assay for measuring the ascorbic acid content within a variety of samples. The assay is based on the Ferric Reducing/Antioxidant Ascorbic Acid (FRASC) chemistry driven by the electron donating reducing power of antioxidants. The kit employs ascorbate oxidase, which allows the user to differentiate the ascorbic acid content from other antioxidants present in the sample. Ascorbic acid levels in samples are determined by measuring the difference in optical density between two sample wells, with and without the oxidase enzyme.

- **Sensitive:** Detect as little as 1 μM of ascorbic acid
- **Fast:** Obtain results in less than 30 minutes
- **Versatile:** Suitable for use with serum, plasma, urine, saliva, tissue homogenates, cell extracts, and purified food or drug extracts



Standard Curve Generated with the OxiSelect™ Ascorbic Acid Assay Kit (FRASC).

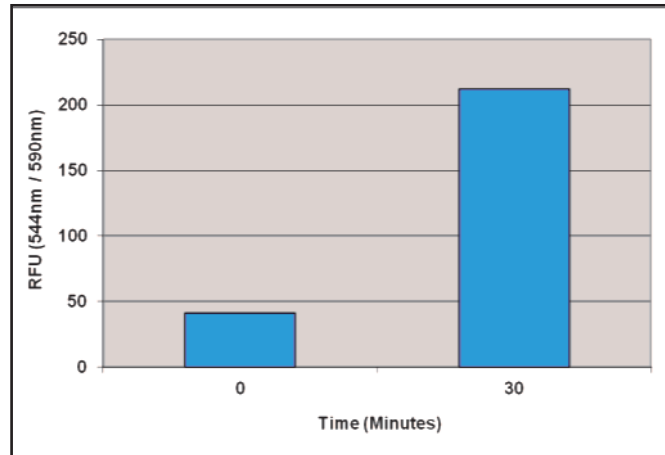
Product Name	Detection	Size	Catalog Number
OxiSelect™ Ascorbic Acid Assay Kit (FRASC)	Colorimetric	200 Assays	STA-860

OxiSelect™ Myeloperoxidase (MPO) Assay Kits

Myeloperoxidase (MPO) is a heme-based peroxidase enzyme that has been implicated in many disease states, and elevated MPO levels have been linked to coronary artery disease. In the presence of hydrogen peroxide, myeloperoxidase is converted to an active redox intermediary form (MPO-I). From there the enzyme plays two roles:

- A chlorination reaction by way of conversion of chloride ions to hypochlorous acid
- A peroxidation reaction where MPO is ultimately converted back to its native state

Our OxiSelect™ Myeloperoxidase Assay Kits provide a convenient way to detect and quantify myeloperoxidase activity levels. Chlorination and peroxidation activities are measured separately.



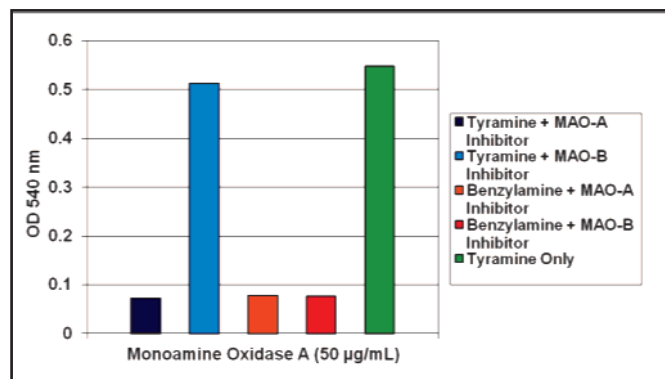
Measurement of the Peroxidation Activity of Purified Human MPO. 650 pM of purified human myeloperoxidase was tested according to the Assay Protocol. The peroxidation activity was determined to be 42 μ U/mL.

Product Name	Detection	Size	Catalog Number
OxiSelect™ Myeloperoxidase Chlorination Activity Assay Kit	Colorimetric	200 Assays	STA-803
	Fluorometric	192 Assays	STA-804
OxiSelect™ Myeloperoxidase Peroxidation Activity Assay Kit	Fluorometric	192 Assays	STA-805

OxiSelect™ Monoamine Oxidase Assay Kits

Monoamine oxidases (MAO) are a collection of enzymes found in the outer mitochondrial membrane that catalyze the oxidative deamination of monoamines. MAO exists as two isoforms, MAO-A and MAO-B, which are differentiated based on localization, substrate affinity, and inhibitor specificity. MAOs regulate neurotransmitters, and dysfunction of MAOs have been associated with depression, drug abuse, migraines, schizophrenia, attention deficit disorder, and Parkinson's and Alzheimer's diseases.

OxiSelect™ Monoamine Oxidase Assay Kits measure MAO-A and MAO-B in biological samples. MAO reacts with a substrate, generating hydrogen peroxide. A reaction between hydrogen peroxide and a probe results in a signal that is directly proportional to the level of MAO in the sample. Quantitation is performed in a colorimetric or fluorescence plate reader.

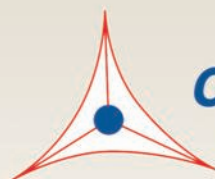


Measurement of MAO-A. 50 μ g/mL of Monoamine Oxidase A was incubated with the MAO-A Inhibitor (Clorgyline) or MAO-B Inhibitor (Pargyline) according to the Assay Protocol. Each was subsequently incubated with the substrates Tyramine or Benzylamine within the Assay Working Solution for 45 minutes. OD values were read at 540 nm on a standard colorimetric plate reader.

Product Name	Detection	Size	Catalog Number
OxiSelect™ Monoamine Oxidase Assay Kit	Colorimetric	96 Assays	XPX-5006
		5 x 96 Assays	XPX-5006-5
	Fluorometric	96 Assays	XPX-5000
		5 x 96 Assays	XPX-5000-5

Cell Signaling and Protein Biology

Small GTPase / G-Protein Signaling	104
Kinase Assays	111
Reporter Assays, Cell Lines and Reagents	113
Epitope Tags / Antibodies	116
Protein Phosphorylation	117
Protein Isolation	118
Protein Detection / Quantitation	119
Antibody Purification	120



CELL BIOLABS, INC.

Creating Solutions for Life Science Research

Small GTPase / G-Protein Signaling

Small GTP-binding proteins (GTPases) regulate a variety of cell signaling pathways and are therefore involved in a wide range of cell functions, processes, and morphology. The most studied small GTPases include Ras, Rac, Rho and Cdc42. We offer a variety of tools to enable the study of these small GTPase family members:

- Small GTPase Activation Assays
- Small GTPase Activation ELISA Kits
- Small GTPase Assay Beads
- Active Rac-GEF Assay
- Small GTPase Expression Vectors
- Small GTPase Premade Adenoviruses
- Small GTPase Retroviral Constructs
- Small GTPase Recombinant Proteins

In addition, we offer sensitive assays to detect cyclic AMP and cyclic GMP, both of which are important regulators in the G-Protein signaling cascade.

Small GTPase Activation Assays

Our Small GTPase Activation Assays use visible agarose beads to selectively pull down the active form of the target of interest. The precipitated GTPase is then detected by Western blot using a target specific antibody included in the kit.

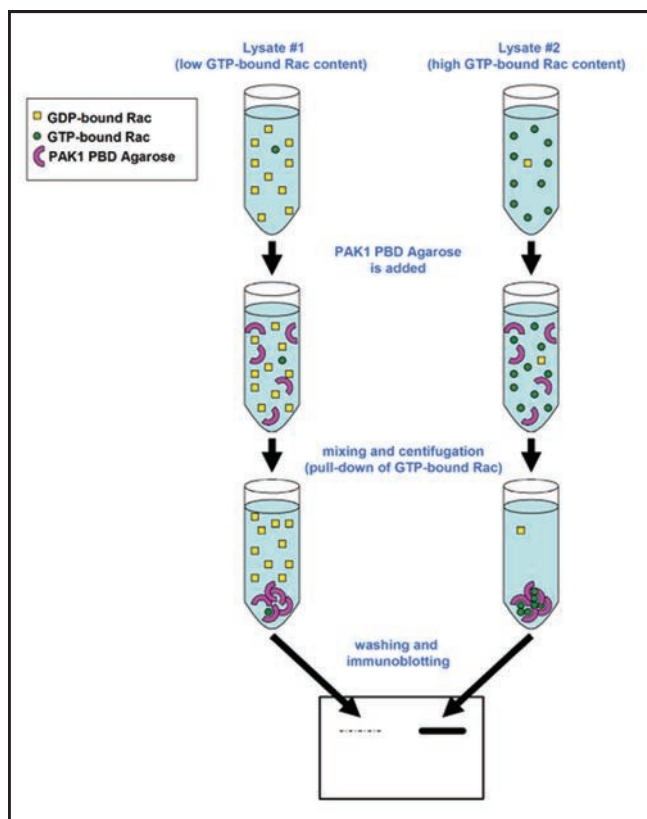
If you are studying more than one small GTPase target, consider one of our Small GTPase Activation Assay Combo Kits. These combo kits allow you to measure the following targets at a savings compared to buying separate kits for each target:

- Rac1 and Cdc42
- RhoA, Rac1 and Cdc42



Visible Agarose Beads Provided in the Small GTPase Activation Assays. Beads are easy to visualize, making it easier to avoid potential loss during washes and aspirations.

- **Safe:** Non-radioactive assay format
- **Visual Check:** Agarose beads can be easily seen
- **Fast Results:** 1 hour plus electrophoresis/blotting



Small GTPase Activation Assay Principle.

Small GTPase Activation Assays (continued)

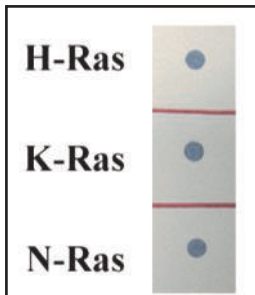
Recent Product Citations

- Nikolos, F. et al. (2014). ER β regulates NSCLC phenotypes by controlling oncogenic RAS signaling. *Mol. Cancer Res.* **12**:843-854. (STA-400)
- Krencik, R. et al. (2015). Dysregulation of astrocyte extracellular signaling in Costello syndrome. *Sci. Transl. Med.* 10.1126/scitranslmed.aaa5645. (STA-400-H)
- Hernandez-Porras, I. et al. (2014). K-RasV14I recapitulates Noonan syndrome in mice. *PNAS USA* **111**:16395-16400. (STA-400-K)
- Gayle, S. et al. (2015). piggyBac insertional mutagenesis screen identifies a role for nuclear RhoA in human ES cell differentiation. *Stem Cell Reports* 10.1016/j.stemcr.2015.03.001. (STA-401-1, STA-403-A)
- Yanagashita, T. et al. (2014). Actin-binding protein, espin: a novel metastatic regulator for melanoma. *Mol. Cancer Res.* **12**:440-446. (STA-401-1, STA-403-A)
- Baetta, R. et al. (2015). Atorvastatin reduces long pentraxin 3 expression in vascular cells by inhibiting protein geranylgeranylation. *Vascul. Pharmacol.* 10.1016/j.vph.2014.11.008. (STA-401-2)
- E-Sayed, F.G. et al. (2014). P2Y2 nucleotide receptor activation enhances the aggregation and self-organization of dispersed salivary epithelial cells. *Am. J. Physiol. Cell Physiol.* **307**:C83-C96. (STA-402)
- Choi, D.S. et al. (2015). SDF-1 α stiffens myeloma bone marrow mesenchymal stromal cells through the activation of RhoA-ROCK-Myosin II. *Int. J. Cancer* **136**:E219-E229. (STA-403-A)
- Ichijo, S. et al. (2014). Activation of the RhoB signaling pathway by thyroid hormone receptor β in thyroid cancer cells. *PLoS One* **9**:e116252. (STA-403-B)
- Tanaka, U. et al. (2015). Sprouty2 inhibition promotes proliferation and migration of periodontal ligament cells. *Oral Dis.* 10.1111/odi.12369. (STA-404)
- Mori, H. et al. (2015). Smad3 deficiency leads to mandibular condyle degradation via the sphingosine 1-phosphate (S1P)/S1P3 signaling axis. *Am. J. Pathol.* 10.1016/j.ajpath.2015.06.015. (STA-405)
- Ishiguro, K. et al. (2014). Suppressive action of acetate on interleukin-8 production via tubulin- α acetylation. *Immunol. Cell Biol.* **92**:624-630. (STA-406-1)
- Monteiro, A.C. et al. (2014). Trans-dimerization of JAM-A regulates Rap2 and is mediated by a domain that is distinct from the cis-dimerization interface. *Mol. Biol. Cell* **25**:1574-1585. (STA-406-2)
- Loskutov, Y.V. et al. (2015). NEDD9/Arf6-dependent endocytic trafficking of matrix metalloproteinase 14: a novel mechanism for blocking mesenchymal cell invasion and metastasis of breast cancer. *Oncogene* 10.1038/onc.2014.297. (STA-407-1)
- Cheung, H.N. et al. (2014). FE65 interacts with ADP-ribosylation factor 6 to promote neurite outgrowth. *FASEB J.* **28**:337-349. (STA-407-6)
- Brasseur, A. et al. (2014). The bi-lobe-associated LRRP1 regulates Ran activity in *Trypanosoma brucei*. *J. Cell Sci.* **127**:4846-4856. (STA-409)

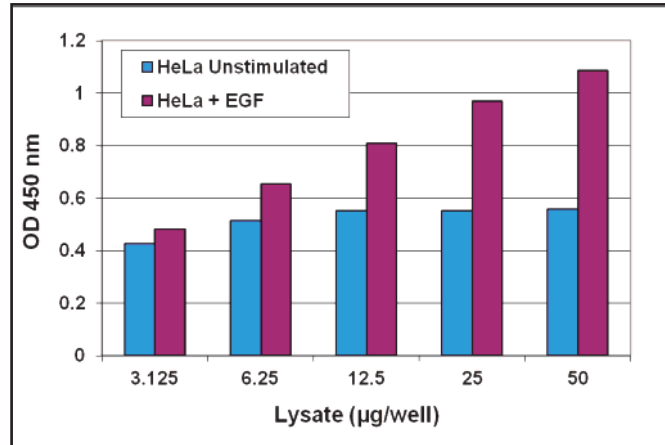
Product Name	Detection	Size	Catalog Number
Arf1 Activation Assay	Immunoblot/ECL	20 Assays	STA-407-1
Arf6 Activation Assay	Immunoblot/ECL	20 Assays	STA-407-6
Cdc42 Activation Assay	Immunoblot/ECL	20 Assays	STA-402
Rac1 Activation Assay	Immunoblot/ECL	20 Assays	STA-401-1
Rac2 Activation Assay	Immunoblot/ECL	20 Assays	STA-401-2
Ral Activation Assay	Immunoblot/ECL	20 Assays	STA-408
Ran Activation Assay	Immunoblot/ECL	20 Assays	STA-409
Rap1 Activation Assay	Immunoblot/ECL	20 Assays	STA-406-1
Rap2 Activation Assay	Immunoblot/ECL	20 Assays	STA-406-2
Pan-Ras Activation Assay	Immunoblot/ECL	20 Assays	STA-400
H-Ras Activation Assay	Immunoblot/ECL	20 Assays	STA-400-H
K-Ras Activation Assay	Immunoblot/ECL	20 Assays	STA-400-K
N-Ras Activation Assay	Immunoblot/ECL	20 Assays	STA-400-N
RhoA Activation Assay	Immunoblot/ECL	20 Assays	STA-403-A
RhoB Activation Assay	Immunoblot/ECL	20 Assays	STA-403-B
RhoC Activation Assay	Immunoblot/ECL	20 Assays	STA-403-C
Rac1/Cdc42 Activation Assay Combo Kit	Immunoblot/ECL	20 Assays/Target	STA-404
RhoA/Rac1/Cdc42 Activation Assay Combo Kit	Immunoblot/ECL	10 Assays/Target	STA-405

96-Well Ras Activation ELISA Kits

Our 96-Well Ras Activation Assays use the Raf1 Rho binding domain (Raf1 RBD) to selectively pull down the active form of Ras from purified or endogenous samples. The captured GTP-Ras is then detected by a pan-Ras antibody and HRP-conjugated secondary antibody. Detection is by either colorimetric or chemiluminescent plate reader.



Pan-Ras Antibody Specificity.
Anti-pan-Ras antibody reactivity with H-Ras, K-Ras and N-Ras human isoforms by dot blot.



EGF Stimulation and Active Ras Detection with the 96-Well Ras Activation ELISA Kit. HeLa cells were serum starved for 18 hours before EGF stimulation of 50 ng/mL for 2 minutes. Lysates were then prepared according to the assay protocol.

Product Name	Detection	Size	Catalog Number
96-Well Ras Activation ELISA Kit	Colorimetric	96 Assays	STA-440
	Chemiluminescent	96 Assays	STA-441

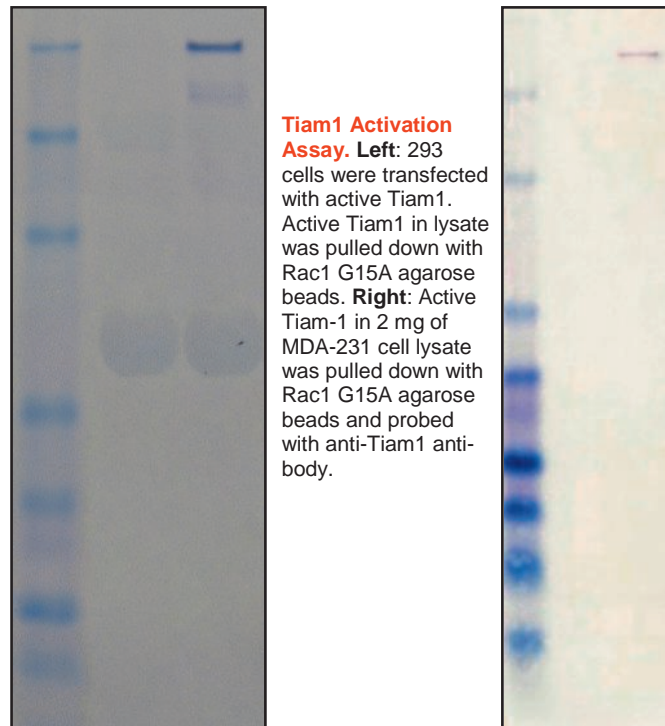
Active Rac-GEF Assay Kit (Tiam1)

Guanine nucleotide exchange factors (GEFs) activate small GTPases by catalyzing the exchange of GDP for GTP.

Our Active Rac-GEF Assay Kit (Tiam1) uses the agarose bead technology of our Small GTPase Activation Assays (previous page). Agarose beads pull down the active form of Rac-GEFs from endogenous lysates or purified samples. The specific GEF known as Tiam1 is then specifically detected with a polyclonal antibody.

Recent Product Citations

1. Wang, P. et al. (2015). Selective killing of K-ras-transformed pancreatic cancer cells by targeting NAD (P) H oxidase. *Chin. J. Cancer* **34**:1-11.
2. Oubaha, M. et al. (2012). Formation of a PKC/ β -catenin complex in endothelial cells promotes angiopoietin-1-induced collective directional migration and angiogenic sprouting. *Blood* **120**:3371-3381.



Tiam1 Activation Assay. **Left:** 293 cells were transfected with active Tiam1. Active Tiam1 in lysate was pulled down with Rac1 G15A agarose beads. **Right:** Active Tiam-1 in 2 mg of MDA-231 cell lysate was pulled down with Rac1 G15A agarose beads and probed with anti-Tiam1 antibody.

Product Name	Detection	Size	Catalog Number
Active Rac-GEF Assay Kit (Tiam1)	Immunoblot/ECL	20 Assays	STA-422

Small GTPase Agarose Assay Beads

Our agarose beads are useful for selectively pulling down only the active form of small GTPases. The beads are colored for easily visualization. These are the same beads used in our Small GTPase Activation Assays (p. 104-105).



Visible Agarose Beads. Beads are easy to visualize, making it easier to avoid potential loss during washes and aspirations.

Recent Product Citations

1. Moniz, S. et al. (2007). Protein kinase WNK2 inhibits cell proliferation by negatively modulating the activation of MEK1/ERK1/2. *Oncogene* **26**(41):6071-6081. (STA-410)
2. Morrison, A.R. et al. (2014). Chemokine-coupled β 2 integrin-induced macrophage Rac2-Myosin IIA interaction regulates VEGF-A mRNA stability and arteriogenesis. *J. Exp. Med.* **211**:1957-1968. (STA-411)
3. Alam, J. et al. (2014). N-acetylcysteine and the human serum components that inhibit bacterial invasion of gingival epithelial cells prevent experimental periodontitis in mice. *J. Periodontal Implant Sci.* **44**:266-273. (STA-411, STA-412)
4. Sabbatini, M. E. et al. (2010). CCK activates RhoA and Rac1 differentially through G-alpha-13 and G-alpha-q in mouse pancreatic acini. *Am. J. Physiol. Cell Physiol.* **298**:C592-C605. (STA-411, STA-412)
5. Levy-Adam, F. et al. (2008). Heparanase facilitates cell adhesion and spreading by clustering of cell surface heparan sulfate proteoglycans. *PLoS ONE* **3**(6):e2319. (STA-411, STA-412)
6. Sabbatini, M. et al. (2008). Rap1 activation plays a regulatory role in pancreatic amylase secretion. *J. Biol. Chem.* **283**:23884-23894. (STA-412)
7. Gibson, C.C. et al. (2015). Dietary vitamin D and its metabolites non-genomically stabilize the endothelium. *PLoS One* **10**:e0140370. (STA-419)

Product Name	Target	Size	Catalog Number
GGA3 PBD Agarose Beads	Arf	400 μ g	STA-419
PAK1 PBD Agarose Beads	Cdc42, Rac	400 μ g	STA-411
Raf1 RBD Agarose Beads	Ras	400 μ g	STA-410
RalBP1 PBD Agarose Beads	Ral	400 μ g	STA-420
RalGDS RBD Agarose Beads	Rap	400 μ g	STA-418
RanBP1 Agarose Beads	Ran	400 μ g	STA-421
Rhotekin RBD Agarose Beads	Rho	400 μ g	STA-412

GEF Agarose Assay Beads

Our GEF agarose beads are useful for selectively pulling down only the active form of guanine nucleotide exchange factors (GEF). The beads are colored for easily visualization.

Recent Product Citations

1. Ngok, S. et al. (2013). Phosphorylation-mediated 14-3-3 protein binding regulates the function of the Rho-specific guanine nucleotide exchange factor (RhoGEF) Syx. *J. Biol. Chem.* **288**:6640-6650. (STA-431)
2. Wu, C.Y. et al. (2014). PI3K regulation of RAC1 is required for KRAS-induced pancreatic tumorigenesis in mice. *Gastroenterology* **147**:1405-1416. (STA-432)
3. Colacios, C. et al. (2011). The p.Arg63Trp polymorphism controls Vav1 functions and Fox3p regulatory T cell development. *J. Exp. Med.* **208**:2183-2191. (STA-432)

Product Name	Target	Size	Catalog Number
Cdc42 G15A Agarose Beads	Cdc42-GEF	800 μ g	STA-433
Rac1 G15A Agarose Beads	Rac1-GEF	800 μ g	STA-432
RhoA G17A Agarose Beads	RhoA-GEF	400 μ g	STA-431

Small GTPase Expression Vector Sets

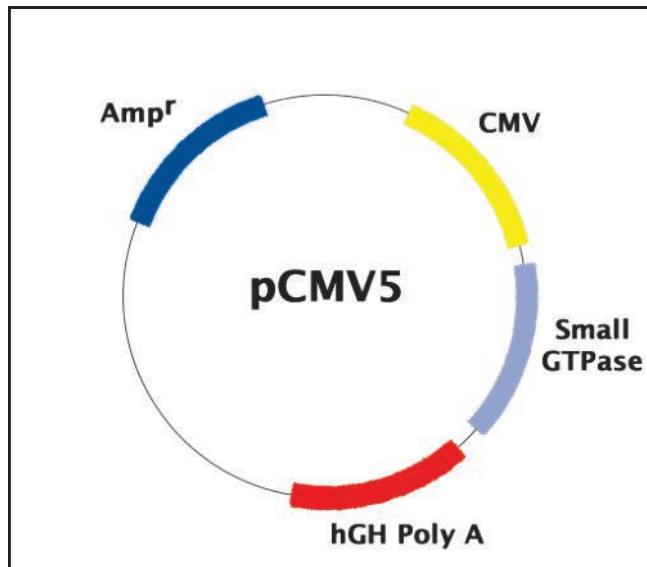
Our Small GTPase Expression Vectors are ideal tools for the study of the most commonly researched small GTPase targets. Each set contains 3 mammalian expression vectors:

- Wild type
- Dominant negative
- Constitutively active

Vectors are available with or without a GFP reporter gene. All vectors are supplied as bacterial glycerol stocks.

Recent Product Citation

Keats, E.C. et al. (2014). Switch from canonical to noncanonical Wnt signaling mediates high glucose-induced adipogenesis. *Stem Cells* 32:1649-1660. (STA-450, STA-452)



Product Name	Vectors	Size	Catalog Number
Cdc42 Expression Vector Set	Wild Type, T17N (Dom. Neg.), Q61L (Active)	3 x 100 µL	STA-455
GFP-Cdc42 Expression Vector Set	Wild Type, T17N (Dom. Neg.), Q61L (Active)	3 x 100 µL	STA-451
Rac1 Expression Vector Set	Wild Type, T17N (Dom. Neg.), G12V (Active)	3 x 100 µL	STA-454
GFP-Rac1 Expression Vector Set	Wild Type, T17N (Dom. Neg.), Q61L (Active)	3 x 100 µL	STA-450
H-Ras Expression Vector Set	Wild Type, T17N (Dom. Neg.), G12V (Active)	3 x 100 µL	STA-457
RhoA Expression Vector Set	Wild Type, T19N (Dom. Neg.), G14V (Active)	3 x 100 µL	STA-456
GFP-RhoA Expression Vector Set	Wild Type, T19N (Dom. Neg.), Q63L (Active)	3 x 100 µL	STA-452

Active Small GTPase Expression Vector Sets

Our Active Small GTPase Expression Vectors are similar to the expression vectors above, except that they are provided as sets of 3 different active mutants for a single small GTPase target. All vectors are supplied as bacterial glycerol stocks.

Product Name	Vectors	Size	Catalog Number
Active Rac1 Expression Vector Set	Q61L, Q61L/F37A, Q61L/Y40C	3 x 100 µL	STA-458
Active H-Ras Expression Vector Set	V12, V12/S35, V12/C40	3 x 100 µL	STA-459

Exoenzyme C3 (Rho Inhibitor) Expression Vector

This vector is supplied as bacterial glycerol stock.

Product Name	Size	Catalog Number
Exoenzyme C3 Expression Vector	3 x 100 µL	STA-460

Gene-Specific Recombinant Retroviral Vectors

Our recombinant retroviral plasmids contain a specific gene cloned into a pBABE vector backbone. Each vector is supplied as bacterial glycerol stock.

Recent Product Citation

Zhao, B. et al. (2012). TNF-induced osteoclastogenesis and inflammatory bone resorption are inhibited by transcription factor RBP-J. *J. Exp. Med.* **209**:319-334. (RTV-101)

Target Name	Vector Backbone	Catalog Number
Cdc42 L61	pBABEhygro	RTV-203
myr-Rac1	pBABEpuro	RTV-201
myr-Rac1 V12	pBABEpuro	RTV-206
Rac1 V12	pBABEhygro	RTV-202

Target Name	Vector Backbone	Catalog Number
Rac3 V12	pBABEhygro	RTV-205
K-Ras	pBABEpuro	RTV-220
K-Ras Q61	pWZLhygro	RTV-221
N-Ras K61	pBABEpuro	RTV-222
Ras V12	pBABEpuro	RTV-101
Ras V12C40	pBABEpuro	RTV-104
Ras V12G37	pBABEpuro	RTV-103
Ras V12S35	pBABEpuro	RTV-102
RhoA L63	pBABEhygro	RTV-204

Small GTPase Recombinant Adenoviruses

Recent Product Citations

- Aissaoui, H. et al. (2015). MDA-9/syntenin is essential for factor VIIa-induced signaling, migration, and metastasis in melanoma cells. *J. Biol. Chem.* **290**:3333-3348. (ADV-149, ADV-152)
- Mao, Y. et al. (2012). Essential diurnal Rac1 activation during retinal phagocytosis requires $\alpha v \beta 5$ integrin but not tyrosine kinases focal adhesion kinase or Mer tyrosine kinase. *Mol. Cell Biol.* **23**:1104-1114. (ADV-150)
- Yu, W.-M. et al. (2009). Laminin is required for Schwann cell morphogenesis. *J. Cell Sci.* **122**:929-936. (ADV-150, ADV-153, ADV-154)
- Salvati, E. et al. (2014). Evidence for G-quadruplex in the promoter of VEGFR-2 and its targeting to inhibit tumor angiogenesis. *Nucleic Acids Res.* **42**:2945-2957. (ADV-151, ADV-157)
- Cheng, Z.-J. et al. (2010). Co-regulation of caveolar and Cdc42-dependent fluid phase endocytosis by phosphocaveolin-1. *J. Biol. Chem.* **285**:15119-15125. (ADV-153)
- Neal M. et al. (2013). A critical role for TLR4 induction of autophagy in the regulation of enterocyte migration and the pathogenesis of necrotizing enterocolitis. *J. Immunol.* **190**:3541-3551. (ADV-156, ADV-157)

Target Name	Catalog Number
Cdc42	ADV-152
Cdc42 L61 (Constitutively Active)	ADV-154
Cdc42 N17 (Dominant Negative)	ADV-153
Rac1	ADV-149
Rac1 L61 (Constitutively Active)	ADV-151
Rac1 N17 (Dominant Negative)	ADV-150
Ras N17 (Dominant Negative)	ADV-145
Ras V12 (Constitutively Active)	ADV-146
Rho L63 (Constitutively Active)	ADV-157
Rho N19 (Dominant Negative)	ADV-156

Small GTPase Recombinant Human Proteins

Protein Name	Tag / Location	Size	Catalog Number
Rac1	6xHis / N-term	50 μ g	STA-728
Ral A	6xHis / N-term	25 μ g	STA-732
Ral B	6xHis / N-term	10 μ g	STA-733
Rap1a	6xHis / N-term	10 μ g	STA-735

Protein Name	Tag / Location	Size	Catalog Number
H-Ras	6xHis / C-term	25 μ g	STA-747
K-Ras	6xHis / N-term	25 μ g	STA-748
N-Ras	None	10 μ g	STA-749
RhoA	6xHis / N-term	20 μ g	STA-740

Recombinant GRP-PH Domain

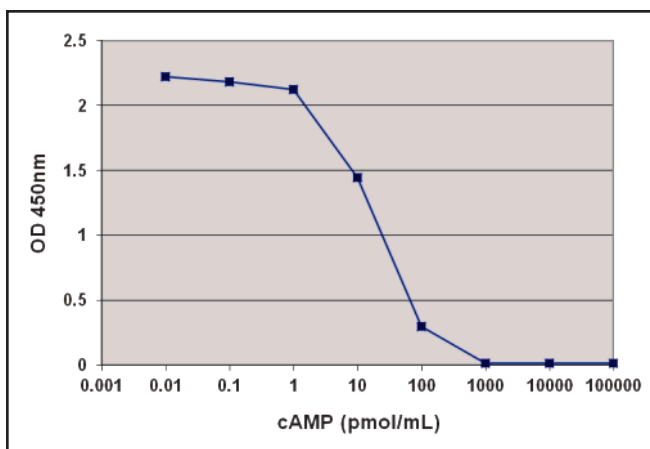
Product Name	Size	Catalog Number
Recombinant GRP-PH Domain	100 μ g	STA-200
	1 mg	STA-200-1MG

Cyclic AMP and GMP ELISA Kits

Cyclic AMP and cyclic GMP are important regulatory molecules in the GPCR signaling cascade. Our cAMP and cGMP ELISA Kits provide a highly sensitive method to measure low levels of cAMP or cGMP in a variety of sample types.

cAMP and cGMP may be tested under either acetylated or non-acetylated conditions. Kits are provided with reagents for acetylation, which may help increase sensitivity when detecting low levels of either analyte.

- **Sensitive:** Detect as little as 1 pmol/mL
- **Versatile:** Suitable for use with cell and tissue lysates, urine, plasma, or culture medium
- **Convenient:** Strip-well plate format with either colorimetric or chemiluminescent detection



Standard Curve Created with the cAMP ELISA Kit, Colorimetric Format.

Recent Product Citations

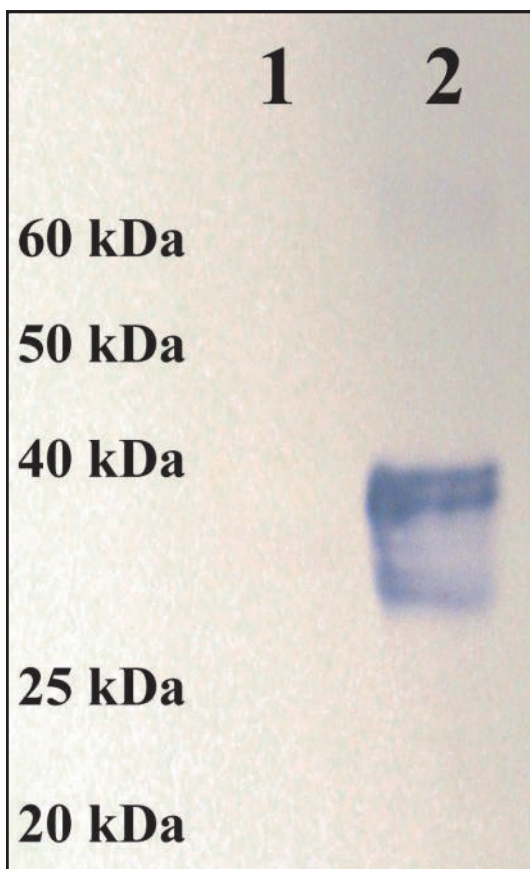
1. He, T. et al. (2015). Role of prostacyclin signaling in endothelial production of soluble amyloid precursor protein- α in cerebral microvessels. *J. Cereb. Blood Flow Metab.* 10.1177/0271678X15618977. (STA-500)
2. Omosun, Y. et al. (2015). IL-10 modulates antigen presentation by dendritic cells through regulation of NLRP3 inflammasome assembly during Chlamydia infection. *Infect. Immun.* 10.1128/IAI.00993-15. (STA-500)
3. Rose, S.J. et al. (2015). A new knock-in mouse model of L-DOPA responsive dystonia. *Brain* 10.1093/brain/awv212. (STA-500)
4. Liu, X. et al. (2015). β -Arrestin-biased signaling mediates memory reconsolidation. *PNAS USA* 10.1073/pnas.1421758112. (STA-500)
5. Cortes, V. et al. (2015). Metabolic effects of cholecystectomy: gallbladder ablation increases basal metabolic rate through G-protein coupled bile acid receptor Gpbar1-dependent mechanisms in mice. *PLoS One* 10:e0118478. (STA-500)
6. Terunuma, M. et al. (2015). Purinergic receptor activation facilitates astrocytic GABA B receptor calcium signalling. *Neuropharmacology* 88:74-81. (STA-500)
7. Jones, A. et al. (2014). Human macrophage SCN5A activates an innate immune signaling pathway for antiviral host defense. *J. Biol. Chem.* 289:35326-35340. (STA-500)
8. Smith, E.P. et al. (2014). The role of β cell glucagon-like peptide -1 signaling in glucose regulation and response to diabetes drugs. *Cell Metab.* 19:1050-1057. (STA-500)
9. Tian, L. et al. (2014). TSH stimulates the proliferation of vascular smooth muscle cells. *Endocrine* 46:651-658. (STA-500)
10. Chen, X. et al. (2014). Identification of serine 348 on the apelin receptor as a novel regulatory phosphorylation site in apelin-13-induced G protein-independent biased signaling. *J. Biol. Chem.* 289:31173-31187. (STA-500)
11. Liu, L. et al. (2014). PKC β II acts downstream of chemoattractant receptors and mTORC2 to regulate cAMP production and myosin II activity in neutrophils. *Mol. Biol. Cell* 25:1446-1457. (STA-501)
12. Santhanam, A.V. et al. (2014). Erythropoietin increases bioavailability of tetrahydrobiopterin and protects cerebral microvasculature against oxidative stress induced by eNOS uncoupling. *J. Neurochem.* 131:521-529. (STA-505)
13. D'Uscio, L.V. et al. (2014). Mechanisms of vascular dysfunction in mice with endothelium-specific deletion of the PPAR- δ gene. *Am. J. Physiol. Hear Circ. Physiol.* 306:H1001-H1010. (STA-505)
14. Yuan, G. et al. (2015). Protein kinase G-regulated production of H₂S governs oxygen sensing. *Sci. Signal* 10.1126/scisignal.2005846. (STA-506)

Product Name	Detection	Size	Catalog Number
cAMP ELISA Kit	Colorimetric	96 Assays	STA-500
		5 x 96 Assays	STA-500-5
	Chemiluminescent	96 Assays	STA-501
		5 x 96 Assays	STA-501-5
cGMP ELISA Kit	Colorimetric	96 Assays	STA-505
		5 x 96 Assays	STA-505-5
	Chemiluminescent	96 Assays	STA-506
		5 x 96 Assays	STA-506-5

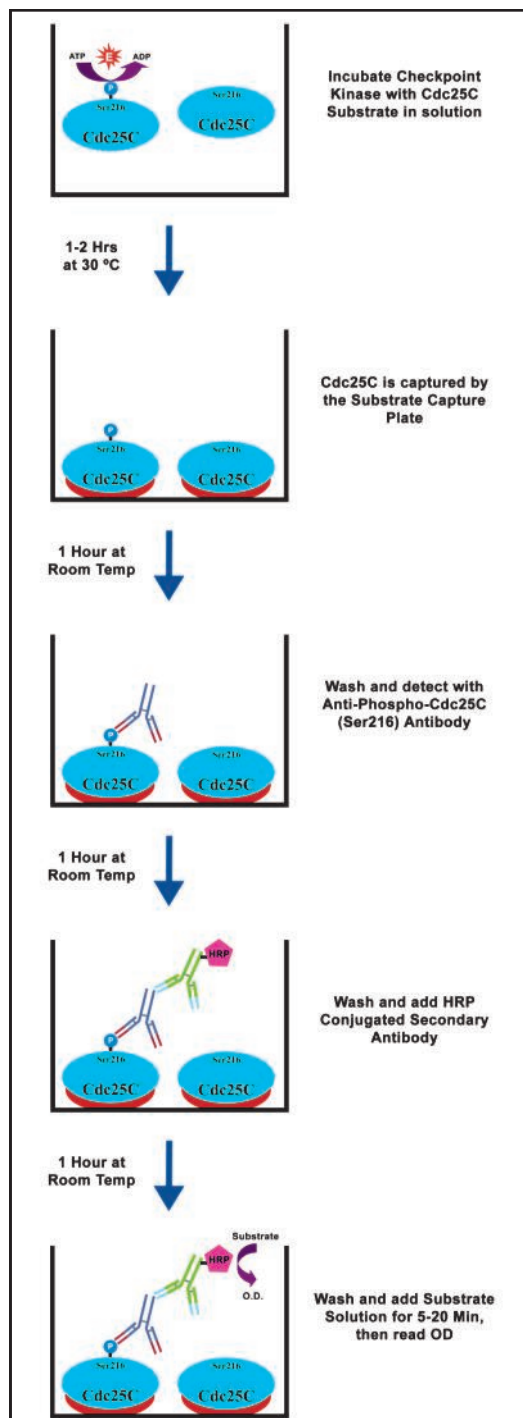
Checkpoint Kinase Activity Assays

Checkpoint kinases, including CHK1 and CHK2, can be activated in response to DNA damage prior to mitosis. These kinases phosphorylate Cdc25C, a protein phosphatase, at Ser-216. This phosphorylation ultimately leads to cell cycle arrest, preventing mitosis and avoiding the passage of DNA damage to daughter cells.

Our Checkpoint Kinase Activity Assays allow you to conveniently measure the activity of CHK1 and CHK2. The assays use recombinant Cdc25C as a checkpoint kinase substrate. Phosphorylated Cdc25C (Ser216) is detected using a phospho-specific antibody. Checkpoint Kinase Activity Assays are available in two formats: a Western blot assay and a 96-well plate-based activity assay.



CHK1 Activity Using the Checkpoint Kinase Activity Immunoblot Kit. Lane 1: Negative Control; Lane 2: 10 ng of active CHK1.



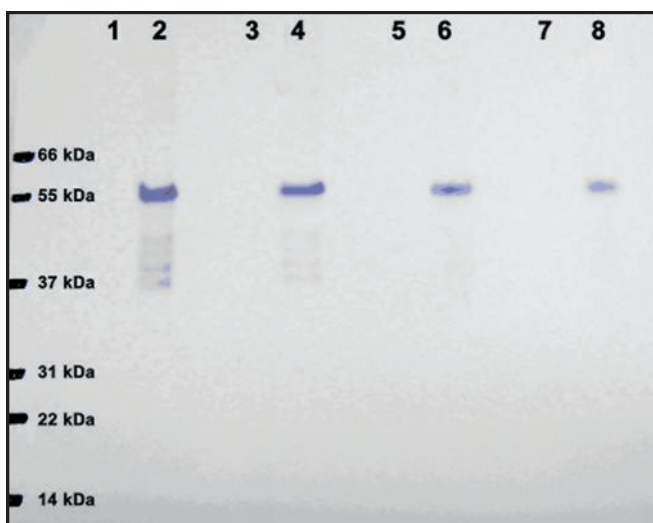
96-Well Checkpoint Kinase Activity Assay Principle.

Product Name	Detection	Size	Catalog Number
Checkpoint Kinase Activity Immunoblot Kit	Immunoblot	20 Assays	STA-413
96-Well Checkpoint Kinase Activity Assay Kit	Colorimetric	96 Assays	STA-414
		5 x 96 Assays	STA-414-5

Rho Kinase (ROCK) Activity Assays

Rho Kinase (ROCK) is a serine/threonine kinase which is a target of Rho. ROCK mediates Rho signaling and reorganizes the actin cytoskeleton via the phosphorylation of several substrates that contribute to contractility and the assembly of actin filaments.

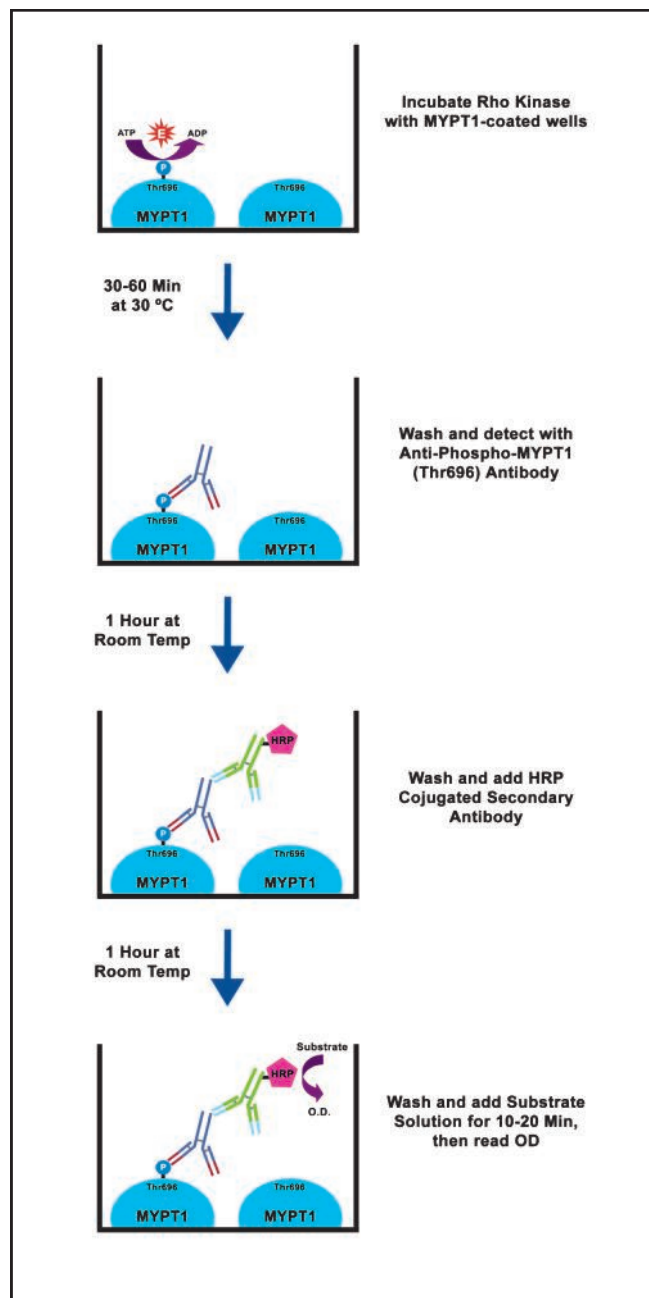
Our ROCK Activity Assays provide a non-radioactive format to measure the level of active ROCK in cell or tissue lysates. The immunoblot kit provides a convenient format for measuring ROCK activity in a few samples, while the 96-well Activity Assay contains a strip-well plate precoated with MYPT1 for higher throughput.



Results Using the ROCK Activity Immunoblot Kit. Lanes 1, 3, 5, 7: Without ROCK (negative control). Lanes 2, 4, 6, 8: With ROCK. Lanes 1 & 2: 200 ng MYPT1; Lanes 3 & 4: 100 ng; Lanes 5 & 6: 50 ng; Lanes 7 & 8: 25 ng. Phosphorylation of MYPT1 substrate was detected by anti-phospho-MYPT1 as described in the protocol.

Recent Product Citations

- Su, C.C. et al. (2015). Phenotypes of trypsin- and collagenase-prepared bovine corneal endothelial cells in the presence of a selective Rho kinase inhibitor, Y-27632. *Mol. Vis.* **21**:633-643. (STA-415)
- Sailland, J. et al. (2014). Estrogen-related receptor α decreases RHOA stability to induce orientated cell migration. *PNAS USA* **111**:15108-15113. (STA-415)
- Liu, Y. et al. (2015). ROCK inhibition impedes macrophage polarity and functions. *Cell Immunol.* 10.1016/j.cellimm.2015.12.005. (STA-416)
- Li, H. et al. (2015). KAP regulates ROCK2 and Cdk2 in an RNA-activated glioblastoma invasion pathway. *Oncogene* **34**:1432-1441. (STA-416)
- Munoz, A. et al. (2015). Aging-related increase in Rho kinase activity in the nigral region is counteracted by physical exercise. *J. Gerontol. A Biol. Sci. Med. Sci.* 10.1093/gerona/glv179. (STA-416)



96-Well ROCK Activity Assay Principle.

Product Name	Detection	Size	Catalog Number
ROCK Activity Immunoblot Kit	Immunoblot	20 Assays	STA-415
96-Well ROCK Activity Assay	Colorimetric	96 Assays	STA-416
		5 x 96 Assays	STA-416-5

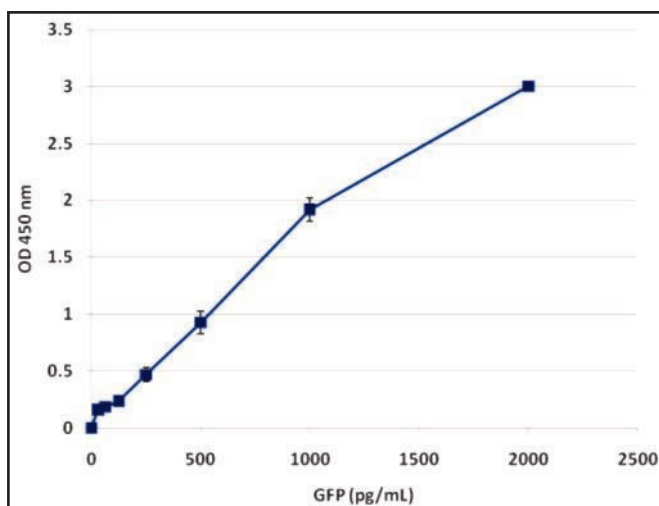
Reporter Assays, Cell Lines and Reagents

We offer a variety of tools for various reporter molecules:

- Reporter Assays
- Reporter Stable Cell Lines
- Recombinant Fluorescent Proteins
- Antibodies to Reporter Molecules
- Reporter Viral Vectors

GFP ELISA Kit

Most imaging studies of rGFP are qualitative, and quantitation by FACS is time consuming and expensive. Our GFP ELISA kit uses a standard microplate reader to quantify GFP levels with extremely high sensitivity. This kit will detect GFP from *Aequorea victoria* as well as its variants.



Standard Curve Generated with the GFP ELISA Kit.

- **Sensitive:** Detection limit of 30 pg/mL
- **Versatile:** Quantify GFP and its variants: BFP, CFP or YFP
- **Easy Quantitation:** Measure GFP levels in a standard microplate reader

Recent Product Citations

1. Borjan, B. et al. (2015). The Aplidin analogs PM01215 and PM02781 inhibit angiogenesis in vitro and in vivo. *BMC Cancer* **15**:738.
2. Gee, H.Y. et al. (2015). KANK deficiency leads to podocyte dysfunction and nephrotic syndrome. *J. Clin. Invest.* **10.1172/JCI79504**.
3. Zhang, Y. et al. (2015). Characterization of the promoter of Grapevine vein clearing virus. *J. Gen. Virol.* **96**:165-169.
4. Anyaegbu, C.C. et al. (2014). Chemotherapy enhances cross-presentation of nuclear tumor antigens. *PLoS One* **9**:e107894.
5. Sendra, L. et al. (2014). Low RNA translation activity limits the efficacy of hydrodynamic gene transfer to pig liver in vivo. *J. Gene Med.* **16**:179-192.
6. Mango, R. et al. (2014). C-C chemokine receptor 5 on pulmonary mesenchymal cells promotes experimental metastasis via the induction of erythroid differentiation regulator 1. *Mol. Cancer Res.* **12**:274-282.
7. Mitchell, A. et al. (2014). Promyelocytic leukemia protein is a cell-intrinsic factor inhibiting parvovirus DNA replication. *J. Virol.* **88**:925-936.
8. Huhtala, T. et al. (2014). Biodistribution and antitumor effect of Cetuximab-targeted lentivirus. *Nucl. Med. Biol.* **41**:77-83.

Product Name	Detection	Size	Catalog Number
GFP ELISA Kit	Colorimetric	96 Assays	AKR-121
		5 x 96 Assays	AKR-121-5

GFP Quantitation Kit

When direct quantitation of GFP fluorescence levels is desired, our GFP Quantitation Kit provides a superior method over time-consuming flow cytometry and semi-quantitative imaging techniques. This kit measures fluorescence levels directly in a plate-based fluorometer.

Recent Product Citations

1. Shim, M.S. et al. (2014). Stimuli-responsive siRNA carriers for efficient gene silencing in tumors via systemic delivery. *Biomater. Sci.* **2**:35-40.
2. Pfeiffer, B. et al. (2012). Using translational enhancers to increase transgene expression in *Drosophila*. *PNAS* **109**:6626-6631.

Product Name	Detection	Size	Catalog Number
GFP Quantitation Kit	Fluorometric	100 Assays	AKR-120

RFP ELISA Kit

Our RFP ELISA Kit provides a convenient, sensitive alternative to imaging systems and time-consuming FACS quantitation. The assay quantifies a wide variety of red fluorescent protein variants including DsRed, TagRFP, TurboRFP, tdTomato, mCherry, mKate, mRuby, mBanana, mOrange, mPlum, and mStrawberry. Detect as little as 150pg/mL.



Recent Product Citation

Fang, J. et al. (2015). COP11 dependent ER export: a critical component of insulin biogenesis and beta cell ER homeostasis. *Mol. Endocrinol.* 10.1210/me.2015-1012.

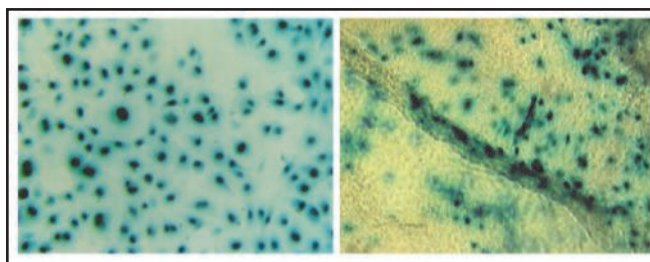
Product Name	Detection	Size	Catalog Number
RFP ELISA Kit	Colorimetric	96 Assays	AKR-122

β -Galactosidase Staining Kit

LacZ is a commonly used reporter gene in transfection experiments because its gene product, β -galactosidase, is extremely stable and resistant to proteolytic degradation, making it easy to assay. Our β -Galactosidase Staining Kit provides an efficient, easy-to-use method to determine the transfection efficiency of the LacZ gene.

Recent Product Citations

- Ge, X. et al. (2015). Mitochondrial catalase suppresses naturally occurring lung cancer in old mice. *Pathobiol. Aging Age Relat. Dis.* 5:28776.
- Xu, X. et al. (2015). Aberrant activation of TGF- β in subchondral bone at the onset of rheumatoid arthritis joint destruction. *J. Bone Miner Res.* 10.1002/jbmr.2550.



X-Gal Staining of Infected HUVEC Cells and Chick CAM Tissue.

Left: HUVEC cells were infected with purified Ad- β -Gal at 50 MOI (multiplicity of infection). X-gal staining was performed after 48 hour infection period. **Right:** Purified Ad- β -Gal was injected intravenously into a 10-day old chick embryo. After three days, X-gal staining was performed on the chick chorioallantoic membrane tissue.

Product Name	Size	Catalog Number
β -Galactosidase Staining Kit	75 Assays	AKR-100

Reporter Stable Cell Lines

Each cell line expresses one or more reporter molecules.

Recent Product Citations

- Irvine, S.A. et al. (2015). Printing cell-laden gelatin constructs by free-form fabrication and enzymatic protein crosslinking. *Biomed. Microdevices* 17:1-8. (AKR-200)
- Carey, S.P. et al. (2015). Comparative mechanisms of cancer cell migration through 3D matrix and physiological microtracks. *Am. J. Physiol. Cell Physiol.* 308:C436-C447. (AKR-201)
- Shopsowitz, K.E. et al. (2015). Periodic-shRNA molecules are capable of gene silencing, cytotoxicity and innate immune activation in cancer cells. *Nucleic Acids Res.* 10.1093/nar/gkv1488. (AKR-209, AKR-213)
- Zhang, K. et al. (2014). Block-cell-printing for live single-cell printing. *PNAS* 111:2948-2953. (AKR-211)

Recent Product Citations (cont'd)

- Tassoni, A. et al. (2015). Molecular mechanisms mediating retinal reactive gliosis following bone marrow mesenchymal stem cell transplantation. *Stem Cells* 10.1002/stem.2095. (AKR-214)
- Huang, F. and Mazin, A.V. (2014). A small molecule inhibitor of human RAD51 potentiates breast cancer cell killing by therapeutic agents in mouse xenografts. *PLoS One* 9:e100993. (AKR-231)
- Tung, C.H. et al. (2015). A quick responsive fluorogenic pH probe for ovarian tumor imaging. *Theranostics* 5:1166-1174. (AKR-232)

Cell Line	Catalog Number
293/GFP	AKR-200
A549/GFP	AKR-209

Cell Line	Catalog Number
HeLa/GFP	AKR-213
MCF-7/GFP	AKR-211
MCF-7/Luc	AKR-234
MDA-MB-231/GFP	AKR-201
MDA-MB-231/Luc	AKR-231
MDA-MB-231/RFP	AKR-251
NIH3T3/GFP	AKR-214
OVCAR-5/RFP	AKR-254
SKOV-3/GFP-Luc	AKR-225
SKOV-3/Luc	AKR-232
T47D/GFP	AKR-208

Recombinant Fluorescent Proteins

Recombinant EGFP and RFP are provided at 1 mg/mL and includes a 6xHis-tag at the C-terminus.

Recent Product Citation

Caschera, F. and Noireaux, V. (2015). Preparation of amino acid mixtures for cell-free expression systems. *Biotechniques* **58**:40-43. (STA-201)

Product Name	Size	Catalog Number
Recombinant EGFP	100 µg	STA-201
	5 x 100 µg	STA-201-5
Recombinant RFP	100 µg	STA-202
	5 x 100 µg	STA-202-5

Monoclonal Antibodies to Reporter Molecules

Antibodies are provided at a concentration of 1 mg/mL. GFP antibody also recognizes EGFP, YFP, EYFP and CFP. RFP antibody recognizes Tag-RFP, Turbo-RFP, DeRed, mCherry and mOrange.

Antibodies are suitable for Western blot, Immunostaining, ELISA and Dot blot.

Recent Product Citation

Maamary, J. et al. (2012). Attenuated influenza virus constructs with enhanced hemagglutinin protein expression. *J. Virol.* **86**:5782-5790. (AKR-021)

Product Name	Size	Catalog Number
Anti-GFP clone GF28R	100 µg	AKR-020
Anti-RFP clone RF5R	100 µg	AKR-021

Gene-Specific Reporter Constructs

Each vector contains a specific gene of interest plus a GFP reporter gene.

Target Name	Catalog Number
AMPA1 / GFP	AKR-515
mCD98 / GFP	AKR-501
CREB / 3' GFP	AKR-504
CREB / 5' GFP	AKR-505
mCrx / GFP	AKR-506

Target Name	Catalog Number
CSF1 / GFP	AKR-500
G-alpha-q / GFP	AKR-507
GAPDH / GFP	AKR-514
Grin1 / GFP	AKR-517
LC3 / GFP	CBA-401

Target Name	Catalog Number
NMDAR1 / GFP	AKR-503
psd95 / GFP	AKR-518
Sec24b / GFP	AKR-512
Sh3glb2 / GFP	AKR-509
SynCAM / GFP	AKR-502

Reporter Viral Vectors

Reporter Adeno-Associated Viruses

Product Name	Catalog Number
AAV1-GFP Control Virus	AAV-301
AAV2-GFP Control Virus	AAV-302
AAV2-Luc Control Virus	AAV-320
AAV3-GFP Control Virus	AAV-303
AAV5-GFP Control Virus	AAV-305
AAV6-GFP Control Virus	AAV-306

Reporter Lentiviruses

Product Name	Catalog Number
GFP Lentivirus Control	LTV-300
RFP Lentivirus Control	LTV-301

Reporter Adenoviruses

Target Name	Catalog Number
β-Galactosidase	ADV-002
Firefly Luciferase	ADV-008
GFP	ADV-004

Reporter Retroviral Plasmids

Target Name	Vector Backbone	Catalog Number
GFP	pBABE	RTV-002
GFP	pMCs	RTV-051
GFP	pMX	RTV-050
GFP	pMYs	RTV-052
GFP-Puro	pMX	RTV-053

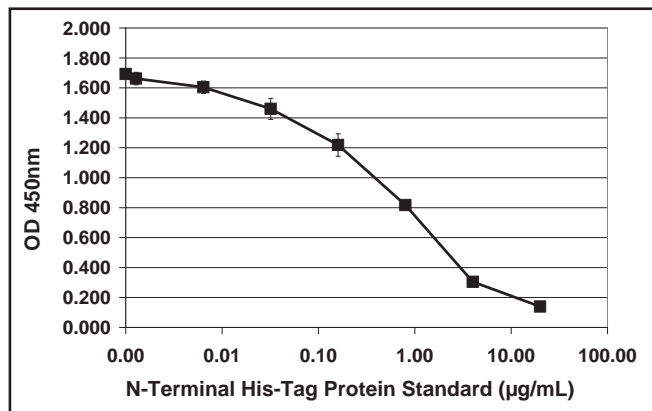
His-Tag Protein ELISA Kit

Our His-Tag Protein ELISA Kit allows you to detect and quantify His-tagged protein samples simply and reliably by comparing unknown samples with a recombinant standard. The kit is suitable for use with cell lysates and tissue homogenates.

- **Sensitive:** Detect as little as 1 ng/mL protein or 50 pM of 6xHis-tag residues
- **Versatile:** Use with proteins containing His-tag at either N- or C-terminus

Recent Product Citations

1. Rinaldo, A.R. et al. (2015). A grapevine anthocyanin acyltransferase, transcriptionally regulated by VvMYBA, can produce most acylated anthocyanins present in grape skins. *Plant Physiol.* **169**:1897-1916.
2. Akiyama, Y. et al. (2014). The identification of affinity peptide ligands specific to the variable region of human antibodies. *Bio-med. Res.* **35**:105-116.
3. Dong, Y. et al. (2013). HMGB1 protein does not mediate the inflammatory response in spontaneous spinal cord regeneration: a hint for CNS regeneration. *J. Biol. Chem.* **288**:18204-18218.



Quantitation of N-Terminal His-Tag Protein.

Product Name	Detection	Size	Catalog Number
His-Tag Protein ELISA Kit	Colorimetric	96 Assays	AKR-130

Monoclonal Antibodies to Epitope Tags

Antibodies are provided at a concentration of 1 mg/mL. GAPDH, β -Actin and β -Tubulin are also available as loading controls. All are suitable for Western blot, Immunostaining, ELISA, Immunoprecipitation, and Dot blot.

Recent Product Citations

1. Sandner, F. et al. (2014). Expression of the oestrogen receptor GPER by testicular peritubular cells is linked to sexual maturation and male fertility. *Andrology* **2**:695-701. (AKR-001)
2. Orlandi, A. et al. (2015). ERCC1 induction after oxaliplatin exposure may depend on KRAS mutational status in colorectal cancer cell line: *In Vitro Veritas. J. Cancer* **6**:70-81. (AKR-002)
3. Satchidanandam, V. et al. (2014). The glycosylated Rv1860 protein of *Mycobacterium tuberculosis* inhibits dendritic cell mediated TH1 and TH17 polarization of T cells and abrogates protective immunity conferred by BCG. *PLoS Pathog.* **10**:e1004176. (AKR-003)
4. Wang, S. et al. (2014). Characterization of two UDP-Gal:GalNAc-diphosphate-lipid β 1,3-galactosyltransferases WbwC from *Escherichia coli* serotypes O104 and O5. *J. Bacteriol.* **196**:3122-3133. (AKR-003)
5. Starostova, M. et al. (2014). The oncoprotein v-Myb activates transcription of Gremlin 2 during in vitro differentiation of the chicken neural crest to melanoblasts. *Gene* **540**:122-129. (AKR-006)
6. Drake, L.L. et al. (2015). Functional characterization of Aquaporins and Aquaglyceroporins of the yellow fever mosquito, *Aedes aegypti*. *Sci. Rep.* **5**:7995. (AKR-007)

Product Name	Size	Catalog Number
Mouse Anti-FLAG Tag Monoclonal Antibody (clone FG4R)	100 μ g	AKR-004
Mouse Anti-GST Tag Monoclonal Antibody (clone GST.B6)	100 μ g	AKR-005
Mouse Anti-HA Tag Monoclonal Antibody (clone HA.C5)	100 μ g	AKR-006
Mouse Anti-His Tag Monoclonal Antibody (clone HIS.H8)	100 μ g	AKR-003
Mouse Anti-Myc Tag Monoclonal Antibody (clone Myc.A7)	100 μ g	AKR-007
Mouse Anti-V5 Tag Monoclonal Antibody (clone E10)	100 μ g	AKR-008
Mouse Anti-GAPDH Monoclonal Antibody	100 μ g	AKR-001
Mouse Anti- β -Actin Monoclonal Antibody	100 μ g	AKR-002
Mouse Anti- β -Tubulin Monoclonal Antibody	100 μ g	AKR-009

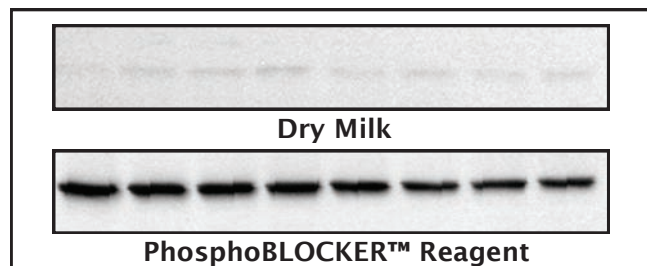
PhosphoBLOCKER™ Western Blot Blocking Reagent

Western blot blockers such as dry milk or serum are sufficient to block unreactive sites on the membrane. However, they are not designed to preserve phosphoprotein antigens during blotting.

- **High Sensitivity:** Enhances low level phosphoprotein signal without increasing background
- **Easy-to-use:** Premixed dry blend

Recent Product Citations

1. Shinoda, K. et al. (2015). Pin1 facilitates NF- κ B activation and promotes tumour progression in human hepatocellular carcinoma. *Br. J. Cancer* 10.1038/bjc.2015.272.
2. Matsushima, M. et al. (2015). Intravesical dual PI3K/mTOR complex 1/2 inhibitor NVP-BEZ235 therapy in an orthotopic bladder cancer model. *Int. J. Oncol.* 10.3892/ijo.2015.2995.
3. Bemben, M.A. et al. (2015). Autism-associated mutation inhibits protein kinase C-mediated neuroligin-4X enhancement of excitatory synapses. *PNAS USA* 112:2551-2556.
4. Shimura, T. et al. (2014). DNA damage signaling guards against perturbation of cyclin D1 expression triggered by low-dose long-term fractionated radiation. *Oncogenesis* 3:e132.

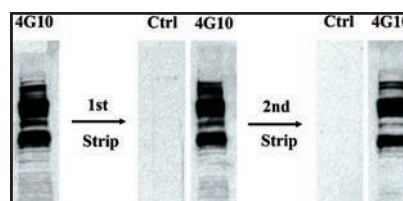


Superior Blocking with PhosphoBLOCKER™ Reagent. A549 cell lysate was blocked with dry milk or PhosphoBLOCKER before detection with anti-Phospho-p38 antibody.

Product Name	Size	Catalog Number
PhosphoBLOCKER™ Western Blot Blocking Reagent	1 L	AKR-103
	4 L	AKR-104

Phospho Antibody Stripping Solution

This solution removes anti-phosphoantibodies selectively from blots without significantly affecting the immobilized proteins, allowing re-probing of the blot with the same or a different antibody. Stripping of antibodies is done at room temperature, so no heating of blots is required.

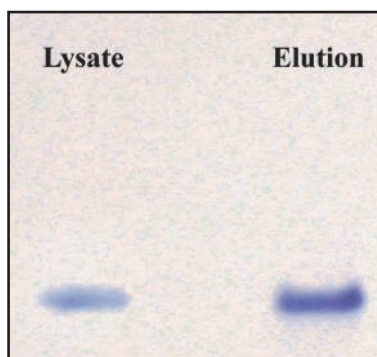


Multiple Blotting and Stripping of 4G10 Phosphotyrosine Antibody.

Product Name	Size	Catalog Number
Phospho Antibody Stripping Solution	10 mL	AKR-102

Phosphoprotein Purification Kit

Our Phosphoprotein Purification Kit allows you to enrich your phosphoprotein samples quickly and easily. Phosphorylated proteins are affinity purified from lysates with a single-step purification / enrichment matrix. The entire procedure takes about 4 hours. Each prep can process 2.5 mg of total lysate protein, or approximately one confluent 10 cm dish.



Enrichment of p-ERK. HeLa cell lysate was incubated with the Phosphoprotein Enrichment Matrix from the Phosphoprotein Purification Kit.

Product Name	Size	Catalog Number
Phosphoprotein Purification Kit	2 preps	AKR-105
	5 preps	AKR-106

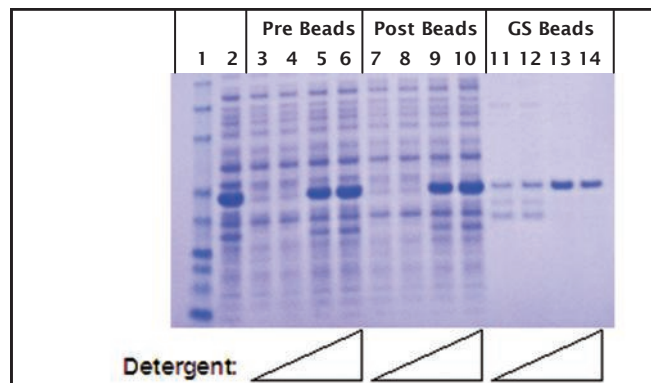
Rapid GST Inclusion Body Solubilization and Renaturation Kit

The Rapid GST Inclusion Body Solubilization and Renaturation Kit is designed to retrieve expressed GST fusion proteins in soluble form after lysis and extraction. Each kit contains sufficient reagents to solubilize and renature up to 5-10 liters of bacterial culture.

- **Fast Results:** No lengthy dialysis or dilution steps
- **Easy-to-Use:** No pH variation or redox pair
- **Optimized:** Designed specifically to solubilize and renature GST inclusion bodies

Recent Product Citations

1. Matsuoka, T. et al. (2014). Expression and characterization of honeybee, *Apis mellifera*, larva chymotrypsin-like protease. *Apidologie* 10.1007/s13592-014-0313-2.
2. Keller, D. et al. (2014). Mechanisms of HsSAS-6 assembly promoting centriole formation in human cells. *J. Cell Biol.* **204**:697-712.



Solubilization and Renaturation of GST-RTK Fusion Protein. Lane 1: MW STD; Lane 2: Whole E.Coli lysate; Lane 3, 7, 11: No detergent; Lane 4, 8, 12: 32-fold dilution; Lane 5, 9, 13: 8-fold dilution; Lane 6, 10, 14: 2-fold dilution.

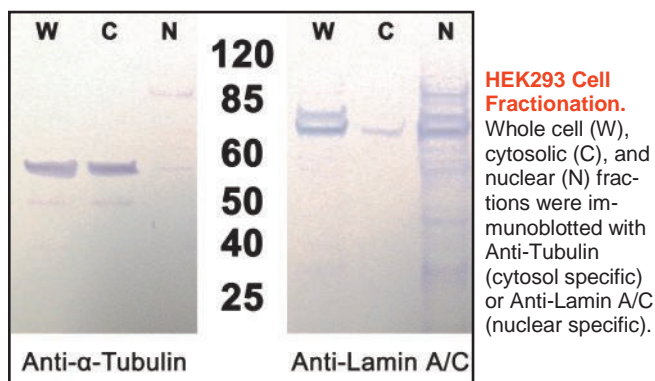
Product Name	Size	Catalog Number
Rapid GST Inclusion Body Solubilization and Renaturation Kit	1 Kit	AKR-110

Nuclear/Cytosolic Fractionation Kit

The Nuclear/Cytosolic Fractionation Kit provides a simple and fast tool to isolate nuclear extract from the cytoplasmic fraction of mammalian cells. The optimized protocol provides high protein recovery and low cross-contamination in less than 2 hours.

Recent Product Citations

1. Jeon, Y.J. et al. (2015). A set of NF- κ B-regulated microRNAs induces acquired TRAIL resistance in lung cancer. *PNAS USA* **112**:E3355-E3364.
2. Zou, J. et al. (2014). A TIR domain protein from *E. faecalis* attenuates MyD88-mediated signaling and NF- κ B activation. *PLoS One* **9**:e112010.



Product Name	Size	Catalog Number
Nuclear/Cytosolic Fractionation Kit	20 preps	AKR-171
	100 preps	AKR-172

Bacterial Protein Extraction Reagents

Our Bacterial Protein Extraction Reagents contain a gentle, non-ionic detergent formulation that quickly extracts functional recombinant proteins from *E. coli* without mechanical disruption. The reagents are compatible with 6xHis and GST affinity purification systems and are suitable for small-scale or large-scale protein extraction.

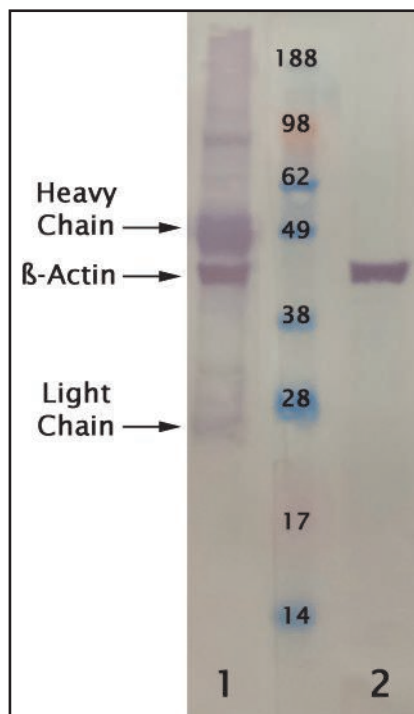
Product Name	Size	Catalog Number
5X Bacterial Protein Extraction Reagent (Phosphate)	50 mL	AKR-181
5X Bacterial Protein Extraction Reagent (Tris)	50 mL	AKR-180

Pure-IP™ Western Blot Detection Kit

Immunoprecipitation (IP) is used to isolate a protein of interest by capturing it with a resin-immobilized antibody specific for that protein. Typically, proteins are eluted from agarose beads under denaturing conditions that also release the IP antibody into solution, and then the protein is detected by Western blot. In many cases the antibody used for IP must also be used for immunoblotting, resulting in massive background due to interference from heavy and light chain antibodies.

The Pure-IP™ Western Blot Detection Kit circumvents this problem by using a proprietary HRP conjugate that cannot bind to contaminating heavy or light chains in the immunoblot lane of interest. The conjugate only detects the antibodies that are properly folded and bound to the protein of interest, resulting in a cleaner immunoblot. The kit works with both colorimetric and chemiluminescent detection methods.

- **Cleaner Results:** Reduces background from heavy and light antibody chains on Western blots
- **Versatile:** Suitable for IgG from most species



Detection of Actin from HeLa Whole Cell Lysate Mixed with Monoclonal Antibody. 20 µg of HeLa lysate and 2 µg of monoclonal antibody were loaded per lane. Lane 1 was probed with goat anti-mouse HRP; Lane 2 was probed with 1X HRP Conjugate Solution from the Pure-IP™ Western Blot Detection Kit.

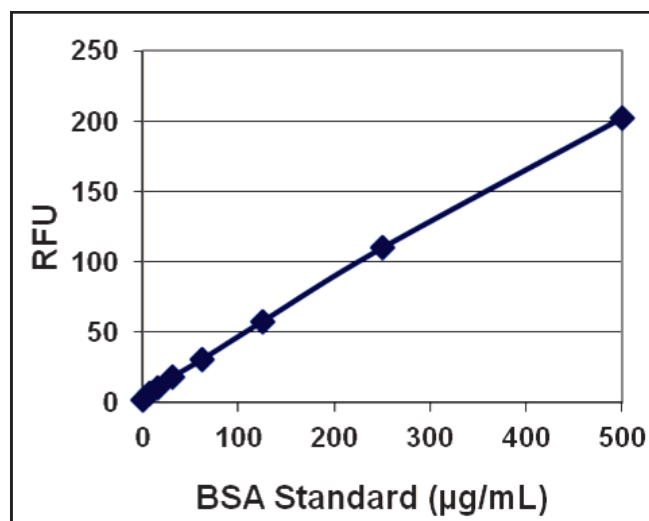
Product Name	Size	Catalog Number
Pure-IP™ Western Blot Detection Kit	20 Blots	PRB-5002

High Sensitivity Protein Quantitation Assay Kit

Our High Sensitivity Protein Quantitation Assay Kit provides a robust method to quantify protein concentrations in the µg/mL range.

The fluorometric format creates a significant sensitivity advantage over standard colorimetric methods such as Bradford or BCA assays.

- **Highly Sensitive:** Quantify protein concentrations as low as 5 µg/mL
- **Fast:** Obtain results in 5 to 15 minutes
- **Easy-to-use:** Read on a 96-well fluorescence plate reader



Standard Curve Generated with the High Sensitivity Protein Quantitation Assay Kit.

Product Name	Size	Catalog Number
High Sensitivity Protein Quantitation Assay Kit	100 Assays	AKR-185

Rapid Antibody Purification Kit

Our Rapid Antibody Purification Kit is designed for fast, single-step purification of high-quality IgG from ascites, serum, tissue culture media or hybridoma supernatants. IgG-containing samples are incubated with immobilized Protein A in the presence of a binding buffer. Non-IgG components are washed and IgG is subsequently eluted.

Recent Product Citation

Ye, J. et al. (2015). Tissue-specific expression pattern and histological distribution of NLRP3 in Chinese yellow chicken. *Vet. Res. Commun.* **39**:171-177.

Species	mg of IgG per Prep
Bovine	15-20
Goat	6-12
Human	20-30
Mouse	6-12
Rabbit	15-20

Capacity per Prep for the Rapid Antibody Purification Kit.

Product Name	Size	Catalog Number
Rapid Antibody Purification Kit	10 Preps	AKR-160

RIPA Buffer

RIPA buffer is a popular reagent for lysis of both adherent and suspension cells in culture, as well as making tissue homogenates. RIPA buffer extracts cytoplasmic, membrane, and nuclear proteins for a variety of downstream protein assays and immunoassays.

Our RIPA Buffer is provided as a 5X concentrate and is available with or without a Protease Inhibitor Cocktail.

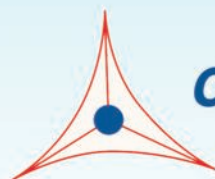
Recent Product Citation

Matsumoto, Y. et al. (2014). Ezrin mediates neuritogenesis via down-regulation of RhoA activity in cultured cortical neurons. *PLoS One* **9**:e105435..

Product Name	Size	Catalog Number
5X RIPA Buffer	20 mL	AKR-191
5X RIPA Buffer, with Protease Inhibitor Cocktail	20 mL	AKR-190

Metabolism Research

Lipoprotein Metabolism	122
Cellular Metabolism	142
Renal Function Assays	148
Alcohol Assays	150



CELL BIOLABS, INC.

Creating Solutions for Life Science Research

Lipoprotein Metabolism Research

Lipoproteins are important assemblies of proteins and lipids that have implications in cardiovascular and related diseases. Our kits and reagents can help streamline the study of various members of lipoprotein metabolism pathways:

- Cholesterol / Lipoproteins
- Apolipoproteins
- Oxidized LDL & HDL
- Lipoprotein Receptors
- Cholesteryl Ester Pathway
- Lipoprotein Lipase
- Triglycerides
- Free Fatty Acids
- Bile Acids
- Phospholipids

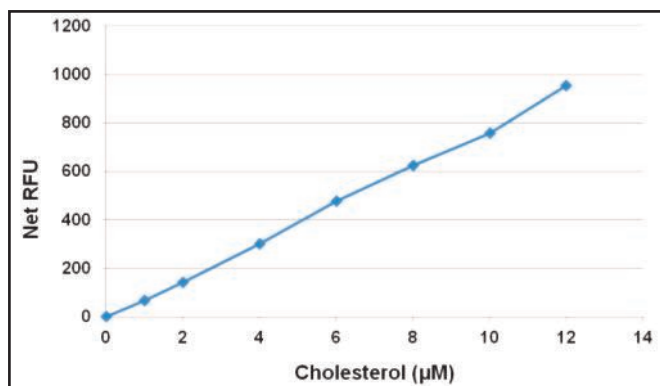
Total Cholesterol Assay Kits

Our Total Cholesterol Assay Kits provide a simple plate-based format that measures the amount of cholesterol in serum, plasma, cell lysates or tissue homogenates.

In the presence of cholesterol esterase, the assay will measure total cholesterol in both forms. In the absence of the esterase, the assay will measure only free cholesterol.

Quantitation is performed in a 96-well plate reader with your choice of colorimetric or fluorescence-based detection.

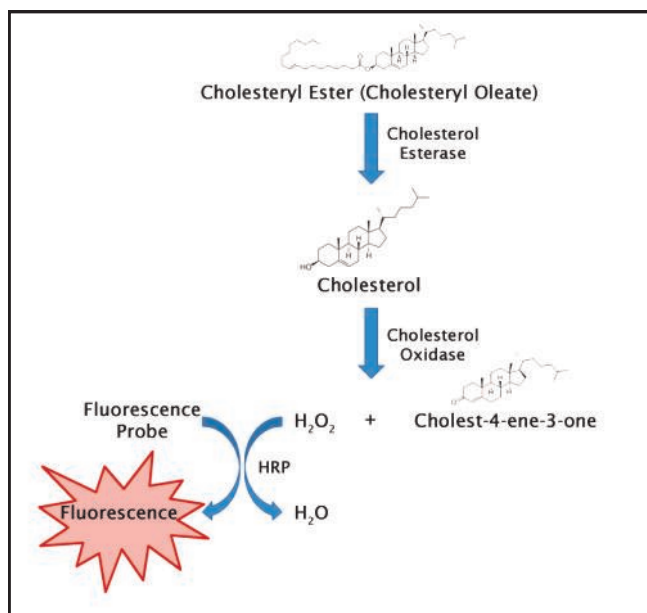
- **Sensitive:** Detect as little as 100 nM
- **Fast:** Simple 30 minute protocol
- **Easy-to-use:** Detect in a 96-well plate reader; colorimetric and fluorometric formats available



Total Cholesterol Standard Curve.

Recent Product Citations

1. Marino, A. et al. (2014). ITCH deficiency protects from diet-induced obesity. *Diabetes* **63**:550-561. (STA-384)
2. Mathews, E. et al. (2014). Mutation of 3-hydroxy-3-methylglutaryl CoA synthase I reveals requirements for isoprenoid and cholesterol synthesis in oligodendrocyte migration arrest, axon wrapping, and myelin gene expression. *J. Neurosci.* **34**:3402-3412. (STA-384)
3. Joseph, B.K. et al. (2015). Inhibition of AMP kinase by the protein phosphatase 2A heterotrimer, PP2APpp2r2d. *J. Biol. Chem.* **10.1074/jbc.M114.626259**. (STA-390)
4. Ananth, S. et al. (2014). Regulation of the cholesterol efflux transporters ABCA1 and ABCG1 in retina in hemochromatosis and by the endogenous siderophore 2,5-dihydroxybenzoic acid. *Biochim. Biophys. Acta.* **1842**:603-612. (STA-390)



Assay Principle for the Total Cholesterol Assay Kit (Fluorometric).

Product Name	Detection	Size	Catalog Number
Total Cholesterol Assay Kit	Colorimetric	192 Assays	STA-384
	Fluorometric	192 Assays	STA-390

HDL-Cholesterol Assay Kit

Our HDL-Cholesterol Assay Kit provides a simple plate-based format similar to our Total Cholesterol Assays (previous page). This kit measures the amount of cholesterol in the HDL fraction isolated from serum, plasma, cell lysates or tissue homogenates.

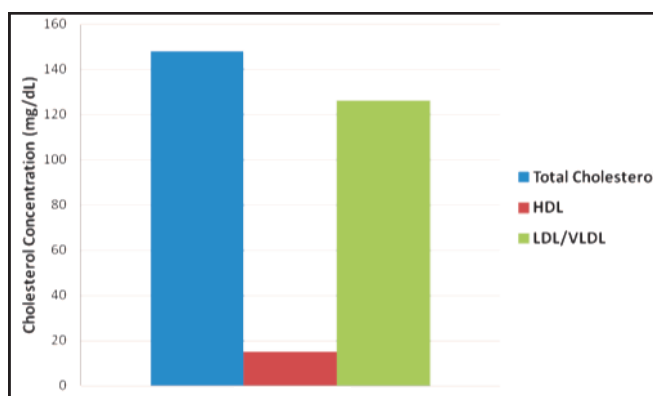
- **Sensitive:** Detect as little as 1 μM
- **Fast:** Simple 45 minute assay protocol
- **Easy-to-use:** Detect in a 96-well plate fluorescence-based plate reader

Product Name	Detection	Size	Catalog Number
HDL-Cholesterol Assay Kit	Fluorometric	96 Assays	STA-394

HDL and LDL/VLDL Cholesterol Assay Kit

Our HDL and LDL/VLDL Cholesterol Assay Kit is similar in principle to our Total Cholesterol Assay Kit, but allows you to quantify HDL and LDL/VLDL separately in serum samples. After separating samples into HDL and LDL/VLDL fractions, the fluorometric assay is run according to the Assay Principle for the Total Cholesterol Assay Kit (previous page).

In the presence of cholesterol esterase, the assay will measure total cholesterol in both free cholesterol and cholesteryl ester forms. In the absence of the esterase, the assay will measure only free cholesterol. Quantitation of cholesteryl ester alone may be calculated by subtracting free cholesterol from total cholesterol levels.



Quantitation of Total Cholesterol, LDL/VLDL, and HDL from Human Serum.

Recent Product Citations

1. Sessions-Bresnahan, D.R. et al. (2015). Effect of obesity on the preovulatory follicle and lipid fingerprint of equine oocytes. *Biol. Reprod.* 10.1095/biolreprod.115.130187.
2. O'Hare, E.A. et al. (2014). Disruption of LDLR causes increased LDL-C and vascular lipid accumulation in a Zebrafish model of hypercholesterolemia. *J. Lipid Res.* 55:2242-2253.

Product Name	Detection	Size	Catalog Number
HDL and LDL/VLDL Cholesterol Assay Kit	Fluorometric	192 Assays	STA-391

Human Lipoproteins

Our human lipoproteins are isolated from human plasma following ultracentrifugation.

Product Name	Size	Catalog Number
Human High Density Lipoprotein (HDL)	100 μg	STA-243
Human High Density Lipoprotein-2 (HDL-2)	100 μg	STA-244
Human High Density Lipoprotein-3 (HDL-3)	100 μg	STA-245
Human Low Density Lipoprotein (LDL)	100 μg	STA-241
Human Low Density Lipoprotein (LDL), Copper (Cu ⁺⁺) Oxidized	100 μg	STA-214
Human Low Density Lipoprotein (LDL), Malondialdehyde Modified	100 μg	STA-212
Human Low Density Lipoprotein (LDL), Nitrated	100 μg	STA-213
Human Very Low Density Lipoprotein (VLDL)	100 μg	STA-242

Human Apolipoprotein ELISA Kits

Apolipoproteins comprise the protein component of lipoprotein assemblies. Apolipoproteins fall into two classes:

- Non-exchangeable Apo B associates with LDL
- Exchangeable Apo A, C and E associate with HDL

Our Human Apo ELISA Kits provide a convenient and sensitive method for quantifying specific apolipoproteins in serum, plasma, or other biological fluids.

Apo (a)	Apo AI	Apo AII	Apo B	Apo CI	Apo CII	Apo CIII	Apo E
1 ng/mL	50 pg/mL	0.3 ng/mL	1 ng/mL	200 pg/mL	1 ng/mL	50 pg/mL	200 pg/mL

Detection Limits of Cell Biolabs' Human Apo ELISA Kits.

Recent Product Citations

1. Bissig-Choisat, B. et al. (2015). Development and rescue of human familial hypercholesterolaemia in a xenograft mouse model. *Nat. Commun.* **6**:7339. (STA-359)
2. Song, X. et al. (2014). APOA-I: a possible novel biomarker for metabolic side effects in first episode schizophrenia. *PLoS One* **9**:e93902. (STA-362)
3. Lee, J.Y. et al. (2014). Apolipoprotein E likely contributes to a maturation step of infectious hepatitis C virus particles and interacts with viral envelope glycoproteins. *J. Virol.* **88**:12422-12437. (STA-364, STA-367)
4. Xu, D.D. et al. (2014). Discovery and identification of serum potential biomarkers for pulmonary tuberculosis using iTRAQ-coupled two-dimensional LC-MS/MS. *Proteomics* **14**:322-331. (STA-365)
5. Rice, S.J. et al. (2015). Proteomic profiling of human plasma identifies apolipoprotein E (APOE) as being associated with smoking and a marker for squamous metaplasia of the lung. *Proteomics* 10.1002/pmic.201500029. (STA-367)
6. Sukhanov, S. et al. (2015). Insulin-like growth factor I reduces lipid oxidation and foam cell formation via downregulation of 12/15-lipoxygenase. *Atherosclerosis* **238**:313-320. (STA-368)

Product Name	Detection	Size	Catalog Number
Human Apo(a) ELISA Kit	Colorimetric	96 Assays	STA-359
Human ApoAI ELISA Kit	Colorimetric	96 Assays	STA-362
Human ApoAII ELISA Kit	Colorimetric	96 Assays	STA-363
Human ApoB ELISA Kit	Colorimetric	96 Assays	STA-368
Human ApoCI ELISA Kit	Colorimetric	96 Assays	STA-364
Human ApoCII ELISA Kit	Colorimetric	96 Assays	STA-365
Human ApoCIII ELISA Kit	Colorimetric	96 Assays	STA-366
Human ApoE ELISA Kit	Colorimetric	96 Assays	STA-367

Human Apolipoproteins

Following ultracentrifugation, lipoproteins are isolated from human plasma. Water-soluble apolipoproteins are then purified from delipidated lipoprotein.

Product Name	Size	Catalog Number
Human Apolipoprotein AI	100 µg	STA-232
Human Apolipoprotein AII	100 µg	STA-233
Human Apolipoprotein B-100	100 µg	STA-234
Human Apolipoprotein B-100, Malondialdehyde Modified	100 µg	STA-211
Human Apolipoprotein CI	100 µg	STA-235
Human Apolipoprotein CIII	100 µg	STA-237

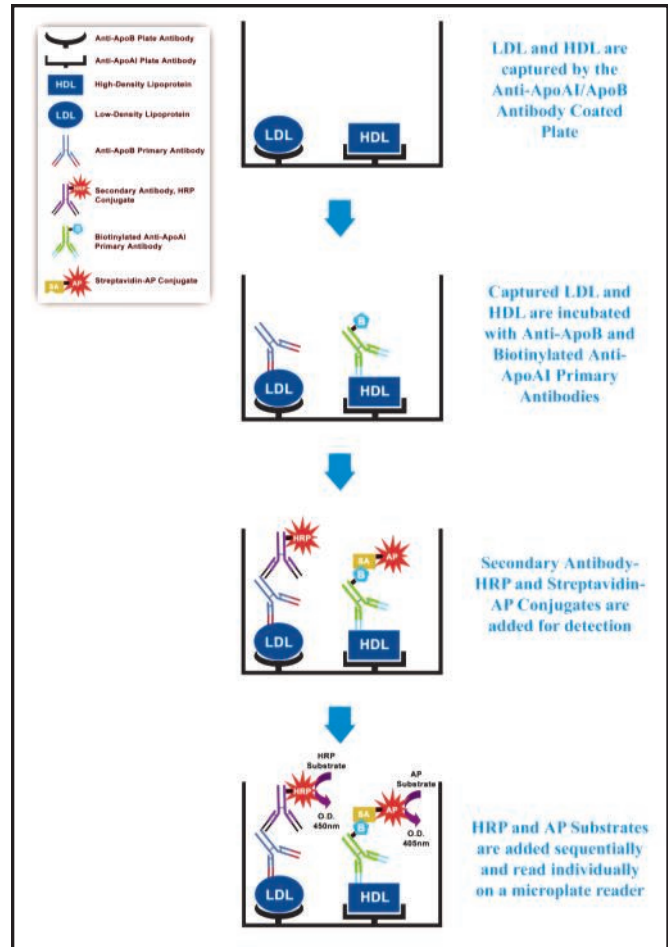
Human ApoA1 and ApoB Duplex ELISA Kit

As the primary protein components of HDL and LDL respectively, ApoA1 and ApoB are arguably the most significant apolipoproteins in lipid metabolism research.

Our Human ApoA1 and ApoB Duplex ELISA Kit provides a convenient tool to quantify both proteins in a single serum or plasma sample. Unlike other multiplex assays, our ApoA1 and ApoB Duplex ELISA does not require a luminometer for detection. Simply quantify both proteins using a standard colorimetric ELISA plate reader.

The ELISA plate is coated with Anti-ApoA1 and Anti-ApoB antibodies, which respectively capture HDL and LDL from the sample. Biotinylated Anti-ApoA1 and Anti-ApoB detection antibodies are added, followed by enzyme conjugates. Alkaline phosphatase substrate is added allowing quantitation of ApoA1. After washing, HRP is added to allow quantitation of ApoB.

- **Efficient:** Quantify two apolipoproteins from the same sample in just a few hours
- **Sensitive:** Detect as little as 0.1 ng/mL of ApoA1 and 1 ng/mL of ApoB from serum or plasma
- **Quantitative:** Compare results to known ApoA1 and ApoB standards



Human ApoA1 and ApoB Duplex ELISA Kit Assay Principle.

Product Name	Detection	Size	Catalog Number
Human ApoA1 and ApoB Duplex ELISA Kit	Colorimetric	96 Assays	STA-361

Antibodies to Apolipoproteins

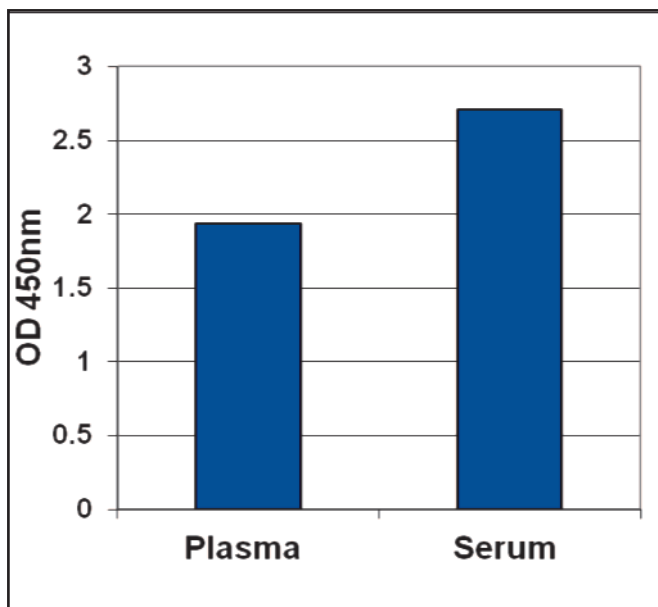
Antibodies are affinity purified.

Product Name	Detection	Size	Catalog Number
Sheep Anti-Human Apolipoprotein (a) Polyclonal Antibody	Immunoblot/ELISA	100 µg	STA-131
Goat Anti-Human Apolipoprotein AI Polyclonal Antibody	Immunoblot/ELISA	100 µg	STA-132
Rabbit Anti-Human Apolipoprotein AII Polyclonal Antibody	Immunoblot/ELISA	100 µg	STA-133
Goat Anti-Human Apolipoprotein B-100/48 Polyclonal Antibody	Immunoblot/ELISA	100 µg	STA-134
Rabbit Anti-Human Apolipoprotein CI Polyclonal Antibody	Immunoblot/ELISA	100 µg	STA-135
Rabbit Anti-Human Apolipoprotein CII Polyclonal Antibody	Immunoblot/ELISA	100 µg	STA-136
Rabbit Anti-Human Apolipoprotein CIII Polyclonal Antibody	Immunoblot/ELISA	100 µg	STA-137
Goat Anti-Human Apolipoprotein E Polyclonal Antibody	Immunoblot/ELISA	100 µg	STA-138

OxiSelect™ Human Oxidized LDL ELISA Kits

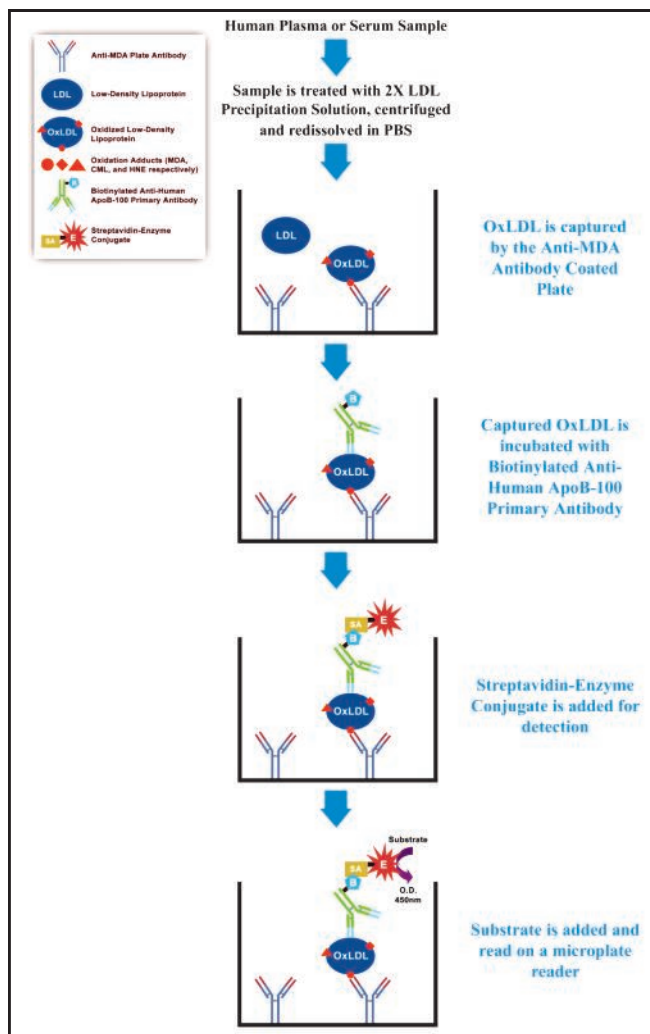
LDL contains a hydrophobic core of various lipids surrounded by one molecule of Apolipoprotein B-100 (ApoB-100), which promotes solubility of the LDL in blood. LDL, often described as “bad” cholesterol, is even more dangerous when it becomes oxidized. Oxidized LDL (OxLDL) is more reactive with surrounding tissues and can collect within the inner lining of arteries.

Our OxiSelect™ Human Oxidized LDL ELISA Kits are designed for the detection and quantitation of modified LDL in human plasma or serum. Kits are available to detect MDA-LDL, CML-LDL, or HNE-LDL in either the protein or lipid component of LDL. Our OxPL-LDL kit specifically detects oxidation in the phospholipid component of LDL.



Quantitation of MDA-LDL in Serum and Plasma Samples. Serum and plasma samples were treated with LDL Precipitation Solution. Precipitated LDL pellets were resuspended in 1.6 mL of PBS before further dilution 1:160 in Assay Diluent according to the Assay Protocol.

- **Sensitive:** Detect as little as 50 ng/mL of MDA-LDL, 150 ng/mL of CML-LDL, 150 ng/mL of HNE-LDL, or 100 ng/mL of OxPL-LDL
- **Quantitative:** Compare unknown samples with provided copper oxidized LDL standard



OxiSelect™ Human Oxidized LDL ELISA Assay Principle.

MDA is the most commonly found damage marker in oxidized LDL, but it can degrade in frozen samples after 1-2 months. CML and HNE, while less commonly found in OxLDL, may be more reliably detectable in samples that have been frozen for several months.

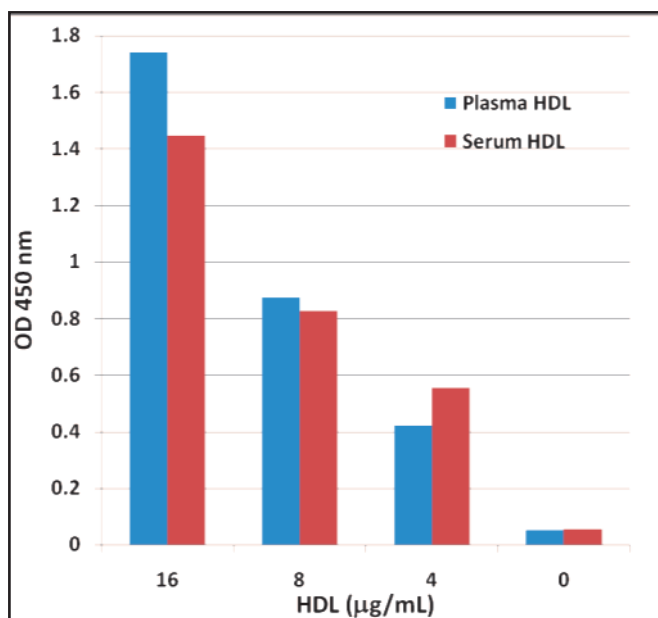
Product Name	Detection	Size	Catalog Number
OxiSelect™ Human Oxidized LDL ELISA Kit (CML-LDL Quantitation)	Colorimetric	96 Assays	STA-388
OxiSelect™ Human Oxidized LDL ELISA Kit (HNE-LDL Quantitation)	Colorimetric	96 Assays	STA-389
OxiSelect™ Human Oxidized LDL ELISA Kit (MDA-LDL Quantitation)	Colorimetric	96 Assays	STA-369
OxiSelect™ Human Oxidized LDL ELISA Kit (OxPL-LDL Quantitation)	Colorimetric	96 Assays	STA-358

OxiSelect™ Human Oxidized HDL ELISA Kits

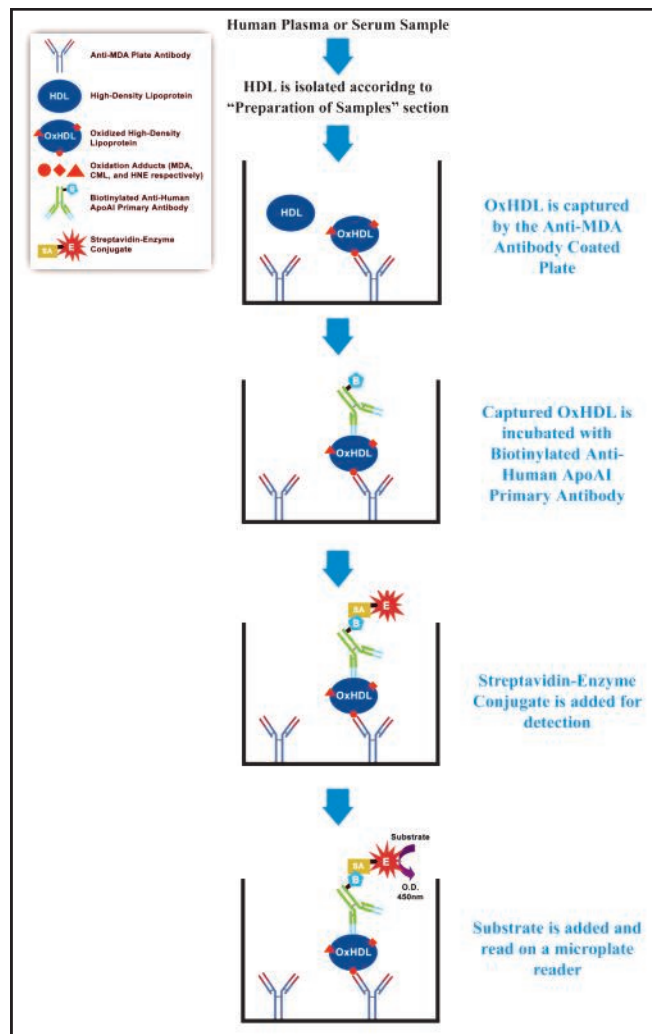
Like LDL, HDL (high density lipoprotein) can become oxidized in either the protein or lipid component. While HDL is often described as “good” cholesterol, oxidation of HDL can cause it to lose its usual cardioprotective properties and cause it to be more dangerous than helpful.

Our OxiSelect™ Human Oxidized HDL ELISA Kits are designed for the detection and quantitation of modified HDL in human plasma or serum. Kits are available to detect MDA-HDL, CML-HDL or HNE-HDL.

- **Sensitive:** Detect as low as 1 ng/mL of MDA-HDL, 1 ng/mL of CML-HDL, or 2 ng/mL of HNE-HDL
- **Quantitative:** Compare unknown samples with provided copper oxidized HDL standard



Quantitation of HNE-HDL in Serum and Plasma Samples. Serum and plasma samples were isolated and diluted in Assay Diluent.



Assay Principle for the OxiSelect™ Human Oxidized HDL ELISA (MDA-HDL Quantitation).

MDA is the most commonly found damage marker in oxidized HDL, but it can degrade in frozen samples after 1-2 months. CML and HNE, while less commonly found in OxHDL, may be more reliably detectable in samples that have been frozen for several months.

Product Name	Detection	Size	Catalog Number
OxiSelect™ Human Oxidized HDL ELISA Kit (CML-HDL Quantitation)	Colorimetric	96 Assays	STA-888
OxiSelect™ Human Oxidized HDL ELISA Kit (HNE-HDL Quantitation)	Colorimetric	96 Assays	STA-889
OxiSelect™ Human Oxidized HDL ELISA Kit (MDA-HDL Quantitation)	Colorimetric	96 Assays	STA-869

Human LDL Receptor ELISA Kit

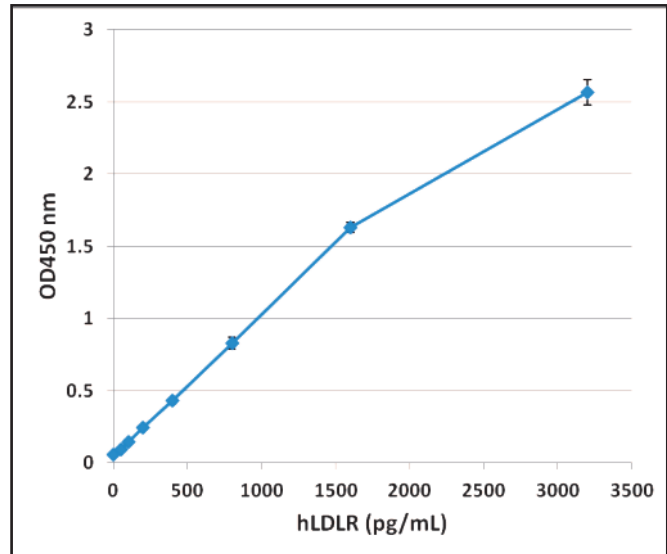
Cholesterol can be toxic when accumulated in excess in cell membranes. The low-density lipoprotein receptor (LDLR) is the primary means of removing cholesterol from the circulation. LDLR is a transmembrane protein that transports cholesterol-carrying lipoprotein particles (primarily LDL) into cells. Receptor-ligand complexes enter the cell by endocytosis; bound lipoproteins are subsequently released in the low-pH setting of the endosome, while the receptors return to the cell surface.

Our Human LDLR ELISA Kit provides a simple, convenient method for the detection and quantitation of LDL receptor in a variety of human sample types.

- **Sensitive:** Detect as little as 50 pg/mL of human LDLR
- **Versatile:** Assay is compatible with plasma, serum, cell lysates and tissue homogenates
- **Quantitative:** Compare results to a known human LDLR standard

Recent Product Citation

Alvarez, M.L. et al. (2015). MicroRNA-271 decreases the level and efficiency of the LDL receptor and contributes to the dysregulation of cholesterol homeostasis. *Atherosclerosis* **242**:595-604.



Standard Curve Generated with the Human LDLR ELISA Kit.

Product Name	Detection	Size	Catalog Number
Human LDLR ELISA Kit	Colorimetric	96 Assays	STA-386

Human LOX-1 ELISA Kit

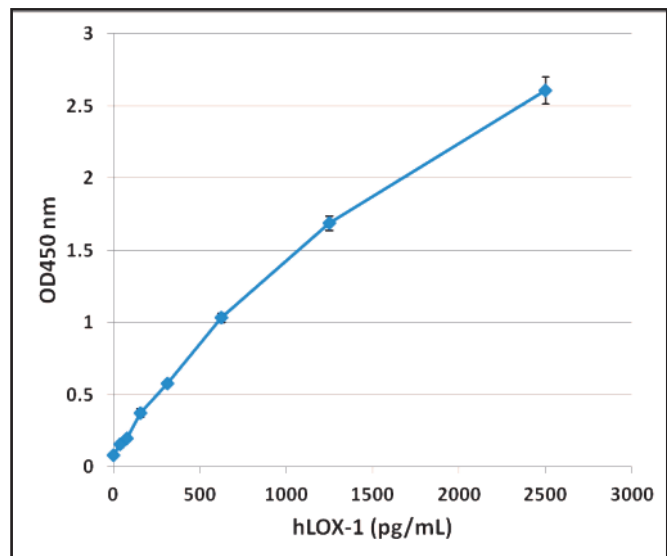
Monocytes and macrophages can form atherosclerotic lesions when they take in oxidized LDL (OxLDL). Uptake is done via the lectin-like oxidized LDL receptor-1 (LOX-1), which is expressed in vascular endothelium as well as in vascular smooth muscle cells, differentiated macrophages and platelets. LOX-1 can be cleaved and released as a soluble form (sLOX-1), which can serve as a prognostic biomarker in serum for early acute coronary syndromes, stroke and coronary heart disease.

Our Human LOX-1 ELISA Kit provides a simple, convenient method for the detection and quantitation of LOX-1 receptor in a variety of sample types.

- **Sensitive:** Detect as little as 40 pg/mL
- **Versatile:** Assay is compatible with plasma, serum, cell lysates, tissue homogenates, or cell culture supernatants
- **Quantitative:** Compare results to a known human LOX-1 standard

Recent Product Citation

Wu, J. et al. (2013). Clinical nephrology—IgA nephropathy, lupus nephritis, vasculitis. *Nephrol. Dial. Transplant.* **28**:i175-i184.



Standard Curve Generated with the Human LOX-1 ELISA Kit.

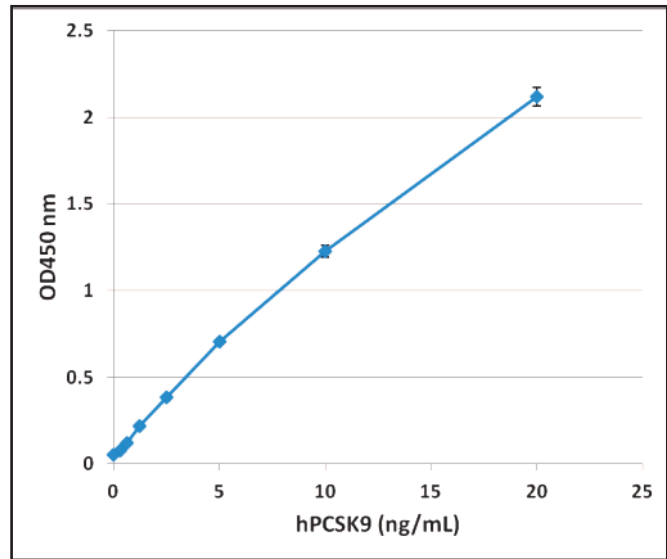
Product Name	Detection	Size	Catalog Number
Human LOX-1 ELISA Kit	Colorimetric	96 Assays	STA-387

Human PCSK9 ELISA Kit

Proprotein convertase subtilisin kexin 9 (PCSK9) is a member of the proteinase K subfamily of subtilisin-related serine endoproteases. PCSK9 mediates LDL receptor (LDLR) degradation by binding to the EGF domain of the LDLR. This binding prevents LDLR from being sorted to the endosomes for recycling back to the cell surface. Instead, the PCSK9/LDLR complex is distributed to the lysosomes for degradation.

Our Human PCSK9 ELISA Kit provides a simple, convenient method for the detection and quantitation of PCSK9 in a variety of human sample types.

- **Sensitive:** Detect as little as 150 pg/mL of human PCSK9
- **Versatile:** Assay is compatible with plasma, serum, and cell and tissue lysates
- **Quantitative:** Compare results to a known human PCSK9 standard



Standard Curve Generated with the Human PCSK9 ELISA Kit.

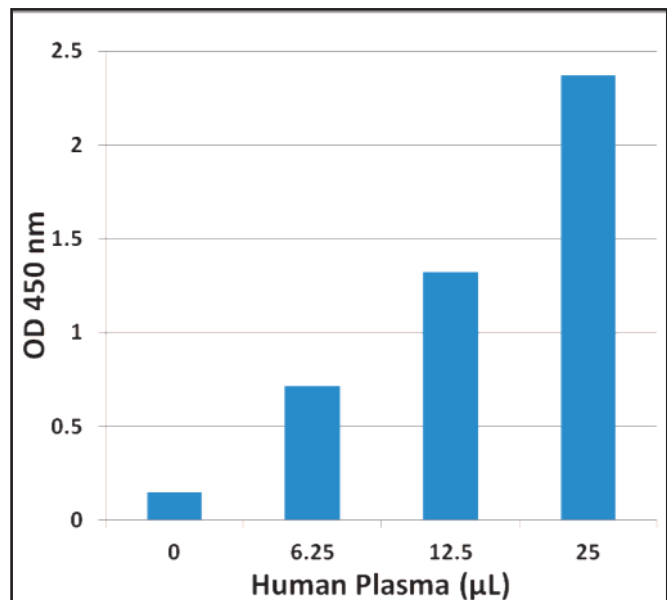
Product Name	Detection	Size	Catalog Number
Human PCSK9 ELISA Kit	Colorimetric	96 Assays	STA-385

Human LRP1 ELISA Kit

LDL Receptor-Related Protein 1 (LRP1), also known as CD91, is a member of the LDL receptor family. LRP1 is involved in many physiological processes including the clearing of a variety of circulatory molecules such as proteinase-inhibitor complexes, serpin enzyme complexes, and activated coagulation factors. It has also been shown to be involved in the regulation of cell migration, macrophage phagocytosis, and blood brain barrier permeability.

Our Human LRP1 ELISA Kit provides a convenient plate-based format for the detection and quantitation of LRP1 in a variety of human sample types. A standard of known concentration of LRP1 is provided against which unknown samples may be quantified.

- **Sensitive:** Detect as little as 50 pg/mL of human PCSK9
- **Versatile:** Assay is compatible with plasma, serum, and cell and tissue lysates
- **Quantitative:** Compare results to a known human LRP1 standard



Detection of Soluble LRP1 in Human Plasma with the Human LRP1 ELISA Kit.

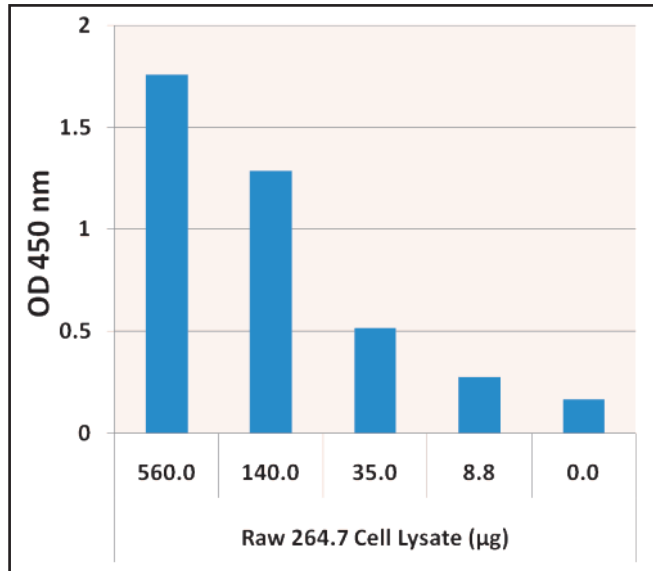
Product Name	Detection	Size	Catalog Number
Human LRP1 ELISA Kit	Colorimetric	96 Assays	STA-609

Scavenger Receptor Class B Member 1 (SRB1) ELISA Kit

Scavenger Receptor Class B Member 1, also known as SRB1 or SCARB1, is a transmembrane protein that plays a critical role in the reverse cholesterol transport pathway where cholesterol is cleared from macrophages and peripheral tissues and transported to the liver. SRB1 appears to mediate binding of HDL and the selective uptake of cholesteryl esters (CE).

Our Scavenger Receptor Class B Member 1 (SRB1) ELISA Kit provides a convenient format for the quantitation of SRB1 in human and rodent samples. Each kit provides sufficient reagents to perform up to 96 assays including standards and unknowns.

- **Sensitive:** Detect as little as 600 pg/mL of human SRB1
- **Versatile:** Assay is compatible with plasma, serum, and cell or tissue lysates
- **Quantitative:** Compare results to a known human SRB1 standard



Detection of SRB1 in Mouse Raw 264.7 Cell Lysate.

Product Name	Detection	Size	Catalog Number
Scavenger Receptor Class B Member 1 (SRB1) ELISA Kit	Colorimetric	96 Assays	STA-630

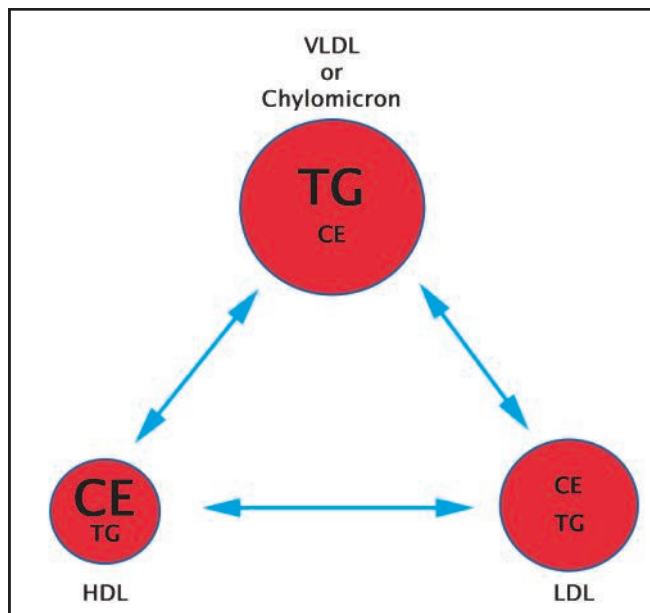
Human Cholesteryl Ester Transfer Protein (CETP) ELISA Kit

Cholesterol exists within lipoproteins in two forms: a free alcohol and a fatty cholesteryl ester. The cholesteryl ester is the predominant form of cholesterol transport and storage.

Cholesteryl ester transfer protein (CETP) promotes the transfer of both cholesteryl esters and triglycerides between various types of lipoprotein particles: HDL, LDL, VLDL, and chylomicrons.

Our Human CETP ELISA Kit provides a simple, convenient method for the detection and quantitation in a variety of human sample types.

- **Sensitive:** Detect as little as 60 ng/mL of human CETP
- **Versatile:** Assay is compatible with plasma, serum, and other biological fluids
- **Quantitative:** Compare results to a known human CETP standard



CETP Promotes Bidirectional Transfer of Cholesteryl Esters (CE) and Triglycerides (TG) Between Lipoproteins.

Product Name	Detection	Size	Catalog Number
Human Cholesteryl Ester Transfer Protein (CETP) ELISA Kit	Colorimetric	96 Assays	STA-614

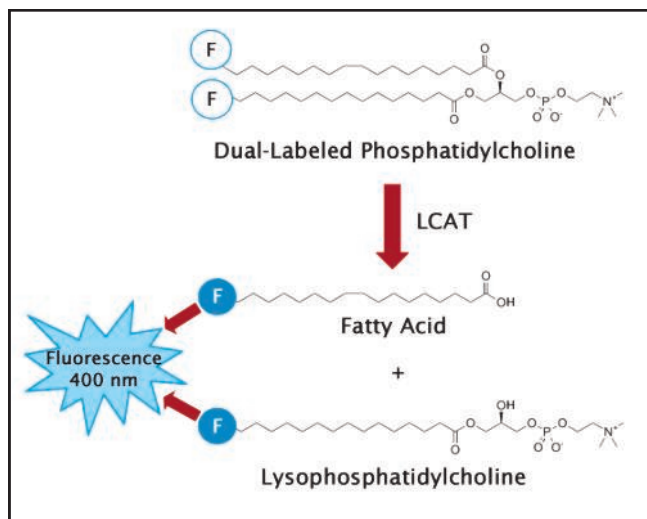
Lecithin Cholesterol Acyltransferase (LCAT) Activity Assay Kit

Lecithin cholesterol acyltransferase (LCAT) is an enzyme associated with lipoproteins and plays a key role in promoting the transfer of excess cell-associated cholesterol from peripheral tissues to the liver to be excreted. LCAT catalyzes the transfer of an sn-2 acyl group from phosphatidylcholine to cholesterol, forming a cholesteryl ester. LCAT is bound to lipoproteins in the blood including HDL and LDL.

Our LCAT Activity Assay Kit provides a simple, convenient method for measuring the phospholipase activity of LCAT in a variety of sample types including plasma, serum, cell lysates and tissue homogenates. Quantitation of LCAT activity is performed in a 96-well fluorescence-based plate reader. This assay may also be used to quantify other calcium independent phospholipase activities such as lipoprotein phospholipase A2 (LP-PLA2).

Recent Product Citation

Jung, M.A. et al. (2015). Hypcholesterolemic effects of *Curcuma longa* L. with *Nelumbo nucifera* leaf in an in vitro model and a high cholesterol diet-induced hypercholesterolemic mouse model. *Animal Cells and Systems* 10.1080/19768354.2014.992953.



Assay Principle for the LCAT Activity Assay Kit. The close proximity of fluorescence labels on a dual-labeled fluorogenic probe keeps the fluorescence quenched. Upon cleavage of the probe by LCAT, fluorescence of the monomers can be measured at an excitation of 342 nm and emission of 400 nm.

Product Name	Detection	Size	Catalog Number
Lecithin Cholesterol Acyltransferase (LCAT) Activity Assay Kit	Fluorometric	100 Assays	STA-615

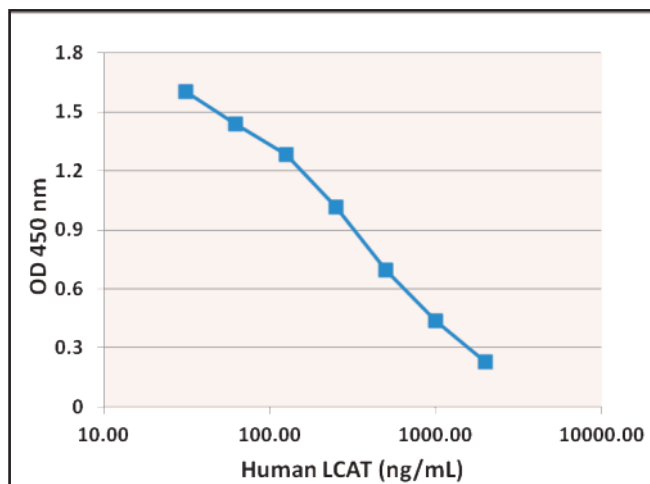
Lecithin Cholesterol Acyltransferase (LCAT) ELISA Kit

Lecithin cholesterol acyltransferase (LCAT) is an enzyme that is associated with lipoproteins and plays a key role in promoting the transfer of excess cell-associated cholesterol from peripheral tissues to the liver to be excreted.

LCAT catalyzes the transfer of an sn-2 acyl group from phosphatidylcholine to cholesterol, forming a cholesteryl ester. LCAT is bound to various lipoproteins in the blood, including HDL and LDL.

Our LCAT ELISA Assay Kit provides a simple, convenient method for quantifying LCAT levels in a variety of sample types including plasma, serum, and cell and tissue lysates. Quantitation of LCAT activity is performed in a standard 96-well plate reader.

- **Sensitive:** Detect as little as 30 ng/mL of LCAT
- **Versatile:** Suitable for human, mouse, rat or rabbit samples



Standard Curve Generated with the Lecithin Cholesterol Acyltransferase (LCAT) ELISA Kit.

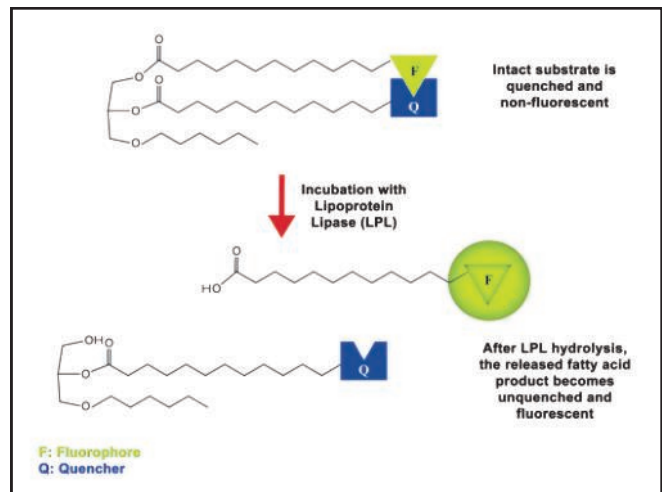
Product Name	Detection	Size	Catalog Number
Lecithin Cholesterol Acyltransferase (LCAT) ELISA Kit	Colorimetric	96 Assays	STA-616

Lipoprotein Lipase (LPL) Activity Assay Kit

Our Lipoprotein Lipase (LPL) Activity Assay Kit provides a simple, convenient method to measure LPL activity in a variety of sample types. This kit uses a fluorogenic triglyceride analog as a lipase substrate. The quenched substrate is cleaved at the sn-1 position by LPL producing a fluorescent product that can be detected in a 96-well fluorescence plate reader. This assay will also measure the activity of endothelial and hepatic lipases. It cannot distinguish between these lipases and LPL.

Recent Product Citations

1. Sun, X. et al. (2015). Insulin dissociates the effects of Liver X receptor on lipogenesis, endoplasmic reticulum stress and inflammation. *J. Biol. Chem.* 10.1074/jbc.M115.668269.
2. Downing, L.E. et al. (2015). A grape seed procyanidin extract ameliorates fructose-induced hypertriglyceridemia in rats via enhanced fecal bile acid and cholesterol excretion and inhibition of hepatic lipogenesis. *PLoS One* 10:e0140267.
3. Kim, H.K. et al. (2015). Regulation of energy balance by the hypothalamic lipoprotein lipase regulator Angptl3. *Diabetes* 64:1142-1153.
4. Dib, L. et al. (2014). LXR α fuels fatty acid-stimulated oxygen consumption in white adipocytes. *J. Lipid Res.* 55:247-257.



Assay Principle for the LPL Activity Assay Kit. The fluorogenic substrate is initially quenched and non-fluorescent. Upon cleavage of the probe by incubation with lipoprotein lipase (LPL), fluorescence can be measured at an excitation of 342 nm and emission of 400 nm.

Product Name	Detection	Size	Catalog Number
Lipoprotein Lipase (LPL) Activity Assay Kit	Fluorometric	100 Assays	STA-610

Lipoprotein Lipase (LPL) ELISA Kit

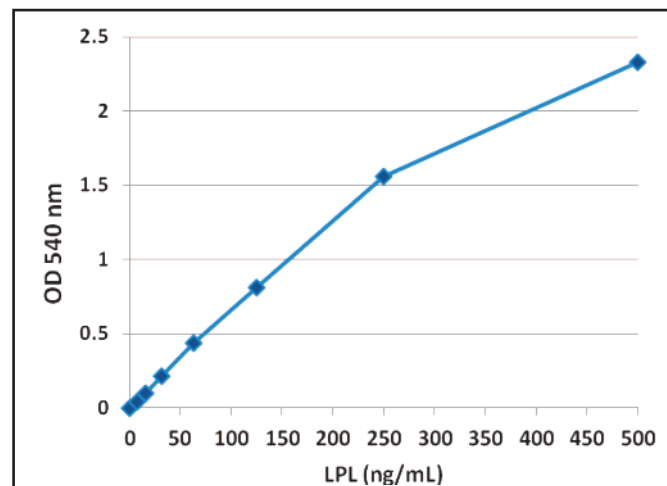
Lipoprotein lipase (LPL) is the key plasma lipase responsible for the hydrolysis of the triglyceride core found in very low density lipoprotein (VLDL) particles formed in the liver. A mutation in the gene coding for LPL can lead to deficiencies in the enzyme, resulting in a diminished ability to breakdown fatty acids. Such LPL deficiency is known as chylomicronemia or Type I hyperlipoproteinemia.

Our Lipoprotein Lipase (LPL) ELISA Kit provides a simple, convenient method to measure LPL levels in plasma, serum or other biological fluids from a variety of species (see below). LPL amounts are quantified against the provided LPL Standard in a colorimetric 96-well microplate reader.

Recent Product Citation

Chan, D.C. et al. (2014). Inter-relationships between proprotein convertase subtilisin/kexin type 9, apolipoprotein C-III and plasma apolipoprotein B-48 transport in obese subjects: a stable isotope study in the postprandial state. *Clin. Sci. (Lond.)* 128:379-385.

- **Sensitive:** Detect as little as 20 ng/mL of LPL
- **Versatile:** Suitable for human, rat, bovine, guinea pig, or chicken samples (but not mouse)



Standard Curve Generated with the Lipoprotein Lipase (LPL) ELISA Kit.

Product Name	Detection	Size	Catalog Number
Lipoprotein Lipase (LPL) ELISA Kit	Colorimetric	96 Assays	STA-611

Serum Triglyceride Quantitation Kits

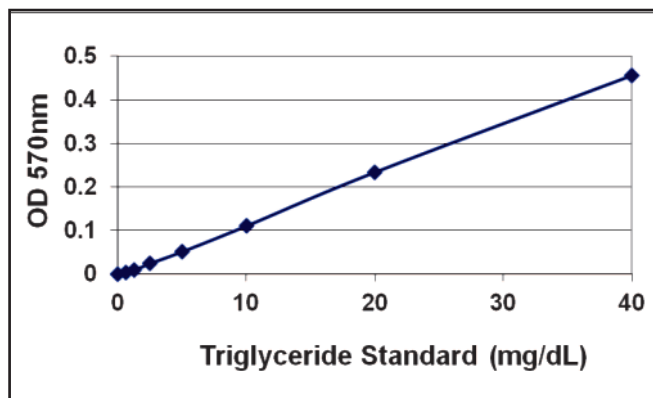
Triglycerides serve as an energy source and play a key role in lipid metabolism. Lipases secreted into the intestines hydrolyze the triglyceride ester bond, producing glycerol and free fatty acids. Hepatic lipases also break down triglycerides in the liver to assemble very low density lipoprotein (VLDL) particles.

Our Serum Triglyceride Quantitation Kits use a coupled enzymatic reaction system to measure triglyceride concentrations. First, a lipase hydrolyzes the ester bond, yielding free glycerol. The glycerol is then phosphorylated and oxidized, producing hydrogen peroxide, which reacts with the probe provided with each kit. Kits are available with either colorimetric or fluorescence-based detection, both of which are performed in a 96-well microtiter plate.

Recent Product Citations

- Chellan, B. et al. (2014). IL-22 is induced by S100/calgranulin and impairs cholesterol efflux in macrophages by downregulating ABCG1. *J. Lipid Res.* **55**:443-454. (STA-396)
- Marino, A. et al. (2014). ITC1 deficiency protects from diet-induced obesity. *Diabetes* **63**:550-561. (STA-396)

- Sensitive:** Detect as little as 10 μM (1 mg/dL) with the colorimetric format and 2 μM (0.2 mg/dL) with the fluorometric format
- Versatile:** Suitable for serum, plasma, and cell and tissue lysates



Standard Curve Generated with the Serum Triglyceride Quantitation Kit (Colorimetric).

Want to measure free glycerol content? See our Free Glycerol Assay Kits on **page 150**.

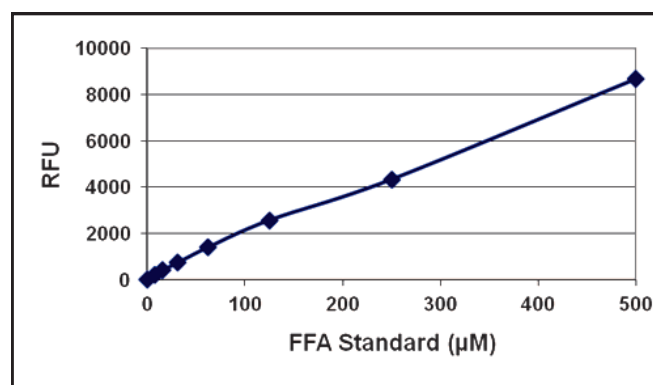
Product Name	Detection	Size	Catalog Number
Serum Triglyceride Quantification Kit	Colorimetric	100 Assays	STA-396
	Fluorometric	100 Assays	STA-397

Free Fatty Acid (FFA) Assay Kits

Our Free Fatty Acid Assay Kits use a coupled enzymatic reaction system to measure free fatty acid concentrations in serum or plasma. Acyl CoA Synthetase catalyzes FFA acylation of CoA. The Acyl-CoA is then oxidized by Acyl CoA Oxidase, producing hydrogen peroxide, which reacts with the kit's probe. Kits are available with either colorimetric or fluorescence-based detection, both of which are performed in a 96-well microtiter plate.

Recent Product Citations

- Kahouli, I. et al. (2015). In-vitro characterization of the anti-cancer activity of the probiotic bacterium *Lactobacillus fermentum* NCIMB 5221 and potential against colorectal cancer. *J. Cancer Sci. Ther.* **7**:224-235. (STA-618)
- Diane, A. et al. (2014). PACAP is essential for the adaptive thermogenic response of brown adipose tissue to cold exposure. *J. Endocrinol.* **222**:327-339. (STA-618)



Standard Curve Generated with the Free Fatty Acid Assay Kit (Fluorometric).

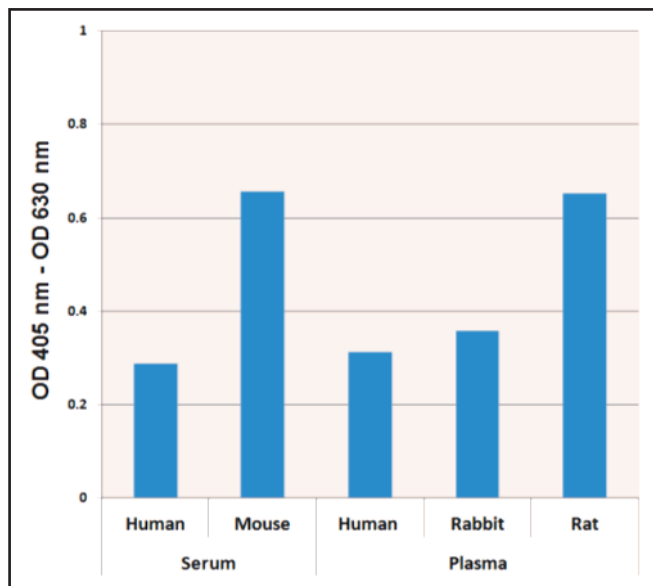
Product Name	Detection	Size	Catalog Number
Free Fatty Acid Assay Kit	Colorimetric	100 Assays	STA-618
	Fluorometric	100 Assays	STA-619

Total Bile Acid Assays

While bile acid synthesis is critical for the removal of cholesterol from the body, bile acids are also required for proper uptake of nutrients in the small intestine. Our Total Bile Acid Assay Kits provide a convenient 96-well plate-based method to measure the total bile acid content in a variety of sample types. These assays are based on an enzyme driven reaction in which bile acids are incubated in the presence of 3-alpha hydroxysteroiddehydrogenase.

The reaction used with the colorimetric kit requires the presence of NADH and thio-NAD⁺. The thio-NAD⁺ is reduced to thio-NADH which is detected by colorimetric absorbance.

The fluorometric kit requires incubation with NAD⁺, which is converted to NADH. Diaphorase then uses NADH to reduce resazurin to resorufin, which is detected fluorometrically at 560 nm excitation and 590 nm emission.



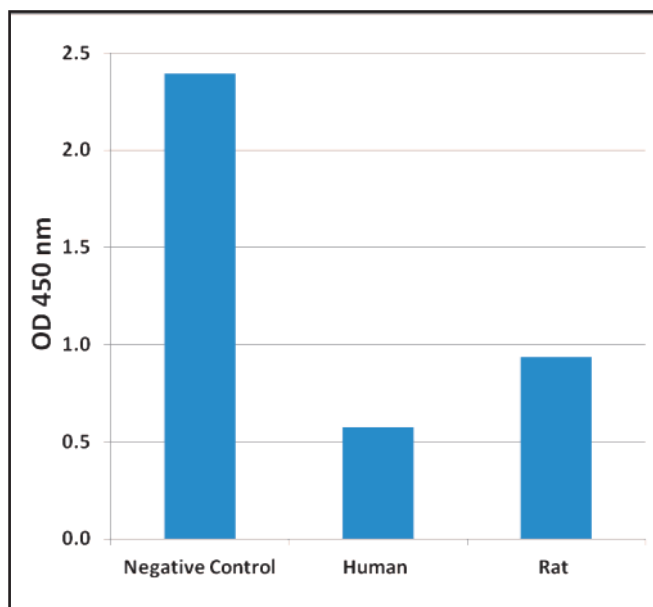
Samples from Various Species Tested with the Total Bile Acid Assay Kit (Colorimetric).

Product Name	Detection	Size	Catalog Number
Total Bile Acid Assay Kit	Colorimetric	100 Assays	STA-631
	Fluorometric	96 Assays	MET-5005

Cholic Acid ELISA Kit

Cholic acid is a primary bile acid that is synthesized from excess cholesterol by the liver. Bile acid synthesis is critical for cholesterol removal from the body as well as uptake of dietary lipids, fat soluble vitamins, and other nutrients from the small intestine. Determining circulatory levels of bile acids may be used to identify certain liver diseases.

Our Cholic Acid ELISA Kit is designed for detection and quantitation of cholic acid in plasma, serum, urine, feces, or lysates. This assay is a competitive ELISA where unknown samples are added to a plate pre-adsorbed with a cholic acid conjugate. An anti-cholic acid antibody is added, and the cholic acid content in unknown samples competes with the cholic acid on the plate for binding to the antibody. High levels of cholic acid in samples will bind most of the antibody, leaving little binding of antibody to the plate and producing a low signal. Low levels of cholic acid result in most antibody bound to the plate, resulting in a higher signal.



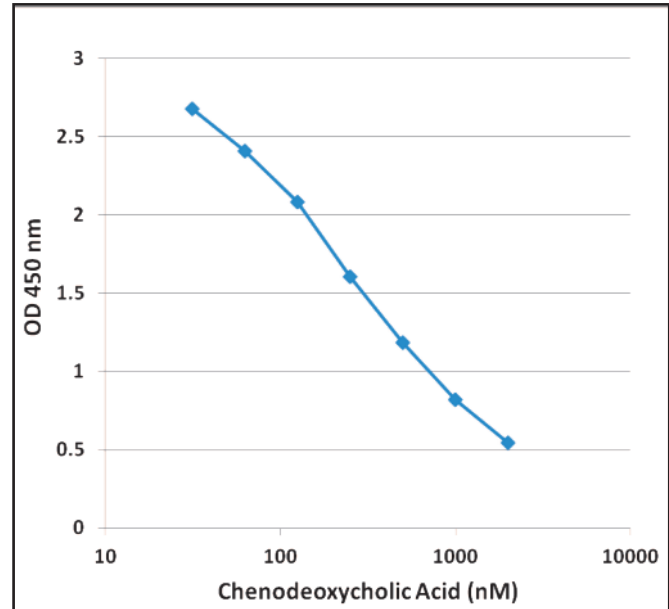
Cholic Acid Levels in Undiluted Human or Rat Serum, Compared to Negative Control.

Product Name	Detection	Size	Catalog Number
Cholic Acid ELISA Kit	Colorimetric	96 Assays	MET-5007

Chenodeoxycholic Acid ELISA Kit

Chenodeoxycholic acid is a primary bile acid that is synthesized from excess cholesterol by the liver. Bile acid synthesis is critical for cholesterol removal from the body as well as uptake of dietary lipids, fat soluble vitamins, and other nutrients from the small intestine. Determining circulatory levels of bile acids may be used to identify certain liver diseases.

Our Chenodeoxycholic Acid ELISA Kit is designed for detection and quantitation of chenodeoxycholic acid in plasma, serum, urine, feces, or lysates. This assay is a competitive ELISA where unknown samples are added to a plate pre-adsorbed with a chenodeoxycholic acid conjugate. An anti-chenodeoxycholic acid antibody is added, and the chenodeoxycholic acid content in unknown samples competes with the bile acid on the plate for binding to the antibody. High levels of chenodeoxycholic acid in samples will bind most of the antibody, leaving little binding of antibody to the plate and producing a low signal. Low levels result in most antibody bound to the plate, resulting in a higher signal.



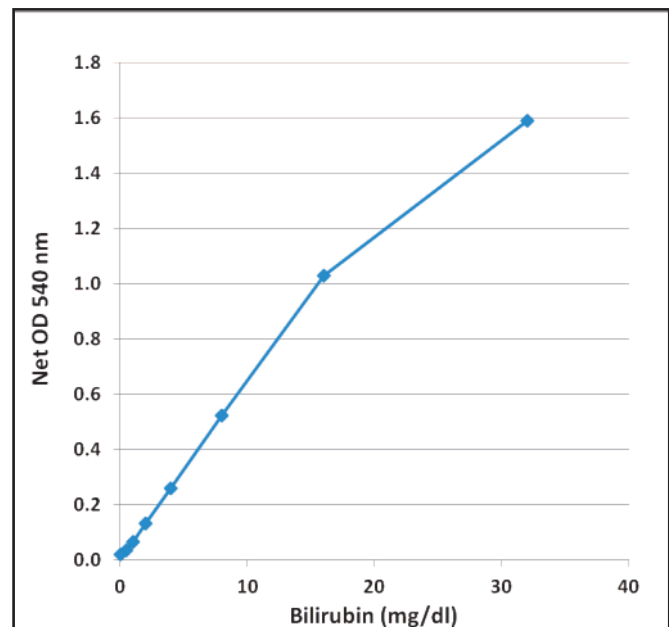
Chenodeoxycholic Acid ELISA Standard Curve.

Product Name	Detection	Size	Catalog Number
Chenodeoxycholic Acid ELISA Kit	Colorimetric	96 Assays	MET-5008

Bilirubin Assay Kit

Bilirubin, a byproduct of heme breakdown, can exist conjugated to glucuronic acid (direct) and as unconjugated (indirect). The unconjugated form is found in the blood bound to albumin and is transported to the liver. Bilirubin becomes conjugated to glucuronic acid in the liver, making it more soluble and allowing for excretion into bile. High levels of bilirubin have been correlated with jaundice and Gilbert's syndrome, while low levels have been associated with cardiovascular disease and diabetes mellitus.

Our Bilirubin Assay Kit measures total and direct bilirubin in plasma, serum, urine, or lysates. This assay is based on the Jendrassik-Grof method, in which diazotized sulfanilic acid reacts with conjugated (direct) bilirubin, forming azobilirubin that is detectable in a colorimetric plate reader. Since unconjugated (indirect) bilirubin reacts slowly, an accelerant can be added to the reaction to measure total bilirubin.



Total Bilirubin Standard Curve.

Product Name	Detection	Size	Catalog Number
Bilirubin Assay Kit	Colorimetric	200 Assays	MET-5010

Phosphatidylcholine Assay Kit

Phosphatidylcholine is the foremost phospholipid in eukaryotic cell membranes and comprises about 70% of the total phospholipids in plasma lipoproteins.

Our Phosphatidylcholine Assay Kit is a simple fluorometric assay that measures phosphatidylcholine in plasma, serum, cell suspensions or tissue homogenates. Phospholipase D enzyme hydrolyzes phosphatidylcholine into phosphatidic acid and choline. The choline is then oxidized by choline oxidase to produce hydrogen peroxide, which is detected by a fluorogenic probe in the presence of horseradish peroxidase (HRP).

Recent Product Citation

Park, E.S. et al. (2014). Phosphatidylcholine alteration identified using MALDI imaging MS in HBV-infected mouse livers and virus-mediated regeneration defects. *PLoS One* **9**:e94127.

Product Name	Detection	Size	Catalog Number
Phosphatidylcholine Assay Kit	Fluorometric	96 Assays	STA-600

Sphingomyelin Assay Kit

Our Sphingomyelin Assay Kit is a simple fluorometric assay that measures sphingomyelin levels in plasma, serum, cell suspensions or tissue homogenates. Sphingomyelinase hydrolyzes sphingomyelin into ceramide and phosphocholine, which in turn is broken down into choline. Choline is enzymatically oxidized to produce hydrogen peroxide, which is detected with a fluorogenic probe in the presence of horseradish peroxidase (HRP).

Recent Product Citation

Winkler, E.A. et al. (2014). Blood-spinal cord barrier disruption contributes to early motor-neuron degeneration in ALS-model mice. *PNAS* **111**:E1035-E1042.

Product Name	Detection	Size	Catalog Number
Sphingomyelin Assay Kit	Fluorometric	96 Assays	STA-601

Total Phosphatidic Acid Assay Kit

Our Total Phosphatidic Acid Assay Kit measures total phosphatidic acid content, including lysophosphatidic acid (LPA), in cell and tissue samples by a coupled enzymatic reaction system. Lipase is used to hydrolyze the phosphatidic acid samples to glycerol-3-phosphate. Then the glycerol-3-phosphate is oxidized by glycerol-3-phosphate oxidase (GPO), producing hydrogen peroxide which reacts with the kit's fluorometric probe.

Product Name	Detection	Size	Catalog Number
Total Phosphatidic Acid Assay Kit	Fluorometric	96 Assays	MET-5019

Acetylcholine Assay Kits

Our Acetylcholine Assay Kits provide a simple, convenient method to quantify acetylcholine in plasma, serum, cell suspensions, or tissue homogenates.

Recent Product Citation

Kim, M.S. et al. (2014). Ginsenoside Re and Rd enhance the expression of cholinergic markers and neuronal differentiation in neuro-2a cells. *Biol. Pharm. Bull.* **37**:826-833. (STA-602)

Product Name	Detection	Size	Catalog Number
Acetylcholine Assay Kit	Colorimetric	100 Assays	STA-603
	Fluorometric	100 Assays	STA-602

Human C-Reactive Protein ELISA Kit

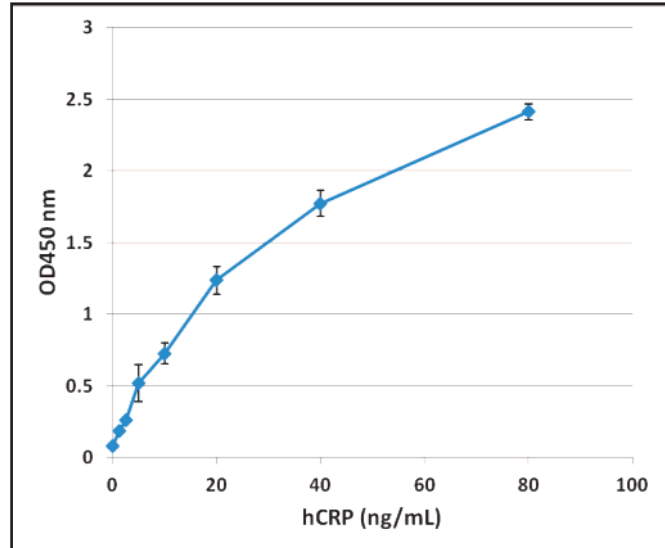
C-Reactive Protein (CRP) is a serum protein that binds with high affinity to phosphocholine residues as well as other autologous and extrinsic ligands. CRP is a well-established marker of inflammation and tissue damage, and it has been associated with cardiovascular disease, atherosclerosis, and other diseases.

Our Human C-Reactive Protein (CRP) ELISA Kit provides a simple, convenient method to measure CRP levels in human plasma, serum, or other biological fluids. CRP amounts are quantified against the provided CRP Standard in a colorimetric 96-well microplate reader.

Recent Product Citations

- Alexandrov, P.N. et al. (2015). Nanomolar aluminum induces expression of the inflammatory systemic biomarker C-reactive protein (CRP) in human brain microvessel endothelial cells (hBMECs). *J. Inorg. Biochem.* 10.1016/j.jinorgbio.2015.07.013.
- Cakar, M. et al. (2015). Arterial stiffness and endothelial inflammation in prediabetes and newly diagnosed diabetes patients. *Arch. Endocrinol. Metab.* 10.1590/2359-3997000000061.
- Chandra, P. et al. (2014). Prospects and advancements in C-reactive protein detection. *World J. Methodol.* 4:1-6.
- Barisione, G. et al. (2014). Mechanisms for reduced pulmonary diffusing capacity in haematopoietic stem-cell transplantation recipients. *Respir. Physiol. Neurobiol.* 194:54-61.

- **Sensitive:** Detect as little as 1 ng/mL of CRP
- **Versatile:** Suitable for plasma, serum, or other biological fluids



Standard Curve Generated with the Human C-Reactive Protein (CRP) ELISA Kit.

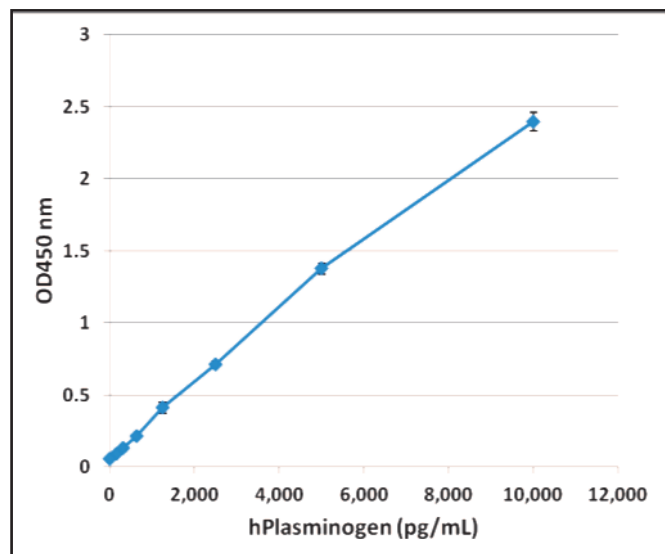
Product Name	Detection	Size	Catalog Number
Human C-Reactive Protein (CRP) ELISA Kit	Colorimetric	96 Assays	STA-392

Human Plasminogen ELISA Kit

Plasminogen is a plasma glycoprotein that plays a role in macrophage recruitment, arterial stenosis, atherosclerosis, aneurysm formation, wound healing, and neovascularization. Plasminogen exists as an inactive proenzyme, but when converted to the active enzyme plasmin it serves to digest fibrin. This activation is catalyzed by tissue-type plasminogen activator (tPA) or urokinase-type plasminogen activator (uPA).

Our Human Plasminogen ELISA Kit provides a simple, convenient method to measure plasminogen levels in human plasma, serum, or other biological fluids. Plasminogen amounts are quantified against the provided Plasminogen Standard in a colorimetric 96-well microplate reader.

- **Sensitive:** Detect as little as 150 pg/mL of plasminogen
- **Versatile:** Suitable for plasma, serum, or other biological fluids



Standard Curve Generated with the Human Plasminogen ELISA Kit.

Product Name	Detection	Size	Catalog Number
Human Plasminogen ELISA Kit	Colorimetric	96 Assays	STA-393

Human Albumin ELISA Kit

Human serum albumin (HSA) is the most abundant protein in human plasma, constituting about half the protein in blood serum. It is typically found in concentrations around 50 mg/mL. Produced in the liver in a prealbumin state, albumin transports hormones, fatty acids, and other compounds through the circulation. It also maintains pH and osmotic pressure.

Our Human Albumin ELISA Kit provides a simple, convenient method to measure HSA levels in human plasma, serum, urine, or other biological fluids. Human albumin amounts are quantified against the provided standard in a colorimetric 96-well microplate reader.

- **Sensitive:** Detect as little as 100 pg/mL of human serum albumin
- **Versatile:** Suitable for plasma, serum, or other biological fluids

Product Name	Detection	Size	Catalog Number
Human Albumin ELISA Kit	Colorimetric	96 Assays	STA-383

BCG Albumin Assay Kit

Our BCG Albumin Assay Kit provides an extremely fast alternative to our Albumin ELISA Kit. This kit uses a proprietary formulation of Bromocresol Green, which forms a color complex specifically with albumin in samples. No pretreatment is required. The assay is performed in a 96-well plate and read using a standard colorimetric plate reader.

- **Fast:** Measure albumin levels in about 5 minutes
- **Versatile:** Suitable for plasma, serum, urine, or other biological fluids
- **Quantitative:** Compare unknown albumin samples to a known standard (provided)

Product Name	Detection	Size	Catalog Number
BCG Albumin Assay Kit	Colorimetric	250 Assays	MET-5017

Human Serum Proteins

Our human albumin and oxidized albumin were isolated and purified by HPLC. C-reactive protein was isolated from human pleural fluid. Plasminogen was isolated and purified from human plasma following an ultracentrifugation procedure.

Product Name	Size	Catalog Number
Human Albumin	100 µg	STA-230
Human Albumin, Malondialdehyde Modified	100 µg	STA-210
Human C-Reactive Protein	100 µg	STA-240
Human Plasminogen	100 µg	STA-239

Antibodies to Human Serum Proteins

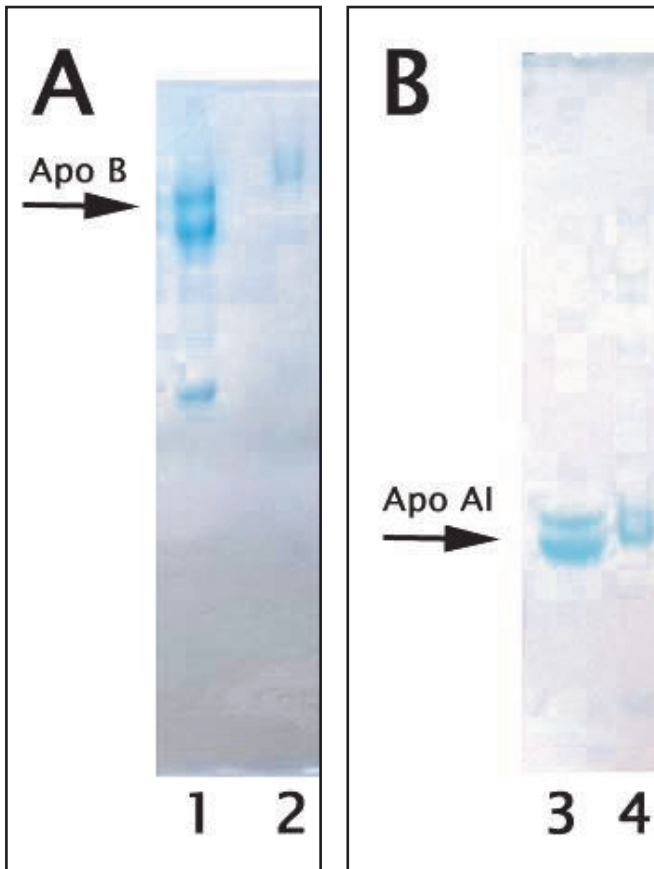
Antibodies are affinity purified.

Product Name	Detection	Size	Catalog Number
Goat Anti-Human Albumin Polyclonal Antibody	Immunoblot/ELISA	100 µg	STA-130
Rabbit Anti-Human C-Reactive Protein Polyclonal Antibody	Immunoblot/ELISA	100 µg	STA-140
Goat Anti-Human Plasminogen Polyclonal Antibody	Immunoblot/ELISA	100 µg	STA-139

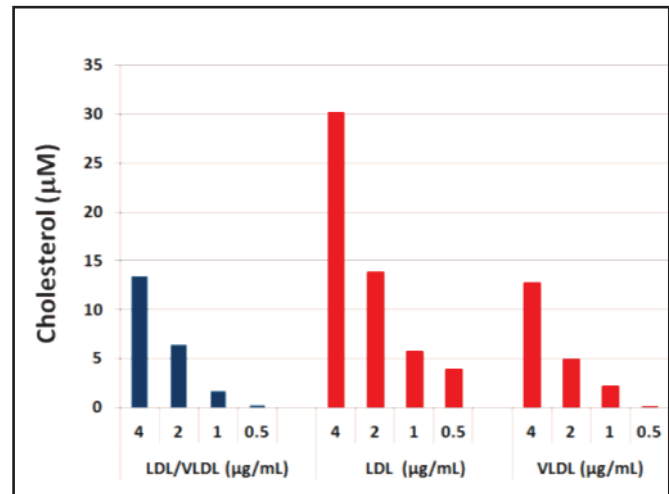
Lipoprotein Purification Kits, Ultracentrifugation Free

Traditionally, lipoproteins such as HDL, LDL and VLDL have been purified from plasma or serum via the use of ultracentrifugation, which can be tedious and time consuming.

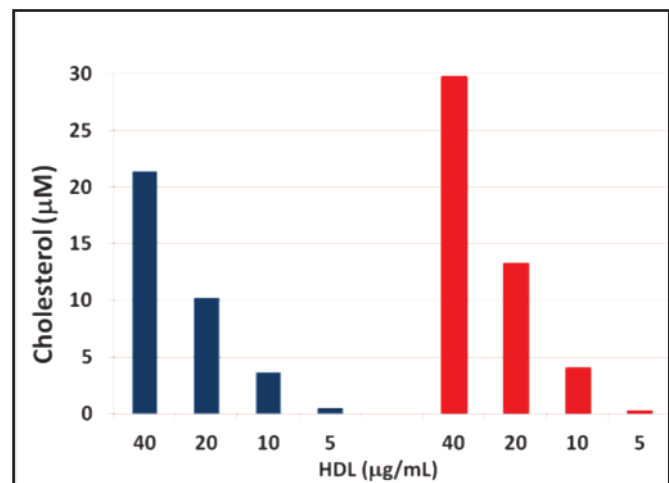
Our Lipoprotein Purification Kits provide comparable purity without the need for an ultracentrifuge. Samples are separate into two fractions, one containing HDL and the other containing LDL and VLDL. Fractions are then further purified using standard table-top centrifugation speeds.



SDS PAGE of Purified Lipoproteins. (A) 20 μ g of LDL/VLDL purified using either the LDL/VLDL and HDL Purification Kit (lane 1) or ultracentrifugation (lanes 2) was loaded on a 3-8% Tris Acetate Gel. (B) 20 μ g of HDL purified using either the LDL/VLDL and HDL Purification Kit (lane 3) or ultracentrifugation (lane 4) was loaded on a 12% Bis Tris gel. Both gels were stained with Coomassie Brilliant Blue Dye.



Detection of Cholesterol in Purified LDL/VLDL Samples. LDL/VLDL purified from the LDL/VLDL and HDL Purification Kit (blue bars) or by ultracentrifugation (red bars) was tested for the presence of cholesterol using Cell Biolabs' Total Cholesterol Assay Kit (Fluorometric).



Detection of Cholesterol in Purified HDL Samples. HDL purified from the LDL/VLDL and HDL Purification Kit (blue bars) or by ultracentrifugation (red bars) was tested for the presence of cholesterol using Cell Biolabs' Total Cholesterol Assay Kit (Fluorometric).

Product Name	Size	Catalog Number
HDL Purification Kit (Ultracentrifugation Free)	10 preps	STA-607
LDL/VLDL Purification Kit (Ultracentrifugation Free)	10 preps	STA-606
LDL/VLDL and HDL Purification Kit (Ultracentrifugation Free)	10 preps	STA-608

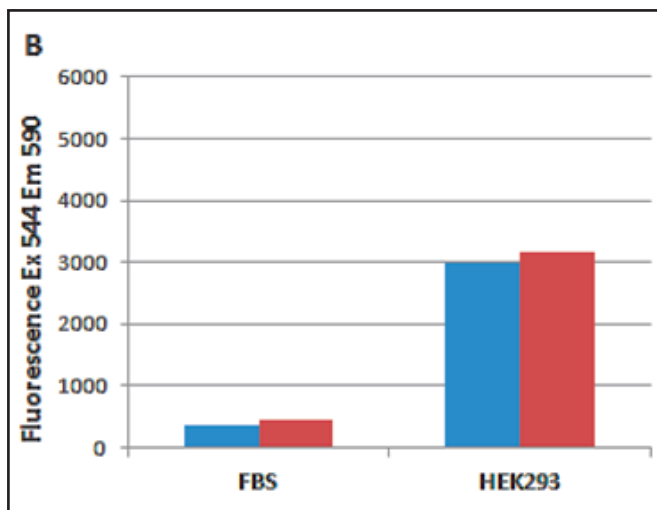
Lipid Extraction and Separation Kits, Chloroform Free

Traditional methods of extracting lipids from tissues or cells, such as the well-published Folch method, use chloroform as the extraction solvent. This method has a couple of disadvantages. First, the organic phase ends up below the aqueous phase, creating problematic removal through the upper phase that risks contamination. Second, chloroform has been classified in many places as a probable carcinogen.

Our Lipid Extraction Kit overcomes both disadvantages of the Folch method. The kit provides a chloroform-free extraction method, and the use of proprietary organic solvents places the organic phase above the aqueous phase, allowing easy removal without disturbing the aqueous layer.

Our Polar/Neutral Lipid Separation Kit allows you to separate polar and neutral lipid fractions from lipids extracted either with our Lipid Extraction Kit or by the Folch method. For best results from start to finish, choose our Lipid Extraction & Polar/Neutral Lipid Separation Combo Kit.

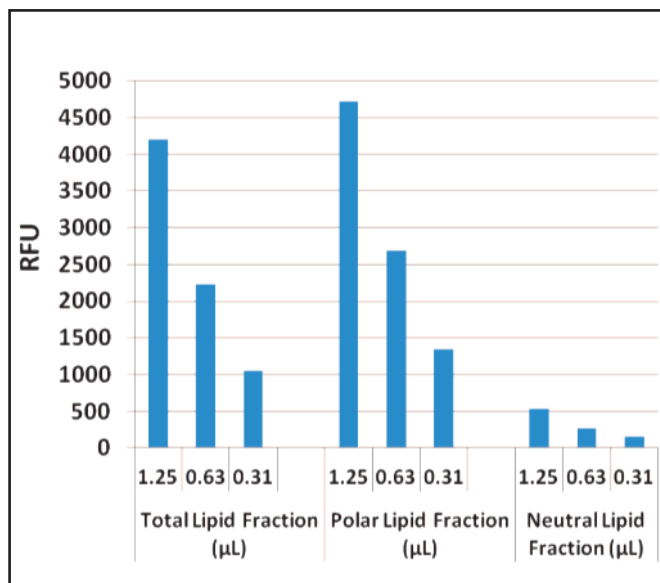
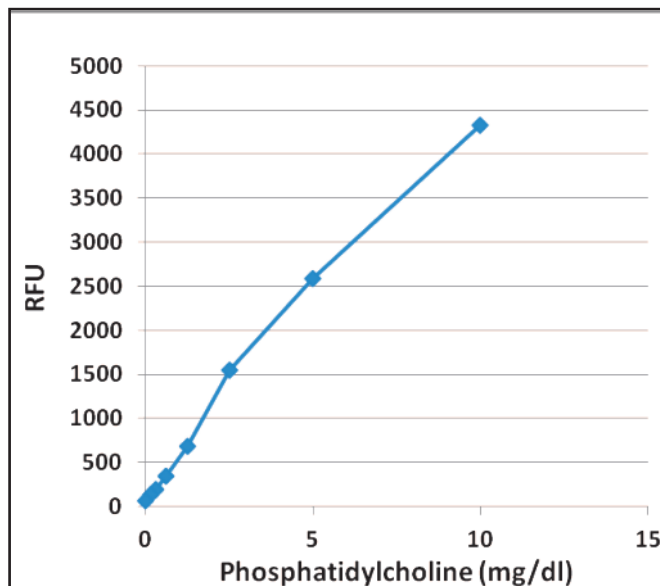
Each kit provides sufficient reagents for 50 extractions from 100 μ L sample sizes, but reagents may be scaled up for larger samples.



Total Cholesterol Assay Performed on Extracted Lipids. Lipids extracted from fetal bovine serum (FBS) and HEK293 cells were prepared using the traditional Folch method (blue) and the Lipid Extraction Kit (red). Samples were tested for the presence of cholesterol in the Total Cholesterol Assay Kit (Cat. #STA-390).

Recent Product Citation

Pamir, N. et al. (2015). Granulocyte macrophage-colony stimulating factor-dependent dendritic cells restrain lean adipose tissue expansion. *J. Biol. Chem.* 10.1074/jbc.M115.645820. (STA-612)



Phosphatidylcholine Assay Performed on Extracted Lipids.

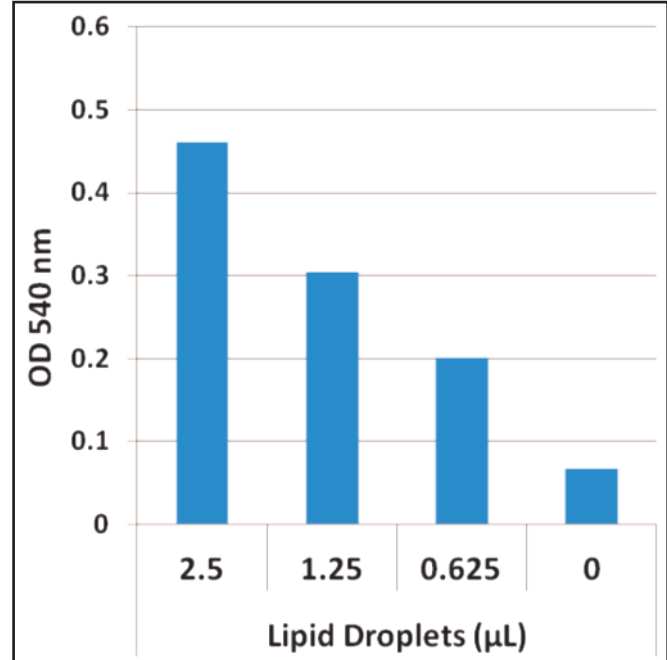
Top: Phosphatidylcholine Standard Curve. **Bottom:** Total, polar and neutral lipids were extracted from homogenized chicken liver using the Lipid Extraction Kit (Chloroform Free) and tested for the presence of phosphatidylcholine according to the Assay Protocol.

Product Name	Size	Catalog Number
Lipid Extraction Kit (Chloroform Free)	50 Preps	STA-612
Polar/Neutral Lipid Separation Kit (Chloroform Free)	50 Preps	MET-5009
Lipid Extraction & Polar/Neutral Lipid Separation Combo Kit (Chloroform Free)	50 Preps	MET-5009-C

Lipid Droplet Isolation Kit

Lipid droplets are organelles that are rich in lipids, contain a lipid rich core, and are surrounded by a phospholipid monolayer as well as outer lipid droplet associated proteins. They are commonly found in adipose tissue of animals, although they are found in all eukaryotes. Lipid droplets function to regulate the hydrolysis and storage of neutral lipids and also serve as storage for cholesterol and acyl-glycerols used to form and maintain cellular membranes.

Our Lipid Droplet Isolation Kit uses simple gradient centrifugation, but circumvents the need for large sample sizes or ultracentrifugation. A lipid droplet source such as tissue or cultured cells is homogenized; a gradient is then created with the homogenate, and the material is centrifuged. The lipid droplets float to the top of the gradient and are recovered by carefully pipetting. Each kit provides sufficient reagents to isolate up to 50 preps based on a 50-100 mg tissue or cultured cell sample size.



Triglyceride Quantification of Lipid Droplets Isolated from Chicken Liver.

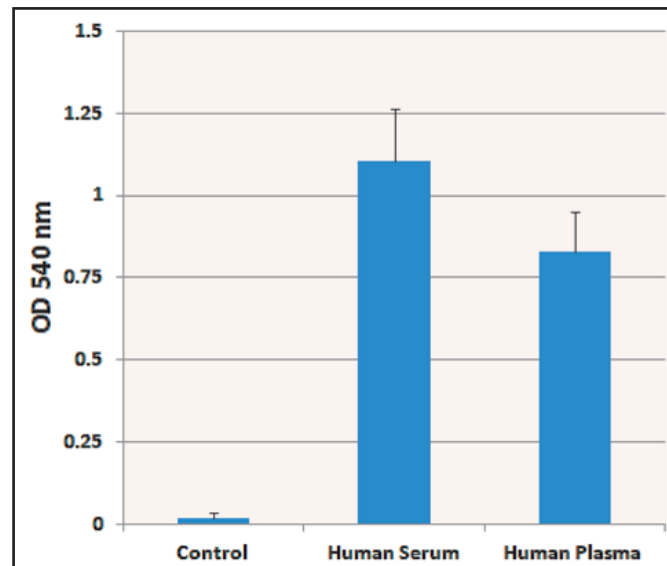
Product Name	Size	Catalog Number
Lipid Droplet Isolation Kit	50 preps	MET-5011

Lipid Quantification Kits

Our Lipid Quantification Kits provide a convenient plate-based method to measure the lipid content in various samples. The colorimetric assay uses a sulfo-phospho-vanillin method to detect unsaturated fatty acids. Samples are acidified and heated to solubilize and prime the lipids. The lipids then react with vanillin in acidic conditions to form a colorimetric product detectable in a standard 96-well microplate reader.

The fluorometric assay specifically measures neutral lipid content from samples and provides a 10-fold sensitivity advantage compared to the colorimetric format.

These kits are compatible with plasma and serum samples, or with crude or purified lipids extracted from cells. Each kit provides sufficient reagents for 100 assays including standards and unknown samples.



Quantification of Lipids from Human Serum or Plasma.

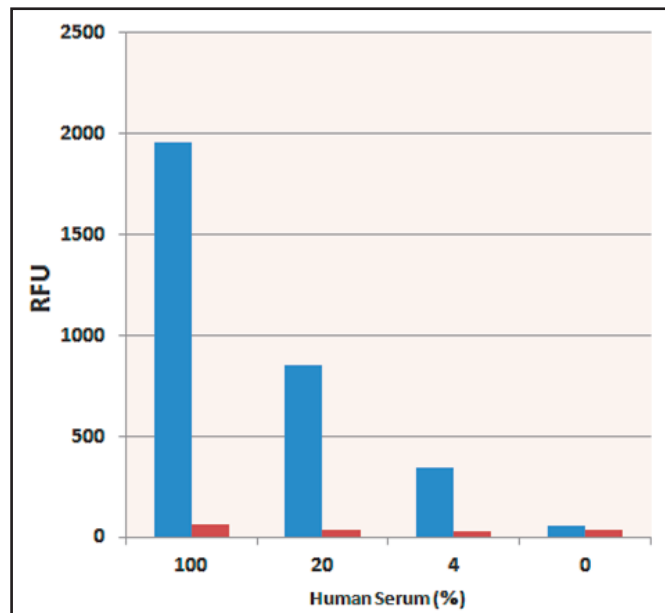
Product Name	Detection	Size	Catalog Number
Lipid Quantification Kit (unsaturated fatty acids)	Colorimetric	100 Assays	STA-613
Lipid Quantification Kit (neutral lipids)	Fluorometric	100 Assays	STA-617

Glutamate Assay Kit

Glutamate is a non-essential amino acid that has a key metabolic role in processes such as the citric acid cycle and removal of excess nitrogen waste. It is one of the major excitatory neurotransmitters of the mammalian brain and is involved in learning and memory.

Our Glutamate Assay Kit is a simple HTS-compatible assay for measuring glutamate levels in biological samples without the need for pretreatment. Glutamate oxidase converts glutamate to α -ketoglutarate while producing ammonia and hydrogen peroxide as byproducts. The hydrogen peroxide reacts with a fluorometric probe in the presence of HRP, producing the highly fluorescent product Resorufin which is measured in a fluorescence-based microplate reader. L-Alanine and glutamate-pyruvate transaminase are added to regenerate glutamate in the reaction.

- **Sensitive:** Detect as little as 0.3 μM of glutamate
- **Versatile:** Suitable for plasma, serum, urine, lysates and cell culture supernatants



Detection of Glutamate in Human Serum. Pooled serum was incubated in the presence (blue bars) and absence (red bars) of glutamate oxidase and glutamate-pyruvate transaminase.

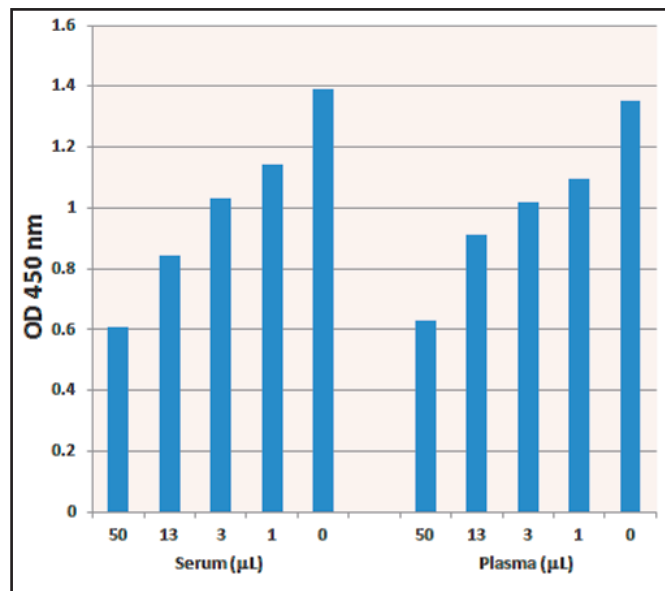
Product Name	Detection	Size	Catalog Number
Glutamate Assay Kit	Fluorometric	200 Assays	STA-674

Homocysteine ELISA Kit

Homocysteine is an amino acid intermediate formed during the production of the essential dietary amino acid methionine. It is a homologue of cysteine, differing only in that it contains an extra side chain methylene bridge. High levels of homocysteine in the blood have been associated with premature incidences of vascular disease, making it a likely risk factor for heart disease.

Our Homocysteine ELISA Kit is competitive ELISA developed for the detection and quantitation of homocysteine in a variety of sample types. Each kit provides sufficient reagents to perform up to 96 assays including standards and unknown samples.

- **Sensitive:** Detect as little as 10 ng/mL of homocysteine
- **Versatile:** Suitable for plasma, serum, lysates, or other biological fluid samples



Detection of Homocysteine in Human Serum and Plasma.

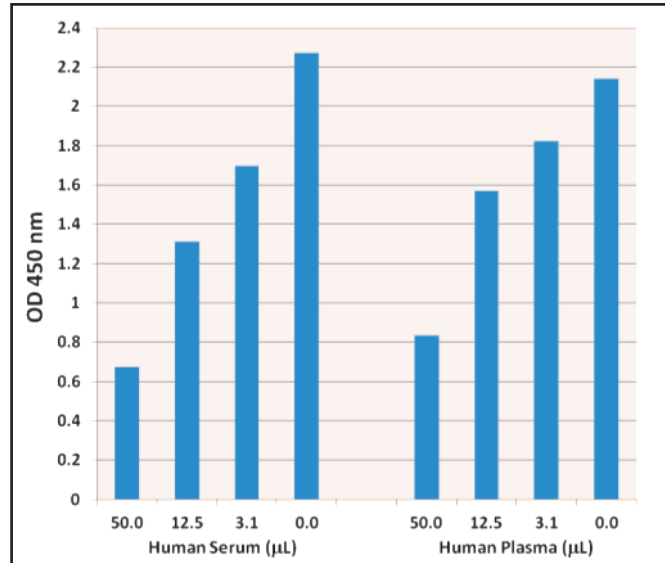
Product Name	Detection	Size	Catalog Number
Homocysteine ELISA Kit	Colorimetric	96 Assays	STA-670

S-Adenosylmethionine and S-Adenosylhomocysteine ELISA Kits

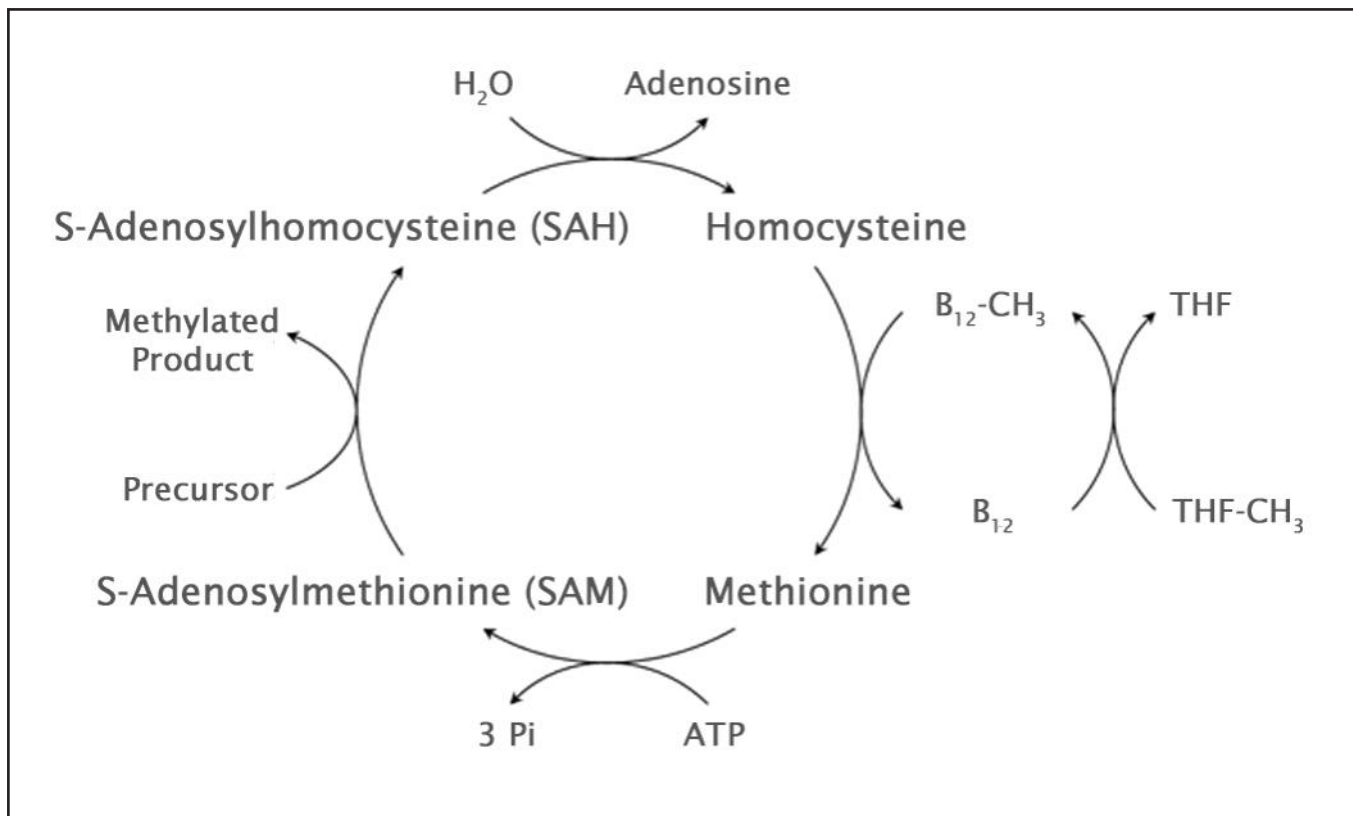
S-adenosylmethionine (SAM) is a methyl donor involved in the transfer of a methyl group to DNA, proteins, phospholipids, RNA, and neurotransmitters. Reactions that break down and regenerate SAM are referred to as the SAM cycle. SAM-dependent methylases convert SAM to S-adenosylhomocysteine (SAH), which is further broken down to homocysteine and adenosine.

Donation of the SAM methyl group converts SAM into SAH, the latter being a potent inhibitor of methylation. For this reason, the SAM/SAH ratio has been used as an index of methylation potentiation in a cell.

Our SAM and SAH ELISA Kits use a competitive ELISA format to detect and quantify SAM and SAH in a variety of sample types. To enable convenient quantitation of the SAM/SAH ratio, we offer the SAM/SAH ELISA Combo Kit.



Detection of S-Adenosylmethionine in Human Serum and Plasma.



The SAM Cycle.

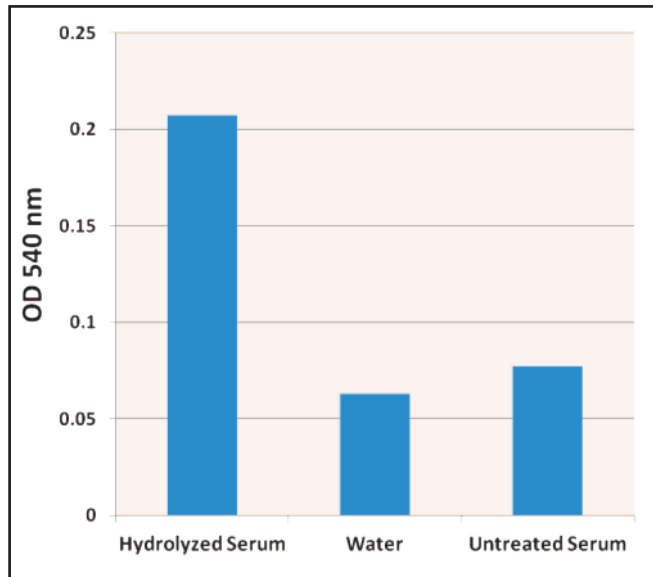
Product Name	Size	Catalog Number
S-Adenosylmethionine (SAM) ELISA Kit	96 Assays	STA-672
S-Adenosylhomocysteine (SAH) ELISA Kit	96 Assays	STA-671
S-Adenosylmethionine (SAM) and S-Adenosylhomocysteine (SAH) ELISA Combo Kit	96 Assays	STA-671-C

Hydroxyproline Assay Kit

Hydroxyproline is an amino acid that is synthesized from the irreversible post-translational hydroxylation of proline by prolyl hydroxylase. Hydroxyproline is found almost exclusively in the protein collagen, in the Y position of the repeating tripeptide Gly-X-Y. By allowing sharp twisting of the collagen helix, hydroxyproline helps to stabilize the collagen structure.

Since hydroxyproline has been found on so few proteins other than collagen, it has been used as a marker to quantify levels of collagen and/or gelatin (partially hydrolyzed collagen).

Our Hydroxyproline Assay Kit is a simple assay for measuring hydroxyproline levels in a variety of sample types. The hydroxyproline is converted to a pyrrole which reacts with the Ehrlich's Reagent to produce a chromophore that is read with a standard microplate reader.



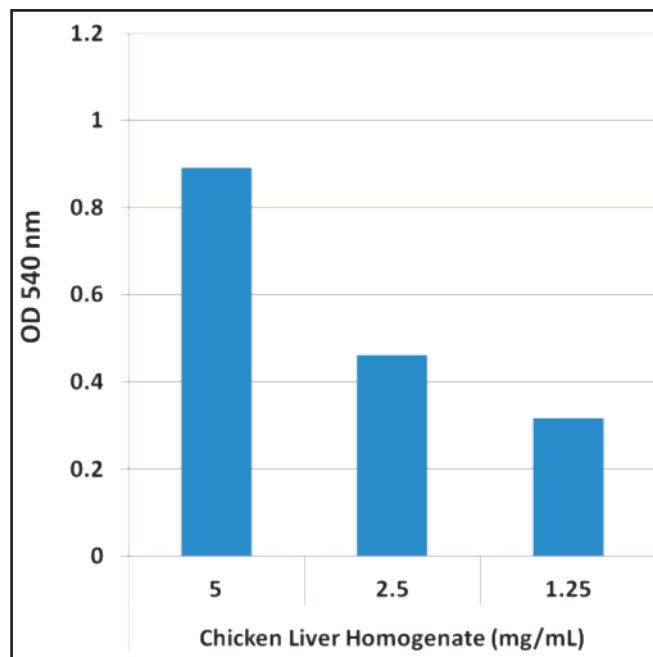
Detection of Hydroxyproline in Human Serum. Pooled serum with (left) and without (right) acid hydrolysis were tested according to the Assay Protocol. Water was included as a negative control.

Product Name	Detection	Size	Catalog Number
Hydroxyproline Assay Kit	Colorimetric	96 Assays	STA-675

Soluble Collagen Assay Kit

Collagen serves as the major structural component of animal connective tissues. Furthermore, collagen comprises about 30% of the total protein content in most animals, making it the most abundant animal protein. This important protein plays an important role in preserving healthy myocardial function, as it contributes to myocyte orientation and heart force transmission.

The Soluble Collagen Assay Kit provides a convenient microplate-based method for the detection of soluble collagen from cell or tissue samples. First, samples are dried down in a 96-well plate. A Sirius Red reagent is added to stain the triple helix structure (Gly-X-Y) of collagen. The stained collagen is then washed with an Acidic Reagent, eluted from the plate with a Basic Reagent, and then quantified in a standard colorimetric plate reader at OD 540 nm.



Detection of Soluble Collagen in Chicken Liver. Chicken liver was homogenized in 0.5M Acetic Acid and 0.1 mg/mL Pepsin.

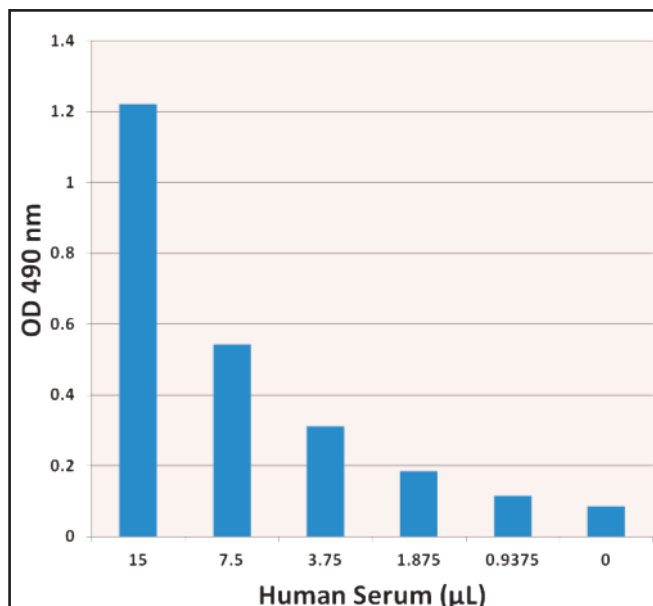
Product Name	Detection	Size	Catalog Number
Soluble Collagen Assay Kit	Colorimetric	96 Assays	MET-5016

Total Carbohydrate Assay Kit

The measurement of total carbohydrate content is important in several fields including food, petroleum, pharmaceutical and environmental research. Many techniques such as light scattering, NMR, capillary electrophoresis, IR spectroscopy and chromatography have been used, but these techniques can be costly, time consuming, and require complex analytical skills.

The Total Carbohydrate Assay kit is a simple, convenient assay that measures the total carbohydrate content of foods or biological samples. Carbohydrates in samples are compared to a known glucose standard provided in the kit.

- **Sensitive:** Detect as little as 62.5 μM
- **Versatile:** Suitable for food samples, plasma, serum, urine, cell lysates, or tissue homogenates



Total Carbohydrate Detection in Human Serum.

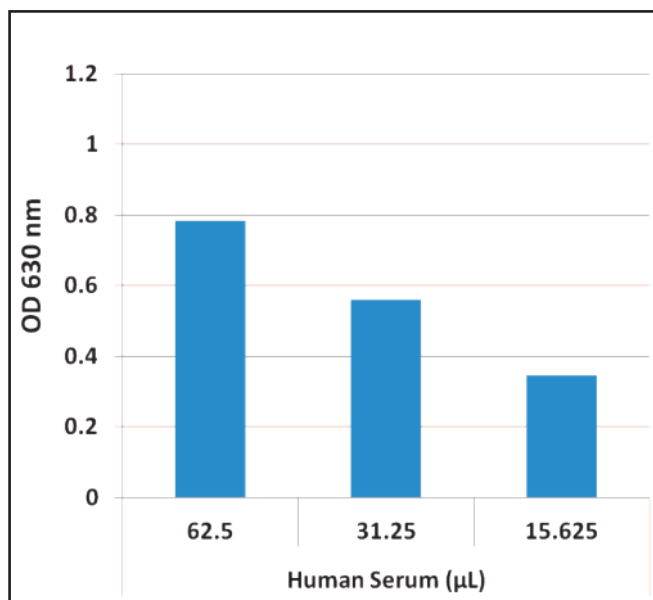
Product Name	Detection	Size	Catalog Number
Total Carbohydrate Assay Kit	Colorimetric	100 Assays	STA-682

Total Sialic Acid Assay Kit

Sialic acids comprise a family of derivatives of nine-carbon monosaccharides. They are found in highest concentrations in brain gangliosides which function in neurotransmission, memory storage, and synapse function. Additionally, sialic acids can bind to proteins to create sialoglycoproteins, a buildup of which can facilitate the entry of metastatic cancer cells into the bloodstream.

Our Total Sialic Acid Assay kit is a simple colorimetric assay that measures the total sialic acid content present in biological samples. Samples are first treated with an Oxidizing Reagent, followed by treatment with Resorcinol Reagent. Under acidic conditions the sialic acid forms a chromophore which is extracted into an alcohol to be read in a standard 96-well microplate reader.

- **Sensitive:** Detect as little as 25 μM
- **Versatile:** Suitable for plasma, serum, saliva, urine, cell lysates, tissue homogenates, or cell culture supernatants



Total Sialic Acid Standard Curve.

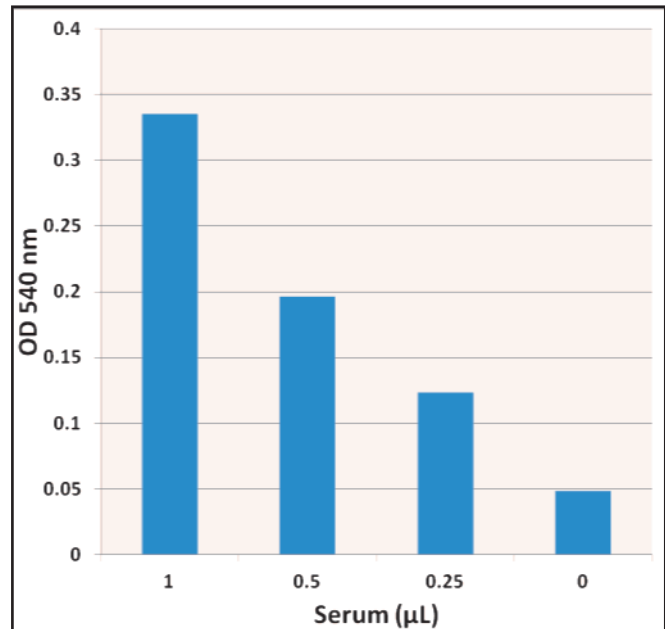
Product Name	Detection	Size	Catalog Number
Total Sialic Acid Assay Kit	Colorimetric	100 Assays	MET-5015

Glucose Assay Kits

Glucose is an important source of energy in plants, prokaryotes, and eukaryotes via processes including respiration and fermentation. Our Glucose Assay Kits are simple microplate-based assays that measure the total amount of glucose present in foods or various biological sample types. In the presence of oxygen, glucose oxidase catalyzes the conversion of glucose to D-gluconic acid, with hydrogen peroxide as the byproduct. Hydrogen peroxide reacts with probe to produce a signal.

Kits are available with either colorimetric or fluorometric detection in a 96-well plate reader.

- **Sensitive:** Detect as little as 6.25 μM in the colorimetric format or 1.56 μM in the fluorometric format
- **Versatile:** Suitable for food samples, plasma, serum, urine, lysates, or other biological fluids



Detection of Glucose in Human Serum.

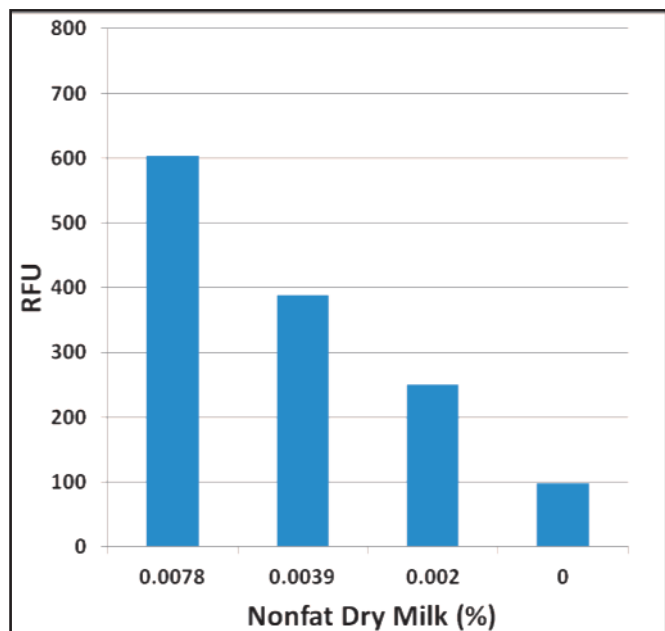
Product Name	Detection	Size	Catalog Number
Glucose Assay Kit	Colorimetric	500 Assays	STA-680
	Fluorometric	500 Assays	STA-681

Lactose Assay Kit

Lactose is a common disaccharide that has implications for a significant portion of the human population due to lactose intolerance, better described as lactase deficiency due to the lack of the enzyme that breaks down lactose.

Since the severity of lactose maldigestion symptoms can depend on the amount of lactose consumed, it is important to quantify the relative amounts of lactose in various food sources.

Our Lactose Assay Kit is a simple plate-based assay that measures the total amount of lactose in milk based food products, as well as biological samples such as blood or urine from lactating animals. The kit can detect lactose levels as low as 10 μM . Quantitation is performed in a 96-well plate using a fluorescence-based microplate reader.



Detection of Lactose in Bovine Nonfat Dry Milk.

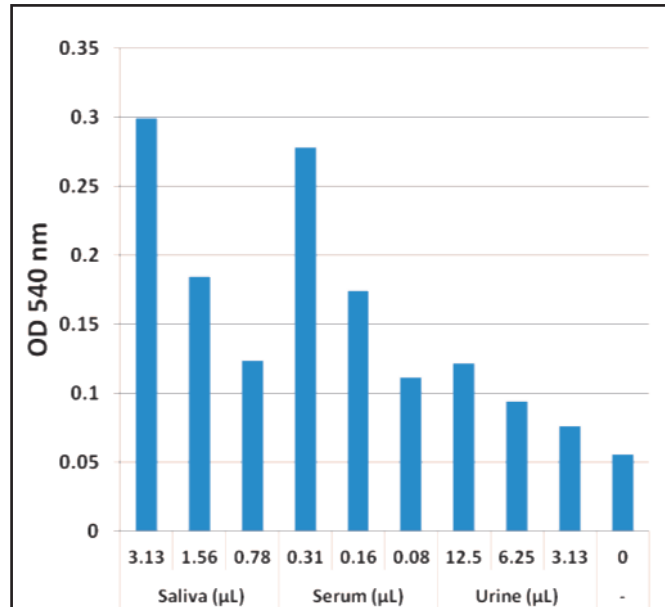
Product Name	Detection	Size	Catalog Number
Lactose Assay Kit	Fluorometric	100 Assays	MET-5001

Lactate Assay Kits

Lactic acid is an alpha hydroxyl acid that can ionize a carboxyl proton to yield the lactate ion. Lactate, like glucose, is thought to be one of the main energy sources in the brain. Lactate is also an important molecule in various industries including food, wine-making, and household detergents.

The Lactate Assay Kits are simple, convenient assays for the detection and quantitation of total lactate levels present in biological samples. In the presence of oxygen, lactate oxidase converts lactate to pyruvate, producing hydrogen peroxide as a byproduct. The hydrogen peroxide reacts with a probe in the presence of HRP and produces a signal.

Kits are available with either colorimetric or fluorometric detection in a 96-well plate reader.



Detection of Lactate in Various Human Biological Samples.

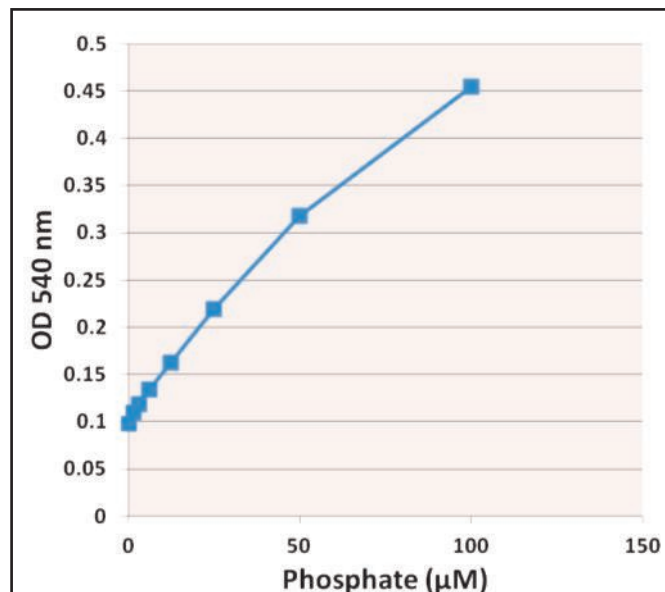
Product Name	Detection	Size	Catalog Number
Lactate Assay Kit	Colorimetric	100 Assays	MET-5012
	Fluorometric	100 Assays	MET-5013

Phosphate Assay Kits

Phosphate is found in biological systems in both organic and inorganic forms. Many metabolic processes are regulated by phosphate such as amino acid metabolism, activation of proteins, carbon metabolism, enzymatic cell signaling, and energy transfer.

Our Phosphate Assay Kits are simple assays that measure total inorganic phosphate (P_i) in solutions, food products, or biological samples in a convenient 96-well microplate format. In the presence of inorganic phosphate, maltose is converted to glucose and glucose-1-phosphate by maltose phosphorylase. The glucose is then converted to D-gluconic acid and hydrogen peroxide by glucose oxidase. The resulting hydrogen peroxide is detected with a highly specific probe.

Kits are available with either colorimetric or fluorometric detection in a 96-well plate reader.



Phosphate Assay Standard Curve.

Product Name	Detection	Size	Catalog Number
Phosphate Assay Kit	Colorimetric	1000 Assays	STA-685
	Fluorometric	1000 Assays	STA-686

Renal Function Assays

Our Renal Function Assays provide a simple, sensitive method to test for various markers related to kidney function:

- Uric Acid / Uricase
- Urea
- Creatinine
- Protein Carbamylation

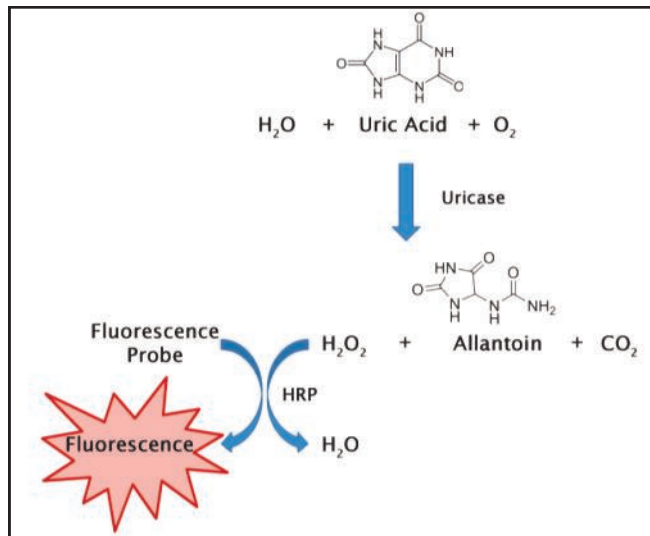
Uric Acid/Uricase Assay Kit

Uric acid is the final oxidation end product of purine nucleotide metabolism. Uric acid is a potent antioxidant that is released during hypoxic conditions and is usually excreted in the urine via glomerular filtration. Our Uric Acid / Uricase Assay Kit is a simple 96-well microplate-based assay for measuring concentrations of either uric acid or uricase in serum, plasma or urine samples. Detection is performed in a fluorescence-based plate reader.

- **Sensitive:** Detect as little as 0.5 μM of uric acid or 1 mU/mL of uricase
- **Quantitative:** Kit includes both uric acid and uricase standards

Recent Product Citation

Leiba, A. et al. (2015). Uric acid levels within the normal range predict increased risk of hypertension—a cohort study. *Am. J. Hypertens. American* 10.1016/j.jash.2015.05.010.



Assay Principle for the Uric Acid / Uricase Assay Kit.

Product Name	Detection	Size	Catalog Number
Uric Acid/Uricase Assay Kit	Fluorometric	400 Assays	STA-375

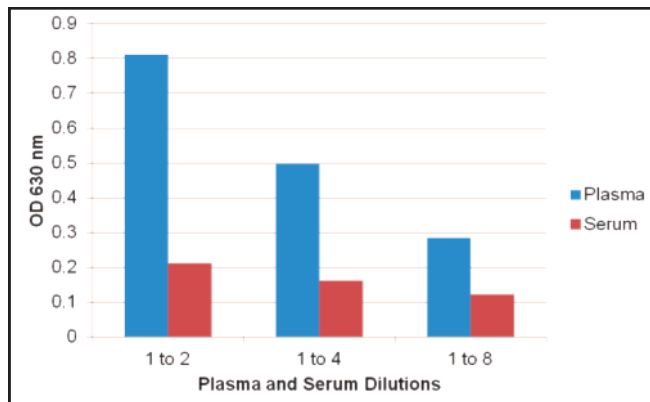
Urea Assay Kit

Urea is the end product of protein nitrogen metabolism and is the primary vehicle for removing toxic ammonia from the body. Urea quantitation is one of the most widely applied tests for kidney function evaluation. Our Urea Assay Kit is a simple 96-well microplate-based assay for measuring urea concentrations in serum, plasma, lysates, or urine samples. Detection is performed in standard colorimetric plate reader.

- **Sensitive:** Detect as little as 1 mg/dL of urea
- **Quantitative:** Measure unknown samples against a known urea standard curve

Recent Product Citation

Bruinsma, B.G. et al. (2014). Subnormothermic machine perfusion for ex vivo preservation and recovery of the human liver for transplantation. *Am. J. Transplant.* 14:1400-1409.



Human Plasma and Serum Samples Tested with the Urea Assay Kit.

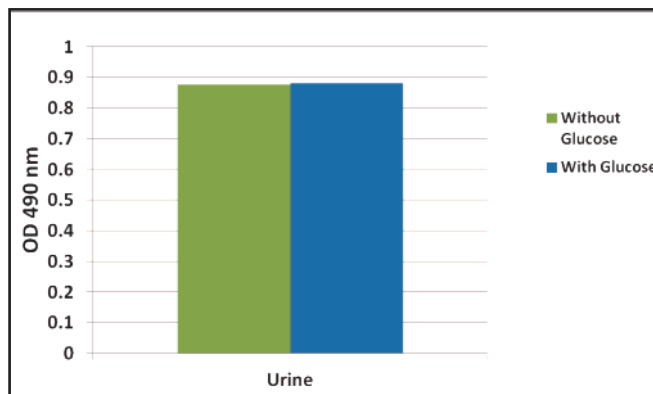
Product Name	Detection	Size	Catalog Number
Urea Assay Kit	Fluorometric	192 Assays	STA-382

Urinary Creatinine Assay Kit

Our Urinary Creatinine Assay Kit is based on the Jaffe reaction between creatinine and alkaline picrate, which produces an orange-red color complex that can be easily read by a standard microplate reader. A creatinine standard is provided to allow quantitative measurements of creatinine levels in urine samples. The assay is simple and takes less than one hour to perform.

Recent Product Citations

1. Bone, R.N. et al. (2015). Inhibition of Ca²⁺-independent phospholipase A2 β (iPLA2 β) ameliorates islet infiltration and incidence of diabetes in NOD mice. *Diabetes* **64**:541-554.
2. Zis, P. et al. (2014). Memory decline in Down syndrome and its relationship to iPF2alpha, a urinary marker of oxidative stress. *PLoS One* **9**:e97709.
3. Day, R. et al. (2013). Apelin retards the progression of diabetic nephropathy. *Am. J. Physiol. Renal Physiol.* **304**:F788-F800.

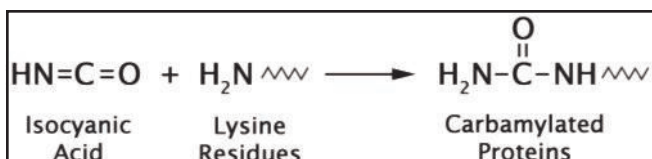


Creatinine Levels in Urine Samples in the Presence and Absence of Glucose.

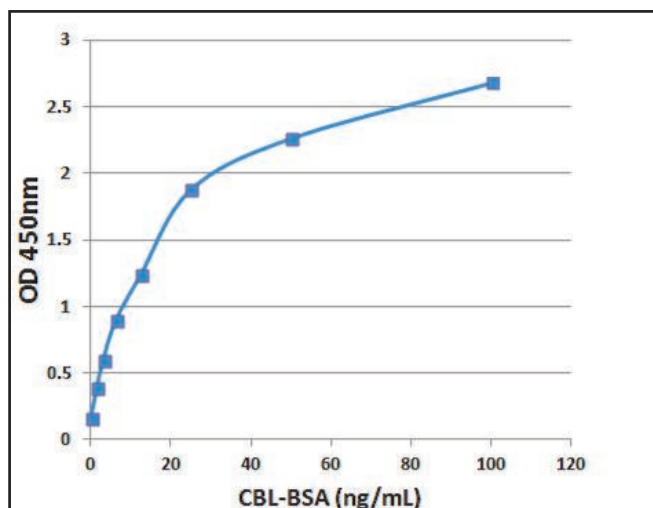
Product Name	Detection	Size	Catalog Number
Urinary Creatinine Assay Kit	Colorimetric	192 Assays	STA-378

Protein Carbamylation ELISA Kit and Antibodies

Carbamylation is a post-translational modification which occurs throughout the lifespan of proteins in vivo. Carbamylation results from the binding of isocyanic acid, which spontaneously arises from high concentrations of urea, to lysine residues of proteins as carbamyl-lysine (CBL). Our Protein Carbamylation Sandwich ELISA Kit is a convenient microplate-based method for the evaluation of protein carbamylation in a variety of sample types. In addition, polyclonal antibodies are available for use in Western blot and ELISA applications.



Formation of Carbamyl-Lysine (CBL) During Carbamylation of Proteins.



Standard Curve Generated with the OxiSelect™ Protein Carbamylation Sandwich ELISA Kit.

Recent Product Citations

1. Joshi, A.D. et al. (2015). Homocitrullination is a novel histone H1 epigenetic mark dependent on aryl hydrocarbon receptor recruitment of carbamoyl phosphate synthase 1. *J. Biol. Chem.* 10.1074/jbc.M115.678144. (STA-077)
2. Koro, C. et al. (2014). Carbamylation of immunoglobulin abrogates activation of the classical complement pathway. *Eur. J. Immunol.* **44**:3403-3412. (STA-078)

Product Name	Detection	Size	Catalog Number
OxiSelect™ Protein Carbamylation Sandwich ELISA	Colorimetric	96 Assays	STA-877
Goat Anti-Carbamyl-Lysine (CBL) Polyclonal Antibody	Immunoblot/ELISA	50 µg	STA-077
Rabbit Anti-Carbamyl-Lysine (CBL) Polyclonal Antibody	Immunoblot/ELISA	50 µg	STA-078
Carbamyl Lysine-BSA	N/A	10 µg	STA-379

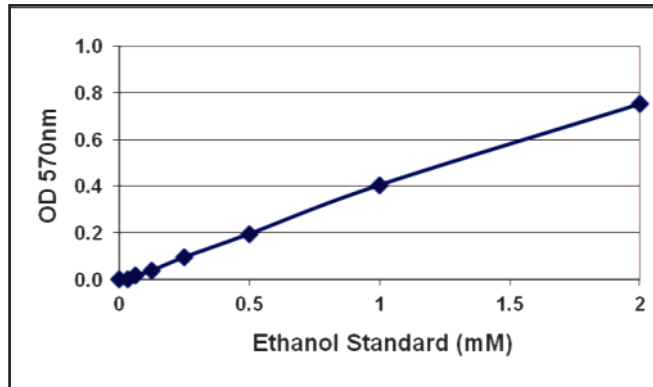
Alcohol Assay Kits

Our Alcohol Assay Kits provide a convenient plate-based method to measure primary alcohols, including ethanol, in plasma, serum or saliva samples.* The kit uses an enzymatic oxidation reaction that produces hydrogen peroxide, which reacts with the provided probe.

Kits are available with either colorimetric or fluorescence-based detection, both of which are performed in a 96-well microtiter plate. The colorimetric assay can detect alcohol levels as low as 30 μM , while the fluorometric assay detects as low as 15 μM .

Recent Product Citation

Wu, Qi et al. (2014). High level expression, efficient purification, and bioactivity of recombinant human metallothionein 3 (rhMT3) from methylotrophic yeast *Pichia pastoris*. *Protein Expr. Purif.* **101**:121-126. (STA-620)



Standard Curve Generated with the Alcohol Assay Kit.

*These assays are not suitable for urine samples.

Product Name	Detection	Size	Catalog Number
Alcohol Assay Kit	Colorimetric	100 Assays	STA-620
	Fluorometric	100 Assays	STA-621

Free Glycerol Assay Kits

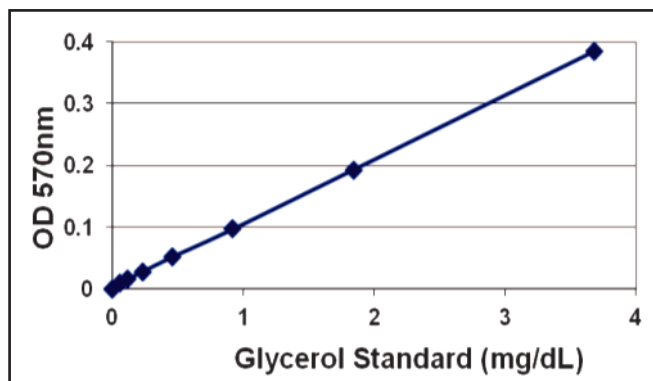
Glycerol is the backbone of triglycerides. Lipases secreted in the intestines hydrolyze the triglyceride ester bond, producing glycerol and free fatty acids.

Our Free Glycerol Assay Kits use a coupled enzymatic reaction system to measure free, endogenous glycerol concentrations. The glycerol is phosphorylated and oxidized, producing hydrogen peroxide, which reacts with the probe provided with each kit.

Kits are available with either colorimetric or fluorescence-based detection, both of which are performed in a 96-well microtiter plate.

Recent Product Citation

Desarzens, S. et al. (2014). Hsp90 blockers inhibit adipocyte differentiation and fat mass accumulation. *PLoS One* **9**:e94127. (STA-398)



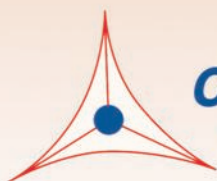
Standard Curve Generated with the Free Glycerol Assay Kit.

Product Name	Detection	Size	Catalog Number
Free Glycerol Assay Kit	Colorimetric	100 Assays	STA-398
	Fluorometric	100 Assays	STA-399

Pathogen and Toxin Assays

Viral Antigen ELISA Kits 152

Toxin Assays 155



CELL BIOLABS, INC.

Creating Solutions for Life Science Research

Virus Antigen Detection

Viral antigens provide a convenient way to detect and quantify certain infectious viruses.

We offer a variety of ELISA kits to measure the specific antigen levels in plasma, serum, or purified virus preps.

- Hepatitis B Core Antigen
- Hepatitis B “e” Antigen
- Hepatitis B Surface Antigen
- Hepatitis C Core Antigen
- MuLV Core Antigen

Note: Assays are for research use only, not for clinical diagnostic use.

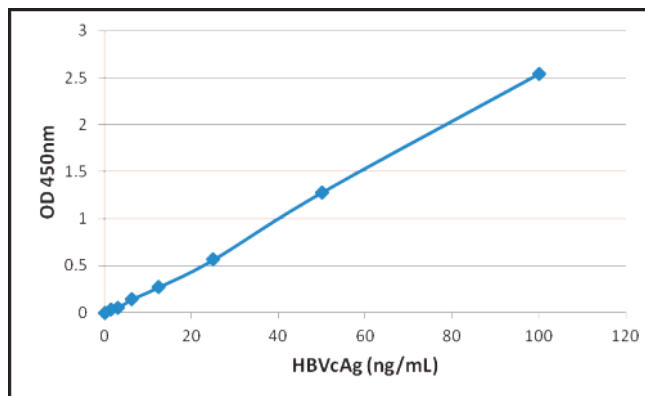
QuickTiter™ HBV Core Antigen (HBVcAg) ELISA Kit

The core antigen of Hepatitis B virus (HBV), also known as HBVcAg, provides a convenient way to quantify HBV in samples. The QuickTiter™ HBV Core Antigen ELISA Kit specifically quantifies this core antigen.

A mouse monoclonal antibody is coated onto an 8 x 12 strip-well plate which allows the flexibility to save some of the wells for later use. After adding unknown samples, a FITC-conjugated mouse anti-HBVcAg antibody is added and binds to the antigen captured on the plate. Then a mouse anti-FITC antibody conjugated to HRP is added, followed by incubation with a substrate solution that reacts with HRP and produces a color measurable in a standard colorimetric plate reader.

The quantity of HBV is compared to the provided HBV Core Antigen Standard. Each kit provides sufficient reagents to run 96 assays including standards and unknown samples.

- **Sensitive:** Detect as little as 1 ng/mL
- **Fully Quantitative:** Recombinant core antigen is included as standard



QuickTiter HBV Core Antigen ELISA Kit Standard Curve.

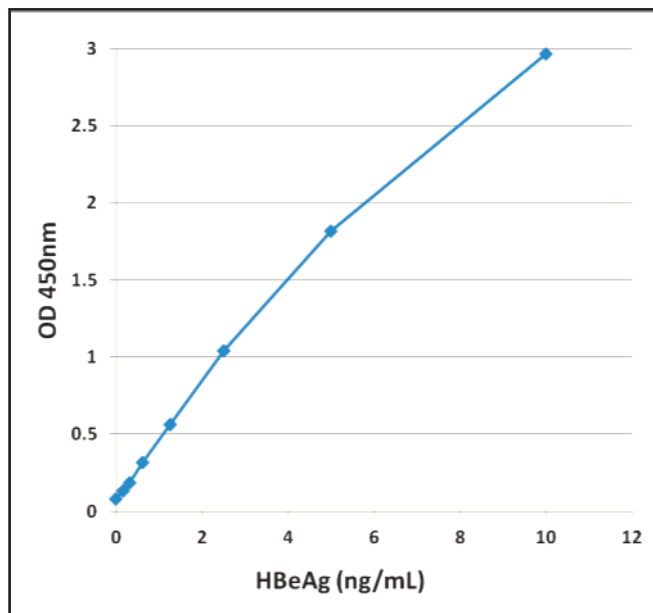
Product Name	Detection	Size	Catalog Number
QuickTiter™ HBV Core Antigen ELISA Kit	Colorimetric	96 Assays	VPK-150
		5 x 96 Assays	VPK-150-5

QuickTiter™ Hepatitis B “e” Antigen (HBeAg) ELISA Kit

The “e” antigen of the Hepatitis B virus (HBV), also known as HBeAg, is an important marker for acute HBV infection. The QuickTiter™ Hepatitis B “e” Antigen ELISA Kit specifically quantifies HBeAg in a 96-well plate format. A mouse monoclonal antibody is coated onto an 8 x 12 strip-well plate which allows the flexibility to save some of the wells for later use.

The quantity of HBV is compared to the provided HBV “e” Antigen Standard. Each kit provides sufficient reagents to run 96 assays including standards and unknown samples.

- **Sensitive:** Detect as little as 150 pg/mL
- **Fully Quantitative:** Recombinant “e” antigen is included as standard



QuickTiter™ Hepatitis B “e” Antigen ELISA Kit Standard Curve.

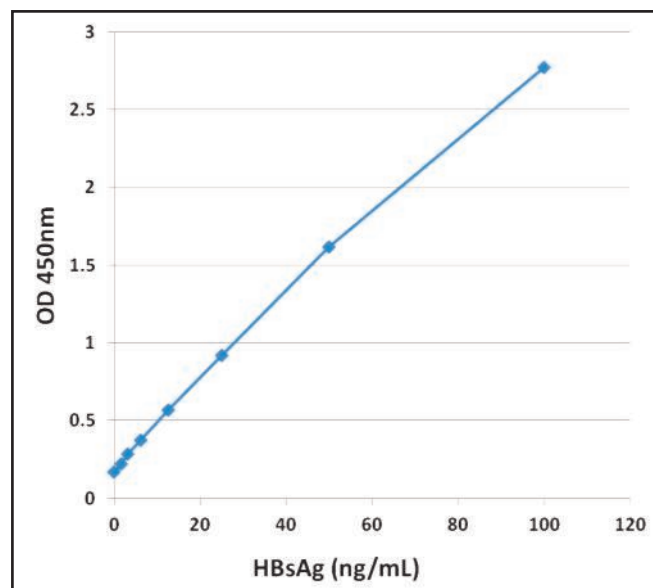
Product Name	Detection	Size	Catalog Number
QuickTiter™ Hepatitis B “e” Antigen (HBeAg) ELISA Kit	Colorimetric	96 Assays	VPK-5003
		5 x 96 Assays	VPK-5003-5

QuickTiter™ Hepatitis B Surface Antigen (HBsAg) ELISA Kit

The surface antigen of the Hepatitis B virus (HBV), also known as HBsAg, is an important marker for acute HBV infection. The QuickTiter™ Hepatitis B Surface Antigen ELISA Kit specifically quantifies HBsAg in a 96-well plate format. A mouse monoclonal antibody is coated onto an 8 x 12 strip-well plate which allows the flexibility to save some of the wells for later use.

The quantity of HBV is compared to the provided HBV Surface Antigen Standard. Each kit provides sufficient reagents to run 96 assays including standards and unknown samples.

- **Sensitive:** Detect as little as 1 ng/mL
- **Fully Quantitative:** Recombinant surface antigen is included as standard



QuickTiter™ Hepatitis B Surface Antigen ELISA Kit Standard Curve.

Product Name	Detection	Size	Catalog Number
QuickTiter™ Hepatitis B Surface Antigen (HBsAg) ELISA Kit	Colorimetric	96 Assays	VPK-5004
		5 x 96 Assays	VPK-5004-5

QuickTiter™ HCV Core Antigen ELISA Kit

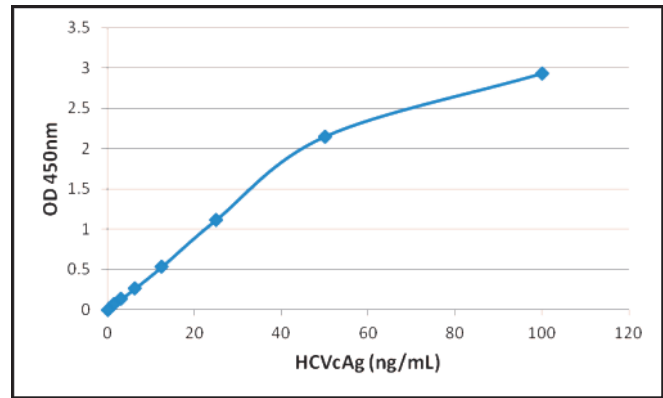
The QuickTiter™ HBV Core Antigen ELISA Kit specifically quantifies the core protein of Hepatitis B virus. A mouse monoclonal antibody is coated onto an 8 x 12 strip-well plate which allows the flexibility to save some of the wells for later use.

The quantity of HBV is compared to the provided HBV Core Antigen Standard.

Recent Product Citations

1. Liu, D. et al. (2015). Downregulation of miRNA-30c and miR-203a is associated with hepatitis C virus core protein-induced epithelial-mesenchymal transition in normal hepatocytes and hepatocellular carcinoma cells. *Biochem. Biophys. Res. Commun.* **464**:1215-1221.
2. Jittavisutthikul, S. et al. (2015). Humanized-VHH transbodies that inhibit HCV protease and replication. *Viruses* **7**:2030-2056.
3. Kong, L. et al. (2014). HIV infection of hepatocytes results in a modest increase in hepatitis C virus expression in vitro. *PLoS One* **9**:e83728.
4. Carpentier, A. et al. (2014). Engrafted human stem cell-derived hepatocytes establish an infectious HCV murine model. *J. Clin. Invest.* **124**:4953-4964.

- **Sensitive:** Detect as little as 1 ng/mL
- **Fully Quantitative:** Recombinant core antigen included as standard



QuickTiter HCV Core Antigen ELISA Kit Standard Curve.

Product Name	Detection	Size	Catalog Number
QuickTiter™ HCV Core Antigen ELISA Kit	Colorimetric	96 Assays	VPK-151

QuickTiter™ MuLV Core Antigen ELISA Kit

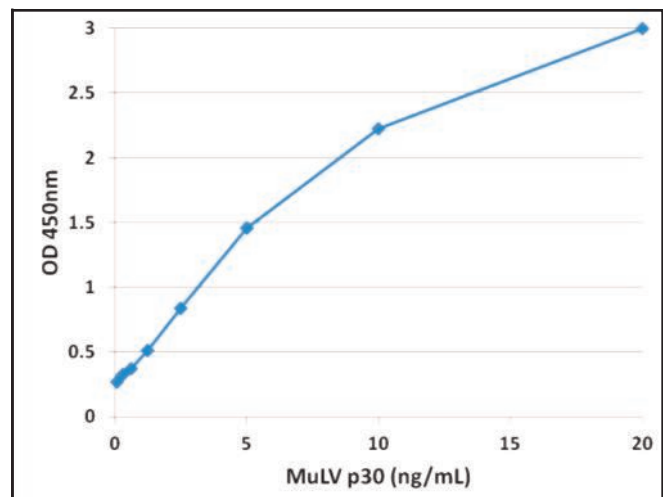
Murine leukemia virus (MuLV) is a retrovirus capable of causing cancer in mice and related vertebrates. Recently discovered in humans, xenotropic murine leukemia virus-related virus (XMRV) is closely related to MuLV; the p30 core antigens share 96% identity.

Our QuickTiter™ MuLV Core Antigen ELISA Kit specifically measures the level of the p30 core antigen in blood or other samples.

Recent Product Citations

1. Rosales Gerpe, M.C. et al. (2015). N-linked glycosylation protects gammaretroviruses against deamination by APOBEC3 proteins. *J. Virol.* **89**:2342-2357.
2. Aydin, H. et al. (2014). Crystal structures of beta- and gamma-retrovirus fusion proteins reveal a role for electrostatic stapling in viral entry. *J. Virol.* **88**:143-153.
3. Nityanandam, R. and Serra-Moreno, R. (2014). BCA2/Rabring7 targets HIV-1 Gag for lysosomal degradation in a tetherin-independent manner. *PLoS Pathog.* **10**:e1004151.
4. Kirchmeier, M. et al. (2014). Enveloped virus-like particle expression of human cytomegalovirus glycoprotein B antigen induces antibodies with potent and broad neutralizing activity. *Clin. Vaccine Immunol.* **21**:174-180.
5. Belanger, K. et al. (2013). Binding of RNA by APOBEC3G controls deamination-independent restriction of retroviruses. *J. Exp. Biol.* **216**:2213-2220.

- **Sensitive:** Detect as little as 300 pg/mL
- **Fully quantitative:** Recombinant core antigen included as standard



Standard Curve Generated with the QuickTiter™ MuLV Core Antigen ELISA Kit.

Product Name	Detection	Size	Catalog Number
QuickTiter™ MuLV Core Antigen ELISA Kit (MuLV p30)	Colorimetric	96 Assays	VPK-156

OxiSelect™ BPDE Adduct ELISA Kits

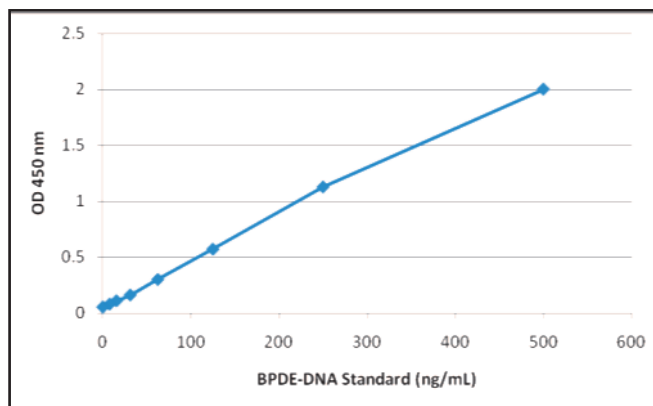
Polycyclic aromatic hydrocarbons (PAH) are potent carcinogenic pollutants commonly associated with oil, cigarette smoke, and automotive exhaust. Benzo(a)pyrene, the first chemical carcinogen discovered, is converted to benzo(a)pyrene 7,8 diol-9,10 epoxide (BPDE) through a series of enzymatic reactions. BPDE can attack both proteins and DNA, forming adducts that can potentially result in tumor formation.

Our OxiSelect™ BPDE Adduct ELISA Kits provide a convenient method to measure BPDE adducts with either DNA or proteins from cells or tissues. Quantitation is performed by comparing unknown values against a standard curve generated with the standard provided in each kit.

- Our BPDE DNA Adduct ELISA can detect adducts as low as 30 ng/mL.
- Our BPDE Protein Adduct ELISA can detect adducts as low as 60 ng/mL.

Recent Product Citation

Chiu, C.Y. et al. (2014). Low-dose benzo(a)pyrene and its epoxide metabolite inhibit myogenic differentiation in human skeletal muscle-derived progenitor cells. *Toxicol. Sci.* 10.1093/toxsci/kfu003. (STA-357)



Standard Curve Generated Using the OxiSelect™ BPDE DNA Adduct ELISA Kit.

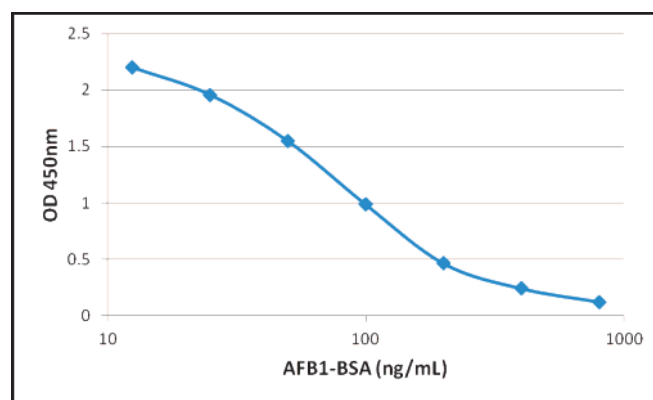
Product Name	Detection	Size	Catalog Number
OxiSelect™ BPDE DNA Adduct ELISA Kit	Colorimetric	96 Assays	STA-357
OxiSelect™ BPDE Protein Adduct ELISA Kit	Colorimetric	96 Assays	STA-301

Aflatoxin ELISA Kits

Aflatoxins are among the most potent genotoxic agents known. They can induce chromosomal aberrations, micronuclei, sister chromatid exchange, unscheduled DNA synthesis, and chromosomal strand breaks. Aflatoxins can form adducts with both DNA and proteins.

Our Aflatoxin Competitive ELISA Kits provide a convenient method for detection of aflatoxin adducts.

- Our Aflatoxin Competitive ELISA Kit measures the total of Aflatoxin B1 and Aflatoxin B2 adducts in protein samples.
- Our Aflatoxin DNA Adduct Competitive ELISA Kit detects total Aflatoxin B1-DNA adducts, both ring-opened and ring-closed forms.



Standard Curve Generated with the Aflatoxin Competitive ELISA Kit.

Product Name	Detection	Size	Catalog Number
Aflatoxin Competitive ELISA Kit	Colorimetric	96 Assays	AKR-350
Aflatoxin DNA Adduct Competitive ELISA Kit	Colorimetric	96 Assays	AKR-351

PRODUCT INDEX

Product	Page	Product	Page	Product	Page
293 Cell Lines		Aflatoxin Assays	155	Antioxidant Assays	
AAV	47	AGE Assays	76-77	(cont'd)	
Adenovirus	52	Albumin		ORAC Assay	100
GFP Stable Expression	114	Antibody	138	Superoxide Dismutase	97
Lentivirus	59	ELISA Kit	138	Activity Assay	
Retrovirus	66	Protein	138	Total Antioxidant Capacity	100
3-Nitrotyrosine		Alcohol Assays	150	Assay	
Antibodies	73	Aldehyde-Induced DNA	89	AOPP Assay	75
ELISA Kit	73	Damage Assays		AP Sites Quantitation Kit	86
4-HNE		Alkaline Phosphatase	38	Apo(a) ELISA	124
Antibodies	79	Assays		ApoAI ELISA	124
ELISA Kit	79	Amino Acid Assays	142-144	ApoAI/ApoB Duplex ELISA	125
6-4PP Quantitation Kits	88	Angiogenesis		ApoAII ELISA	124
8-Iso-Prostaglandin F2α ELISA	79	Recombinant Adenovirus	50	ApoB ELISA	124
8-Isoprostane ELISA Kit	79	Tube Formation Assay	30	ApoCI ELISA	124
8-Nitroguanine ELISA Kit	85	Anoikis Assays	23	ApoCII ELISA	124
8-OHdG ELISA Kit	84	Antibodies		ApoCIII ELISA	124
8-OHG ELISA Kit	85	Albumin	138	ApoE ELISA	124
A549/GFP Cell Line	114	Apolipoproteins	125	Apolipoproteins	
AAV (Adeno-Associated Virus)		Beta-Actin	116	Antibodies	125
Cell Line	47	Beta-Tubulin	116	ELISA Kits	124
Expression Systems	41-45	Carboxymethyl Lysine (CML)	77	Proteins	124
Expression Vectors	46	C-Reactive Protein	138	Arf1 Activation Assay	105
Helper Free Systems	41-45	Flag Tag	116	Arf6 Activation Assay	105
Packaging Systems	45	Fluorescent Proteins	115	Ascorbic Acid Assay	101
Premade Control Viruses	47	GAPDH	116	AUF1 Retroviral Vector	68
Purification Kits	48	GFP	115	Autophagy Expression Vectors	30
Quantitation Kit	49	GST Tag	116	β-Actin Antibody	116
shRNA Expression	41-45	HA Tag	116	β-Galactosidase	
Titer Kit	49	His Tag	116	Recombinant Adenovirus	50
Transduction Reagent	49	HNE (4-Hydroxynonenal)	79	Reporter Assays	114
Acetylcholine Assays	136	MDA (Malondialdehyde)	80	β-Tubulin Antibody	116
Active Rac-GEF Assay	106	Methylglyoxal (MG)	77	Bacterial Protein Extraction Reagents	118
Adenovirus		Myc Tag	116	BCG Albumin Assay	138
Cell Line	52	Nitrotyrosine	73	Bile Acid Assays	134-135
Expression Systems	53	Plasminogen	138	Bilirubin Assay	135
Premade Recombinant	50-52	RFP	115	Blocking Reagent	117
Purification Kits	54	Antibody Tools		BPDE	
Quantitation Kits	55	Blocking Reagent	117	DNA Adduct ELISA	155
RCA Assay	56	Purification Kit	120	Protein Adduct ELISA	155
shRNA Expression	53	Western Stripping Solution	117	BrdU ELISA Kit	25
Titer Kits	55	Antioxidant Assays		C3 Expression Vector	108
Transduction Reagent	56	Catalase Activity Assay	96	c-Abl Retroviral Vector	66
Adhesion Assays	10-11	Cellular Antioxidant Assay	99	cAMP ELISA Kits	110
Adipogenesis Assay	27	Glutathione Assay	98	Cancer Cell Assays	
Advanced Glycation End Products Assay	76-77	Glutathione Reductase Assay	98	Angiogenesis	30
Advanced Oxidation Protein Products Assay	75	HORAC Assay	100	Anoikis	23

PRODUCT INDEX

Product	Page	Product	Page	Product	Page
Cancer Cell Assays (cont'd)		Cell Cycle (cont'd)		Cholesteryl Ester Transfer Protein Assay	130
Cell Adhesion	10-11	Cell Viability Assay	22	Cholic Acid ELISA	134
Cell Invasion	18-19	Cytotoxicity Assay	22	Clonogenic Tumor Cell Isolation Kit	9
Cell Migration	12-19	Retroviral Vectors	66	CML (Carboxymethyl Lysine) Antibodies Assays	77
Cell Transformation	6-7	Senescence Assays	23	CML-LDL ELISA Kit	82
Colony Formation	6-9	Cell Fractionation Kits	118	c-Myc Retroviral Vectors	67
Soft Agar	6-9	Cell Invasion Assays	18-19	Colony Formation Assays	
Tumor Cell Isolation Kit	9	Cell Lines		Cell Transformation Assays	6-7
Tumor Sensitivity	8	293AAV	47	Hematopoietic Colony Forming Cell Assay	36
Carbamyl Lysine		293AD	52	Stem Cell Colony Assay	37
Antibodies	149	293LTV	59	Tumor Cell Isolation Kit	9
ELISA Kits	149	293RTV	66	Tumor Sensitivity Assay	8
Carbohydrate Assays	145-146	293/GFP	114	Collagen Assay	144
Carbonyl Assays	74	A549/GFP	114	Collagen Cell Contraction Assays	29
Carboxyethyl Lysine ELISA	76	HeLa/GFP	114	Comet Assay Kits & Slides	87
Carboxymethyl Lysine Assays	77	JK1 Feeder Cells	35	Contraction Assays	29
Catalase Activity Assays	96	MCF-7/GFP	114	Core Antigen Assays	152-154
Cdc42		MCF-7/Luc	114	CPD Quantitation Kits	88
Activation Assay	105	MDA-MB-231/GFP	114	C-Reactive Protein	
Agarose Beads	107	MDA-MB-231/Luc	114	Antibody	138
Recombinant Adenovirus	52	MDA-MB-231/RFP	114	ELISA	137
Retroviral Vector	67	MEF Feeder Cells	35	Protein	138
CEL ELISA Kit	76	NIH3T3/GFP	114	Cre Recombinant Adenovirus	50
Cell-Based Assays		OVCAR-5/RFP	114	Creatinine Assay	149
Adhesion	10-11	Plat-A Retroviral Packaging Cells	63	Cyclic AMP ELISA Kits	110
Angiogenesis	29	Plat-E Retroviral Packaging Cells	63	Cyclic GMP ELISA Kits	110
Anoikis	23	Plat-GP Retroviral Packaging Cells	63	CytoSelect™ Cell-Based Assays	
Cell Contraction	29	SKOV-3/GFP-Luc	114	Anoikis	23
Cell Viability	22	SKOV-3/Luc	114	Cell Adhesion	10-11
Chemotaxis	15, 19	SNL Feeder Cells	35	Cell Contraction	29
Colony Formation	6-9	T47D/GFP	114	Cell Invasion	18-19
Cytotoxicity	22	Cell Migration Assays	12-19	Cell Migration	12-19
Haptotaxis	16	Cell Proliferation Assays	24-25	Cell Transformation	6-7
Invasion	18-19	Cell Transformation Assays	6-7	Cell Viability	22
Migration	12-19	Cell Viability Assay	22	Chemotaxis	15, 19
Phagocytosis	28	Cellular Antioxidant Assay	99	Colony Formation	6-9
Proliferation	24-25	Cellular Senescence Assays	23	Cytotoxicity	22
Senescence	23	CETP ELISA Kit	130	Haptotaxis	16
Soft Agar	6-9	cGMP ELISA Kits	110	Phagocytosis	28
Transformation	6-7	Checkpoint Kinase Assays	111		
Transmigration	17	Chemotaxis Assays	15, 19		
Tumor Sensitivity	8	Chenodeoxycholic Acid ELISA	135		
Wound Healing	20	Cholesterol Assays	122-123		
Cell Cycle					
Adenoviruses	52				
Anoikis Assay	23				

PRODUCT INDEX

Product	Page	Product	Page	Product	Page
CytoSelect™ Cell-Based Assays (cont'd)		FFA Assay Kits	133	HBV Surface Antigen ELISA	153
Soft Agar	6-9	Firefly Luciferase Recombinant Adenovirus	50	HCV Core Antigen ELISA	154
Transmigration	17	Flag Tag Antibody	116	HDL Assay	123
Tumor Sensitivity	8	FRAP Assay	101	Lipoprotein, Human	123
Wound Healing	20	FRASC Assay	101	Oxidized	127
Cytoskeleton Regulation		Free Fatty Acid Assays	133	HEK 293 Cell Lines	
Activation Assays	104	Free Glycerol Assays	150	AAV	47
Adenoviruses	52	Gap Closure Migration Assays	13	Adenovirus	52
Expression Vectors	108	GAPDH Antibody	116	GFP Stable Expression	114
Retroviral Vectors	67	GEF (Guanine Exchange Factors)		Lentivirus	59
Cytotoxicity Assay	22	Activation Assays	106	Retrovirus	66
DNA Damage Assays		Agarose Beads	107	HeLa/GFP Cell Line	114
6-4PP Quantitation	88	GFP		Hematopoietic Colony Forming Cell Assay	36
8-Nitroguanine ELISA Kit	85	Antibody	115	Hepatitis B Core Antigen ELISA	152
8-OHdG ELISA Kit	84	ELISA Kit	113	Hepatitis B "e" Antigen ELISA	153
Aldehyde-Induced Damage	89	Lentiviral Vectors	59	Hepatitis B Surface Antigen ELISA	153
AP Sites Quantitation Kit	86	Quantitation Kits	113	Hepatitis C Core Antigen ELISA	154
BPDE Adduct ELISA	89	Recombinant Adenovirus	50	HIF-1α	
Comet Assays	87	Recombinant Lentivirus	59	Assays	26, 91
CPD Quantitation	88	Recombinant Protein	115	Recombinant Adenovirus	50
Double-Strand Break Assay	86	Retroviral Vectors	66	High Density Lipoprotein Assay	123
UV Damage	88	Stable Cell Lines	114	Protein	123
DNA Methylation Assays	90	GGA3 Agarose Beads	107	His Tag	
ECM Assays		Global DNA Methylation Assays	90	Antibody	116
Cell Adhesion Assays	10	Glucose Assays	146	Protein ELISA	116
Cell Invasion Assays	18-19	Glutamate Assay	142	HIV-1 p24 ELISA Kits	60-61
Tube Formation Assay	30	Glutathione Adduct Assay	78	HNE	
Endothelial Tube Assay	30	Glutathione Assay	198	Antibodies	79
Epitope Tag Antibodies	116	Glutathione Reductase Assay	198	Assays	79
ERK2		Glycerol Assays	150	HNE-LDL Assay	82
Recombinant Adenovirus	51	Glycoaldehyde-BSA	76	hnRNPA0 Retroviral Vector	68
Retroviral Vector	68	GST		Homocysteine ELISA	142
ES/EC Cells		Antibody	116	HORAC Assay Kit	100
Alkaline Phosphatase Assays	38	Inclusion Body Solubilization and Renaturation Kit	118	H-Ras	
Colony Formation Assays	37	GTPase Assay Kits	104-105	Activation Assay	105
Retroviral Expression Systems	34	Guanine Exchange Factors		Recombinant Protein	109
Ethanol Assays	150	Activation Assays	106	HuB Retroviral Vector	68
Exoenzyme C3 Expression Vector	108	Agarose Beads	107	HuC Retroviral Vector	68
Extracellular Matrix Kits		HA Tag Antibody	116	HuD Retroviral Vector	68
Cell Adhesion Assays	10	Haptotaxis Assays	16	HuR Retroviral Vector	68
Cell Invasion Assays	18-19	HBV Core Antigen ELISA	152		
Tube Formation Assay	30	HBV "e" Antigen ELISA	153		
Feeder Cells	35				
Ferric Reducing Antioxidant Power Assay	101				

PRODUCT INDEX

Product	Page	Product	Page	Product	Page
Hydrogen Peroxide Assays	94	Lecithin Cholesterol Acyl-	131	MAPKAPK2	
Hydroxyl Radical Antioxidant Capacity Assay	100	Lentivirus		Recombinant Adenovirus	51
Hydroxyproline Assay	144	Cell Line	59	Retroviral Vector	68
Hypoxia Assays	26, 91	Control Plasmids	59	MCF-7/GFP Cell Line	114
IFN Recombinant Adenovirus	51	Expression Systems	57-58	MCF-7/Luc Cell Line	114
IKK Recombinant Adenovirus	52	Expression Vectors	59	MDA (Malondialdehyde)	
Immunoblot Blocking Reagent	117	Packaging Systems	58	Antibodies	81
<i>In Vitro</i> Angiogenesis Assay	29	Premade Control Viruses	59	Assays	80-81
<i>In Vitro</i> Tumor Sensitivity Assay	8	Purification Kits	62	MDA-LDL Assay	82
Inclusion Body Solubilization Kit	118	Quantitation Kits	60-61	MDA-MB-231/GFP Cell Line	114
Induced Pluripotent Stem Cells		shRNA Expression	57-58	MDA-MB-231/Luc Cell Line	114
Lentiviral Vectors	33	Titer Kits	60-61	MDA-MB-231/RFP Cell Line	114
Retroviral Packaging Cells	32	Transduction Kits	62	MEF Feeder Cells	35
Retroviral Vectors	32-33	Leukocyte Assays		MEK1	
Invasion Assays	18-19	Adhesion	11	Recombinant Adenovirus	51
IP Western Blot Detection Kit	119	Transmigration	17	Retroviral Vector	68
iPS Cell Reprogramming	32-33	Lin-28 Retroviral Vectors	67	MEK5 Recombinant Adenovirus	51
JK1 Feeder Cells	35	Lipid Droplet Isolation Kit	141	MEKK1 Recombinant Adenovirus	51
JNK1		Lipid Extraction Kits	140	Methylglyoxal (MG)	
Recombinant Adenovirus	51	Lipid Peroxidation Assays		Antibody	77
Retroviral Vector	68	8-Isoprostane ELISA	79	ELISA Kits	77
Klf4 Retroviral Vectors	67	HNE Adduct ELISA	79	microRNA	
KOSM Viral Vectors	33	Malondialdehyde (MDA) Assays	80-81	Adenoviral Expression	53
K-Ras		TBARS Assay	80	Retroviral Expression	65
Activation Assay	105	Lipid Quantification Assays	141	Migration Assays	12-19
Recombinant Protein	109	Lipid Separation Kits	140	MKK3	
Lactate Assays	147	Lipoprotein Lipase Assays	132	Recombinant Adenovirus	51
Lactose Assay	146	Lipoproteins		Retroviral Vector	68
LC3 Expression Vectors	30	Assays	122-125	MKK4 Recombinant Adenovirus	51
LCAT Assays	131	Human	123-124	MKK6	
LDH Cytotoxicity Assay	22	Oxidized	126	Recombinant Adenovirus	51
LDL		Purification Kits	139	Retroviral Vector	68
Assays	123	LOX-1 Assay	128	MKK7 Recombinant Adenovirus	51
Lipoprotein, Human	123	LPL Assays	132	MPO Assays	102
Oxidized	126	LRP1 ELISA	129	MTT Cell Proliferation Assay	24
LDL Receptor Assay	128	Luciferase		MuLV p30 Core Antigen ELISA	154
		Recombinant Adenovirus	50	Myc Tag Antibody	116
		Reporter Cell Lines	114	Myeloperoxidase Assay Kits	102
		Malondialdehyde		MyoD Recombinant Adenovirus	52
		Antibodies	81	myr-Akt Retroviral Vectors	68
		Assays	80-81		
		MAO Assays	102		
		MAP Kinase Signaling			
		Recombinant Adenovirus	51		
		Retroviral Vectors	68		

PRODUCT INDEX

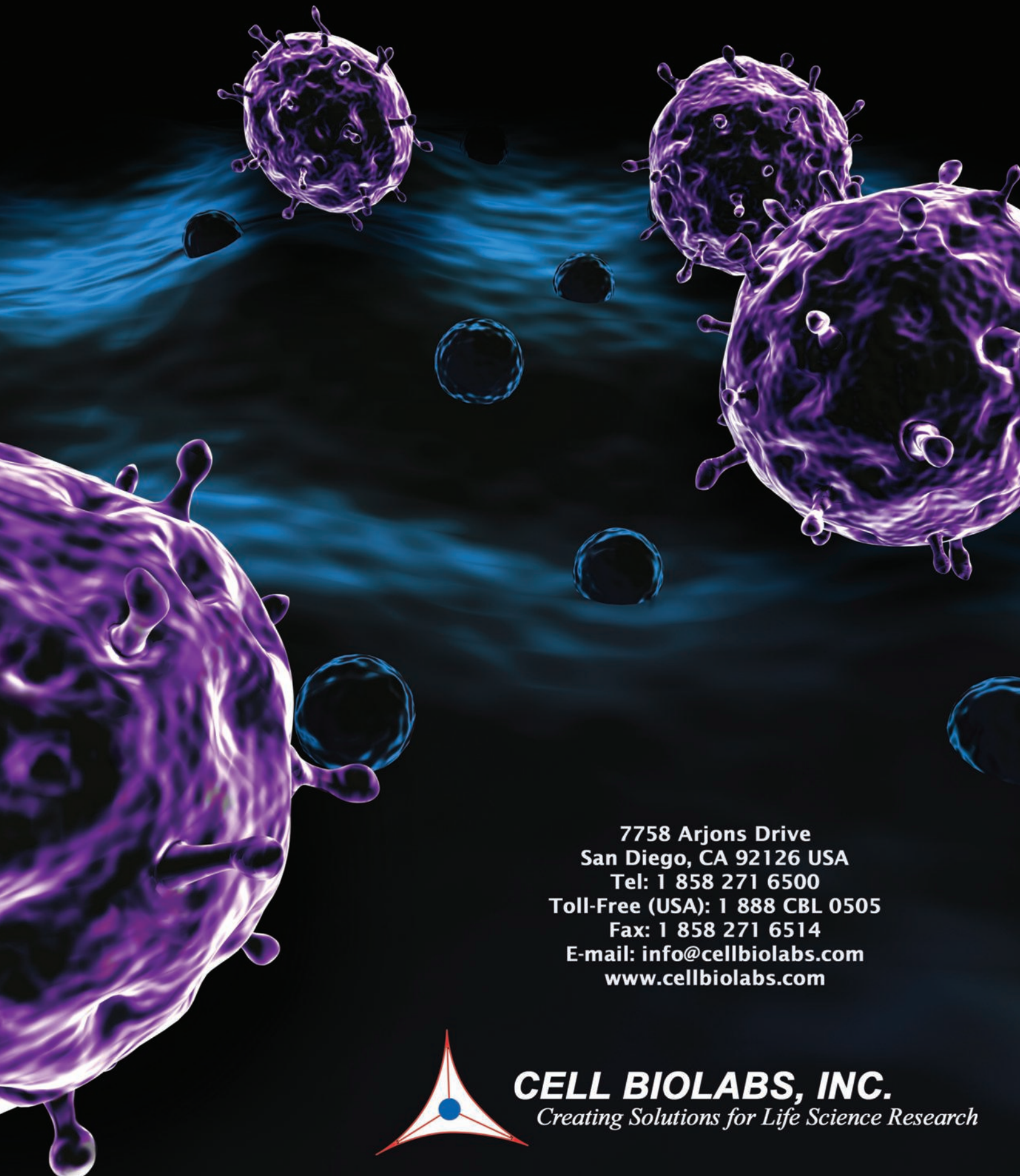
Product	Page	Product	Page	Product	Page
myr-Rac1 Retroviral	67	PABP Retroviral Vector	68	Protein Oxidation Assays	
NANOG Retroviral Vectors	67	PAK1 PBD Agarose Beads	107	(cont'd)	
N ^ε -Carboxyethyl Lysine		PCNA ELISA Kit	25	CML (Carboxymethyl	77
ELISA	76	PCSK9 ELISA Kit	129	MG (Methylglyoxal)	77
N ^ε -Carboxymethyl Lysine		Peroxide Detection Assays	94	Nitrotyrosine	73
Antibody	77	Phagocytosis Assays	28	Protein Phosphorylation	
Assay Kits	77	Phosphatidic Acid Assay	136	Antibody Stripping	117
NIH3T3/GFP Cell Line	114	Phosphatidylcholine	136	Solution	117
Nitrated LDL	123	Assay	136	Blocking Reagent	117
Nitric Oxide Assays	95	Phospho Antibody Strip-	117	Purification Kit	117
Nitroguanine ELISA Kit	85	ping Solution	117	Protein Quantitation Kit	119
Nitrotyrosine		PhosphoBLOCKER™		Proteins	
Antibodies	73	Western Blot Blocking	117	Albumin	138
Assay Kits	73	Reagent	117	Apolipoproteins	124
N-Ras		Phosphoproteins		EGFP	115
Activation Assay	105	Antibody Stripping	117	GRP-PH Domain	109
Recombinant Protein	109	Solution	117	Oxidized/Nitrated	77
Nuclear / Cytosolic Cell		Blocking Reagent	117	Purification Kits	
Fractionation Kits	118	Purification Kit	117	AAV	48
Oct-3/4 Retroviral Vectors	67	PI3K Retroviral Vector	68	Adenovirus	54
OHdG ELISA Kit	84	Plasminogen		Antibodies	120
OHG ELISA Kit	85	Antibody	138	Lentivirus	62
ORAC Assay Kit	100	ELISA Kit	137	Phosphoproteins	117
OVCAR-5/RFP Cell Line	114	Protein, Human	138	QuickTiter™ Viral Titer	
Oxidized HDL ELISA Kits	127	Plat-A Retroviral Packag-	63	& Quantitation Kits	
Oxidized LDL		ing Cells	63	AAV	49
ELISA Kits	126	Plat-E Retroviral Packag-	63	Adenovirus	55
Lipoprotein, Human	123	ing Cells	63	HBV Core Antigen	152
Oxidized Proteins	77	Plat-GP Retroviral Packag-	63	HBV “e” Antigen	153
OxiSelect™ Oxidative		ing Cells	63	HBV Surface Antigen	153
Stress / Damage Assays		Platinum Retroviral		HCV Core Antigen	154
Antioxidant Assays	96-101	Expression		HIV p24	60-61
DNA / RNA Damage Kits	84-90	Expression Systems	64	Lentivirus, Recombinant	60-61
Lipid Peroxidation Assays	79-83	Packaging Cell Lines	63	MuLV p30	154
Protein Oxidation Assays	73-78	pMX Retroviral Vectors	65-68	Retrovirus, Recombinant	69
ROS Assays	92-95	PRAK Retroviral Vector	68	Rac	
OxHDL Assay Kits	127	Proliferating Cell Nuclear	25	Activation Assays	105
OxLDL Assay Kits	126	Antigen Assay	25	Agarose Beads	107
OxPL Assay	126	Proliferation Assays	24-25	GEF Assay	106
Oxygen Radical Antioxi-		Protease Retroviral	67	Recombinant Adenovirus	52
dant Capacity (ORAC)		Vectors	67	Recombinant Proteins	109
Assay	100	Protein Extraction	118	Retroviral Vectors	67
p24 ELISA Kits	60-61	Reagents	118	Radius™ Cell Migration	13
p38		Protein Oxidation Assays		Assays	
Recombinant Adenovirus	51	Advanced Glycation		Raf1	
Retroviral Vectors	68	End Products (AGE)	76-77	Recombinant Adenovirus	51
p53		Advanced Oxidation Pro-	75	Retroviral Vectors	68
Recombinant Adenovirus	52	tein Products (AOPP)	75	Ral	
Retroviral Vectors	66	BPDE Adduct	75	Activation Assay	105
		Carbonyl	74	Agarose Beads	107
		CEL (Carboxyethyl Lysine)	76		

PRODUCT INDEX

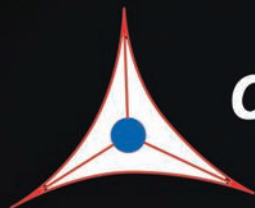
Product	Page	Product	Page	Product	Page
Ral (cont'd)		RFP (cont'd)		Small GTPase (cont'd)	
Recombinant Proteins	109	Recombinant Protein	115	Agarose Beads	107
Ran		Stable Cell Lines	114	Expression Vectors	108
Activation Assay	105	Rho		Premade Adenoviruses	52
Agarose Beads	107	Activation Assays	105	Retroviral Vectors	67
Rap		Agarose Beads	107	SNL Feeder Cells	35
Activation Assays	105	Recombinant Adenovirus	52	SOD Activity Assay Kit	97
Recombinant Proteins	107	Recombinant Proteins	109	Soft Agar Colony Assay Kits	
RAPAd® Adenoviral Expression Systems	53	Retroviral Vector	67	Cell Transformation Assays	6-7
Rapid GST Inclusion Body Solubilization and Renaturation Kit	118	RhoA Activation Assay	105	Hematopoietic Colony Forming Cell Assay	36
Rapid RCA Assay	56	RhoB Activation Assay	105	Stem Cell Colony Formation Assay	37
Ras Superfamily		RhoC Activation Assay	105	Tumor Cell Isolation Kit	9
Activation Assays	105	Rho Kinase Activity Assays	112	Tumor Sensitivity Assay	8
Agarose Beads	107	RIPA Buffer	120	Soluble Collagen Assay Kit	144
Expression Vectors	108	RNA Damage ELISA Kit	85	Sox2 Retroviral Vector	67
Recombinant Adenovirus	52	ROCK Activity Assay Kits	112	Sphingomyelin Assay	136
Recombinant Proteins	109	ROS Assays	92-95	SRB1 Assay Kit	130
Retroviral Vectors	67	S-Adenosylhomocysteine ELISA Kit	143	Stat5 Retroviral Vectors	68
RCA Assay Kit	56	S-Adenosylmethionine ELISA Kit	143	Stem Cell Research Products	
Reactive Oxygen Species (ROS) Assays	92-95	SAH ELISA Kit	143	Alkaline Phosphatase Detection Kits	38
Recombinant Adenoviruses	50-52	SAM ELISA Kit	143	Feeder Cells	35
Recombinant Proteins		scAAV		Hematopoietic Colony Forming Cell Assay	36
Fluorescent Proteins	115	Control Vector	46	iPS Cell Reprogramming	32-33
GRP-PH Domain	109	Expression Systems	42-45	PCR Primers	38
Small GTPase	109	Expression Vector	46	Retroviral Expression Systems	34
Renal Function Assays	148-149	Scavenger Receptor Class B Member 1 Assay Kit	130	Stem Cell Colony Assay	37
Reporter Genes		SCGE Assay Kits	87	Superoxide Dismutase Activity Assay	97
Lentiviral Vectors	59	SEAP Recombinant Adenovirus	50	T47D/GFP Cell Line	114
Quantitation Assays	113-114	Senescence Assays	23	TAC Assay	100
Recombinant Adenovirus	50	S-Glutathione Adduct Assay Kit	78	TBARS Assay Kit	80
Recombinant Lentivirus	59	shRNA Expression		TIA1 Retroviral Vector	68
Retroviral Vectors	66	Adeno-Associated Virus	41-45	Tiam1 Assay Kit	106
Stable Cell Lines	114	Adenovirus	53	TIAR Retroviral Vector	68
Retrovirus		Lentivirus	57-59	Total Antioxidant Capacity Assay	100
Expression Systems	64	Retrovirus	65	Total Bile Acid Assay Kits	134
Expression Vectors	65	Sialic Acid Assay Kit	145	Total Carbohydrate Assay Kit	145
Gene-Specific Vectors	66-68	Single Cell Gel Electrophoresis Assays	87	Total Cholesterol Assay Kits	123
Packaging Cell Lines	63	SKOV-3/GFP-Luc Cell Line	114	Total Phosphatidic Acid Assay	136
Quantitation Kits	69	SKOV-3/Luc Cell Line	114		
shRNA Expression	65	SKOV-3/RFP Cell Line	114		
Transduction Kits	70	Small GTPase			
RFP		Activation Assays	104-105		
Antibody	115	Active GEF Assays	106		
ELISA Kit	114				

PRODUCT INDEX

Product	Page	Product	Page
Transcription Regulation		Viral Core Antigen Assays	
Retroviral Vectors	68	HBVcAg	152
Transduction Reagents		HCVcAg	154
AAV	49	MuLV p30	154
Adenovirus	56	Viral Expression Systems	
Lentivirus	62	AAV	41-45
Retrovirus	70	Adenovirus	53
Transformation Assays	6-7	Lentivirus	57-58
Transmigration Assays	17	Retrovirus	64
Triglyceride Assays	133	Viral Packaging Cells	
TTP Retroviral Vector	68	AAV	47
Tube Formation Assay	30	Adenovirus	52
Tumor Cell Assays		Lentivirus	59
Cell Adhesion	10-11	Retrovirus	63, 66
Cell Invasion	18-19	Viral Titer Kits	
Cell Migration	12-19	AAV	49
Cell Transformation	6-7	Adenovirus	55
Chemosensitivity	8	Lentivirus	60-61
Soft Agar Colony Formation	6-9	Retrovirus	69
Transmigration	17	Viral Transduction	
Tumor Cell Isolation	9	Reagents	
uPA / uPAR Retroviral Vectors	67	AAV	49
Urea Assay	148	Adenovirus	56
Uric Acid / Uricase Assay	148	Lentivirus	62
UV DNA Damage Assays	88	Retrovirus	70
V5 Tag Antibody	116	ViraSafe™ Lentivirus	
VEGF Recombinant		Expression Systems	57-58
Adenovirus	50	Virus Purification Kits	
Very Low Density Lipoprotein Assay	123	AAV	47
Lipoprotein, Human	123	Adenovirus	54
ViraBind™ Purification Kits		Lentivirus	62
AAV	47	Virus Quantitation Kits	
Adenovirus	54	AAV	49
Lentivirus	62	Adenovirus	55
ViraDuctin™ Transduction Kits & Reagents		Lentivirus	60-61
AAV	49	Retrovirus	69
Adenovirus	56	VLDL	
Lentivirus	62	Assay	123
Retrovirus	70	Lipoprotein, Human	123
		VSV-G Retroviral Vector	66
		Western Blot Blocking Reagent	117
		Wound Healing Assay	20
		WST-1 Cell Proliferation Reagent	24



7758 Arjons Drive
San Diego, CA 92126 USA
Tel: 1 858 271 6500
Toll-Free (USA): 1 888 CBL 0505
Fax: 1 858 271 6514
E-mail: info@cellbiolabs.com
www.cellbiolabs.com



CELL BIOLABS, INC.
Creating Solutions for Life Science Research